SIM AUD 2014

Tampa FL USA

2014 Proceedings of the

Symposium on Simulation for Architecture and Urban Design

Edited by

Dr. David Gerber and Rhys Goldstein

2014 Proceedings of the

Symposium on Simulation for Architecture and Urban Design

Edited by

Dr. David Gerber and Rhys Goldstein

Cover by

Justin Matejka

Layout by

Stephen Gaebel, Michael Glueck, John Yee

2014 Proceedings of the Symposium for Architecture and Urban Design
Dr. David Gerber and Rhys Goldstein, editors

ISBN: 978-1-312-08357-8

Contents

Preface 1

Session 1: Role of Simulation in Design (Part 1) 5

Prototyping Interactive Nonlinear Nano-to-Micro Scaled Material Properties and Effects at the Human Scale 7
Jenny E. Sabin, Andrew Lucia, Giffen Ott, and Simin Wang
College of Architecture, Art, and Planning, Cornell University; Sabin Design Lab, Cornell AAP; Jenny Sabin Studio.

Session 2: Role of Simulation in Design (Part 2) 15

Parametric Spatial Models for Energy Analysis in the Early Design Stages 17
Wassim Jabi
Welsh School of Architecture, Cardiff University.

Simulation Supported Precedent Analysis: Disclosing the Sustainable Attributes of Vernacular Structures in the Southern U.S. 25
Tim Frank
Mississippi State University.

Session 3: Occupant Simulation and Visualization 33

SAFEgress: A Flexible Platform to Study the Effect of Human and Social Behaviors on Egress Performance 35
Mei Ling Chu, Paolo Parigi, Kincho Law, Jean-Claude Latombe
Dept. of Civil & Environmental Eng., Stanford University; Dept. of Sociology, Stanford University; Computer Science Dept., Stanford University.

Using Agent-Based Modelling to Simulate Occupants' Behaviours in Response to Summer Overheating 43
Alaa Alfakara, Ben Croxford
Bartlett School of Graduate Studies, UCL.

Towards Visualization of Simulated Occupants and their Interactions with Buildings at Multiple Time Scales 51
Simon Breslav, Rhys Goldstein, Alex Tessier, Azam Khan
Autodesk Research.

Session 4: Interactive Environments 59

Tangible 3D Urban Simulation Table 61
Flora Salim
RMIT University.

Typologies of Architectural Interaction: A Social Dimension 65
Seoug Oh, Veronica Patrick, Daniel Cardoso Llach
Design Ecologies Laboratory, The Pennsylvania State University.

Designing Fluvial Sites: Digitally Augmented Physical Hydraulic Modeling 73
Alexander Robinson
USC School of Architecture.

Session 5: Design Search and Optimization 75

Parameters Tell the Design Story: Ideation and Abstraction in Design Optimization 77
Erin Bradner, Francesco Iorio, Mark Davis
Autodesk Research.

Genetic Based Form Exploration of Mid-Rise Structures Using Cell Morphologies 85
Ornid Oliyan Torghabehi, Peter von Buelow
Taubman College of Architecture and Urban Planning, University of Michigan.

Design Agency: Prototyping Multi-Agent System Simulation for Design Search and Exploration 91
David Jason Gerber, Rodrigo Shiordia, Sreerag Veetil and Arjun Mahesh
School of Architecture, University of Southern California.

Session 6: Fabrication and Design **99**

Visual Robot Programming — Linking Design, Simulation, and Fabrication **101**
Johannes Braumann, Sigrid Brell-Cokcan
Association for Robots in Architecture.

A Freeform Surface Fabrication Method with 2D Cutting **109**
Andres Sevtsuk, Raul Kalvo
City Form Lab, Singapore University of Technology and Design.

Design-Friendly Strategies for Computational Form-Finding of Curve-Folded Geometries: A Case Study **117**
Shajay Bhooshan, Mustafa El-Sayed, Suryansh Chandra.
Zaha Hadid Architects.

Session 7: Computational Fluid Dynamics **125**

Tensegrity Systems Acting as Windbreaks: Form Finding and Fast Fluid Dynamics Analysis to Address Wind Tunnel Effect **127**
Panagiota Athanailidi, Ava Fatah gen Schieck, Vlad Tenu, Angelos Chronis
Bartlett School of Architecture, University College London.

Optimizing the Form of Tall Buildings to Achieve Minimum Structural Weight by Considering Along Wind Effect **135**
Matin Alaghmandan, Mahjoub Elnimeiri, Andres Carlson, Robert Krawczyk
Illinois Institute of Technology; University of Southern California.

Approximating Urban Wind Interference **143**
Samuel Wilkinson, Gwyneth Bradbury, Sean Hanna
University College London.

Session 8: Learning from Buildings **151**

Comparison of Control Strategies for Energy Efficient Building HVAC Systems 153
Mehdi Maasoumy, Alberto Sangiovanni Vincentelli
Dept. of Mechanical Engineering, University of California, Berkeley; Department of Electrical Engineering and Computer Science, University of California, Berkeley.

Causality in Hospital Simulation Based on Utilization Chains 161
Gabriel Wurzer, Wolfgang E. Lorenz
Vienna University of Technology.

Full-Automated Acquisition System for Occupancy and Energy Measurement Data Extraction 165
Dimosthenis Ioannidis, Stelios Krinidis, Georgios Stavropoulos, Dimmitrios Tzovaras, Spiridon Likothanassis
Information Technologies Institute, Centre for Research & Technology Hellas; Pattern Recognition Laboratory, Computer Engineering and Informatics,, University of Patras.

Session 9: Green Buildings and Cities **173**

Experimental Design of Energy Performance Simulation for Building Envelopes Integrated with Vegetation 175
Xiao Sunny Li, Ultan Byrne, Ted Kesik
John H. Daniels Faculty at the University of Toronto.

Transit-Oriented Development (TOD): Analyzing Urban Development and Transformation in Stockholm 179
Todor Stojanovski, Tesad Alam, Marcus Janson
KTH Royal Institute of Technology.

Scenario Modeling for Agonistic Urban Design 187
Trevor Patt, Jeffrey Huang
Ecole Polytechnique Federale de Lausanne.

Session 10: Smart and Sustainable Façades **191**

Acacia: A Simulation Platform for Highly Responsive Smart Facades 193
Daniel Cardoso Llach, Avni Argun, Dimitar Dimitrow, Qi Ai
Design Ecologies Laboratory, The Pennsylvania State University; Giner, Inc.

Sustainability Performance Evaluation of Passivhaus in Cold Climates 201
Kyoung-Hee Kim, Ph.D, Seung-Hoon Han, Ph.D
University of North Carolina at Charlotte and FrontInc.; Chonnam National University.

Presenting Author Biographies **205**

Organizers **211**

Sponsors **213**

Cover Image Credits **215**

Author Index **217**

Preface

Among the numerous endeavors supported by simulation, design is unique in the extent to which it combines the idiosyncratic with the empirical, the human with the computer, and the modeled with the real. Consistent with the truisms espoused by Rittel and Simon who describe design problems as "wicked" or "ill-defined", design as an activity is one fraught with uncertainties. These uncertainties are addressed through synthesis normally based on iterations of modeling and simulation, and here one must immediately acknowledge that designers, architects, urbanists, and building scientists rely on simulation in most aspects of how they conceive, explore, validate and learn from their ideas. SimAUD showcases the breadth and depth of research enhancing and employing sophisticated computationally focused simulation for challenges that range in scale from that of cities and regions, to that of buildings, down to that of human-computer interaction and interfaces. In this symposium we see simulation deployed through a variety of techniques, from discrete-event simulation and multi-agent systems, to CFD and FEA analysis through to material aggregation and robotics. What the culmination of this work speaks to is that the wicked and ill-defined nature of design can be tackled through iteration and refinement, and with simulation as part of this process the designer has both a greater number of options to choose from and a better understanding of which options are most likely to perform as intended or conceived.

It has been our pleasure to chair the fifth Symposium on Simulation for Architecture and Urban Design. SimAUD 2014 has highlighted simulation across a broad spectrum of research thrusts all relating to improving the processes we use to achieve a positive and lasting impact on society though architecture, urbanism, landscape architecture, and now the design of intelligent and interactive environments. This year we received 60 submissions, of which 40 were completed and peer-reviewed, from which 26 were selected for presentation and publication. The high caliber of the papers included in this year's proceedings attests to the talent and dedicated efforts of some of the leading researchers in the application of computer simulation, as evidenced by examples of constructed works, large-scale fluid dynamics models, the real-time capture and modeling of occupant behavior, and the use of multi-agent systems for form finding and optimization. Particularly worthy of acknowledgement is the geographic and disciplinary diversity represented by this year's presenters, who include our distinguished keynote speakers Yehuda Kalay, Professor and Dean of Architecture and Town Planning at the Technion, and Jenny Sabin, Assistant Professor at Cornell University.

Many people contributed to making SimAUD 2014 a success. The efforts of the Scientific Program Committee and referees were instrumental in shaping the program by facilitating the peer-review process as well as in supporting the organization of the symposium. As a testament to the quality of our Peer Review process all papers were reviewed by 4 and sometimes 5 reviewers and where necessary detailed suggestions and requirements were provided for ensuring the papers acceptance and meeting of the conference standards. These efforts have continued to be above the norm

and have provided our community with additional input and care in the dissemination of quality research. We would like to thank our international Peers for their tireless efforts once again. We would like to thank John Yee both for his fantastic work assembling this proceedings book and for providing ongoing administrative support. We also thank Michael Glueck for his help with the SimAUD website. We are grateful to have received guidance from former SimAUD chairs Ramtin Attar, Lira Nikolovska, and Liam O'Brien in all aspects of planning, and a special thanks goes to SimAUD founder Azam Khan for his vision and dedication in helping all participants and contributors get as much as possible out of the event. Most importantly, we wish to recognize all of this year's authors for their hard work and ingenuity. Given the quality and competitiveness of the research and papers submitted to this year's symposium, we are hopeful and confident that future SimAUD symposiums will continue to build on this success and advance our collective knowledge of simulation-supported urban design, landscape architecture, architecture, and design of intelligent and interactive environments.

Dr. David Gerber
Assistant Professor
University of Southern California
School of Architecture

Rhys Goldstein
Principal Research Scientist
Autodesk Research

All accepted papers will be published in the ACM Digital Library at the SpringSim Archive.
Sponsored by The Society for Modeling and Simulation International.

Keynote Presentations

Simulating Human Behavior in Built Environments

Yehuda Kalay
Technion, Israel Institute of Technology

Yehuda Kalay has been serving as the elected dean of the Faculty of Architecture and Town Planning at the Technion, Israel Institute of Technology, since October 2010. Prof. Kalay also holds an appointment as Professor in the Graduate School, at the University of California, Berkeley, where for 18 years he served as Professor of Architecture prior to assuming his current position at the Technion.

Kalay's research explores the implications and applications of digital technologies to architectural design. Specifically, his research explores the mutual interactions between space, the people who inhabit it, and the activities they engage in, for the purpose of improving that interaction through the use of digital media at all phases of the building's lifecycle (design, construction, and use).

Professor Kalay has published more than 120 scholarly papers (over 70% of them peer-reviewed) and nine books, the most recent of which are: Collaborative Working Environments for Architectural Design (Palombi, 2009), with Prof. Carrara of the University of Rome, Italy; New Heritage: Cultural Heritage and New Media (Routledge, 2008), with Prof. Kvan of the University of Melbourne, Australia; and Architecture's New Media (MIT, 2004).

Elastic Matters: The Role of Simulation and Visualization in Trans-disciplinary Research

Jenny Sabin
Cornell University

Jenny E. Sabin's work and research is at the forefront of a new direction for 21st-century architectural practice---one that investigates the intersections of architecture and science, and applies insights and theories from biology and mathematics to the design of material structures. Sabin is an Assistant Professor in the area of Design and Emerging Technologies in Architecture at Cornell University. She is Principal of Jenny Sabin Studio, an experimental architectural design studio based in Philadelphia USA and director of the Sabin Design Lab at Cornell AAP, a hybrid research and design unit with specialization in computational design, data visualization and digital fabrication.

Sabin was awarded a Pew Fellowship in the Arts 2010 and was recently named a USA Knight Fellow in Architecture. She has exhibited nationally and internationally most recently at Nike Stadium NYC, the American Philosophical Society Museum and at Ars Electronic, Linz, Austria. Her work is currently exhibited in the internationally acclaimed 9th ArchiLab at FRAC Centre, Orleans, France. Her work has been published extensively including in The Architectural Review, A+U, Mark Magazine, 306090, 10+1, ACM, American Journal of Pathology, Science, the New York Times, Wired Magazine and various exhibition catalogues and reviews.

Session 1: Role of Simulation in Design (Part 1) **5**

Prototyping Interactive Nonlinear Nano-to-Micro Scaled Material Properties and Effects at the Human Scale 7
Jenny E. Sabin, Andrew Lucia, Giffen Ott, and Simin Wang
College of Architecture, Art, and Planning, Cornell University; Sabin Design Lab, Cornell AAP; Jenny Sabin Studio.

Prototyping Interactive Nonlinear Nano-to-Micro Scaled Material Properties and Effects at the Human Scale

Jenny E. Sabin[1,2,3], Andrew Lucia[1,2], Giffen Ott[1,2], and Simin Wang[1,2]

[1]College of Architecture, Art, and Planning
Cornell University
139 E. Sibley Hall,
Ithaca, NY 14853

[2]Sabin Design Lab
Cornell AAP
101 Rand Hall,
Ithaca, NY 14853

[3]Jenny Sabin Studio
Middle City
P.O. Box 30368,
Philadelphia, PA 19103

Keywords: Adaptive Architecture, Materials Science, Matrix Biology, Simulation, Interaction, Nano, Prototype, Scale.

Abstract

The goal of the eSkin project is to explore materiality from nano to macro scales based upon an understanding of the dynamics of human cell behaviors. Immediately at hand is the necessity to understand, speculate, test and simulate which nonlinear nano to micro scaled material properties are possible at the architectural scale. The synergistic, bottom-up approach across diverse disciplines, including cell-matrix biology, materials science and engineering, electrical and systems engineering, and architecture brings about a new paradigm to construct intelligent and sustainable building skins that engage users at an aesthetic level. In this paper, we present two human scale prototypes combining real-time presence detection with specialized display technology and interactive computer simulation. The prototypes probe the possible features and effects of eSkin at the scale of a building façade unit.

1. INTRODUCTION

1.1. Background

How might architecture respond to issues of ecology and sustainability whereby buildings behave more like organisms in their built environments? We are interested in probing the human body for design models that give rise to new ways of thinking about issues of adaptation, change and performance in architecture. The eSkin project starts with these fundamental questions and applies them towards the design and engineering of responsive materials and sensors. The work presented here, titled *eSkin*, is one subset of ongoing trans-disciplinary research spanning across the fields of cell biology, materials science, electrical and systems engineering, and architecture. The goal of the eSkin project is to explore materiality from nano to macro scales based upon an understanding of nonlinear, dynamic human cell behaviors on geometrically defined substrates. To achieve this, human smooth muscle cells are plated on polymer substrates at a micro scale. Sensors and imagers are then being designed and engineered to capture material and environmental transformations based on manipulations made by the cells, such as changes in color, transparency, polarity and pattern. Through the eSkin project, insights as to how cells can modify their immediate extracellular microenvironment are being investigated and applied to the design and engineering of highly aesthetic passive materials, sensors and imagers that will be integrated into responsive building skins at the architectural scale.

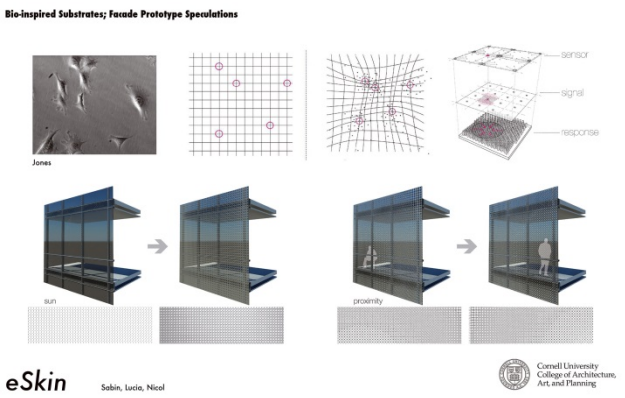

Figure 1. Previous simulations and architectural speculations using eSkin. Cell data originally produced in Dr. Peter Lloyd Jones's lab, University of Pennsylvania. Our emphasis continues to rest heavily upon the study of natural and artificial ecology and design, especially in observing how cells interacting with pre-designed geometric patterns alter these patterns to generate new surface effects. These tools and modes of design thinking are then applied towards the design and engineering of passively responsive materials, sensors and imagers.

A building's envelope must consider a number of important design parameters, including degrees of

transparency, overall aesthetics and performance against external conditions such as sunlight levels, ventilation and solar heat-gain. In contrast to existing examples of adaptive architecture, we are specifically interested in the role of the human in response to changing conditions within the built environment. Additionally, our group is carrying out fundamental and applied research to develop novel materials synthesis and fabrication methods not yet available on the market. Our applied design offers additions to the paradigm of responsive and adaptive architecture through architectural treatments in the form of an adaptive building skin, eSkin, which modulates passive solar, light and moisture control with embedded sensors that ultimately (re)configure their own performance based upon local criteria.

Our role as architects involves generating tools to visualize and simulate cell attraction forces and cell behavior, such as forces distributed via a virtual extracellular matrix environment over multiple time-states, while also incorporating micro scale material constraints. Beyond visualization, we also direct the architectural intent of the project by constantly speculating on how results at the nano and micro level will potentially look, feel, and assemble at the building scale (Figure 1). For example, one of the interactive prototypes featured in this paper integrates actual simulation data from micro-scale material substrates to speculate upon how these complex behaviors and effects may translate to the building scale and initiate human interactivity. Based upon these nonlinear and dynamic responses that human cells generate, we are redesigning and re-engineering interfaces between living and engineered systems with the ultimate goal of implementing some of the key features and functions revealed by cells on a chip for sensing and control at the building scale.

1.2. Background on Materials Research and the Importance of Scaled Prototypes

The particular material research presented in this paper focuses on one subset of study within the eSkin project, the optical simulation and application of geometrically defined nano to micro scale substrates that display the effects of nonlinear structural color change (Figure 2) when deployed at the building scale. Specifically, nano/micro scale pillar substrates, designed in the Yang lab, form the basis of this investigation. These substrates are fabricated via microlithography and softlithography, first requiring a negative nano/micro pattern to be etched into a substrate in which PDMS is subsequently cast, cured, and removed, thus producing a positive relief of nano/micro pillars. For a full description of the materials used in the context of this investigation, please see Wang, et al. 2013.

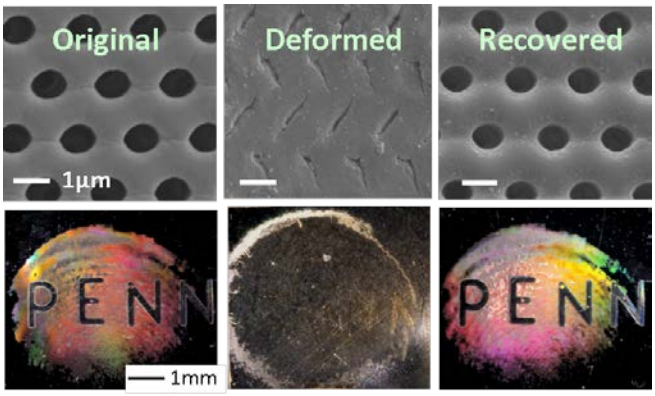

Figure 2. Example of a predefined geometric pattern embedded within a shape memory polymer material displaying structural color change under deformation and recovery. Here we exhibit SEM images of membranes consisting of a hexagonal array of micron-sized circular holes (top row) and demonstrated dramatic color switching as a result of pattern transformation (bottom row). Image originally published in Li, J., et al, 2012.

Though these specific types of optical qualities can be seen by the naked eye (Figure 2), extracting their optical performance quantitatively for speculation at larger architectural scale applications is necessary given (1) the current limitations in which these substrates can be fabricated (currently 4 inches maximum), and (2) the necessity to speculate on large scale deployments of potential materials without the need to actually fabricate. Thus, simulating the effects of larger swathes of these materials has been a goal and focus of this research: to speculate as to the larger scale application and effect of these substrates in an architectural context.

Thus, as actual fabrication of the desired nano material is still unattainable, we demonstrate in principle two distinct types of speculation for the architectural scale. The first is a simulated, digital, real-time and interactive prototype that harnesses the optical properties and attributes of the particular desired nano materials being designed and tested within the Yang Lab for the eSkin project. Here, through the use of video input, a viewer's proximity and movement trigger a simulated response in the virtual substrate's appearance (Figure 8).

The second output aimed at advancing speculative design trajectories within the eSkin project is a physical, interactive, and scaled component prototype whose properties behave in a comparable manner to those sought, but which can be fabricated at a larger scale. Importantly,

this second scaled prototype provides a test bed for another fundamental element in the conception of eSkin, that of local adaptation to environmental stimuli. Here, we consider the role of the individual sensing node and its effects upon a local region of change within a global surface substrate. To this end, our scaled prototype makes use of sensing and control technologies developed in the labs of Van der Speigel and Engheta, which then influence local regions of change within the eSkin prototype (Figures 6 and 9). While the adaptive materials, colloidal particles, used in this prototype are not the intended final material output for eSkin, they allow for a rapidly responsive testing ground for the local sensors' adaptive technologies. The thrust of this paper demonstrates these two distinct trajectories, both of which offer insights and allow for development of further architectural speculation as we traverse scalar-dependent properties generated at the nano and micro levels, yet that are applied at the macro human scale.

2. METHODS

2.1. Prototyping Optical Properties at the Nano Micro Scale

Previously (Wang et al, 2013), we have demonstrated the extraction of simulated optical properties and their deployment through a suite of off-the-shelf and custom written software, enabling the speculation of nano/micro scaled material properties at an architectural scale.

First, the unique physical and angle dependent optical properties of a small portion of these periodic geometric substrates are simulated in the labs of Van der Spiegel and Engheta through the use of Lumerical FDTD Solution, material simulation software. Due to the periodic nature of the substrates in question, only a portion of these substrates need be simulated, after which the characteristics of the material would "repeat" itself. These simulations, which derive the angle-dependent optical properties of the material substrates, ultimately form the basis for larger scale simulations of potential material applications within the eSkin system. The angle-dependent property can be formatted into a function of reflection coefficient and transmission coefficient versus wavelength of light.

Initially, at the architectural scale, speculations as to the extracted performative and aesthetic qualities of these nano/micro materials were deployed using custom written algorithms in conjunction with the Rhinoceros (NURBS modeling) software environment. We would later rewrite these algorithms in alternate software to facilitate a smoother real-time simulation. To maximize the color changing effect and efficiency calculation, the simulated geometry was approached as a tessellation of panels that

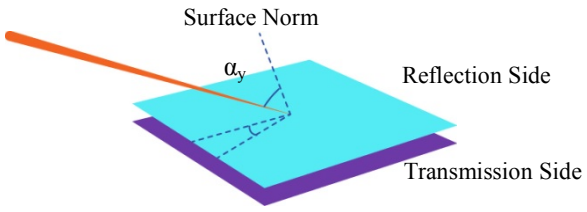

Figure 3. Incident light angle on two sides of a surface.

respond to peoples' movement in front of a video camera serving as a sensor. Each panel can be treated as an individual surface with a single light source of uniform distribution, with each point on the surface having the same optical properties. Therefore, evaluation of the center point upon each discrete tessalated surface represents properties of the whole. With one single light, the two sides of the surface can be named as the reflection side (C_r) and transmission side (C_t) (Figure 3). After calculating the incident angle, a matrix of C_r and C_t at different wavelength (λ) can be obtained by interpreting the measured data. For a given light source with a specific spectral power distribution ($I(\lambda)$), reflected/transmitted spectral power distribution can be obtained by $C_r(\lambda)\ I(\lambda)$ and $C_t(\lambda)\ I(\lambda)$, so that an XYZ color can be generated for the surface. (Figure 4).

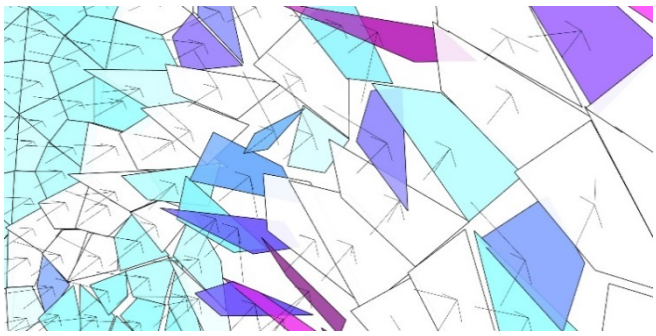

Figure 4. Incident light and normal of tessellated surfaces.

2.2. Interface Design for Simulation: Prototype 1

As mentioned, in the context of the prototypes and simulations, the previously constructed suite of digital tools proved too computationally heavy and burdened with a significant temporal delay to perform adequately in a real-time situation, operating at speeds of 1 second plus between

refresh. As a result, it became necessary to rebuild the same properties, qualities, and interactions within a single software environment rather than across platforms. Having resolved networking issues across platforms, the remaining performance criteria largely surrounded issues of spatial and temporal fidelity. Issues of efficiently computing movement and coloration of mesh faces were important design constraints. Similarly, spatial fidelity of the environmental triggering stimuli (here taken from differences across a real-time temporal pixel array) was minimized to avoid unnecessary lag in computation. Temporally, frame rates were a limiting factor based upon the amount of computation required per frame. A sufficiently smooth frame rate was set empirically and weighed against all other spatial parameters.

While using the prior studies as a framework (Wang et al, 2013), the open-source scripting environment Processing was chosen to work within, firstly for its computational efficiency. In addition, Processing allows an ability to easily import geometry and optical data from the prior simulations, as well as having the capability to easily interface with real-time interactive inputs via a camera installed in the prototype, thus integrating a viewer's experience as part of the simulation (Figure 7). For the purposes of this simulation, the new application retains much of the original functionality of the initial studies (i.e., rotation and color change), querying simulated angle-dependent optical data arrays as a user moves about the environment, ultimately affecting the viewers' virtual angular difference with respect to the simulated substrate.

This interactive simulation features a built-in camera that detects your motion through a custom script. When one waves their hand or moves in front of the screen—to the left, right, or center—the input adjusts the virtually simulated eSkin in real time (Figure 8). The simulation incorporates real optical data in the form of color and geometric transformation from micro scale material substrates to speculate upon how these nano to micro scale material effects and related geometries may be applied at the architectural scale. Here, visitors are able to interact with the actual material effects of eSkin in real time and in a scaled way.

In order to achieve this, a faceted mesh "wall" model composed of 1,728 individual faces was generated in the Rhinoceros modeling environment. The number and geometry of mesh subdivisions was based on empirical design decisions goverened by spatial fidelity (impacting computational speed) and aesthetics. This mesh was then imported into a Processing sketch (workspace in Processing) as a .obj file via the external OBJLoader library by Saito and Ditton. Next, each mesh facet within the sketch is embedded with an identical angle-dependent optical color data array extracted from simulated nano/micro materials fabricated in the Yang Lab. At its inception, this color data appears generic, but is given specificity per simulated viewing angle. Within the simulation this color data is then queried through time as a list array of RGB values corresponding to virtual incident dependent viewing angles initially established according to actual material testing in the Yang Lab (for a full discussion of color simulation prodedures, please see Wang et al, 2013).

In order to engage with viewers in an environment external to the simulation, a video camera captures a real-time image feed and a resultant low fidelity image difference is taken (Figure 5a). This image difference is achieved by simply comparing corresponding pixel brightnesses at each pixel (x_i, y_i) of a possible 256 values through time and at each frame of image capture (designated *i*). If the difference in brightness between two spatially coincident pixels (x_i, y_i) and (x_{i+1}, y_{i+1}) is sufficiently changed through time, the resultant pixel is said to have changed and is added to a counter for further inquiry. In order to increase computational speed for real-time interaction, not every pixel in the initial image array is considered for calculation. Thus, every n^{th} pixel in the array is queried; in the prototype simulation presented here, the fidelity was chosen to be every 300^{th} pixel in both the x and y dimensions. For the purposes of this study and simulation, the optimal fidelity of the differenced pixel array was set emperically, satisfying outcomes based upon speed and the amount of sensitivity to environmental stimuli deemed sufficient. To this end, the image capture and differencing occurs at a rate of 7 frames per second. Ultimately, this crude image difference is mapped to an underlying grid of circular bins whose regions correspond to mesh facet centroids (Figure 5c). Depending on the amount of difference at a given moment within the underlying grid of circular bins, varying degrees of rotation about each mesh centroid are triggered within the corresponding meshes (Figure 5d). Finally, based upon the amount of rotation and each corresponding mesh normal to the viewing plane of the simulation screen, the array of simulated angle-dependent color data from the Yang Lab is accessed, assigning appropriate color data to the mesh at each instant in the

simulation. Thus within the overall field of change, as a single mesh facet is allowed to rotate within the model, a resultant color variation is expressed within each facet, corresponding to the optical color data array (Figure 5e-5f).

The implementation of incident light source and transmission properties in the real-time simulation is still being developed further through ongoing iterations of the software. While the work presented here relies on the assignment of one color value per mesh, ongoing investigations are the subject of more advanced and accurate shading techniques such as vertex interpolation.

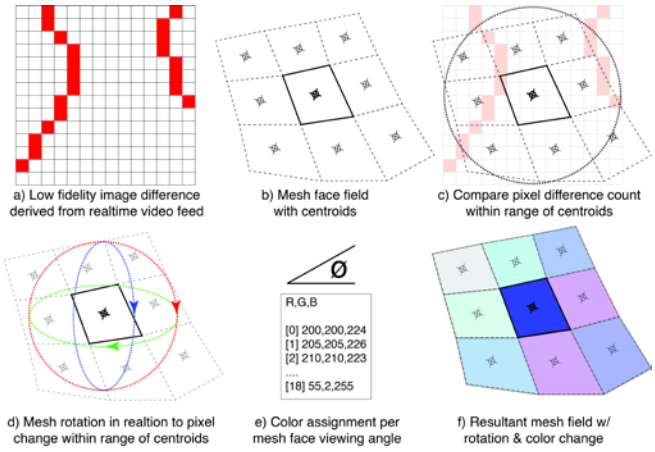

Figure 5. Schematic Diagram of Real-time Simulation. A real-time image feed is subject to low-fidelity image differencing. The virtual resultant difference map (a) is compared to the actual mesh face field visible in the simulation (b). Within a given range of every unique mesh centroid, the number of changed pixels is quantified (c). Each mesh is then rotated about its centroid, corresponding to the given pixel count (d), while a corresponding viewing angle is calculated and coupled with a change in color (e).

2.3. Interface Design for Scaled eSkin Components: Prototype 2

The second prototype aims to advance speculative design trajectories within the eSkin project as a physical, interactive, and scaled component prototype whose properties behave in a comparable manner to those observed at a nano to micro scale, but which can be fabricated at a human scale. Silica colloidal nano particles dispersed in an organic medium (solvent) are sandwiched between two transparent conductively treated Indium Tin Oxide (ITO) pieces of glass, housed within an assembly of three laser-cut plexiglass frames. The light reflected from the ordered structure (depending on the particle size, distance and reflective index contrast between the silica nanoparticles and the organic medium) provides a specific wavelength of light. When a voltage is applied to the particulate solution, the surface charge of the particles is altered, thus changing the distance between the particles, leading to the change of color appearance. At each intersection between the color cells, a sensor based on shifts in light intensity levels actuates voltage change between the adjacent color cells. Thus, when a finger, hand, or figure passes by a sensor, a detected shift in light intensity level triggers a voltage shift across the ITO component, reorganizing the distribution of particles in the solution, ultimately affecting the reflected appearance of color from the nano-particle solution (Figure 6).

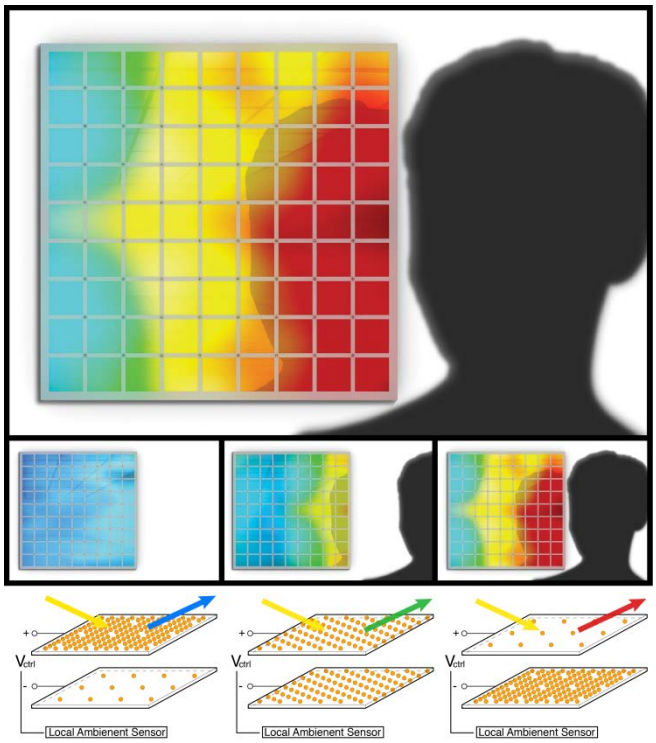

Figure 6. Rendering of eSkin material prototype demonstrating user interaction as an active input with resultant speculative transformation of the material substrate (top). Schematic diagram of circuit design interfacing with nano-colloidal particle solutions through voltage control. Individual sensing nodes interact with the material substrates locally through voltage control via the sensing of changes in ambient light, ultimately affecting the appearance of the prototype components (bottom).

3. RESULTS

3.1. Interface for Simulation: Prototype 1

While the primary aim of the first prototype is to simulate macro scale possibilities of nanoscale technologies and the effects of eSkin, it was also important to create a provocative representation of the technology at hand through an interesting and dynamic simulation that exemplifies the capabilities of the technology and suggests further real-world applications. Therefore, we approached

this installation as an interface that alludes to the possible spatial characteristics of a thin film laminate in relation to the tangible built environment. In order to distance the installation from a typical screen displaying an interactive simulation, we disassembled a contemporary Liquid Crystal Display monitor, removed everything nonessential to the display, and applied the LCD panel to a box of our own creation. The liquid crystal screen serves as a façade for the box, constructed of frosted plexiglass, mirrored plexiglass, and an array of high-voltage cold-cathode fluorescent bulbs, 2mm in diameter. The pattern of the bulb array within the box, in conjunction with the mirrored surface, provides a seemingly infinitely deep space that expands within the box and behind the screen, lit at a standard interval by bulbs that resemble typical office fluorescent lights. Along with the screen, at the face of the box is an embedded camera. This camera is the input for the simulation run on the machine hidden in the underside of the box that is in turn displayed upon the front of the box as a mock interactive building façade/curtain wall (Figures 7 & 8).

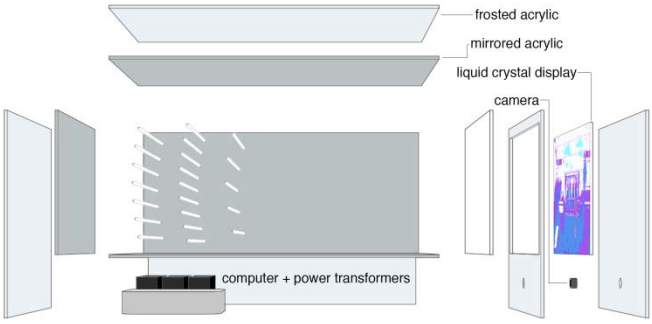

Figure 7. Diagram of simplified installation assembly. An array of cold cathode fluorescent bulbs is housed within a mirrored box. The face of this box is a sandwich of a liquid crystal display and clear acrylic. The mirrored box provides a reflective depth that is much more vast than the actual volume of the box.

3.2. Interface for Scaled eSkin Components: Prototype 2

Rather than purely display a simulation based upon actual data as recorded from the original nano-pillar material simulation, we were able to create a panel that displayed the dynamism and control achieved with an actual nanoparticle suspension. In collaboration with the labs of Yang, Van der Speigel and Engheta we present a modular component design that exhibits the structural color adaptation of the nanoparticles in relation to variable voltage.

Using Indium Tin Oxide (ITO) treated glass acting both as the frame and the conduit for the nanoparticles within, we were able to create a mosaic of a variety of individual units, of multiple sizes. Each of these contained components is then mounted to a printed circuit board (PCB), with its own control circuit that adjusts the charge across the glass according to the dynamic impedance of an arrangement of photoresistors. These photoresistors, acting as sensing nodes, are placed at each corner of the cells, and react to the presence of the participant/spectator.

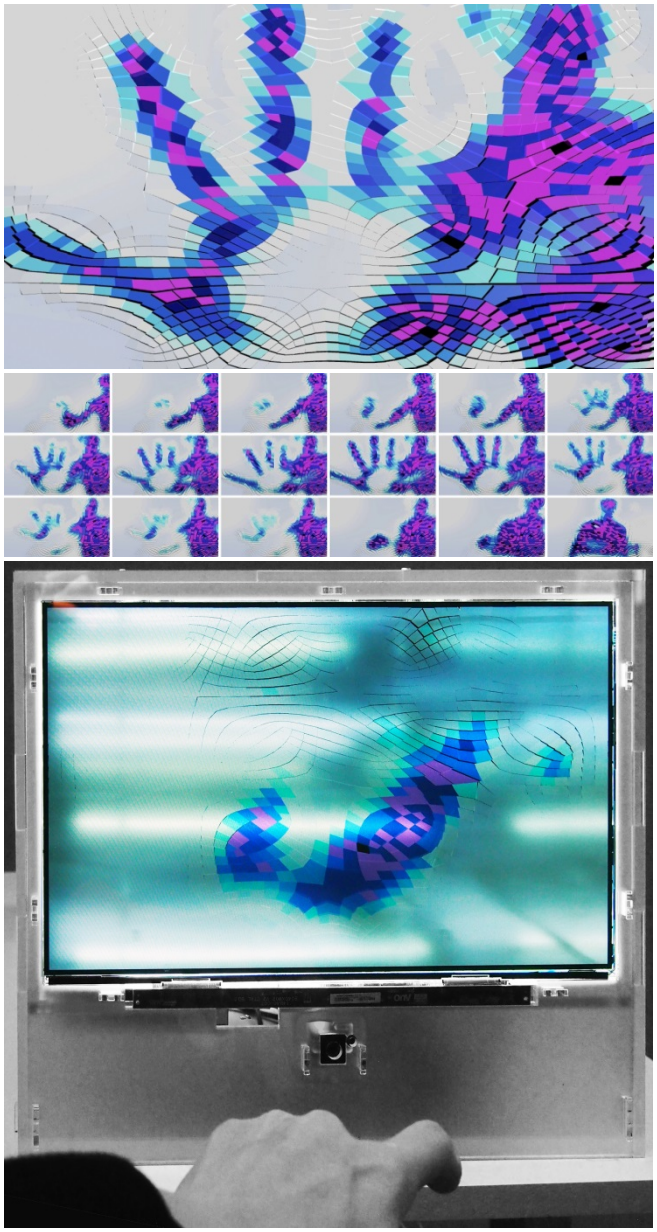

Figure 8. Still image (top) and sequential still images (middle) taken from real-time simulation built with Processing, harnessing geometric variation, optical data arrays, and user input as parameters. Simulation presented on custom LCD monitor, backlit with cold-cathode fluorescent bulbs, and embedded in custom-built plexiglass housing.

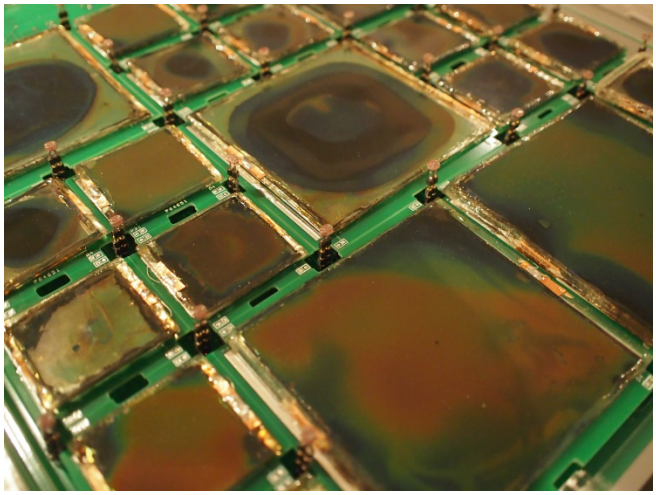

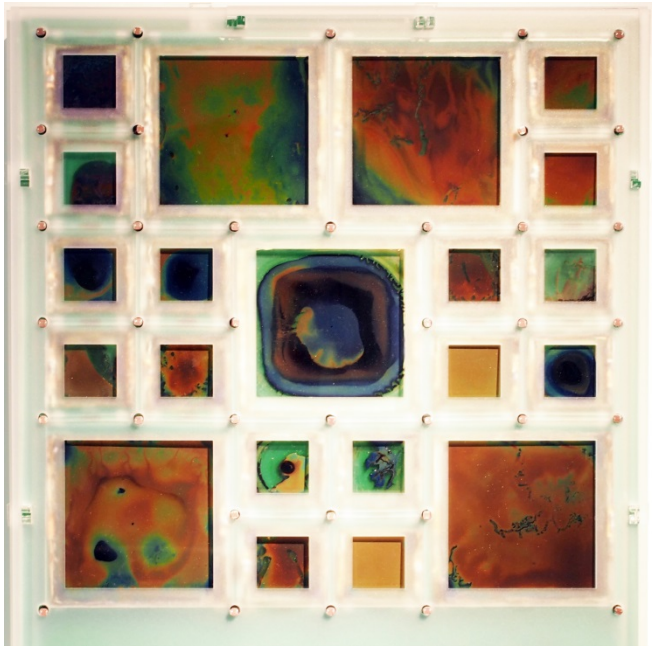

Figure 9. ITO treated glass cells with voltage controlled nanoparticle solution within, housed on a custom-built PCB substrate, and controlled locally via ambient sensing nodes. Note, front face of prototype housing removed to reveal component arrays (top). Component material prototype with local sensing nodes affecting component cells, harnessing user interaction as an active input and resultant transformation of the material substrate (bottom).

4. DISCUSSION

Within the context of the two prototypes presented here, the practical inability to fabricate nano/micro patterned materials at a human scale in turn inspired a speculation as to the behavior of these materials' effects as scale increases were taken into consideration. We found that the scalability of effects and material fabrication to be the largest challenge to the group at hand. Specifically, the micro and nano lithography arrays we intend to utilize cannot currently be fabricated above roughly a 2cm x 2cm feasible sample size, with an absolute maximum of 4in x 4in. The 2 prototypes presented in this paper can thus be seen as a designed response and speculation to this limitation as well as a test for more advanced human interaction, including local and regional environmental stimuli.

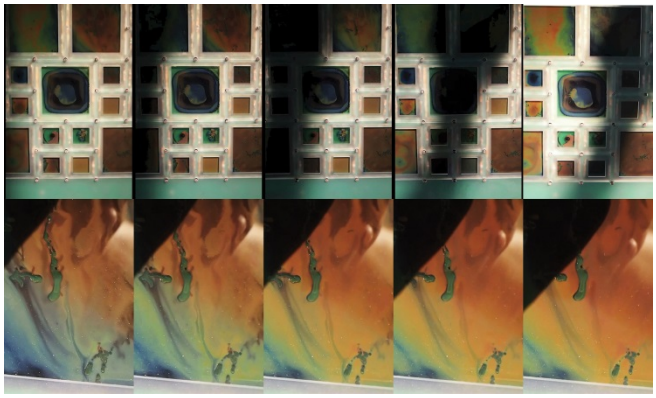

Figure 10. Image stills from a movie demonstrating structural color adaptation of the nanoparticles in relation to variable voltage due to the presence or absence of a hand and arm (as seen in silhouette) passing in front of the sensing nodes.

Through simulation, modeling, and prototyping, unique non-linear aspects of the desired eSkin materials—and projected use of these materials in situ—were extracted and redeployed through a series of prototypes. Through each of the prototypes (the simulation and the scaled components) presented here, we were limited to the exploration of aspects of the nano to micro material behavior and its application in part, but never as a whole. Thus, for each investigation we took this limitation as an opportunity to interrogate and expand upon particular behavioral aspects of the eSkin materials, while not trying to merely mimic the total functionality within a single prototype.

By their very nature, the eSkin materials in question demonstrate optical variability based upon the relative location between a viewer and the surface. In an ideal large scale application of an eSkin prototype, material effects, specifically color change, transparency, and transmission, would be the result of geometric variation within a surface, a viewer's relative position with respect to that surface, and the source of illumination upon or from behind the surface. Naturally, it is impossible to take all of these parameters into consideration in a single virtual modeled environment, especially one in which a viewer's interaction with the simulation space is transmitted to an entire audience via a flat screen display (Figure 8). In the case of the simulation,

multiple angle-dependent observation points cannot be accounted for, given the singular nature of the flat screen display technology deployed here. However, this optical simulation space is essential, given the inadequate scalability of the material at hand. While a single virtual simulation allows for a robust overall speculation of material behavior and effect, it does not truly allow for the simulation of a curved geometry in actual space from multiple observational vantages. In order to overcome this limitation of a virtually variegated geometric interactive surface, the use of a gently rotating faceted surface geometry was deployed, one that could approximate multiple viewers' interaction and involvement with the virtual environment.

In the case of the second prototype, we were able to test changes in color and to some degree, transparency, through nuanced environmental stimuli including multiple participants and changes in light intensity (day to night light shifts in a gallery room) that in turn affected features of the prototype in local, regional and global ways. The ability to 'tune' the second prototype to specific environments was made possible through the incorporation of individual potentiometers located in the back of the control board of the prototype. This enabled adjustments of local thresholds of illumination relative to each component for the control of the materials across the entire prototype. While the selected material for the second prototype, silica colloidal nano particles, is not the actual material being tested currently at the nano to micro scale, these interim material assemblies behave in a comparable manner to those observed at a nano to micro scale, but can be fabricated at a human scale, thus providing a useful testing ground for eSkin.

Lastly, though not a criticism but a reality of the interdisciplinary nature of the team, we found the ability to fabricate in an applied fashion to be more or less beyond the scope of scientists and engineers whose areas of expertise reside in fundamental research. Simply put, prototyping through scaled applications is not necessarily the purview or area of expertise of scientists and engineers whose specialty is fundamental research. As a reality of the interdisciplinary work, next steps might include pairing with industry partners who would aid in the development of applied applications.

5. CONCLUSION

Having learned from the two prototypes discussed in this paper, we are currently developing a hybrid large-scale prototype whereby the material effects sought are simulated in a manner in which multiple viewers' unique experiences are the consequence of variegated geometry and relative viewing relationship to the surface of interest. Though again this prototype will not be constructed of the specific nano to micro materials fabricated in the Yang Lab, our aim is to architecturally prototype the behaviors of the intended materials. From the virtual simulation presented here we are maintaining the modeled material properties of angle dependent color change, coupled with a regioned notion of triggered event space within the surface. This regioned event surface is further controlled and evolved by the motion of bodies in space relative to their unique viewing of the prototyped surface. Aspects of this behavior that were explored in the second prototype presented here will continue to be refined and incorporated in this forthcoming prototype. To this end we are integrating the material substrate's transparency and reflectivity with respect to unique viewing angle via geometry and projection. Taking cues from the second physical prototype discussed here, the large-scale work in progress will maintain an aggregate of faceted surfaces whose variation will be the result of nodal characteristics, or regions of change. These prototypes serve as an interactive testing ground for selecting and refining nonlinear nano to micro scaled material effects at the human and architectural scale.

Bibliography

LI, J., SHIM, J., OVERVELDE, J., DENG, J., ZHU, X., BERTOLDI, K., YANG, S. 2012. Switching Reflective Color to Transparency in Photonic Membranes via Pattern Transformation and Shape Memory Effect. *Soft Matter*. Vol. 8. Num 40. 10322 – 10328

KRETZER, M., IN, J., LETKEMANN, J., JASKIEWICZ, T., 2013. Resinance: A (SMART) Material Ecology. ACADIA 2013 Adaptive Architecture, Edited by Beesley, Khan and Stacey. 137-146.

SAITO, T & DITTON, M. .OBJ loader for Processing. http://code.google.com/p/saitoobjloader/

WANG, S., LUCIA, A. SABIN, J. 2013. Simulating Nonlinear Nano-to-Micro Scaled Material Properties and Effects at the Architectural Scale. Proceedings of SIMAUD 2013. San Diego, CA.

Session 2: Role of Simulation in Design (Part 2) **15**

Parametric Spatial Models for Energy Analysis in the Early Design Stages 17
Wassim Jabi
Welsh School of Architecture, Cardiff University.

Simulation Supported Precedent Analysis: Disclosing the Sustainable Attributes of Vernacular Structures in the Southern U.S. 25
Tim Frank
Mississippi State University.

Parametric Spatial Models for Energy Analysis in the Early Design Stages

Wassim Jabi

Welsh School of Architecture
Cardiff University
Cardiff, United Kingdom, CF10 3NB
jabiw@cardiff.ac.uk

Keywords: Spatial Models, Energy Analysis, Parametric Design, Thermal Simulation, Non-manifold Geometry.

Abstract

Much of the research into integrating performance analysis in the design process has focused on the use of Building Information Modeling (BIM) as input for analysis engines. The main disadvantage of this approach is that BIM models are resource intensive and thus are usually developed in the later stages of design. BIM models are also not necessarily compatible with energy analysis engines and thus a conversion and export process is needed. This can lead to data loss, calculation errors, and failures.

Starting with the premise that energy analysis is more compatible with earlier design stages where simpler schematic models are the norm, this paper presents a software system that integrates non-manifold spatial topology, a parametric design environment and an energy analysis engine for a more seamless generate-test cycle in the early design stages. The paper includes a description of the system architecture, initial results, and an outline of future work.

1. INTRODUCTION

The noted architect Steven Holl has written, "While artists work from the real to the abstract, architects must work from the abstract to the real" (Holl 2013). Underpinning this quote is the notion that architects invariably begin their design process with representations that are not merely simpler models of what they would construct in later stages, but ones that are abstracted to encompass only the ideas, concepts, and information necessary to move the design process forward. As the design process unfolds, architects create models that more closely correspond to the real project. They also then start to analyse the implications of their design decisions and simulate performance aspects of their project. Unfortunately, most of these analyses happen later in the design process when design modification may not be feasible or be very costly. In many cases, the analysis (e.g., thermal and daylight analysis) is conducted to measure compliance with external regulations or to satisfy the client regarding the performance of the project rather than to fundamentally reflect on the parameters of the design (Mhadavi et al. 2003). Many researchers, architects, and clients wish to have that analysis done earlier in the design process so that they discover and avoid problems earlier and create a more considered design solution (Brahme et al. 2001). Unsurprisingly, the difficulty with conducting performance analysis in the early design stage stems mainly from the lack of appropriate representations and information. Current performance analysis software such as daylighting requires detailed inputs of materials and constructions that are simply not available during the early design stages.

While architects create several types of analogue and digital representations and conduct several types of analyses, the focus in this paper is on spatial digital representations and models of their work and the role of energy analysis in the early stages of design. The aim of this research project is to more closely harmonise the outputs of parametric digital spatial representations with the input requirements for building performance simulation. The goal is to better integrate energy analysis in the design process and thus improve the overall outcome of design.

DSOS is software that was developed by the author to analyse the energy use of a parametrically designed building using Autodesk DesignScript and the U.S. Department of Energy (DOE) EnergyPlus software through the use of the

OpenStudio Software Development Kit (SDK). EnergyPlus is a whole building energy simulation program that allows building professionals and researchers to better understand the performance of the simulated building and optimise its design to use less energy and resources (Crawley et al. 2000). It was chosen over other tools such as ECOTECT due to the fact that it is an industry standard and offers a robust API that is easy to work with. Additionally, EnergyPlus is being incorporated in cloud-based solutions that promise to vastly increase processing speed. However, additional analysis engines should be considered in the future. OpenStudio is a collection of software tools developed by the U.S. National Renewable Energy Laboratory (NREL) to support whole building energy modelling using EnergyPlus and advanced daylight analysis using Radiance (Guglielmetti et al. 2011). OpenStudio is an open source project to facilitate community development, extension, and private sector adoption. OpenStudio includes graphical interfaces along with an SDK. The DSOS plugin exposes many of these services in scripts, handling most of the process of sorting, labelling, and otherwise abstracting a model into OpenStudio's specifications. To generate an analysis, a scriptwriter simply needs to specify the building's location through a weather file, specify which days and conditions to simulate, its general program (architectural use), and a spatial representation of the form. Once the simulation is complete, the results are displayed in the parametric design environment. This workflow allows the users to iterate parametrically through multiple design alternatives and even display a matrix of alternatives side-by-side for comparative analysis without the need to export to different software packages and use file formats that may lose information in the process.

2. MODELS FOR ENERGY SIMULATION

While daylight simulations are most accurate when models closely represent reality in detail and material (Ibara and Reinhold 2009), energy analysis software such as EnergyPlus requires input models to consist of infinitesimally thin surfaces that represent walls or partitions between thermal zones. This has presented a problem for the simulation of models built within Building Information Modeling (BIM) environments. BIM models strive to include all details needed to construct and manage a building (Figure 1). Yet, energy simulation requires a simplified and abstracted version of that model. As Jackubiec and Reinhart report, this has divided the building simulation community because while BIM strives for a single model, there are advantages of using hybrid models that combine several models for several types of analyses (Jackubeic and Reinhart 2011).

Figure 1. A typical *mature* BIM model from industry.

Interestingly, architects and designers generally use these types of 'sketch models' in the early stages of design (Granadeiro 2012). Architects frequently think of their design projects to be made out of spaces that are enclosed by boundaries that have yet to acquire thickness and materiality (Figure 2). They place these spaces intuitively and visually in proportion to each other without much attention to tectonic detail (Jabi 1998). This conceptual or idealised approach allows designers to "build the lightest possible model using the least effort that gives the most accurate feedback about their design …" (Aish and Pratap 2013).

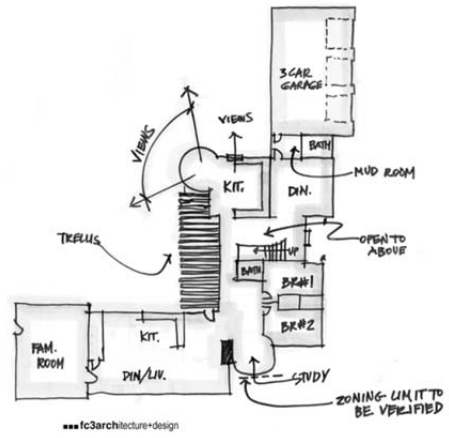

Figure 2. A typical architect's sketch from the early design stages. Image courtesy of fc3 architecture+design.

If architects and designers sketch and build idealised analogue spatial models that can be a good fit with energy simulation, the question then becomes: do they do the same when building digital models? Sadly, in most cases the answer is no. One example is the use of SketchUp as a generator of models for energy analysis. SketchUp is one of

the most popular tools used in the early stages of design. Its power stems from the fact that it allows users to quickly build schematic massing models that can be easily modified. Indeed, NREL's OpenStudio heavily depends on SketchUp (through their own plugin) to create input geometry for EnergyPlus analysis (Figure 3). Unfortunately, SketchUp suffers from two main shortcomings in the context of energy analysis. The first shortcoming is that SketchUp is not truly a parametric system. Thus, changes need to be made manually and are thus time consuming. The second shortcoming is that models created in SketchUp are not necessarily compatible with the zero-thickness requirements for energy analysis. This means that manual work needs to be undertaken to convert any existing geometry to a set of conceptual masses that represent thermal zones. A more ideal workflow in SketchUp is to create idealised conceptual masses from the start so that the resulting models are compatible with the input requirements of EnergyPlus. Even then, modelling errors in SketchUp can lead to failures in energy simulation. The main issue is that SketchUp cannot guarantee that surfaces that belong to different spaces exactly match and that the constructions on these surfaces also match (i.e. are mirror reflections of each other) as required by EnergyPlus.

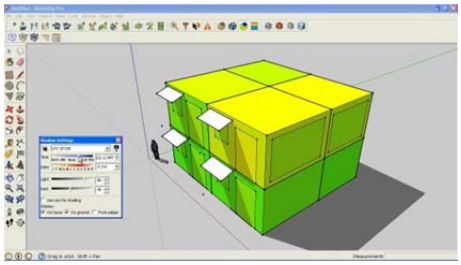

Figure 3. An example of a *shoebox* model. Image courtesy of NREL.

These problems point to the fact that the problems associated with input models for energy analysis have yet to be solved. The current workaround has been to either abstract more complex models, as is the case with BIM models that are far too detailed for energy analysis, or to try to automatically convert general massing models into spatially and topologically inter-connected models that are suited for energy simulation. The third prevalent alternative is to build extremely simple shoebox models in order to understand the effects of design decisions at the most basic level. While these approaches are routinely used, they are not ideal solutions. There is a need for a new way of thinking about and building models in the early design stages.

3. PARAMETRIC DESIGN SPACE EXPLORATION

Another important aspect of work in the early design stages is that of design space exploration. As the project progresses, the design space of possible solutions is not merely expanded and populated with more alternatives. Previous analysis of artefacts produced during the early design stages by individuals found that artefacts share two dichotomous characteristics: divergence and convergence (Jabi 1996). While providing divergence by broadening the design space under exploration, the depiction of multiple alternatives also leads to the elimination of undesirable solutions and, through progressive refinement, to convergence on satisfactory ones. Interesting artefacts were drawn with more detail and level of craft while uninteresting artefacts were quickly abandoned in an incomplete state. One could almost retrace the design process by examining and comparing the resulting artefacts. The work of Woodbury and Burrow asserts that computers and parametric design systems are particularly suited for this exploration: "Design space exploration is the idea that computers can be used to help designers by representing many designs, arraying them in a network structure (the space part), and by assisting designers to make new designs and to move amongst previously discovered designs in the network (the exploration part)" (Woodbury and Burrow 2006). The ability to explore the design space depends heavily on the ability of the software to quickly vary the parameters of the design (i.e. parametric design) and generate potential design solution candidates (i.e. generative design). Judging by the proliferation of papers in conferences and seductive student work in progressive schools of architecture, parametric and generative design systems, such as Grasshopper, have become the most popular digital tools for the exploration of design alternatives (Figure 4). Despite the existence of plugins that link Grasshopper to energy simulation (e.g. Gerilla and Geco), the majority of these explorations remain in the realm of geometric form finding where variations in the design are not usually tested or compared from a performance aspect.

The problem of reaching an optimal solution by carefully conducting a multi-variate parametric analysis of *relevant* parameters—as opposed to focusing exclusively on aesthetic and formal parameters—remains a vexing

problem. Some researchers have made progress by using evolutionary heuristic methods to quickly evolve and search the solution space for a set of potentially optimal candidates (Figure 5). For example, Gerber and Lin have researched and integrated computational strategy using genetic algorithms to "expand the solution space of a design problem as well as presort and qualify candidate designs." Their approach avoids the pitfall of attempting to find *the perfect* solution: "… What is not afforded nor necessarily expected is the solving for a single optimal result … the experiment is still inclusive of designer-driven choice, where the [chosen alternatives] exhibit some improved scoring, they are not necessarily the aggregate best scores as form and implicit architectural constraints come into play and become major factors for consideration in the design decision making."

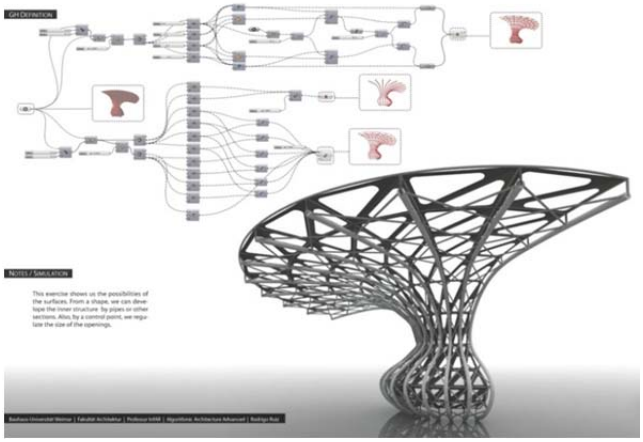

Figure 4. A typical exploration of architectural form using Grasshopper. Image courtesy of Rodrigo Ruiz.

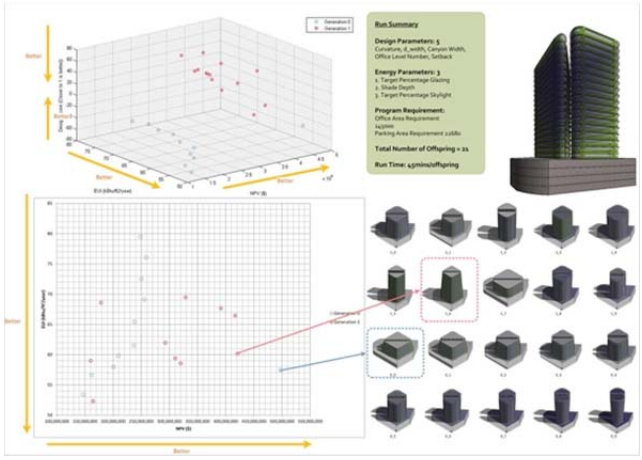

Figure 5. Multi-variate parametric design space exploration. Image courtesy of Dr. David Gerber, USC School of Architecture.

Combining rapid design alternative generation with evolutionary heuristic methods can enable complex geometries to be better understood beyond their aesthetics and significantly strengthen the relationship between geometry and performance (Gerber and Lin 2012).

4. INTEGRATING NON-MANIFOLD TOPOLOGY, PARAMETRIC DESIGN AND ENERGY ANALYSIS

As stated earlier, the aim of this research is to integrate parametric systems and performance analysis engines. We envisage a seamless generate-test cycle that will ultimately be conducted in real-time and is invisible to the user (Figure 6). Such a cycle would avoid the drawbacks of file import and export and data loss due to subtle incompatibilities. This research project seeks to find out spatial representations and parametric digital workflows that are suitable for early design stages as well as energy simulation. The research starts with two premises based on the work of (Aish and Pratap 2013). The first premise is that a non-manifold topology, as explained below, satisfies the requirement for conceptual design as well as energy analysis. The second premise is that integrating a generative/parametric scripting environment with an energy simulation engine can help the designer make better decisions in the early design stages.

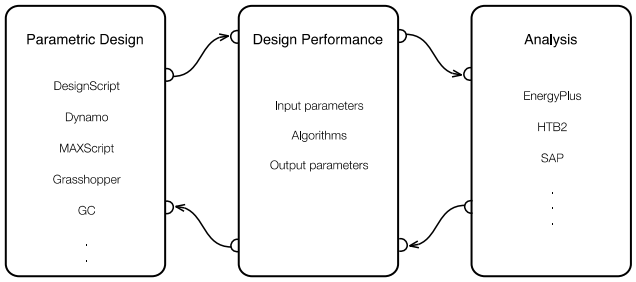

Figure 6. The design-analyse cycle.

4.1. Manifold and Non-Manifold Topology

While it is beyond the scope of this paper to delve into the mathematics of manifold topology, for the purposes of this paper one can think of three-dimensional manifold geometries with boundaries to be polyhedral solids such as cuboids. In manifold polyhedral geometries, each surface separates the interior solid condition of the object from the exterior world. Each edge is shared by exactly two surfaces of the solid. All surfaces form the outer boundary of the solid such that it is said to be *watertight*. These guaranteed attributes allow 3D software to easily operate on such geometry (e.g. calculating surface area, volume and

centroid, and intersecting the solid with other solids). Non-manifold geometry is also made of surfaces, edges, and vertices. However, edges can be shared by more than two surfaces (Figure 7). Furthermore, surfaces can either be a boundary between the solid interior of the object and the exterior world or between two spatial *cells* within the object. The implementation of non-manifold topology within DesignScript allows the scriptwriter to create regular polyhedral geometries at the start and then boolean them with other geometries using a non-regular (i.e. non-manifold) operation that maintains the interior surfaces that would have been otherwise lost (Aish and Pratap 2013). The implementation also allows the scriptwriter to slice a manifold geometry using a series of planes in order to create a non-manifold geometry with cells and surfaces. The scriptwriter can then query the non-manifold geometry for its vertices, its edges, its surfaces, and its cells. Methods within the non-manifold class return useful information, such as the cells at each side of a surface or whether the surface is a boundary between the inside and the outside of the object.

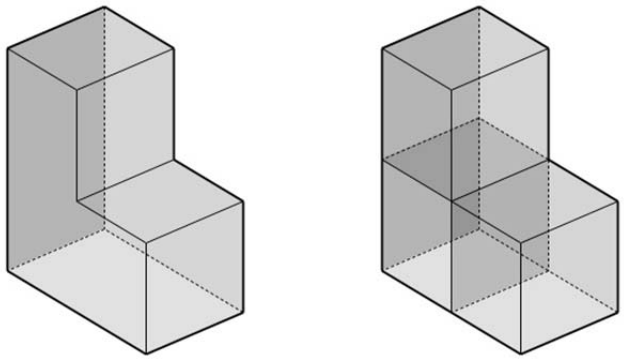

Figure 7. (Left) A manifold polyhedral geometry; (Right) a non-mainfold geometry.

4.2. The DSOS System Architecture

The DSOS software architecture is composed of a dynamically linked library (.dll) written in C# and a set of scripts using DesignScript which in turn runs as a plugin within the AutoCAD environment (Figure 8). In order to use the DSOS plugin, one must first install AutoCAD, the DesignScript software, EnergyPlus, and the DSOS files. DSOS provides the needed OpenStudio .dll files. The DSOS plugin generates files that are fully compatible with OpenStudio and EnergyPlus. Thus, a user can optionally install the OpenStudio graphical user interface software to further investigate the generated models or use other software that can read EnergyPlus file formats.

The DSOS system architecture is composed of the following files and parameters:

1) ***dsos.dll***. This is a dynamically linked library that provides the *dsos.Utility* object. This object provides the main functionality (methods and attributes) for specifying an OpenStudio model. For example, the *dsos.Utility* object can create the main abstract model, the building, the building storeys, the spaces and thermal zones, and save the model in preparation for EnergyPlus analysis.

2) ***DSProtoGeometry.dll***. This is a special version of the DesignScript ProtoGeometry library. In order to avoid naming conflicts with OpenStudio, this library prefixes all DesignScript geometries with the letters "DS" (e.g. DSCuboid instead of Cuboid). This is a temporary workaround. Autodesk is working to resolve this issue so that DSOS scriptwriters can revert to using the regular ProtoGeometry.dll file.

3) ***OpenStudio.dll***. This is the NREL OpenStudio suite of linked libraries.

4) ***EPW file***. This is the standard EnergyPlus Weather data file. This file describes the weather data for a specific geographic location.

5) ***DDY file***. This is the ASHRAE Design Conditions Design Day Data file. These files specify the *design days* and their conditions that EnergyPlus uses to run its simulation.

6) ***OSM file***. This is the NREL OpenStudio Template File. This file provides a minimal template for a particular building type. NREL provides several templates. A template usually contains default construction sets and schedule sets, but no geometry.

7) ***Initialise.ds***. This script imports the required classes for DSOS to function properly. It initialises certain parameters with default values that can be changed by the user.

8) ***Building.ds***. This script can be named by the user and is where the user constructs a parametric building using a non-manifold topology.

9) ***Analyse.ds***. This script loads the building from the previous scripts, conducts the analysis and displays the results.

10) ***Building.osm***. This is the OpenStudio model generated by the DSOS software. It serves as the input to the analysis cycle.

11) ***eplusout.sql***. This is the standard SQL database file generated by EnergyPlus. This file gets read back into the software and can be queried using the standard SQL format.

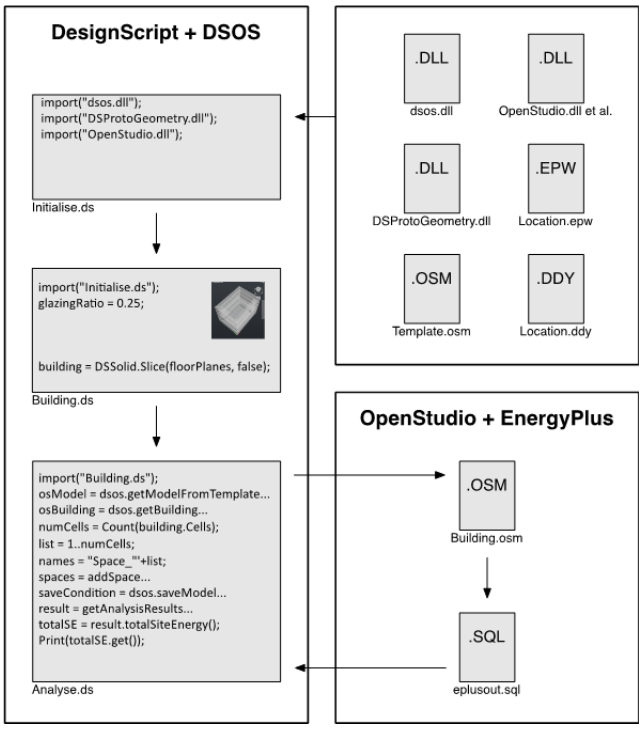

Figure 8. The DSOS system architecture.

4.3. The DSOS Workflow

The DSOS Workflow is quite simple. The user structures their design scripts by modifying default scripts organised in three stages (e.g. *Initialise.ds*, *Building.ds*, *Analyse.ds*). The initialisation script usually remains as is with only a change to some path names depending on the installation. The second file is where the user can generate any parametric non-manifold geometry they wish. This geometry can be derived from the parametric process at any time. The only three requirements for that script are: 1) Define a global variable called `building` to store the resulting non-manifold geometry of the building. 2) Define a global variable called `numFloors` with a value greater than 1 that represents the number of floors (stories) in the building. 3) Define a global variable called `glazingRatio` that represents the ratio of glazing to exterior wall surfaces.

Within the analysis script a user can request that the analysis is conducted and then construct an SQL query to retrieve any results from the EnergyPlus analysis. These results can then be visually displayed to the user or used to further investigate and modify the design.

The usual steps to build a parametric model and visualise analysis results consist of the following steps:

1) Import the Initialise.ds file:

```
import("C:\dsos\Scripts\Initialise.ds");
```

2) Define the required parameters for the building. The script assumes the dimensions of the building are in metres and the temperatures in degrees Celsius. The glazing ratio applies to each exterior wall surface individually.

```
buildingWidth  = 40;
buildingLength = 30;
buildingHeight = 15;
numFloors = 5;
glazingRatio = 0.5;
```

3) Generate a non-manifold geometry (to be called building). Each cell in the non-manifold geometry translates into a space in the OpenStudio model and has its own thermal zone. Each horizontal slice of the geometry will translate into an OpenStudio Building Storey.

4) Create an Analyse.ds script (starting from the given default file) that imports the previous script:

```
import("C:\dsos\Scripts\MyBuilding.ds");
```

5) Get the OpenStudio Model from the template:

```
osModel =
dsos.getModelFromTemplate(templatePath,
EPWPath, DDYPath);
```

6) Get the OpenStudio Building from the osModel:

```
osBuilding = dsos.getBuilding(osModel,
buildingName, buildingType, buildingHeight,
numFloors, spaceType);
```

7) Create a space for each cell in the non-manifold geometry:

```
numCells = Count(building.Cells);
list = 1..numCells;
names = "Space_" + list;
spaces = addSpace(building.Cells, names,
osModel, WCS.ZAxis);
```

8) Save the model and run the analysis:

```
saveCondition = dsos.saveModel(osModel,
outputPath);
result = getAnalysisResults(logPath,
outputPath, EPWPath, outDirPath);
totalSE = result.totalSiteEnergy();
Print("Total Site Energy use:
"+totalSE.get());
```

The scriptwriter can then experiment with retrieving and displaying different energy simulation results. Further information regarding NREL's sqlFile object specification can be found at: `http://goo.gl/jfnKtq`

5. INITIAL RESULTS

This paper reports on initial results from test runs of the software where some analysis results such as peak temperatures for cooling loads were translated into colours and assigned to the respective spaces in the model (Figure 9).

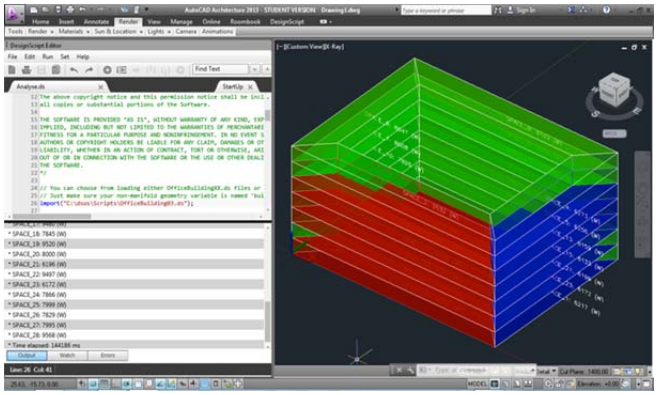

Figure 9. The DSOS graphical user interface.

The resulting geometry is overlaid with the original parametric model. These results should not be considered indicative of the full extent of the capabilities of the software. For example, the parametric software can create geometry of any degree of complexity and is not limited to orthogonal structures (Figure 10). Multiple parametric studies can also be conducted and presented to the user in a matrix, or browsed through. The results indicate that using non-manifold topology is a powerful representation of both parametric spatial constructs and input models for energy analysis. The tight integration of parametric design system and an energy analysis engine created a reasonably seamless experience and, more importantly, avoided the pitfalls of file export and import. By being mostly script-based, DSOS can be considered an open platform for scriptwriters to develop their own spatial parametric constructs and analysis scenarios.

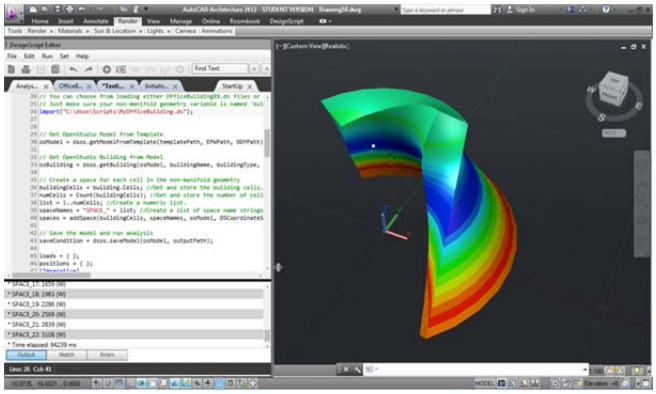

Figure 10. Parametric modeling and analysis of non-orthogonal building.

6. FUTURE WORK

The DSOS software is under active development. One of the main obstacles to overcome is the amount of time it takes EnergyPlus to complete its analysis. A possible solution is to integrate distributed high performance computing (HPC) with DSOS. We are pursuing that solution with our university's HPC centre as well as investigating NREL's new initiative to offer OpenStudio as server software on Amazon's Elastic Compute Cloud (EC2). In doing so, we will thrive to maintain a seamless generate-test cycle. Another option would be to use HPC to generate a vast array of possible candidates, similar to (Gerber and Lin 2012), and invent user-friendly ways to visualise, explore and select optimal pre-analysed solutions. The current implementation of non-manifold topology in DesignScript does not allow for the specification of sub-surfaces (e.g., glazing subsurfaces). In DSOS, we opted to use a glazing ratio as a temporary substitute for a more accurate representation of glazing surfaces. While it is not impossible to add the ability to model glazing surfaces in DSOS itself, it would be preferable if the non-manifold topology itself were extended to handle subsurfaces. Finally, we intend to offer DSOS on as many platforms as possible. To that end, we are currently developing a version that will run within Autodesk's 3ds Max since it too can create and represent non-manifold geometries. We are also planning support for Autodesk's Vasari and Revit if and when Autodesk incorporates non-manifold geometry into DesignScript and/or Dynamo for these platforms. Finally, we are keenly interested in verifying the software against industry standard case studies to find out if energy analysis in the early design stages using idealised spatial models is

comparable in accuracy to analysis conducted using more complex and mature BIM models. The comparison to real world case studies is always of interest, but we are cognisant that even the most sophisticated energy analysis results are far from their real-world values. Because this software is intended for the early stages of design, we are less interested in exact measures and more interested in trend analysis based on parametric variation.

7. CONCLUSION

This paper provided an alternative approach to the integration of energy analysis in the design process. Rather than rely on file export and import of BIM models and their associated pitfalls, energy analysis can be conducted much earlier in the design cycle using far simpler and more idealised models. We presented the DSOS software that integrated the use of non-manifold topology, a parametric design system, and an energy analysis engine for use in the early design stages. The results of this software can be visualised using user-friendly methods to investigate trends rather than focus on precise values. We believe this is an appropriate approach for designers and architects in the early design stages where complete building information is not available and precise numeric information is not needed. Since analysis data is present in the software as it is running, it can be both visualised and used to affect the parameters of the design. Although DSOS is in its initial development stages, initial results indicate that energy analysis in the early design stages is possible and can raise awareness of the energy implications of early design decisions.

Acknowledgements

This research would not have been possible without the contribution of Dr. Robert Aish, who suggested I research non-manifold geometries and helped me develop my ideas. I am also grateful for the invaluable help of Daniel Macumber and the whole OpenStudio team at NREL. I would also like to thank Prof. Ian Knight, Simon Lannon, and Enrico Crobu at the Welsh School of Architecture for their insights and help in developing the ideas behind this paper.

References

AISH, R. AND PRATAP, A. 2013. Spatial Information Modeling of Buildings Using Non-Manifold Topology with ASM and DesignScript. Advances in Architectural Geometry 2012. 25-36.

BRAHME, R. ET AL. 2003. Complex Building Performance Analysis in Early Stages of Design. Seventh International IBPSA Conference, Rio de Janeiro, Brazil, August 13-15, 2001. 661-668.

CRAWLEY, D. ET AL. 2000. EnergyPlus: Energy Simulation Program. ASHRAE Journal Online. Vol. 42, No. 4, April 2000. 49-56.

GERBER, D., LIN, S. 2012. Synthesizing Design Performance: An evolutionary approach to multidisciplinary design search. 32nd Annual Conference of the Association for Computer Aided Design in Architecture (ACADIA), San Francisco 18-21 October 2012. 67-75.

GRANADEIRO, V., ET AL. 2013. Building Envelope Shape Design in Early Stages of the Design Process: Integrating architectural design systems and energy simulation. Automation in Construction 32 (2013). 196–209.

GUGLIELMETTI, R., MACUMBER, D. AND LONG, N. 2011. OpenStudio: An Open Source Integrated Analysis Platform. Twelfth International IBPSA Conference, Sydney, Australia, November 14-16, 2011. 442-449.

HOLL, S. 2013. What is Architecture? (Art?). The Brooklyn Rail: Critical Perspectives on Arts, Politics, and Culture. September 2013. Available at: http://www.brooklynrail.org/2013/09/criticspage/what-is-architecture-art. (Accessed on 8 November 2013).

IBARRA, D. AND REINHART, C. 2009. Daylight Factor Simulations – How Close Do Simulation Beginners 'Really' Get?. Eleventh International IBPSA Conference, Glasgow, Scotland, July 27-30, 2009. 196-203.

JABI, W. 1996. An Outline of the Requirements for a Computer-Supported Collaborative Design System. Open House International 21/1 (March 1996). 22-30.

JABI, W. 1998. The Role of Artifacts in Collaborative Design. Proceedings of the Third Conference on Computer-Aided Architectural Design Research in Asia, Osaka, Japan: CAADRIA, Department of Architecture and Civil Engineering, Kumamoto University, 1998. 271-280.

JACKUBEIC, J.A. AND REINHART, C. 2011. Diva 2.0: Integrating Daylight And Thermal Simulations Using Rhinoceros 3d, Daysim And EnergyPlus. Twelfth International IBPSA Conference, Sydney, Australia, November 14-16, 2011. 2202-2209.

MAHDAVI, A. ET AL. 2003. An Inquiry into The Building Performance Simulation Tools Usage By Architects in Austria. Eighth International IBPSA Conference, Eindhoven, Netherlands, August 11-14, 2003. 777-784.

NAGHMI I.S. ET AL. 2011. Design Space Exploration in Parametric Systems: Analyzing effects of goal specificity and method specificity on design solutions. ACM Creativity & Cognition, Atlanta, Georgia, November 3-6, 2011. 249-258.

WOODBURY, R. AND BURROW, A. 2006. Whither Design Space? AIE EDAM: Artificial Intelligence for Engineering Design, Analysis, and Manufacturing, Vol. 20, No. 02, May 2006. 63-82.

Simulation Supported Precedent Analysis: Disclosing the Sustainable Attributes of Vernacular Structures in the Southern U.S.

Tim Frank

Mississippi State University
899 Collegeview St., 240 Giles Hall
Mississippi State, MS 39762
tfrank@caad.msstate.edu

Keywords: Vernacular Structures, Performance Analysis, Multi-domain Testing, Result Corroboration | Reciprocation

Abstract

Environmental case study analysis has long served the design profession in describing complex building behavior, putting architectural design strategies to task in order to offset the need for supplemental high-grade energy systems. Knowledge of these strategies becomes crucial for designers practicing in the Southern United States, a region that demands effective low-cost strategies that perform well within a fully humid climate marked by distinct variations. However, traditional case study methods rely heavily upon methods of approximation, basing results on commonly held assumptions with little regard for the particular characteristics of place, people, and purpose that animate building performance. Rather than relying upon rule-of-thumb conjecture, low-resolution simulation platforms offer a highly interactive and diverse toolset to designers, facilitating testing sequences which acutely disclose how a range of geometric building configurations intensively shape the behavior of light, heat, and airflow present within the extensive environment. This paper explores the role of building simulation tools in the analysis of Southern vernacular structures, with emphasis on the tool's capacity to support heuristic procedures. Through multi-domain functionality, these tools enable iterative analysis across numerous time frames, producing and advancing crucial knowledge about the performance of vernacular building attributes. The findings from simulation supported precedent analysis underscore this role, expanding upon the inventory of passive architectural devices highlighted by James Marston Fitch to include permeable enclosures, centralized wind chambers, and narrow floor plates (Fitch, 1961).

1. INTRODUCTION

Today's performance modeling platforms provide the opportunity for architects to embrace environmental challenges with a first-principles approach toward design innovation, developing a practice that advances the reintegration of classical building design concerns including firmness, utility, and delight (Lam, 2012). These platforms retract our over-reliance on mechanical systems, favoring instead passive design strategies that attune the physical enclosure to the unique characteristics of local micro-climates. Designers can now systematically evaluate the consequences of design decision-making due to the inextricable linkage that performance modeling platforms provide between the building's physical constituents and the natural environment. Within the spectrum of performance modeling platforms, low-resolution simulation tools are those that provide a highly interactive graphic user interface and are appropriate for use during early design stages. Due to the wide ranging analysis options provided by low-resolution tools, they are well suited for use by non-experts who seek to examine the various parameters that characterize high performance building attributes.

While many low-resolution building simulation tools offer well-designed graphical user interfaces, they need to be carefully vetted since their target audience operates these systems at an entry level with limited domain knowledge. One of the well documented disadvantages of using low-resolution performance modeling programs is their lack of reliability due to the limited nature of their simulation engines (Attia, 2011). Even though weaknesses and gaps in tool reliability are clear, experts in the field of building simulation are calling for improved integration of low-resolution performance modeling platforms within all

phases of the design process (Augenbroe, 2003). In order to circumvent the limitations of low-resolution simulation engines, users of these tools can embrace the abstract nature of simulation results, using these outcomes to promote a heuristic process instead of attempting to predict the performance of lone solutions. Unlike predictive modeling, a heuristic process promotes the progressive production of localized design knowledge and supports the development of new lines of inquiry from feedback obtained in earlier stages. Countering the mentality that these performance platforms operate in a vacuum, simulation results can be used to frame questions that are further pursued through alternative means such a physical prototypes or even companion programs. Moreover, the interoperable functionality of these programs can be exploited to examine specific design attributes through a range of domain types.

This paper presents a simulation supported precedent analysis methodology that extends the promise of simulation platforms for architects who aim to disclose the operation of historical structures within complex eco-social systems. To overcome limitations in tool precision, the work leverages the usability, interoperability, and recursivity of simulation platforms to circumscribe the complex behavior of a building, gauging its effectiveness in constructing intensive environments that occupants find to be equally sound, useful, and delightful. The role of simulation in bridging the divide between an architect's intent to create passively acclimatized buildings and consequent architectural design strategies are framed through the analysis of formative buildings in the Southern United States. With each case study, architects disclose passive design strategies and associated performance outcomes prevalent within the region; a region that demands affordable construction strategies that effectively operate within a fully humid climate demarcated by distinct variations.

2. OUTLINE: CURRENT ANALYSIS TECHNIQUES

2.1. Architectural Precedent Analysis

Architectural precedent analysis refers to the study of existing buildings to uncover strategies of form, space, order, and structure. The exercise aims to identify archetypal patterns of form and space, highlighting underlying geometric shifts and continuities across distinct periods in the architectural tradition (Allen, 2008). Architectural precedent analysis operates largely in diagrammatic form, whereby all content deemed irrelevant is removed except the singular trait that the author deems most relevant. By and large, because the architect's primary means to examine the built environment carries a deeply formal bias, attempts to unpack the language of historical structures tend to isolate the built environment from its natural setting. This kind of analysis within the discipline of architecture operates in a vacuum, excluding the influence of environmental, social, or material influences in the construction of built form (Clark and Pause, 2012). By placing overt emphasis upon the dimensional and compositional properties of the physical enclosure itself, it considers the building to be an inert object, standing rigid and intractable to the ever-changing social and environmental conditions which pervade any work of architecture.

2.2. Environmental Case Studies

Environmental case studies are exercises which focus on issues of energy and environment, providing for the architect a window into how architectural design strategies respond to a wide array of climatic factors such as heat, light, and airflow. These exercises are a crucial component within the discipline of architecture today because most architects have exclusively designed structures that use non-architectural means, primarily chemical and mechanical, to achieve environmental adaptation (Knowles, 1981). These exercises reconnect architects to first-principles approaches utilized prior to the introduction of active building technologies, which use high-grade energy to maintain steady interior states. Environmental case studies describe how the building design passively modulates climatic shifts to provide quality conditions for interior occupants. With the knowledge acquired in such exercises, the architect can close the gap between architectural design strategies and high performance outcomes, underscoring the notion that the most energy critical decisions are made in the schematic design phases (Thomas, 2006).

While environmental case studies are capable of highlighting formal building strategies in the context of climatic factors, they do not reside wholly in the realm of empirical inquiry. In most cases, the relationships outlined between architectural elements and environmental factors are derived via approximation methods founded on basic assumptions (Brown and DeKay, 2001). Therefore, traditional case study methods are more descriptive and less exploratory, relying on projective techniques to generate

outcomes based upon absolute principles with little to no regard for the particular characteristics of place, people, and purpose that animate a building's performance. With the introduction of computer simulation in the environmental case study process, one is able to conduct heuristic practices that measure the fine-grain operation of a building within differentiated situations through procedures such as testing, experimentation, and re-evaluation.

One such example is the analysis of Mies van der Rohe's Courtyard Houses at the 6th International Space Syntax Symposium (Choudhary et al., 2007) whereby building simulation tools are used to test a series of Modern free-plan configurations against factors such as view and sunlight. The authors use computer simulation platforms to systematically experiment with various geometric plan configurations to ascertain how different layouts would be perceived by inhabitants. The study highlights the process of analyzing case studies using computer simulation tools to emphasize that perceived space is not solely derived by geometric factors alone. In testing a range of plan configurations, the authors advance the practice of precedent analysis, enabling feedback from the simulation platform to inform conclusions drawn. In this way, simulation can be credited for revealing the efficacy of approaches, enabling the comparison of a broader range of design variations and providing a better understanding of the consequences of design decisions (Augenbroe, 2001).

This study challenges the approximation methods found in traditional environmental case studies. Rather than rely upon rule-of-thumb conjecture, simulation platforms enable one to challenge assumptions about how a building behaves relative to its ever-changing context. These platforms allow unique geometric configurations to be placed within the flow field of a specific context, increasing our capacity to visualize and measure a variety of architectural strategies that intensively shape the behavior of light, temperature, and airflow present within the extensive environment.

3. SIMULATION SUPPORTED PRECEDENT ANALYSIS

3.1. Exercise Overview

The intent of simulation supported precedent analysis is to deliver a behavioral building modeling platform capable of "sketching-out" a building's heterogeneous environmental design system. Introducing simulation tools into the precedent analysis workflow is based on the need to establish a parametric relationship between a building's form and its immediate environment. This method combines multiple domains including light, thermo-dynamics, and air-dynamics in a shared simulation environment; animating each domain across multiple temporal and spatial scales. A model domain is comprised of mathematical boundaries representing the building configuration, variable input states, and related calculations of environmental behavior across a defined area of investigation. Variations to the domain model systematically introduced by the user foregrounds this crucial link between building form and environmental factors. Yet, one of the immediate challenges that this paper addresses involves the modeling of complex environmental systems with low-resolution computer programs that are better suited toward abstraction, not exact concretization. How can one acutely disclose the complex totality of any building system, constituted by numerous domains across an array of time frames, with such low-resolution simulation programs?

The principal requirement for using computer simulation tools when analyzing precedents is to instill accountability, as one cannot assume that the non-expert user will use the tool correctly. We should remember that for the initial user, these tools are essentially a 'black box' whereby the mathematical methods used to model real-world complexity remains a mystery to the non-expert (Augenbroe, 2003). Therefore, the proposed methodology approaches the use of simulation as a way to understand the character of building behavior in lieu of using simulation to predict singular optimizations.

3.2. Exercise Constituents

Simulation supported precedent analysis is comprised of four main constituents: computational modeling, multi-domain simulation, output corroboration, and parametric analysis. The base platforms used to carry out the analysis are McNeel® Rhinoceros™ and Autodesk® Ecotect Analysis™, with plug-in components such as Desktop Radiance and WinAir4 used to expand the domain range of the basic platform.

McNeel® Rhinoceros™ is a NURBS (non-uniform rational B-spline) based geometric modeling program developed by Robert McNeel & Associates favored for its concise scripting language and its ease in translation across primary geometric elements. Autodesk® Ecotect Analysis™

is an environmental analysis tool developed by Andrew Marsh & Square One Research preferred for its user-friendly interface and ease of interactivity during multi-domain analysis stages. Desktop Radiance is ray-tracing simulation software written by Greg Ward at Lawrence Berkeley Laboratories used to compute interior spectral radiance and irradiance values used for its advanced and comprehensive daylighting analysis. Using boundary conditions exported from the base Ecotect modeling platform, WinAir4 is a plug-in component used to perform computational fluid dynamics analysis on building geometry.

3.3. Exercise Methodology

The initial step in the simulation supported precedent analysis workflow involves the digital reconstruction of each historical structure to be studied using McNeel's® Rhinoceros™ 3D geometrical modeling software. Background bitmaps representing the historical structure are scaled and located within the NURBS modeling workspace, serving to generate the geometric armature of the reconstruction. Boundary conditions are modeled using NURB surfaces whose directional normals are coordinated according to the space being analyzed. Layer control dialogs are used to organize boundary surfaces by material assembly. They are then converted to polygonal mesh objects whose resolution and subsequent triangulation can be set within the conversion process.

Once the polygonal mesh boundaries are imported into the Ecotect Analysis workspace, they are systematically exposed to external factors such as changing light, heat, and airflow patterns culled from weather data sourced from the nearest gathering location. The ability to conduct multiple domain simulations using the Ecotect Analysis platform enables the architect to circumscribe the building's performance, examining its response to multiple environmental factors. Conducting integrated thermal, ventilation, and lighting calculations on singular attributes enables the architect to visualize how such attributes begin to achieve a level of polyvalence necessary for passive climatization and energy efficiency. Additionally, Ecotect offers the ability to simulate different sub-domains within the same workspace, providing the capability to look at multiple characteristics of environmental effects such as light.

Simulating multiple domains within the same model also provides the opportunity to instill reciprocity protocols within the reiterative process. Using highly interoperable simulation platforms enables the system to attune itself, whereby one domain branch can reinforce or critically examine the relative reliability of another. Instead of relying heavily upon high-resolution simulation engines to corroborate results, the non-expert user can compare and contrast the output from within the integrated system. Further extending its interoperable functionality, models can also be exchanged between the native Ecotect platform and outside sub-domain simulation engines like Desktop Radiance and WinAir4. By expanding the functional network of the system to incorporate outside engines, the system increases its functionality, enabling the non-expert to hold the overall system reciprocally responsible. With such an approach, the results from the simulation engine are not accepted blindly by the non-expert, but are held accountable relative to the larger system. (Figure 1)

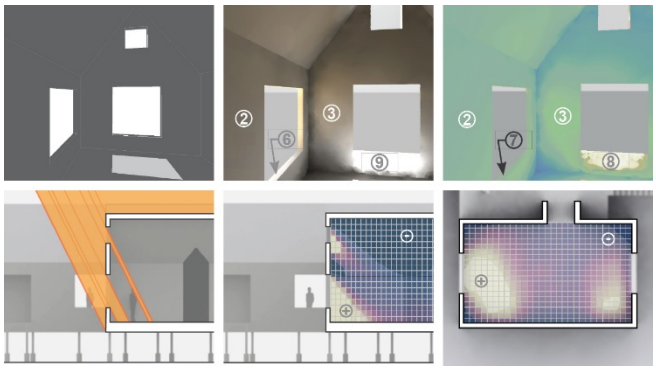

Figure 1. Multi-domain lighting simulations of the Modified Shotgun House: from left to right, the top row shows direct shading analysis, illuminance rendering and color field analysis while the bottom row shows, from left to right, solar ray tracing analysis and incident solar gain analysis in orthographic views.

As each historic structure is simulated and the results are corroborated using multiple domains during critical time frames, variations to geometric models are introduced to gain a sense of how the immediate environment changes accordingly. This 'flexing' of the model measures the inextricable linkage that is present between the physical enclosure and the behavior of the built environment itself. Parametric associations typically enable architects to survey the network of relationships that are integral to an array of architectural assemblies. The unique contribution made by simulation tools is that they expand these relationships to incorporate the locally specific environmental conditions that permeate the building itself. As a complete package

with inherent modeling, simulation, and post-processing capabilities, it is a platform that effectively supports the introduction of geometric variables that demand quick turnaround times to produce relative comparison across a range of geometric alternatives. (Figure 2)

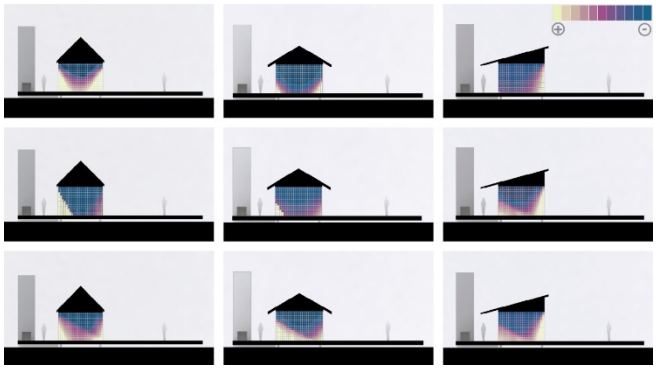

Figure 2. Flexing the parasol roof geometry of the Dogtrot House: each column represents a different parasol roof configuration. From top to bottom, each row shows the cumulative daily solar radiation levels under the roof on June 21st, March 21st and December 21st.

In leveraging the multiple domain functionality of low-resolution simulation platforms such as Ecotect, the above approach supports the exploratory nature of design research. While scientific inquiry is instrumental in its detailed calculation and quantification of environmental behavior, design research requires a holistic approach which accounts for social, environmental and material factors across various temporal and spatial scales. By focusing on geometric variability, interoperability, and multiple domain functionality, the proposed approach responds to the request by industry experts to embrace low-resolution tools as an evaluative instrument for the assessment of geometric alternatives exposed to multiple states (Hensen, 2004).

4. PRECEDENT ANALYSIS RESULTS

4.1. Southern U.S. Vernacular Building Analysis

In order to appraise the effectiveness of building simulation tools when analyzing architectural precedents, formative vernacular building types located within the Southern United States are examined to determine how systems of physical enclosure are put to task to achieve high performance outcomes. With the advantages provided by building simulation tools, architects are able to disclose passive design strategies and associated performance outcomes prevalent within the region; a region that demands affordable construction strategies that effectively perform within a fully humid climate marked by distinct seasonal and daily variations. It is a community that relies heavily upon the use of high-grade energy sources for provisions of indoor air quality, human comfort and adequate illumination within the built environment. Therefore, it is imperative for architects in this region to develop design strategies that passively modulate extremes of this hot-humid climate to create inhabitable spaces that are environmentally sustainable.

4.2. Dogtrot House

During the 19th century, the Dogtrot House emerged within the Southern United States, ranging from places such as the southern Appalachians down to the Gulf Coast. Notable examples of this building type include the James Jackson Bryan House in Webster Parish Louisiana (ca. 1840), the Noel Neal House in Arkansas (ca. 1840), and the Zachary House designed by Stephen Atkinson now located in North Carolina (ca. 1999). (Figure 3)

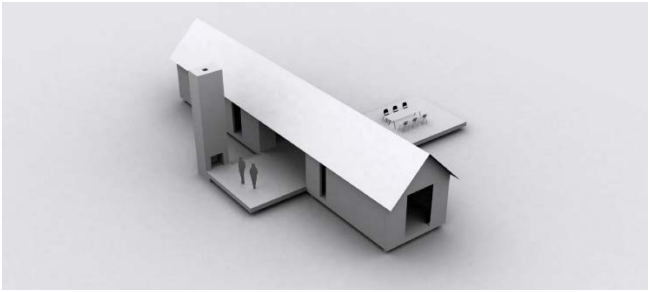

Figure 3. Zachary House, Stephen Atkinson

Surrounded by tree-lined open meadows, the Dogtrot House inflects the traditional southern cabin by dividing it into two equal units. The plan organization reflects a binuclear scheme, creating two dominant enclosed programmatic spaces connected by a central wind chamber, all of which are unified by a large parasol roof that extends beyond the footprint of the two enclosed spaces to create a deep perimeter porch. The organization of space in this precedent intelligently intertwines the way in which space is used with passive ventilation and cooling strategies, an essential characteristic of structures located within the hot and humid climate of the Southern US. And yet, these strategies do not utilize mechanical or chemical means to cool these spaces, they modulate the harsh climate through the building design itself, utilizing a series of well-crafted devices. In this example, building simulation tools disclose the inventory of building design attributes which shape the passive climatization of the structure including the central wind chamber, parasol roof and programmatic separation.

The wind chamber central to the structure carves out of the building mass an indoor-outdoor space, providing increased potential for cross ventilation in all zones of the building. Low-resolution CFD simulations and prevailing wind frequency data are used in combination to visualize the Bernoulli Effect, which increases air velocity through the central chamber, drawing air through the enclosed areas that flank the space. With the tendency of air to move from areas of high to low pressure, simulating pressure zones and flow vectors attunes the reliability of simulated velocity differentials. To further examine the parametric relationship between the rate at which air flows through the building and the configuration of physical enclosures themselves, a number of changes are enacted on the model to examine the nature of this relationship. Transformations to the model geometry include adjustments in the sizing of both the windward and leeward wind chamber apertures in order to examine the resultant rates of air change within the chamber space. (Figure 4)

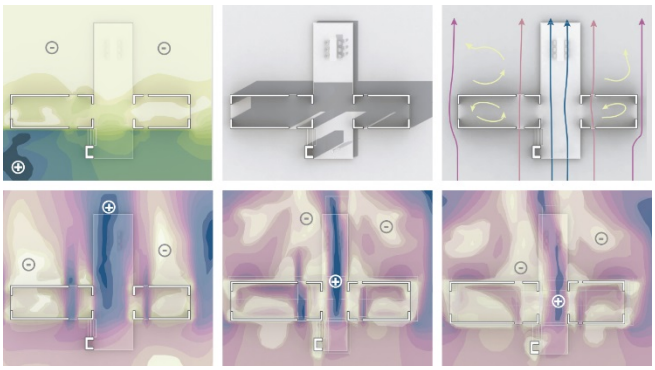

Figure 4. Flexing the central wind chamber of the Dogtrot House: from left to right, the top row shows pressure zones, shading patterns and airflow vectors while the bottom row shows changing wind velocity rates with geometric modifications.

The expansive parasol roof shields and protects all areas of the structure from strong direct sunlight in the summer and heavy seasonal rain. Polar sky dome projections, solar ray tracing and moisture frequency data are used to examine how the roof plane protects inhabitable areas of the house during numerous storm events and during cloud-free days in the summer. Changes are introduced to the roof's area of coverage and geometry to examine how the roof plane responds continuously to the most severe climatic events such as tropical storms and also low sun angles during extreme heat days, both of which are modeled using a ray tracing analysis tool. (Figure 5)

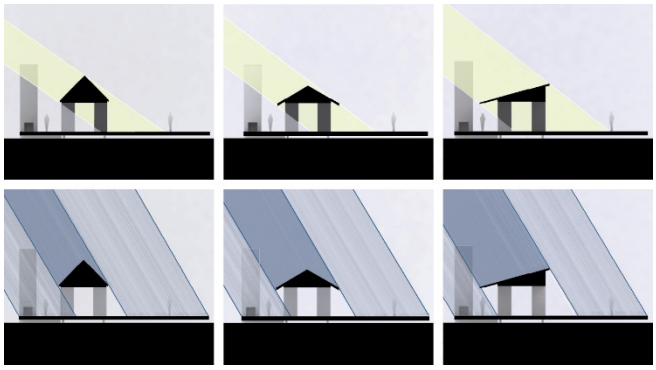

Figure 5. Varying the parasol roof of the Dogtrot House: each column shows a different roof geometry and coverage level. The top row shows shadow patterns at noon on December 21st and the bottom row shows wind-driven rain from a prevailing storm direction.

The binuclear organization of space separates the program into halves, one for the serving areas of the program which generate a considerable source of internal heat gain and the served areas of the program which require a considerable amount of cooling during hot and humid seasons. Thermal analysis focusing on internal heat gains and heat transfer are conducted to study the impact of internal heat sources on the overall comfort of those occupying adjacent spaces. Adjustments in the location of heating elements within the plan organization examine how heat gains are mitigated to minimize transfer into adjacent spaces and evacuated through cross ventilation strategies.

4.3. Modified Shotgun House

Following Hurricane Katrina in 2005, towns along the Gulf Coast such as Biloxi, Mississippi began rebuilding using sustainable building techniques which were mindful of the need to conserve energy use while minimizing operational costs for its owners. One such strategy employed by a number of architects rebuilding within the area was to adapt a building type found throughout the region, the Shotgun House. The Shotgun House is a narrow unit that was most prominently constructed in the area in the late 19th – early 20th centuries. It was favored by architects rebuilding after Katrina because of its modularity and potential for passive climatization. Notable examples of this adaptation located in Biloxi, Mississippi include the Parker Residence (ca. 2007) by Brett Zamore Design along with the Tran (ca. 2007) and Nguyen (ca. 2007) Residences by MC2 Architects (Figure 6).

Elevated above the storm surge elevation, the modified version of the shotgun type uses multiple units to generate an abundance of intermediary spaces between the structure's

interior and its immediate context. While the plan organization follows its Shotgun predecessor in its linearity, the stacking and repositioning of multiple linear blocks begin to create outdoor courts that expose more of the interior space to the outside. The organization of space in this precedent intelligently incorporates passive heating control mechanisms, natural daylighting provisions, and cross ventilation strategies which are crucial for a community such as Biloxi where structures operating with low energy costs are an absolute necessity. In this example, building simulation tools reveal the range and effectiveness of sustainable design strategies which include the deep perimeter porch, narrow building footprint, and high volume interior space.

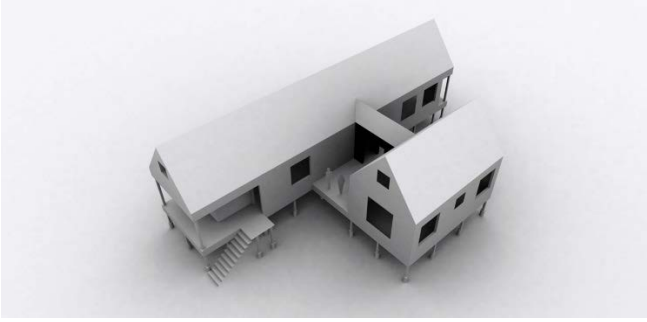

Figure 6. Parker Residence, Brett Zamore

The deep perimeter porch around the structure creates an intermediary indoor-outdoor space which facilitates shading for the interior zones and evaporative cooling through cross ventilation during hot summer months. During the cool winter months, the porch is configured to benefit from direct radiant heat gain while the enclosed programmatic units serve to block the cool northerly winds. Low-resolution CFD simulations, prevailing wind frequency data, and polar shading projections are used in combination to visualize the rate of air change within the predominately shaded areas around the perimeter structure. With the propensity of constricted air to increase in velocity when moving around objects, simulating wind velocity calibrates the reliability of flow vector simulations to visualize the path of airflow around the porch volume. Alterations to the geometry are introduced to examine ways to maximize passive summer cooling by minimizing direct solar gain and increasing prevailing air change through the space. These changes also focus on the potential for passive winter heating whereby the direct solar gain is invited into the space while cool prevailing winds are blocked from entering the space. (Figure 7)

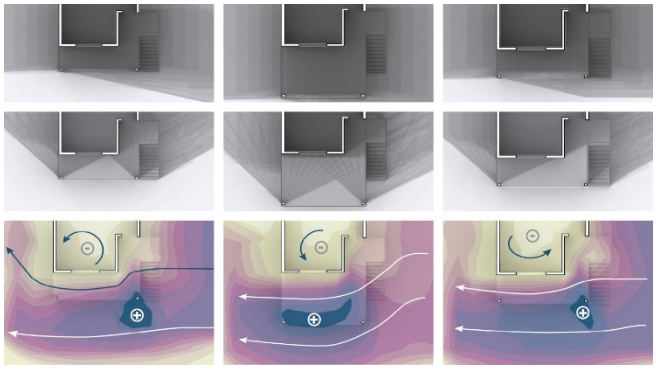

Figure 7. Altering the porch of the Modified Shotgun House: each column represents a different porch configuration. The top row shows the shadow range on June 21st, the middle row shows the shadow range on December 21st and the bottom row shows airflow velocity and vector path from a prevailing wind direction.

The permeability of the building perimeter along with the high volume interior space allows buoyant hot air to settle in the unoccupied upper level zones of the home where it is evacuated through upper story apertures. Low-resolution CFD simulations along with heat gain analysis are used to track the displacement of hot air within the structure's volume. Ventilation velocity and flow vector simulations together reveal the rate and direction of air change within the interior volume. Changes in the volume's height along with changes in upper and lower level apertures are used to explore the expedited removal of hot air during the summer season (Figure 8).

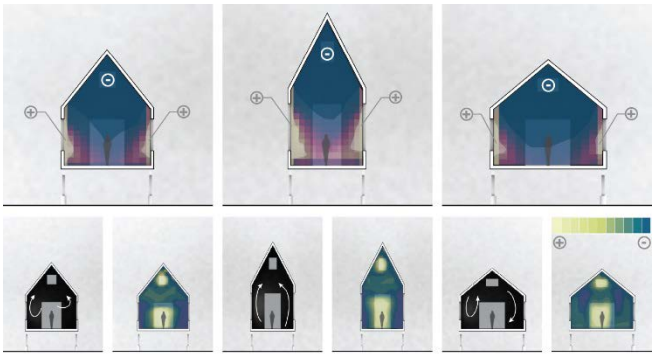

Figure 8. Adjusting the inhabitable volume of the Modified Shotgun House: each column represents a different volume configuration. The top row shows daily cumulative incident gains on June 21st and the bottom row shows flow paths (left) and ventilation velocities (right) for each.

The building's permeability is established by a multitude of oriented apertures and a narrow footprint that aids in ventilating and daylighting the interior spaces. Daylighting factor calculations, illuminance simulations, and glare control renderings are used to assess the levels and qualities of natural daylight on the interior. These improvements are

provided by both a thin building footprint and aligned openings that repeat along the length of the volume. Adjustments to room proportion, room size, and window placement are introduced to examine how the positioning of apertures relative to exterior shading devices influence the degree of even interior illumination within the space.

5. CONCLUSION

While the role of building simulation tools within architectural precedent analysis is still in its initial growth period, it has established a new way for architects to examine buildings of the past. Reintroducing issues of performance and function back into the early design field, this method provides a critical approach to the use of new computer-aided analysis tools. It achieves this through an iterative and integrated process, using the quick and interoperable capabilities of low-resolution simulation tools to assess the polyvalent nature of sustainable design strategies. This approach significantly improves upon conventional forms of architectural precedent analysis as it establishes a parametric relationship between the building's physical form and its exterior environment, revealing how sustainable space is evoked by building attributes themselves. This method also embraces the use of highly abstract low-resolution simulation platforms as an analytical sketch tool appropriate for non-expert users in considering the functional implications of a wide range of conceptual design alternatives. The objective of this approach is to offer the non-expert user a way to incorporate contemporary environmental principles into the development of conceptual design thinking through the use of abstract testing and experimentation. While questions still remain about the accuracy of results that stem from native simulation engines, this method instills accountability for the non-expert user through reciprocity protocols engrained within the system's ability to configure analysis sequences to rapidly evaluate the veracity of previous findings. With the use of an experimental digital model and an analysis sequence which critically circumscribes the various performance aspects of a design, the architect can begin to frame questions and propose contemporary environmental design approaches that can be explored further by expert collaborators. While the field appears to be moving toward the integration of simulation engines within highly deterministic computer-aided modeling programs (i.e., BIM platforms), there remains a need to continue to develop tools which ease the examination of singular structures through multiple domain analysis. There is an equal need to facilitate the rapid adjustment of custom geometries themselves, establishing a direct parametric link between a variety of physical enclosures and their impact on the immediate environment. In conclusion, the prospective of this methodology is to highlight the important role that functionality occupies within a design culture, introducing an approach to low-resolution simulation that does not attempt to optimize building design in a singular sense but that advances innovations in high performance building systems through a heuristic process.

References

ALLEN, S. 2008. Forward. Ten Canonical Buildings 1950-2000. New York: Rizzoli.

ATTIA, S. 2011. State of the Art of Existing Early Design Simulation Tools for Net Zero Energy Buildings: A Comparison of Ten Tools. Architecture et climat at Université catholique de Louvain. Louvain, Belgium.

AUGENBROE, G. 2003. Trends in Building Simulation. Advanced Building Simulation. New York, Spon Press. Pages 4-24.

AUGENBROE, G. 2001. Building Simulation Trends Going into the New Millennium. Proceedings of the Seventh International IBPSA Conference. Rio de Janeiro, Brazil.

BROWN, G.Z. AND DEKAY, M. 2001. Introduction. Sun, Wind & Light: Architectural Design Strategies. New York: Wiley.

CHAUDHARY, R., YEONSOOK, H. AND BAFNA, S. 2007. A Study of Variations among Mies's Courtyard Houses by a Combined Set of Visual and Environmental Properties. Proceedings of the Sixth International Space Syntax Symposium. İstanbul, Turkey.

CLARK, R. AND PAUSE, M. 2012. Introduction. Precedents in Architecture: Analytic Diagrams, Formative Ideas, and Partis. Hoboken, NJ: John Wiley & Sons.

FITCH, J.M. 1961. The Uses of History. Architecture and the Aesthetics of Plenty. New York. Pages 244-245.

HENSEN, J.L.M. 2004. Towards More Effective Use of Building Performance Simulation in Design. Proceedings of the Seventh International Conference on Design & Decision Support Systems in Architecture and Urban Planning. Eindhoven, Netherlands.

KNOWLES, R.L. 1981. Sun Rhythm Form. Cambridge, MA: MIT.

LAM, K.P. 2012. Sustainability Performance Simulation Tools for Building Design. Encyclopedia of Sustainability Science and Technology. Pages 10192-10260.

THOMAS, R. 2006. Environmental Design: An Introduction for Architects and Engineers. London: Taylor & Francis.

Session 3: Occupant Simulation and Visualization **33**

SAFEgress: A Flexible Platform to Study the Effect of Human and Social Behaviors on Egress Performance 35
Mei Ling Chu, Paolo Parigi, Kincho Law, Jean-Claude Latombe
Dept. of Civil & Environmental Eng., Stanford University; Dept. of Sociology, Stanford University; Computer Science Dept., Stanford University.

Using Agent-Based Modelling to Simulate Occupants' Behaviours in Response to Summer Overheating 43
Alaa Alfakara, Ben Croxford
Bartlett School of Graduate Studies, UCL.

Towards Visualization of Simulated Occupants and their Interactions with Buildings at Multiple Time Scales 51
Simon Breslav, Rhys Goldstein, Alex Tessier, Azam Khan
Autodesk Research

SAFEgress: A Flexible Platform to Study the Effect of Human and Social Behaviors on Egress Performance

Mei Ling Chu[1], Paolo Parigi[2], Kincho Law[1], Jean-Claude Latombe[3]

[1]Stanford University,
Dept. of Civil & Environmental Eng.
473 Via Ortega, Y2E2, Room 279,
Stanford, CA 94305
{mlchu, law}@stanford.edu

[2]Stanford University,
Department of Sociology
450 Serra Mall, Bldg 120, Rm 132,
Stanford, CA 94305
pparigi@stanford.edu

[3]Stanford University,
Computer Science Department,
353 Serra Street, Room 146,
Stanford, CA, 94305
latombe@cs.stanford.edu

Keywords: Social Behavior, Egress, Crowd Simulation, Multi-Agent Based Modeling, Building Safety.

Abstract

Studies of past emergency events have revealed that occupant behavior, local geometry, and environmental constraints affect crowd movement and govern evacuation. Occupants' social characteristics and the unique layout of buildings should be considered to ensure that egress systems can handle evacuee behavior. This paper describes an agent-based egress simulation tool, SAFEgress, which is designed to incorporate human and social behaviors during evacuations. Simulation results on two scenarios are presented. The first scenario illustrates the effects of the exiting strategies adopted by occupants on evacuation. The second scenario shows the influence of social group behavior on evacuations. By assuming different behaviors using this prototype, engineers, designers, and facility managers can study the important human factors during an emergency situation and thereby improve the design of safe egress systems and procedures.

1. INTRODUCTION

Computer simulations are often used to evaluate building egress and occupant safety. Despite observations and studies about human behaviors during emergencies, most simulation tools assume simplistic behavioral rules and mostly ignore the social behaviors of the occupants. The deficiencies in modeling human behaviors for egress simulations have been echoed by authorities in fire engineering and social science (Aguirre et al. 2011; Kuligowski 2011). To address the need to incorporate human and social behaviors, we designed SAFEgress (Social Agent For Egress), an agent-based model for egress simulation. SAFEgress models occupants as agents with affiliation to social groups, each defined by a unique social structure and group norm. The agents, being part of their own group rather than isolated individuals, make decisions considering group members and neighbors, in addition to individual preferences. Moreover, each agent is equipped with capabilities of sensing, cognitive reasoning, memorization, and locomotion to decide and execute its actions. By incorporating plausible behaviors with these agents, SAFEgress can be used to study the effects of human and social behaviors on collective crowd movement patterns and egress performance.

The focus of this paper is to show the effects of human and social behaviors on egress performance. Simulation results from our case studies indicate that occupants' exit strategies and social behavior can lead to very different congestion patterns and evacuation times. This kind of analysis can be useful in many applications. For example, architects can design occupant-centric floor layouts and ensure that the egress design can handle a wide range of occupant behaviors. The simulation results can also help in designing and placing signage to guide evacuation. As echoed by our collaborators from theme parks and sports stadiums, such analysis can be useful for facility management to plan evacuation strategies and design emergency training programs.

2. RELATED WORK

2.1. Human behaviors during emergencies

Researchers have proposed a variety of social theories regarding human behavior during emergencies. For example, the affiliative and place script theories examine the behavior of individuals based on their personal knowledge, risk perceptions, experience, and routines (Mawson 2005;

Sime 1983). The emergent norm theory and the pro social theory suggest that people continue to maintain group structure and behave in a pro-social manner during emergencies (McPhail 1991; Aguirre et al. 2011). The social identity theory infers that people have a tendency to categorize themselves into one or more "in-groups," building their identity in part on their membership in the groups and enforcing boundaries with other groups (Drury et al. 2009). Moreover, studies in sociology and psychology suggest that people influence each other's behaviors by spreading information and emotions (Rydgren 2009).

Social theories can provide valuable insights into the behavior of occupants during emergencies. However, developing a unified theory that fully explains occupants' behaviors in different situations is difficult. We conjecture that egress models require individual, group, and crowd level characteristics and mechanisms to predict the outcome of an egress situation. At the individual level, occupants may refer to their past experiences and knowledge to decide on their actions. At the group level, the pre-existing social structure (relations between group members) and group norms (expectations of others' behavior) would affect the behavior of an individual. Crowd-level behaviors are emergent phenomena and often follow social norms. As evidenced from recent studies of emergency incidents, occupants interact with their group members and the people nearby to guide their decision-making process (Kuligowski 2011). Therefore, an egress model should properly reflect the social structure and capture the social interactions among the occupants, in addition to assuming occupants as individual constructs (Macy and Flache 2009).

2.2. Human and crowd simulations

Humans, instead of moving randomly, tend to perform wayfinding when navigating their environment (Gärling et al. 1986). During the wayfinding process, they examine the surrounding layout and perceive sensory (visual or audio) information, and then move toward a direction based on their purpose of navigation, their destination(s), and their knowledge of the space (Turner and Penn 2002). The wayfinding process, unlike the motion of molecules or particles that are determined by interaction with their immediate neighbors, depends on both short-term, nearby information and the long-term decision goal. Since human movements aggregate to form collective crowd flow, egress simulations need to model properly the individual agent navigation decision in order to predict the overall egress performance.

Agent-Based Modeling (ABM) has been widely adopted for crowd simulation, among many other simulation approaches. In most ABM systems, the agent navigation routes are pre-defined by specifying explicitly the origins and destinations of the occupants (Aguirre et al. 2011; Veeraswamy et al. 2009). Optimal routes (usually defined in terms of travel time or distance) are obtained by assuming that the agents have good, often perfect, knowledge of the environment. Examples are the wayfinding model in EXODUS (Veeraswamy et al. 2009) and the simulation model proposed by Kneidl et al. (2013). In real situations, however, occupants usually decide their final destinations dynamically in real time and may not have complete knowledge of the space, particularly during emergencies in an unfamiliar environment. Researchers in environmental and cognitive psychology have argued that people use their perceptions to guide their navigation (Gärling et al. 1986). With proper spatial representation of the environment, Turner and Penn (2002) have shown that natural human movement can be reproduced in simulations without the need to assign agents with extra information on the location of a destination or escape routes.

Other ABM systems model agents' navigation decisions as the outcome of decision-making processes, rather than pre-defined or optimized routes. For example, ViCrowd is a crowd simulation tool in which crowd behaviors are modeled as scripted behaviors, as a set of dynamic behavioral rules using events and reactions, or as externally controlled behaviors in real time (Musse and Thalmann 2001). MASSEgress gauges the agents' urgency and invokes a particular behavior implemented using a decision tree (Pan 2006). These models consider agent behavior as a perceptive and dynamic process subject to external changes. SAFEgress also adopts the perceptive approach when updating agent knowledge of the environment. The agents, each representing an occupant, use both the perceived states of the environment and their background knowledge of the building to determine their behavior.

3. SAFEGRESS

SAFEgress is an agent-based model designed to simulate human and social behaviors during evacuation. Figure 1 depicts the system architecture of SAFEgress. The key modules are described below.

- The Global Database holds all the information about the geometry of the building, the status of emergency situations, and the agent population, which are input through the Situation Data Input Engine, the Geometry Engine, and the Population Generator.
- The Crowd Simulation Engine interacts closely with the Agent Behavior Models Database. It keeps track of the simulation, and records and retrieves information from the Global Database. The generated simulation results are sent to the Event Recorder and the Visualizer.
- The Agent Behavior Models Database contains the individual, group, and crowd behavioral models. Apart from the default models, new models can be added to investigate different behaviors and different scenarios.

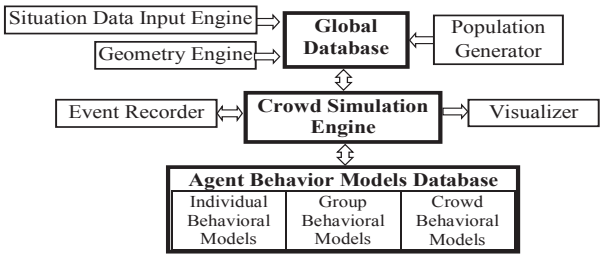

Figure 1. System architecture of SAFEgress.

Details of the system have been described in our previous work (Chu and Law 2013). In particular, algorithms (proximity and visibility computation) have been carefully designed to handle a large number of agents.

3.1. Spatial representation of the environment

A floor space includes physical obstacles, such as walls and furniture. Agents navigate the virtual space and avoid colliding with physical obstacles. To enable the agents to "sense" the vicinity of the physical obstacles and the visible space, an obstacle model is built according to user-input building geometry, which describes the locations and the dimensions of different building objects such as walls, doors, and windows. The obstacle model is constructed to represent the boundary surfaces of the physical obstacles as a set of polygonal planes. Using the obstacle model, an agent can perform proximity tests to determine the distances from nearby obstacles and visibility tests to determine if a given point in the virtual space is visible to the agent.

Besides avoiding collisions with obstacles, agents also need to detect the obstacle-free space in their surroundings in order to navigate. According to prior wayfinding studies, the choice of next navigation direction is motivated by subsequent movements to get closer to the final destinations (Gärling et al. 1986). To facilitate this navigation decision process, a navigation map to represent obstacle-free space is constructed. This map is used by SAFEgress to facilitate the computations that allow agents to "perceive" the possible navigation directions in the virtual space. The navigation map is constructed using the following procedure:

1) The continuous space is discretized into square cells to form a 2D grid. Those cells containing building features (such as exits, doors, and windows) are identified and form the initial set of navigation points (Figure 2a).
2) The algorithm computes the area of visibility for each cell on the 2D grid. Then, each cell's visibility area is compared to the area of its neighboring cells. The cells with the largest locally visible areas become additional navigation points (Figure 2b).
3) Edges are added to link the navigation points that are visible to each other within a certain radius. The resulting navigation map is a graph representing the connectivity of the obstacle-free space (Figure 2c).

In the real world, humans can only perceive their local obstacle-free surroundings. Similarly, in SAFEgress, the virtual agents can access only the "visible" portion of the navigation map to decide their navigational direction. More precisely, every agent can query the navigation map to identify navigation points that are visible from the agent's current position. Then, the agent selects its navigation target based on motivation and prior knowledge and working

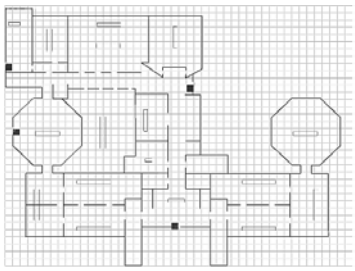

(a) Subdividing the space into square cells and initializing exits as navigation points

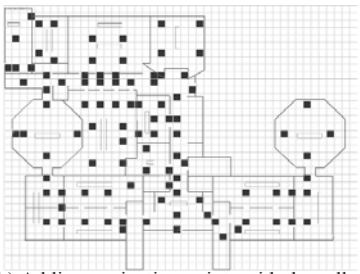

(b) Adding navigation points with the cells with large areas of visibility

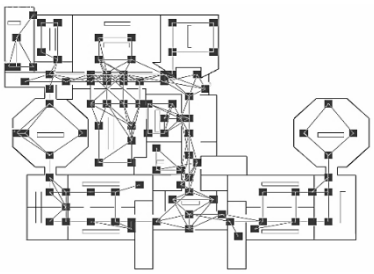

(c) Linking the navigation points which are visible to each other within a certain radius

Figure 2: Procedure for generating navigation map

memory of the building layout. For example, an agent having the knowledge of a familiar exit might choose a navigation point toward the familiar exit.

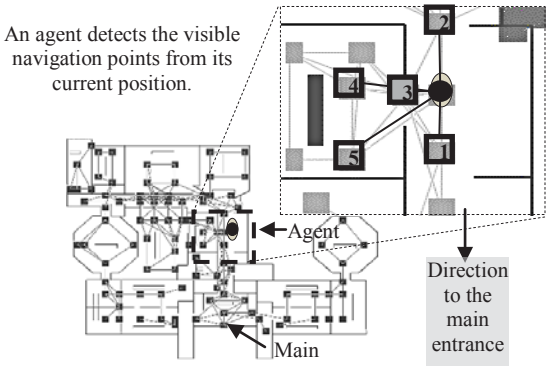

Figure 3: Illustration of an agent's visible navigation points.

In Figure 3, the agent, with knowledge of the main entrance, can choose the point labelled "1" to move closer to the main entrance among the 5 visible navigation points. On the other hand, if an agent does not have prior knowledge of the spatial layout, the agent would assign equal weight to all the options and choose a navigation target randomly. For example, if the agent in Figure 3 is unfamiliar with the environment, it can choose randomly one of the five navigation points to explore the space. Finally, each agent can "memorize" the areas traveled by registering the visited navigation points in its cognition module. Therefore, an agent can avoid repeated visits to the same area, because it will assign less weight to the visible navigation points that it visited before. This cognitive ability to memorize the previously travelled areas is particularly important for modeling a natural navigation trajectory when an agent has no prior knowledge of the environment and needs to explore its surroundings to find an exit.

3.2. Agent representation of occupants

In modeling the occupants, each agent is given a set of static and dynamic attributes. Static attributes are defined prior to the simulation, and dynamic attributes are updated during the simulation. The choice of attributes is crucial, since it implicitly determines the range of tests that the users can do with SAFEgress. To make this choice, we relied mainly on published work. (See Section 2.) The agents' attributes, listed in Table 1, can be further categorized into three levels—individual, group, and crowd—as described below with the static attributes shown **in bold**:

Level	Individual	Group	Crowd
Static	• Physical Profile[1] • Familiarity • Known Exits	• Group Affiliation[2]	• Social Order • Assigned Roles
Dynamic	• Spatial Position • Urge • Spatial Knowledge	• Visible Group Member	• Neighboring Agents

[1] The physical profile includes attributes such as age, gender, body size, travel speed, and personal space.
[2] The group characteristics include group leader(s), group intimacy level, group seeking, and group influence.

Table 1: Agents' static and dynamic attributes

- At the individual level, an agent has a **physical profile**, a **level of familiarity** with the building, and **known exits** of at least one through which the agent entered the building (Mawson 2005; Sime 1983).
- At the group level, social groups are defined by the following attributes (Aguirre et al. 2011; McPhail 1991): a **group leader** (each group has one default leader), the **group intimacy level** (e.g., high intimacy among a family group), the **group-seeking property** (describing willingness to search for missing members), and the **group influence** (describing the influence of a member to the others in the same group). The agents belonging to the same group share the same group attributes.
- At the crowd level, an agent's social position is defined by the **social order**, stating the likelihood to exhibit deference behavior (Drury et al. 2009). The lower the social order, the higher the chance for the agent to defer to other agents when negotiating the next move. A special agent may have **assigned roles** (such as authority, safety personnel, etc.) and this agent would be responsible for executing actions such as sharing information or giving instructions (Kuligowski 2011).

Based on studies by researchers in disaster management and fire engineering on occupant behavior during emergencies, a five-stage process model—perception, interpretation, decision-making, execution, memorization—is executed to update the agents' behaviors (Lindell and Perry 2011; Kuligowski 2011). Each stage may lead to changes in the parameter values of the dynamic attributes (shown **in bold**), as described below:

- At the perception stage, the agents perceive the nearby environment by detecting threats and visible features such as exits and doors (Lindell and Perry 2011). They also detect **neighboring agents** within a certain radius (Aguirre et al. 2011). If an agent is affiliated with a social group, it updates the **visible group members**. If

the default group leader is not visible, the agent searches for a temporary group leader with the highest group influence among the visible group members**.**

- At the interpretation stage, the agents revise their internal **urge level** according to the perception and the perceived urge level of the visible social group and neighbors (Rydgren 2009).
- At the decision-making stage, the agents select and invoke the behavioral decision trees according to their urge level, social affiliation, and crowd condition. A behavioral decision tree consists of intermediate nodes (which compare the agents' attributes and parameter values to the threshold values defined by users) and leaf nodes (which are either conditional checks leading to another decision tree, or low-level locomotion functions). The outcomes of decision-making are the exhibited behaviors and navigation targets. The current implementation is a rule-based reasoning system.
- At the execution stage, the agents perform low-level locomotion to move toward a navigation target determined by the decision-making process.
- Finally, at the memorization stage, the agents register the decision made and update their **spatial knowledge** about their previous locations and visited areas (Turner and Penn 2002; Sime 1983).

Each stage mimics a cognitive process or an act by an occupant during evacuation. Collectively they define the behavioral process of the occupants.

4. CASE STUDIES

In this section, we demonstrate the flexibility of SAFEgress to explore different human and social behaviors on egress performance. Two different case studies are presented. In the first case study, we vary the level of familiarity with the surroundings and the known exit to examine the effect of individual knowledge on evacuation patterns. In the second case study, we test the group effects by varying the intimacy level of the groups that the agents are affiliated with. The agents' static attributes are defined prior to simulation. In all cases, the population consists of 50% male and 50% female. None of the agents have assigned roles, all have equal social order, and they begin to evacuate immediately upon the start of the simulation (with no delay time).

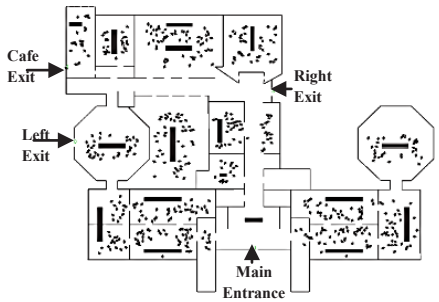

Figure 4: Geometry of the building and initial locations of 550 agents

Based on real-life observations and social studies, we construct different plausible agent behavioral models and compare the results of different simulations using a museum as the physical setting. The museum consists of several exhibition halls with four exits (the main entrance, the right exit, the left exit, and the café exit), as highlighted in Figure 4. A total of 550 agents are assigned in the simulation runs.

4.1. Effects of different individual exiting behaviors

In an emergency situation, the primary goal of the occupants is to exit the building safely. Depending on their familiarity with the building and previous experience, the occupants may adopt a broad range of strategies in choosing an evacuation route. For example, occupants who are unfamiliar with the building may select the entrance they used to enter the building as the possible exit (Mawson 2005; Sime 1983). On the other hand, occupants who visit the building regularly may have learned their preferred exit over time or have knowledge of the nearest exit. We study the effect of individual exit knowledge by varying the values assigned to the **known exits** and assume no agents have group affiliation. We conjecture and design four simple individual exiting behaviors as follows:

- Case 1: agents have knowledge of the main entrance of the museum and exit through the main entrance.
- Case 2: agents have knowledge of all four exits and choose to evacuate through the nearest exit given their initial starting position.
- Case 3: agents have knowledge of one pre-defined familiar exit and escape through familiar exits; agent population is assigned evenly to the four exits.
- Case 4: agents have no prior knowledge of any exits and solely follow the visual cues at their spatial position to guide their navigation and exit the building when a visible exit is detected.

Agent exiting behavior	Egress time (s)[1]	Exit usage			
		Main	Left Exit	Right Exit	Cafe Exit
1-Main Entrance	200 +/- 5	100%	-	-	-
2-Nearest Exit	84 +/- 4.5	39%	16%	31%	14%
3-Known Exit	180 +/- 10	25%	25%	25%	25%
4-Visible Exit	166 +/- 22.6	30%	30%	30%	10%

[1] Results are averaged over 10 runs, with +/- one standard deviation

Table 2: Results assuming different exiting strategies

Table 2 summarizes the results for the four cases, assuming all agents act as an individual (without group affiliation) and exhibit the same behavior on exiting. The average computation time for each simulation run is 4 minutes 30 seconds using an Intel Core i5-650 machine at 3.2 GHz.

The result from Cases 1 and 2 are consistent with the common understanding of crowds: occupants who are familiar with the building evacuate faster than occupants who are just used to a single exit. From the simulation result, we explore how familiarity leads to faster evacuation. In Case 1, as all the agents travel to the main entrance, high levels of congestion occur at the main entrance, as shown in Figure 5a, which leads to long egress times. In Case 2, when all agents exit through the nearest exit, the distance travelled for each agent is shorter and, because various exits are being used, much less congestion occurs at the exits (see the crowd density at the exits in Figure 5b to that in Figure 5a). In this setting, escaping through the nearest exit is the most efficient exiting strategy.

By giving spatial cognitive ability and visual sensing capability to the agents, we observe some interesting results in the egress patterns and performances. In Case 3, wherein all agents "know" and follow their familiar exit, the evacuation time is only slightly less than that for Case 1, implying that the situation where agents go to familiar exits may well be as inefficient as the one where most agents head to the main entrance. In Case 3, the inefficiency and prolonged egress times are due to the long distances required by some agents to travel from their initial position to their familiar exit. As shown in Figure 5c, congestion due to cross flow at narrow corridors occurs. For Case 4, when agents follow visual cues as a guide, evacuation appears to be a more random process, as reflected in a large standard deviation (shown in Table 2) on egress times. This situation may occur when the occupants are unfamiliar with the building and have to explore it. The prolonged egress time is due to the time spent exploring the space, with no predefined routes before the agents can "see" an exit for evacuation. Congestion occurs at the connections between the rooms and main corridors and the two atriums (as indicated by the arrows in Figure 5d), instead of at the exits. As depicted in Figure 5, the agents' knowledge of the building and visual capability can affect the choice of egress route, and thus lead to different flow patterns. The higher congestion level at the atriums also suggests that signage should be placed at the atriums to provide navigation guidance to occupants who are unfamiliar with the building.

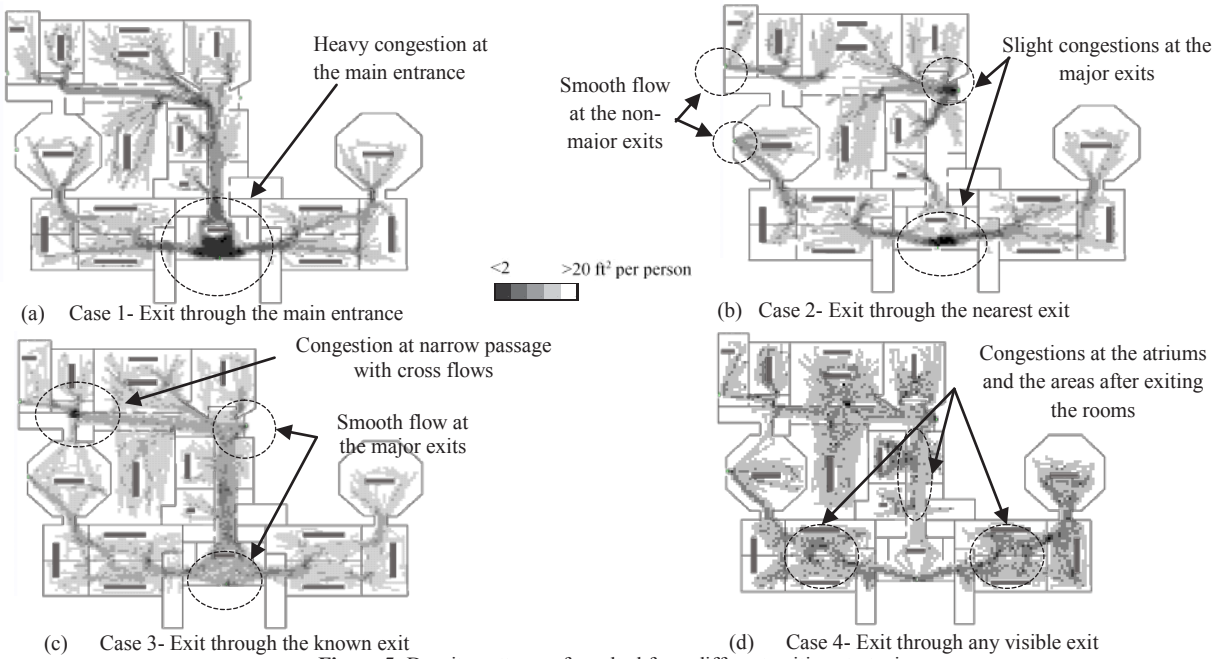

Figure 5: Density patterns of resulted from different exiting strategies

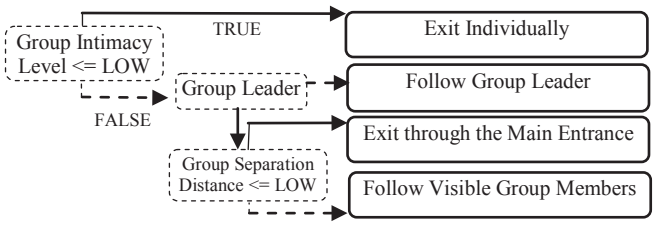

Figure 6: Group exiting behavioral decision tree, BEHAVIOR [Exiting with Group]

4.2. Effects of social group

Studies have shown that people in the same group tend to evacuate as a group and escape using the same exit (Aguirre et al. 2011). The social structure and norms persist and guide the evacuation behaviors. As depicted in Figure 6, we simulate the social effect of group behavior by constructing a decision tree that takes into consideration group-level parameters: "group intimacy level", "group leader(s)", and "group separation distance". In this study, each agent is assigned to a group of one to six agents, and each group has one default group leader. Group members start in the same room and are visible to each other at the beginning of the simulation. We vary the value of **group intimacy level** of the groups to test the effect of group behaviors. A group with a high intimacy level is a closely-related group, like a family or couple, while a group with a low intimacy level is a loosely-related group, such as a team of co-workers. In the baseline model, Case 1, all groups are defined to have a low group intimacy level, so all agents are loosely affiliated to their group and choose to exit individually through either the main entrance or a visible exit. In Case 2 and Case 3, a high group intimacy level is assigned to 50% and 100% of the groups, respectively. Table 3 summarizes the simulation results for the three cases with different group assumptions. The average computation time for each simulation run is 5 minutes 45 seconds using an Intel Core i5-650 machine at 3.2 GHz.

Group intimacy level assumption	Egress time (s)[1]	Exit usage			
		Main	Left Exit	Right Exit	Cafe Exit
1 - low intimacy; exit Individually	120 +/- 15	58%	7%	29%	6%
2 - 50% high intimacy	140 +/- 16.5	59%	6%	28%	7%
3 - 100% high intimacy	152 +/- 18	58%	6%	28%	8%

[1]Results are averaged over 10 runs, with +/- one standard deviation

Table 3: Results assuming different group traits of the agent population

As shown in the simulation results, we found that the group behaviors can have significant effects on the evacuation patterns and performances. In Case 1, as shown in Figure 7a, congestion occurs at the exits where the agents exhibit individual behaviors exiting the building. In Case 2 and Case 3, as shown in Figure 7b and 7c, the crowding is less serious at the exits, but high crowd densities are observed at the intersections of corridors and at the locations connecting the exhibition halls to the corridor. The result also shows that group behaviors have a prolonging effect on evacuation. The effects on congestion patterns and lengthened evacuation are due to the waiting time for group members as well as the fact that agents may take a detour in order to move closer to the group, thereby causing congestion at the corridors and the intersections as they leave the exhibition halls.

5. DISCUSSION

To realistically predict building egress performance, designers and managers of the building need to consider the building geometry unique to each building, and more importantly, occupants' individual and social characteristics. With the proper representations of space and occupant variables, SAFEgress allows users to assume a wide range of combinations of occupant populations and behaviors in a convenient and flexible manner. Agent behavior is modeled as different behavioral decision trees, representing plausible occupant behaviors in emergencies. Sensitivity analysis on the static attributes of different agents can be conducted to identify and assess the impacts of social factors in different

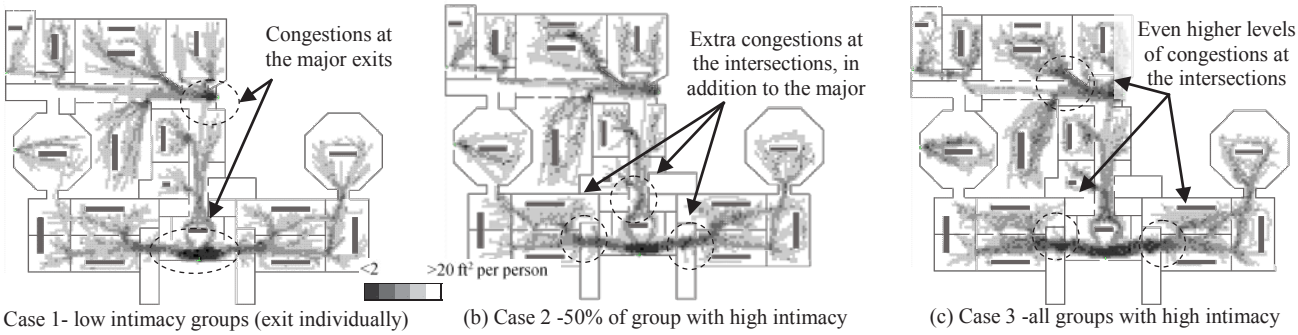

(a) Case 1- low intimacy groups (exit individually) (b) Case 2 -50% of group with high intimacy (c) Case 3 -all groups with high intimacy

Figure 7: Density patterns of Case 1, 2, and 3 assuming different group intimacy levels

physical and environmental settings, such as the case studies presented in this paper. This kind of analysis can give insights to architects, building designers, and facility managers to design user-centric safe egress and improve emergency procedures and training programs.

Through the case studies in this paper, we have shown that the inclusion of a social parameter like group intimacy significantly alters the behavior of agents during evacuation. By embedding individuals into groups, our model adds flexibility to established plausible occupant models based on the spreading of information within social groups and crowds and the role of authorities (Rydgren 2009; Hoogendoorn et al. 2010; Kuligowski 2011). The described platform represents a step forward toward incorporating social interactions into engineering models that capture human behaviors.

Based on the synthesis of social studies of past emergencies, we conjecture that SAFEgress is a reasonable and sufficient platform to model a range of evacuation behaviors of occupants. Given the flexibility of the framework, reasonable initial assumptions of the occupants' characteristics (such as demographics, how familiar the occupants are with the building, and their preference to use different exits) are important in order to generate realistic and relevant simulation results. We continue to gather feedback on the framework from our industry collaborators. Moreover, as a part of our on-going validation effort, we establish benchmark scenarios based on modeling guidelines and real-life data (Chu and Law 2013; videos: eig.stanford.edu/SAFEgress).

Acknowledgments

This research is partially supported by the Center for Integrated Facility Engineering at Stanford University. The first author is also supported by the Croucher Foundation Scholarship and the Leavell Fellowship.

References

AGUIRRE, B. E., TORRES, M. R., GILL, K. B., AND HOTCHKISS, H. L. (2011). "Normative collective behavior in the station building fire," Social Science Quarterly, 92(1), 100–118.

CHU, M. L., AND LAW, K. H. (2013), "A Computational Framework Incorporating Human Behaviors for Egress Simulations, " ASCE Journal of Computing in Civil Engineering, 27(6), 699–707.

DRURY, J., COCKING, C., AND REICHER, S. (2009). "Everyone for themselves? A comparative study of crowd solidarity among emergency survivors," British Journal of Social Psychology, 48, 487–506.

GÄRLING, T., BÖÖK, A., AND LINDBERG, E. (1986). "Spatial orientation and wayfinding in the designed environment: A conceptual analysis and some suggestions for post-occupancy evaluation," Journal of Architectural and Planning Research, Vol 3(1), 55-64.

HOOGENDOORN, M., TREUR, J., WAL, C. V. D., AND WISSEN, A. V. (2010). "An agent-based model for the interplay of information and emotion in social diffusion," Proceedings of: Web Intelligence and Intelligent Agent Technology (WI-IAT), 439–444.

KNEIDL, A., HARTMANN, D., AND BORRMANN, A. (2013). "A hybrid multi-scale approach for simulation of pedestrian dynamics." Transportation Research Part C: Emerging Technologies, available online 18 April 2013, http://dx.doi.org/10.1016/j.trc.2013.03.005

KULIGOWSKI E. D. (2011). Terror defeated: occupant sensemaking, decision-making and protective action in the 2001 World Trade Center disaster, Ph.D. Thesis, University of Colorado, Boulder.

LINDELL, M. K., AND PERRY, R. W. (2011). "The Protective Action Decision Model: Theoretical Modifications and Additional Evidence," Risk Analysis, 32(4), 616-632.

MACY M, AND FLACHE A. (2009). "Social dynamics from the bottom up: Agent-based models of social interaction," In: Hedström P, Bearman P (eds) The Oxford Handbook of Analytical Sociology. Oxford: Oxford University Press, 245–268.

MAWSON, A. R. (2005). "Understanding mass panic and other collective responses to threat and disaster," Psychiatry, 68, 95–113.

MCPHAIL, C. (1991). The Myth of the Madding Crowd, Aldine de Gruyter, New York.

MUSSE, S. R., AND THALMANN, D. (2001). "Hierarchical model for real time simulation of virtual human crowds," IEEE Transactions on Visualization and Computer Graphics, 7, 152-164.

SIME, J. D. (1983). "Affiliative behavior during escape to building exits," Journal of Environmental Psychology, 3(1), 21–41.

TURNER, A., AND PENN, A. (2002). Encoding natural movement as an agent-based system: an investigation into human pedestrian behaviour in the built environment. Environment and Planning B: Planning and Design, 29(4), 473-490.

PAN, X. (2006). Computational modeling of human and social behavior for emergency egress analysis, Ph.D. Thesis, Stanford University.

RYDGREN, J. (2009). "Beliefs." In: Hedström P, Bearman P (eds) The Oxford Handbook of Analytical Sociology. Oxford: Oxford University Press, 72–93.

VEERASWAMY, A., LAWRENCE, P., AND GALEA, E. (2009). "Implementation of cognitive mapping, spatial representation and wayfinding behaviours of people within evacuation modelling tools," 2009 Human Behavior in Fire Symposium. Available at: http://gala.gre.ac.uk/1297/.

Using Agent-Based Modelling to Simulate Occupants' Behaviours in Response to Summer Overheating

Alaa Alfakara and Ben Croxford

[1]Bartlett School of Graduate Studies, UCL
14 Upper Woburn Place,
London, UK, WC1H 0NN
alaa.alfakara.09@ucl.ac.uk, b.croxford@ucl.ac.uk

Keywords: Agent-Based Modelling (ABM), Occupant Behaviour, Dynamic Building Simulation Tools.

Abstract

This paper presents a pilot investigation of an ongoing research to model detailed occupants' behaviours when dealing with summer overheating in UK domestic buildings using agent-based modelling and a dynamic simulation model. The pilot model was built in REPAST to initially model the behaviours of two adults in a flat, controlling windows and mechanical cooling systems to achieve comfort. Two cases were considered; a base-case behaviour, and an improved-case behaviour. Thermal Analysis Simulation software (TAS) was used to model the flat, where hourly cooling and windows schedules produced by agents were fed into TAS to estimate cooling load and internal temperatures. Initial results showed a reduced usage of mechanical cooling and reduced cooling load under improved-case behaviour.

1. INTRODUCTION

Carbon dioxide emissions due to energy use are increasing at an alarming rate. Over 50% of global energy consumption is attributed to the building industry (MacKay 2009). Summertime temperatures in UK homes are of increasing concern, particularly with the growing evidence that the UK climate is warming and is expected to continue (Murphy et al. 2009). Under the medium emissions scenario, UK Climate Projections predicted an increase in summer average temperatures by up to 5.4°C (2.2- 9.5°C) in parts of southern England by 2080 (Jenkins et al. 2009). UK dwelling refurbishment has been focusing on reducing heating demand. According to (Boardman et al. 2005), over 70% of the dwellings that will be in use in 2050 have already been built. This imposes uncertainty about the resilience of UK homes to climate change, and the impact on energy consumption and CO_2 emissions due to the predicted increase in the use of cooling systems. Thus, a holistic approach is needed that includes measures to reduce overheating and address cooling demands as well. To cope with a changing climate, numerous changes to occupant behaviour will be required, and these changes should be considered by simulation models. Current models have to be further developed so that they can incorporate a range of current and future dynamic occupants' behaviours to improve the accuracy of building performance estimations, and to properly assess energy efficiency measures in buildings. Even though a number of studies attempted to construct behavioural models to analyse occupants' impact on energy consumption levels, most of these behavioural models are for occupant behaviour in commercial buildings, which limit their applicability to the home context where the behaviour of occupants tends to be more complex and unpredictable.

This paper presents an initial attempt to construct Agent-Based Modelling (ABM*)* to simulate occupant behaviour in residential buildings in response to summer overheating that can be linked to a dynamic building simulation model to assess the impact of occupant behaviour on comfort and energy consumption, and to start bridging the gap between actual and estimated energy consumption in current building simulation models. The paper first presents a literature review, followed by a methodology section, the initial case study, a discussion and an outline of future work.

2. LITERATURE REVIEW

The literature review will cover the concepts of agent-based modelling and how occupant behaviour has an impact on energy consumption. It will focus more on presenting

current attempts to model occupant behaviour using ABM to pinpoint the gap in current research.

2.1. Agent-Based Modelling (ABM*)*

ABM is a rather new approach, which since 1990 has begun to gain popularity as a method for modelling complex systems with interacting, autonomous agents. A significant amount of research has been accomplished, which has further advanced the application of agent-based modelling into various fields such as engineering, economics, biology and social sciences (Macal and North 2007, 2011). While the definition of agent-based modelling varies depending on the field, the general philosophy is that ABM consists of individual, autonomous, interacting objects called "agents" where each agent has a state and a rule, and the model aims to identify, explain, and generate emergent behaviours (Axtell 2000; Chan et al. 2010). Agents' relationships, interactions, and behaviours are the main focus of agent-based modelling, and it can explicitly model the complexity arising from these individual behaviours and interactions (Macal and North 2011). This gave rise to using ABM to model social systems of interacting agents that can influence each other, learn from their experiences, and adapt their behaviours. Macro phenomena emerges from the micro-level behaviours and interactions among the heterogeneous agents (Janssen 2005; Macal and North 2011). Generally speaking, the structure of ABM consists of three elements:

1) A set of agents.
2) A topology: a set of rules that defines the relationship and interaction between agents.
3) An environment in which the agents interact.

To create such models, you must first define a population of agents, their environment and behavioural rules; then, run the simulation and monitor what happens.

2.2. Occupant behaviour

Energy consumption in buildings is closely related to occupants and their interactions with building systems such as windows, heating and cooling, lighting, etc. (Peng et al. 2011; Hoes et al. 2009). Several studies suggested significant variations in energy use among similar apartments with identical appliances, due to differences in occupant behaviour (Peng et al. 2011; Gram-Hanssen 2010; Fabi et al. 2012; Gram-Hanssen 2004). Moreover, a number of studies pointed out that energy savings in excess of 40% in buildings can result from changes in how occupants behave (Bourgeois et al. 2006; Azar and Menassa 2012).

With the push towards sustainable buildings, many energy simulation tools are now commonly used in the industry—eQuest, EnergyPlus, TAS—as assessment tools to estimate building energy performance (Hoes et al. 2009). However, results show variations in estimates of over 30% between actual and predicted energy consumption levels (Azar and Menassa 2012; Yudelson 2010; Turner & Frankel 2008; Dell'lsola and Kirk 2003). Many factors that relate to the complexity of buildings and weather can limit the accuracy of energy simulation models (Turner and Frankel 2008). However, the way occupants are represented in these models may also contribute to the disparity of estimates (Hoes et al. 2009). Traditional energy software is sensitive to occupancy related inputs such as energy consumption rates and occupant schedules. Although this software allows for variations in hourly occupancy loads and schedules, occupants are considered as static entities in the modelling process with similar schedules and energy consumption rates, and occupancy-related actions or behaviours typically are not considered (EnergyPlus 2013; eQuest 2009; Hoes et al. 2009; Turner & Frankel 2008). A study by (Clevenger and Haymaker 2006) examined the impact of occupancy variations on energy simulation models. It was reported that estimates can vary by more than 150% when using low vs. high energy consumption rates. Furthermore, a change in only one factor (such as open windows or doors) might result in up to a 40% change in total estimated consumption. Therefore, many researchers are now focusing on understanding occupants' energy behaviours to bridge the gap between predicted and actual energy use in buildings. The ability of ABM to model complex systems can be facilitated to simulate occupants' energy use characteristics and its change over time, and assist traditional energy simulation software.

2.3. Agent-based modeling of occupants in buildings

Over the last few years, there have been many studies that used ABM as a method to simulate occupant behaviour in buildings. Erickson et al. (2009) deployed ABM to optimise HVAC loads by modelling the room's occupancy in commercial buildings in order to achieve energy savings. It was concluded that HVAC energy savings of approximately 14% could be achieved by simulating occupancy presence. Another study by Li et al. (2009) used ABM to model occupancy in the emergency department of a health care facility so it could be used to optimise the sizing

of the HVAC system; the study showed a reduction of 43% in the required HVAC capacity when occupancy was properly estimated. Azar and Menassa (2012) used ABM to estimate energy consumption in commercial buildings where occupants had control over lighting and window blinds. Different energy categories were considered, and agents were considered to be constantly trying to influence other occupants to change their energy use. The study concluded that a reduction of 23% in electricity consumption was achieved, while gas consumption only dropped by 5% because agents had no control over space heating. Kashif et al. (2011, 2013) proposed using ABM to simulate occupant behaviour for energy-smart homes, and assessed the sensitivity of occupant behaviour for energy management. The model was constructed based on a user behaviour modelling approach of "5W's and 1H", and a causal model of occupant behaviour was built using Brahms (Sierhuis et al. 2007). The paper pinpointed the importance of dynamic behaviours for an accurate energy simulation in order to predict energy trends and reduce energy consumption.

Literature specific to the use of ABM to simulate occupant behaviour tends to focus mainly on commercial buildings, where agents simulate occupants' presence rather than occupants' detailed energy behaviour, and are based on controlled activity profiles aimed at occupant behaviour in commercial buildings. The study by Azar and Menassa (2012) showed the potential of modelling occupant behaviour and interactions, rather than only modelling the presence of occupants. However, only a narrow stream of interactions was included. The model presented by Kashif (2011, 2013) presented the significance of dynamic behaviour within the home context; however, not all behavioural aspects were covered because the study included buildings with power management systems where space heating, which accounts for over a half of domestic energy consumption in both UK and USA (Pérez-Lombard et al. 2008), was centrally controlled. Moreover, energy consumption was estimated using Matlab rather than a validated building simulation tool, which may affect the accuracy of the simulator predictions. As a consequence, there is a need to broaden the scope of research to include more detailed energy usage of occupants and its change over time, and to use these behaviours in a validated dynamic building simulation tool to estimate the occupancy effect on energy consumption, which is the aim of this ongoing research.

3. METHODOLOGY

Occupant behaviour, when dealing with summer overheating in a residential context, is simulated using ABM. It has been proposed to start with a pilot ABM model where factors that affect occupant behaviour in response to overheating are initially assumed; different hypotheses such as occupant response to physical stimulus, energy policies, and increased energy prices are tested. The model is built using REPAST Simphony (REPAST 2013); an open source agent-based modelling library specifically developed for ABM of complex adaptive systems (North et al. 2013). The ABM is linked to a dynamic building simulation model, where at every time interval, agent actions—such as changing the lighting, opening the window, using cooling systems, etc.—are fed into the building simulation model. Based on agent actions, the resulting physical parameters (such as internal temperature, air velocity, and luminance) are estimated and used in the next time interval. Initial tests and sensitivity analyses to identify key input parameters that the model is sensitive to are performed to identify key variables that need to be monitored and acquired during data collection from operational residential buildings. Collected data will be used to test and modify the model, leading to the final step of validating and verifying the model. This general methodology is summarised in (Figure1).

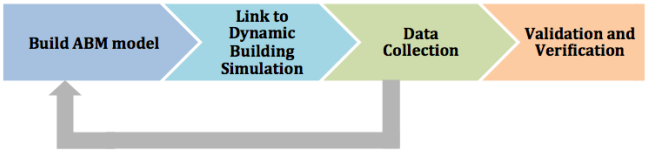

Figure 1. General methodology for the model.

4. INITIAL CASE STUDY

For the purpose of this study, an initial experimental ABM was built to simulate a flat occupied by two adults for 24 hours a day, where the occupants are awake from 8:00 AM until 11:00 PM. The model currently covers only the interactions of the occupants with the flat's windows (opening or closing) and the mechanical cooling system AC (turning on or off), but will be expanded to cover more actions as research progresses. The model produced window opening and AC usage schedules that were used in TAS building simulation model (EDSL 2012) to estimate the building's energy performance and the resulting internal temperature. Two cases were considered: a base-case behaviour that represented a typical behaviour, and an improved-case behaviour where occupants attempted to

save energy.

It is worth mentioning that building an ABM with few human agents has been used by many authors to model micro-behaviour and interactions of occupants with building systems, such as in the work of (Kashif 2011; Kashif et al. 2013; Azar and Menassa 2012; Kim et al. 2013). The current model of two occupants is just the first step in this research, which as explained in future work will expand to include different family sizes, and will also model the effect of social interactions of "neighbour" agents to influence behavioural changes.

4.1. The thermal model of the building

A virtual model of a high-rise residential building block was built in TAS to model the dynamic thermal performance of the flat in response to different occupancy cooling behaviours (Figure 2). The flat included a living room, bedroom, kitchen and bathroom. A geometry and construction materials were specified for the various building elements, besides defining the internal conditions, aperture openings, schedules based on hourly time intervals, and weather information. For the sake of this experimental test, a hot weather profile was used to ensure necessary actions in response to overheating. The simulation in TAS covered one flat (highlighted in red) for the summer period (from 21 Jun to 21 Sep), with two adults occupying the flat.

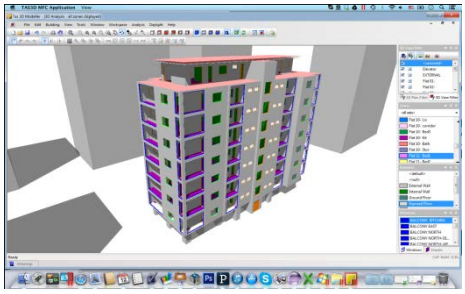

Figure 2. Building model in TAS.

The first simulation of the flat in TAS assumed no cooling or window openings, and estimated the initial internal temperatures of every room in the flat. These initial internal temperatures were used as initial ABM inputs only for the first time. Thereafter, more accurate schedules were produced by the ABM model. There were hourly schedules over the entire simulation period, a "summer season", which included window openings and mechanical cooling usage in the living room, master bedroom and the kitchen. Doors, were assumed to be closed by default in TAS. These new schedules were then fed into TAS to re-estimate internal temperatures and the cooling load for the flat model, based on agent actions. The updated internal temperatures generated in TAS were, thereafter, used as input for the next simulation of the ABM as illustrated in (Figure 3). The entire cycle shown in the following figure is currently considered as "one iteration", where TAS uses hourly schedules for window and AC changes over the entire summer period, produced by ABM, while ABM uses the hourly room temperatures of the entire summer period, produced by TAS. As research progresses, a dynamic link between the two models will be established to allow instant transfer of input/output at every time interval of 15 minutes.

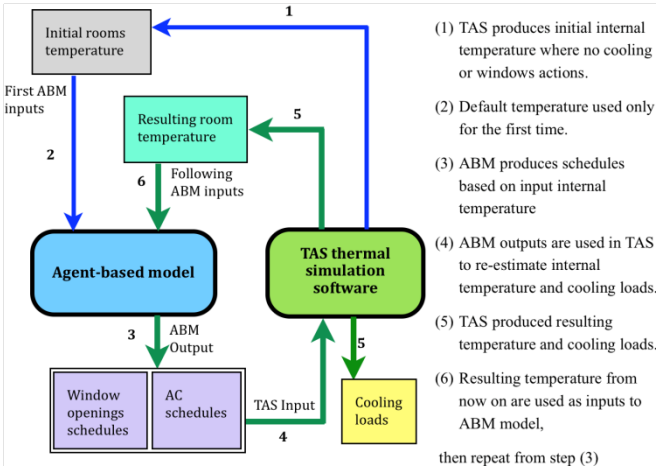

Figure 3. The process of a full simulation between the ABM model and TAS

4.2. The agent-based model

The pilot ABM was built using Repast Symphony, which initially used hourly time intervals and included two different types of agent classes: 1) Person class and 2) Room class. Person class included all the information regarding the current occupants, including ID, seniority, temperatures, threshold, location, and awake status. Occupants' location probability determined their location at every time interval, and the temperatures threshold profile (probability profile) calculated the probability of taking an action based on internal temperature. It was proposed to use this profile to test if changing these profile set points would induce changes in agent behaviour. Also, the concept of seniority was introduced in this model where the occupant with higher seniority is the one responsible for decision making when present with another occupant in the same room; however decision making and interaction amongst "occupant" agents will only be thoroughly investigated and

deployed in future work. As for the room class, this class held attributes of the room such as ID, room temperature, the status of window and AC, and number of occupants in the room. At every hourly time interval, the initial model executed a number of functions. The first function was to calculate the time, and to get each room's default temperature, which was extracted from TAS. Then, based on the time, the model checked if the agent was asleep or not, and got the location probability for each agent. Checking if a person was asleep was purely based on time, while location probability was extracted from an input-data file that provided dummy data for each occupant's location. Using dummy data was just for the sake of exploring the model; later on, real data will be used in the model. Thereafter, the model checked the following:

1) For each room, the model checked if any agent was in the room.

2) If more than one agent was in the room, a function was built to determine which agent was the most senior agent, the one who would be making decisions regarding interaction with the room's systems at every time interval. The agent with the highest rank is assigned as the most senior one. If the agent is alone in the room, it is considered to be the decision maker.

3) Based on internal temperature, the model calculated the probability that the agent would open/close the window or turn the *AC* on/off. (Figure 4) illustrates the temperature threshold profile (probability profile) that an agent would take an action based on the internal temperature. Every agent has a different probability profile based on personal preference for internal temperature. The predicted probability Y_i for a certain temperature T_i is then calculated using the following linear formula (1):

$$Y_i = b_0 + b_1 \times T_i \quad (1)$$

Where b_0 is the intercept point with probability-axis, and b_1 is the gradient of the line.

After calculating the probability of taking an action, if the agent was the most senior then a random probability number was generated. If the random probability was less

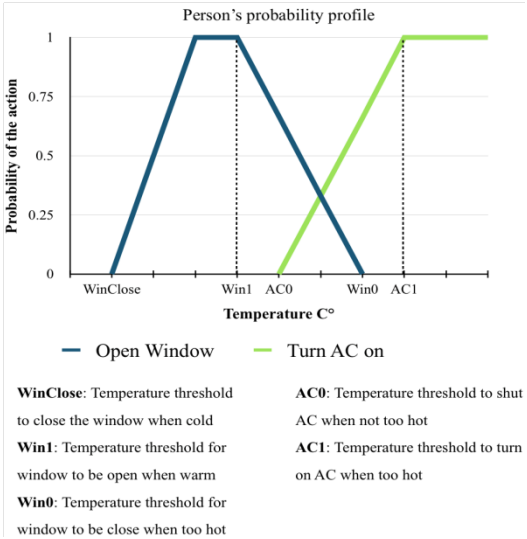

Figure 4. Probability profile to take a certain action**.**

than the predicted probability, then the required actions took place; otherwise nothing happened. This simple function was aimed at initially avoiding having a fixed output, while maintaining the likelihood of making an action with a higher probability (i.e., the higher the predicted probability was, the higher likelihood of the random number being smaller). This function will be replaced in the next phase of the research with more complex learning algorithms to allow agents to learn which actions to take based on the current event. The aforementioned functions were repeated for every time interval until the model reached the maximum tick count of ~2232 hours (the number of hours in a 3 month summer period), and all information was exported.

Two different energy consumption profiles were tested. It was proposed to initially use temperature threshold as a method to categorise cooling use patterns where a higher temperature threshold (probability profile) represented a more efficient use of cooling systems. The first case study was on "base-case" behaviour, while the second case study was on "improved-case" behaviour, which was represented by a changing temperature threshold profile for occupants. (Figure 5) shows the temperature threshold profile for both cases for both occupants. Using different profiles with different set points for every occupant was intended to introduce diversity and conflicts between agents when it came to deciding what is "comfortable".

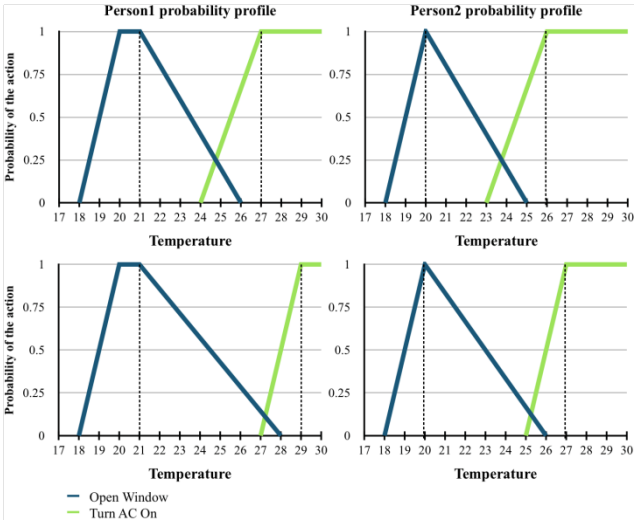

Figure 5. Occupants' probability profile for "base case" (top) and "improved behaviour" (bottom).

For each case, six iterations were performed of the process illustrated in (Figure 3). Currently, the difference between successive iterations is minimal, as agents in the current model lack the ability to learn. In the current model it was expected that windows would be open more when the temperature was cooler, and cooling systems would be used more when it was hot, and that AC would be shut down when opening windows. For improved-case behaviours, AC should be used less, and more windows should be open even in hotter temperatures.

4.3. Simulation results

Table 1 shows the average number of hours windows are open and AC is used over the 3 month simulation period. For all rooms, it shows an increase in the number of hours windows are open for the improved case, with the number of hours of AC use reduced.

	Window		AC			
Room	Base case	Improved case	Base case	Improved case	Change in Win	Change in AC
Living	965	1,096	620	562	+13.6%	-9.3%
Bed	394	444	105	93	+12.7%	-11.4%
Kitchen	207	260	237	224	+25.6%	-5.5%

Table 1. Average number of hours window are open and AC is used.

Figure 6 represents the average frequency of open windows and AC turned on, in relation to internal temperature ranges (of 1 °C) in the living room, for each case.

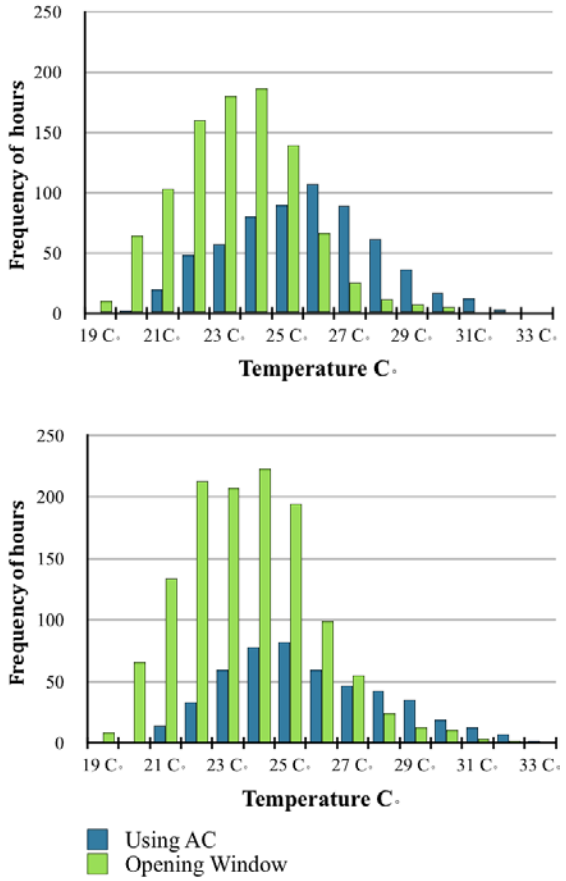

Figure 6. Average frequency of turning AC on and opening the window in the living room for "base-case" behaviour (top) and "improved-case" behaviour (bottom).

In general, the frequency of window opening outweighed the frequency of turning the AC on. For the improved case behaviour, with agent temperature profiles increased by 2°C, more open windows and a reduction in AC use were observed. At a temperature range of 26–27°C, for instance, AC usage in the living room dropped by around 40%, and the average frequency of window opening was almost double to that of using the AC. The resulting cooling load was estimated by using the TAS building simulation tool. Under the base-case behaviour the thermostat setting was considered as 24°C, while under improved-case behaviour it was set at 26°C. For the hottest day in the entire simulation period, day 230 August the 18th, the following figure (Figure 7) shows the average cooling load in individual rooms and on the flat level. For the hottest day, in both simulations, cooling load peaked at 15:00 with

an external temperature of 36°C. Under the base-case simulation, peak cooling load was at 4.3 KW, whereas for the improved-case behaviour the cooling load peaked at 3.1KW; a reduction of almost 30% in cooling loads.

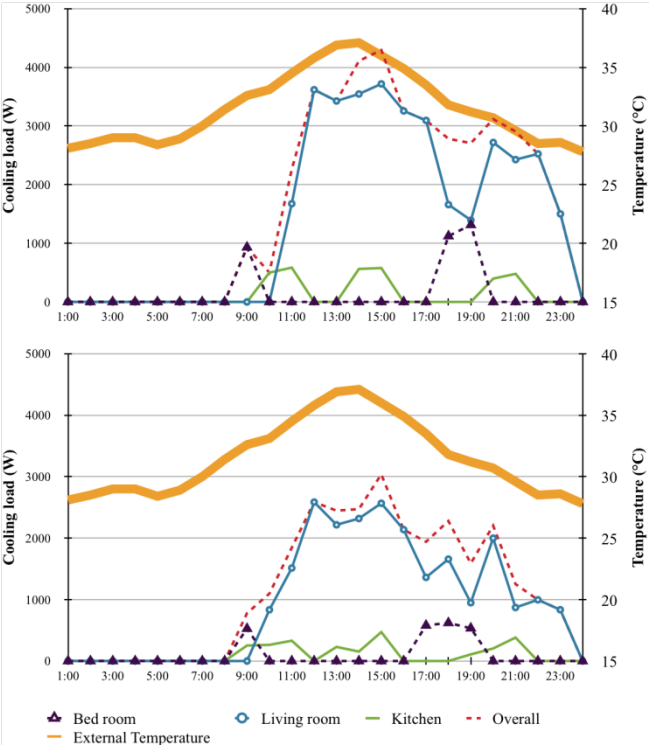

Figure 7. Average cooling load on the hottest day under "base-case" behaviour (Top) and "improved-case" behaviour (bottom)

5. CONCLUSION

This paper presented initial Agent-Based Modelling (ABM) of ongoing research that was linked to Thermal Analysis Simulation (TAS) to simulate the interactions of occupants with residential building systems in response to overheating. The current range of interactions included opening/closing windows and using AC. The use of personal temperature threshold profiles (probability profiles) was tested to observe if they would induce changes in agent behaviour when changes in temperature threshold set points were introduced. The initial results of the model showed changes in agent behaviour when changing the agent's temperature profile–the higher the temperature set point, the less use of cooling systems and more use of open windows took place. Results showed a reduction in using AC by up to 11.4% under improved-case behaviour, while the use of open windows increased by up to 25.6%. When linked to TAS, the average cooling load for the hottest day was reduced by over 30%. Thus, this study showed the potential for this approach to be used in a more dynamic representation of occupant behaviour within the home context, and to obtain a more realistic estimation of energy consumption levels.

The model used simplified parameters, as the purpose was to set the foundation for the next stages of this research. The next step is to expand the model to include multiple flats and cover several families with different behaviour and occupancy patterns. Also, more occupant actions will be included, such as the use of blinds, lighting, fans, heating systems, etc. One of the objectives of this research is to investigate how occupants can optimise their response to overheating, so optimal and sub-optimal behaviours will be built into the model to identify ways to avoid sub-optimal behaviours. As for personal preference, it currently includes thermal preference, which will be thoroughly investigated during data collection and linked to a thermal comfort model, along with other parameters such as the control of clothing, metabolism, age, etc. Moreover, currently the model assigns seniority as a simple way to represent decision-making; however, modelling decision-making and negotiation within the household, the social interaction, and the influence of other agents in neighbouring households to change energy behaviours will be properly investigated and included in the model. Future steps also include data collection from operational residential buildings, by monitoring and interviewing occupants, learning how they deal with overheating and how they change their behaviours. This data will be used to test the assumptions made in the model about occupant behaviour, and to validate the model after making any necessary changes. Currently, the researcher is working on expanding the model and preparing the data collection process to closely monitor a recently built residential development in North London.

References

AXTELL, R., 2000. Why Agents? On The Varied Motivations For Agent Computing In The Social Science. www.brookings.edu, pp.1–23. http://www.brookings.edu/~/media/Files/rc/reports/2000/11technology_axtell/agents.pdf [Accessed June 10, 2013].

AZAR, E. & MENASSA, C.C., 2012. Agent-Based Modeling of Occupants and Their Impact on Energy Use in Commercial Buildings. Journal of Computing in Civil Engineering, 26(4), pp.506–518.

BOARDMAN, B. ET AL., 2005. 40% House, Environmental Change Institute, University of Oxford.

BOURGEOIS, D., REINHART, C. & MACDONALD, I., 2006. Adding advanced behavioural models in whole building energy simulation: A study on the total energy impact of manual and automated lighting control. Energy & Buildings, 38, pp.814–823.

CHAN, W.K.V. ET AL., Agent-based simulation tutorial of emergent behavior and differences between agent-based simulation and discreet-event simulation. In Proceedings of the 2010 Winter Simulation Conference. pp. 135–150.

CLEVENGER, C.M. & HAYMAKER, J., 2006. The impact of the building occupant on energy modeling simulations. In Proceedings of Joint International Conference on Computing and Decision Making in Civil and Building Engineering. Monteral, Canada, pp. 1–10.

DELL'LSOLA, A. J., AND KIRK, S. J. (2003). "Life cycle costing of facilities." Reed Construction Data, Kingston, MA.

ENERGYPLUS. (2013). "Input/output reference: The encyclopaedic reference to EnergyPlus input and output." The Board of Trustees of the University of Illinois and the Regents of the University of California through the Ernest Orlando Lawrence Berkeley National Laboratory. http://apps1.eere.energy.gov/buildings/energyplus/pdfs/inputoutputreference.pdf (Jan. 27, 2014).

EQUEST. (2009). "Introductory tutorial, version 3.63." http://doe2.com/download/equest/eQ-v3-63_Introductory-Tutorial.pdf (Jul. 1, 2011).

ERICKSON, V.L. ET AL., 2009. Energy Efficient Building Environment Control Strategies Using Real-time Occupancy Measurements. In Proceedings of the First ACM Workshop on Embedded Sensing Systems for Energy-Efficiency in Buildings. pp. 19–24.

FABI, V. ET AL., 2012. Occupants' window opening behaviour: A literature review of factors influencing occupant behaviour and models. Building and Environment, 58(C), pp.188–198.

GRAM-HANSSEN, K. 2004. Domestic electricity consumption – consumers and appliances, in L. Reisch and I. Røpke (eds.): The Ecological Economics of Consumption, Edward Elgar, Camberley, pp. 132–150.

GRAM-HANSSEN, K., 2010. Residential heat comfort practices: understanding users. Building Research & Information, 38(2).

HOES, P. ET AL., 2009. User behavior in whole building simulation. Energy & Buildings, 41(3), pp.295–302.

HULME, M., TURNPENNY, J. & JENKINS, G., 2002. Climate change scenarios for the United Kingdom The UKCIP02, Norwich, UK: Tyndall Centre for Climate Change Research, School of Environmental Sciences, University of East Anglia.

JACKSON, T., 2005. Motivating Sustainable Consumption, Sustainable Development Research Network.

JANSSEN, M.A., 2005. Agent-Based Modelling. In J. Proops & P. Safonov, eds. Modelling In Ecological Economics. Glos, UK: Modelling In Ecological Economics, pp. 155–172.

JENKINS, G.J. ET AL., 2009. UK Climate Projections. Met Office Hadley Centre: Exeter, UK.

KASHIF, A. ET AL., 2013. Simulating the dynamics of occupant behaviour for power management in residential buildings. Energy & Buildings, 56, pp.85–93.

KIM ET AL., 2013. Traditional VS. Cognitive agent simulation. Proceedings of BS 2013: 13th Conference of the International Building Performance Simulation Association. pp 2020-2027.

LI, Z., HEO, Y. & AUGENBROE, G., 2009. HVAC design informed by organizational simulation. pp.1–6.

MACAL, CHARLES M & NORTH, M.J., 2011. Introductory tutorial: agent-based modeling and simulation. pp.1–14.

MACKAY, D.J., 2009. Sustainable Energy without the hot air. 3rd ed. CAMBRIDGE, ENGLAND: UIT Cambridge Ltd.

MURPHY, J.M. ET AL., 2009. UK Climate Projections Science Report. Met Office Hadley Centre: Exeter, UK.

NORTH, M.J. & MACAL, CAHRLES M, 2007. Managing Business complexity, Oxford: Oxford University Press.

NORTH, M.J. ET AL., 2013. Complex adaptive systems modeling with Repast Simphony. Complex Adaptive Systems Modeling, 1(3), pp.1–26.

PENG, C. ET AL., 2011. Quantitative description and simulation of human behavior in residential buildings. Building Simulation, 5(2), pp.85–94.

PÉREZ-LOMBARD, L., ORTIZ, J. & POUT, C., 2008. A review on buildings energy consumption information. Energy & Buildings, 40(3), pp.394–398.

REPAST. (2013). http://repast.sourceforge.net. (Oct 8, 2013).

SIERHUIS, M., CLANCEY, W.J. & VAN HOOF, R.J.J., 2007. Brahms: a multi-agent modelling environment for simulating work processes and practices. International journal of Simulation and Process Modelling, 3(3), pp.134–152.

SUSTAINABLE BUILDING INDUSTRY COUNCIL (SBIC). (2012). "Mastering Energy-10® software user manual." SBIC, http://www.sbicouncil.org/store?page=shop.browse&category_id=2 (Jan. 27, 2014).

TAS BY EDSL .2013. http://www.edsl.net/main// [Accessed Jan 14, 2014].

TURNER, C. & FRANKEL, M., 2008. Energy Performance of LEED® for New Construction Buildings, Washington DC, USA: U.S. Green Building Council.

YUDELSON, J. (2010). Greening existing buildings, McGraw-Hill: New York.

Towards Visualization of Simulated Occupants and their Interactions with Buildings at Multiple Time Scales

Simon Breslav, Rhys Goldstein, Alex Tessier and Azam Khan

Autodesk Research
210 King St. East,
Toronto, Ontario, Canada, M5A 1J7
{firstname.lastname}@autodesk.com

Keywords: Sustainable Design, Design Tools, Perception, Occupant Behavior, Stylized Computer Animation.

Abstract

While most building simulation tools model occupancy using simple 24-hour profiles, researchers are applying machine learning and other advanced modeling approaches to simulate individual occupants and their interactions with buildings. For building designers to fully benefit from these increasingly advanced occupant models, visualizations must ultimately reveal subtle yet informative patterns contained in the simulation results. As a step in this direction, we focus on 3D animation and the challenges that arise when multiple time scales are involved. Specifically, we explore the use of stylized computer animation to clarify occupant movement, the use of cueing to draw attention to key events, and an original clock widget to consolidate time-related information.

1. INTRODUCTION

Numerous experts have pointed out, through informal observations and formal experiments, that humans can have a dramatic effect on the energy required by the buildings they occupy. This understanding has motivated researchers to apply machine learning, complex scheduling algorithms, and other advanced modeling approaches to simulate individual occupants and their interactions with buildings. These detailed models may soon begin to replace the simple 24-hour profiles used in most building simulation tools intended for sustainable design.

This paper is concerned not with development of advanced occupant models, but rather with the visualization of the simulation results they produce. To understand the role of visualization, it is important to note that simulation results comprise not only a final set of calculated quantities such as heating and cooling loads; they also contain subtle yet informative patterns. One example of such a pattern is a high overnight heating load following certain afternoons in which a particular window is manually opened and left open. Simple tables and plots may suffice to show that the overnight heating load is excessive, but they may not provide an explanation. An advanced visualization tool is more likely to reveal that the root cause of the problem is a poorly designed room that overheats under certain conditions, inducing occupants to open the window. The room might then be redesigned to prevent overheating, or repurposed such that it is occupied late in the day when the cooler outdoor air reminds occupants to close the window. This example illustrates that in order for designers to fully benefit from increasingly advanced occupant models, visualization techniques must advance as well.

As a step toward developing effective visualization tools that reveal subtle patterns in occupant simulation results, we focus on 3D animations representing real-world events that unfold over different time scales. The emphasis on multiple time scales reflects the fact that humans can move between rooms or perform short actions in a matter of seconds, whereas longer activities require several minutes or a few hours. Humans also vary their behavior over the course of a day, between days, and between seasons. Naïve attempts to include different time scales in an animation tend to result in complex and rapidly changing scenes, undermining one's perception of motion, events, and time. To address these challenges, we borrow from computer graphics, cognitive psychology, and human-computer interaction. Specifically, we explore the use of stylized computer animation to clarify occupant movement, the use of cueing to draw attention to key events, and an original clock widget to consolidate time-related information.

2. RELATED WORK

2.1. Occupant Simulation

Experts who record and analyze the day-to-day energy-related actions of building occupants tend to reach the same general conclusions: that occupant behavior has a significant impact on building energy requirements; that this behavior is highly variable and therefore hard to predict; and that more realistic occupant models are needed. According to Haldi (2013), the performance of two identical buildings can vary by roughly a factor of two due to diversity in occupant behavior. Therefore, in the same work, diversity is modeled using probabilities derived from eight years of observed window-opening behavior. Urban and Gomez (2013) report that real-world manual thermostat adjustments, recorded over winter in 82 residential units, show that the standard ASHRAE 90.2 model is likely to oversimplify occupant behavior and underestimate heating loads.

Three Ph.D. theses written in the last decade suggest a trend in academia towards increasingly detailed occupant models. Bourgeois (2005) shows how simulations which distinguish between individual occupants can be used to predict the performance of both manual and automated lighting control systems. Page (2007) proposes a method for simulating rooms as they alternate between vacant and occupied states. Because the state transitions are generated randomly based on probabilities derived from measured occupancy data, Page's method represents an example of machine learning and a clear departure from the static 24-hour profiles used to estimate occupancy in most energy modeling tools. Tabak (2008) demonstrates an alternative to machine learning: a complex scheduling algorithm that accounts for the role of each occupant in an organization, the tasks they perform alone and with other occupants, and the layout of a building. A journal paper by Hoes et al. (2009) combines the work of Tabak and Bourgeois and shows that increasing the level of detail of an occupant model may significantly change energy use predictions.

Narahara (2007) approaches occupant simulation from an architectural perspective as opposed to an engineering point of view. The idea is that the observation of simulated occupants may provide various insights into the design of a building, such as the level of privacy offered by each space. Goldstein et al. (2010) also strive to address the needs of designers. They propose a machine learning method which outputs randomly generated schedules of occupant activities reflecting both real-world measurements and architect-supplied personas. This work is extended in Goldstein et al. (2011) to provide a location for each activity that accounts for a building's layout.

Because buildings must be designed to support the day-to-day activities of their occupants, and because early design decisions are widely believed to have a disproportionately large impact on a building's ultimate energy requirements, we anticipate further model developments reflecting a vision of designers as expert practitioners of occupant simulation.

2.2. Visualization of Building Simulation Results

One may expect widespread interest in the modeling and simulation of a particular domain to be followed by a growing interest in visualizing the resulting data. In the field of computation fluid dynamics (CFD), for example, a recent literature review by McLoughlin et al. (2010) cites no fewer than 70 original contributions to the visualization of flow. However, despite recent advances in modeling, the visualization of simulated occupants and their interactions with buildings has received little attention.

In claiming that the visualization of occupant simulation results has received relatively little attention, we must point out that the numerous 3D animations of simulated crowds address only a few of the many aspects of building design. Crowd simulations tend to emphasize survival instincts and adversity towards collisions. While these aspects of human behavior are critical for the study of pedestrian flow and building evacuation, a multitude of other factors are of greater importance for predicting and minimizing a building's energy requirements. Furthermore, animations of crowd simulations are generally restricted to relatively short time periods over which the movement of each simulated occupant is clear. Visualizations of energy-related occupant simulations must be effective for both short and long time scales. The reason is that a single action may require only a few seconds while patterns of human behavior and energy use may unfold over hours, days, or seasons.

A number of techniques proposed for the visualization of measured data could be repurposed to show simulated data instead. Hailemariam et al. (2010) demonstrate various ways to superimpose building performance data on renderings of 3D building geometry. For example, simple geometric shapes are used to represent occupants detected by motion sensors. Also, walls, floors, and furniture are

colored by interpolating data from nearby temperature sensors. Rassia (2008) uses flow maps to show the recorded paths of 56 real-world occupants carrying location tracking devices. Although the flow maps do not represent time and are not presented as the main contribution of the paper, they have the potential to inform design and could easily be adapted to show simulation results instead of measured data. Wijk and van Selow (1999) address the issue of visualizing recurring 24-hour patterns in non-spatial datasets over the course of a year. Any recurring patterns are detected automatically and displayed alongside time series plots using a calendar-inspired graphical tool.

Little previous work can be found in the building simulation field on what we call *multiscale visualization*: the visualization of both recurring and anomalous patterns that involve multiple length scales and time scales.

2.3. Related Work in Other Fields

Formal studies suggest that animations produce better learning and pattern recognition than static images (Höffler and Leutner 2007), and in this work we apply this principle to simulated occupant motion. One of many challenges associated with the multiscale visualization of simulation results is that, if there are movements that are clear when animated over short periods of simulated time, these movements may become incoherent when longer time periods are animated. To address this problem, we turn to non-photorealistic rendering, a sub-discipline of computer graphics which investigates various stylistic techniques to emphasize or communicate certain aspects of a scene or scenario. Of particular interest is the work of Joshi et al. (2005) exploring the application of illustration techniques from traditional hand-drawn images to convey motion. Whereas Joshi et al. focus on movements extracted from CFD results, Haller et al. (2004) present similar stylized computer animation techniques in the context of computer games. The specific techniques considered in Joshi et al. (2005) and Haller et al. (2004) include *speedlines* (called *motion lines* in Haller), *flow ribbons* (only in Joshi), and *strobe images* (referred to as *opacity modulation* in Joshi, *multiple images* in Haller). We explain these techniques and apply them to occupant simulation results in Section 4.

A key visualization challenge is the fact that important events in a simulation may be overlooked if presented while a viewer's attention is focused on other more prominent animated objects. For example, the opening of a window may be a key event with a long-lasting effect on a building's indoor climate and energy requirements. However, because the act of opening of a window is associated with a small region of space and a short period of time, it may go completely unnoticed. The obvious strategy for addressing this problem is to alter animations in a way that draws attention to certain parts of the screen at appropriate points in time. This is one of several goals of *attention cueing* as described in de Koning et al. (2009), a review of related experiments in the field of cognitive psychology. One example of an attention cue is the glowing effect used in animated organizational graphs showing how a company changes structure over time (Khan et al., 2009a).

A third challenge is that, when visualizing multiscale data in animations or interactive software, users can become disoriented in space (McCrae et al. 2009), in time, or in both dimensions. To reduce disorientation in the perception of time, inspiration can be drawn from various graphical tools in the field of human computer interaction (HCI). Dachselt et al. (2008) propose a timeline graphic in which the user can zoom in or out to see representations of time periods of dramatically different durations. Khan et al. (2009b) present a clock-inspired graphic with concentric circles that show how much progress has been made through a presentation, and how much time has elapsed.

3. PROTOTYPE SIMULATION AND RESULTS

We developed a prototype occupant simulation in order to obtain a set of 3D simulation results suitable for exploring a variety of visualization techniques. The model will be explained in detail elsewhere, though here we give a brief overview. The simulation represents the hypothetical two-storey hotel shown in Figure 1, which features 11 guest rooms, a restaurant, a kitchen, an office, circulation areas, and storage space. At any given time the hotel may be occupied by about 10 employees and two or three dozen guests. The simulation tracks the position of each simulated occupant. It also predicts air temperatures, which vary smoothly over the interior of the hotel and change gradually over time.

Each activity and action of each simulated occupant is determined randomly according to probabilities influenced by their role, the time of day, and comfort level. Most of the probability distributions were chosen arbitrarily to produce realistic behavior adequate for visualization research. Guests tend to visit the restaurant during meal times, for example,

whereas employees tend to exit the hotel in the evening. While energy and water consumption were modeled, the only form of occupant-building interaction with a visible effect was the manual opening of windows in response to high indoor temperatures. One run covering 18 hours of simulated time provided a time series of each occupant's changing coordinates and activities. These results were used to produce roughly 40 experimental videos exploring the visualization techniques presented in the following sections.

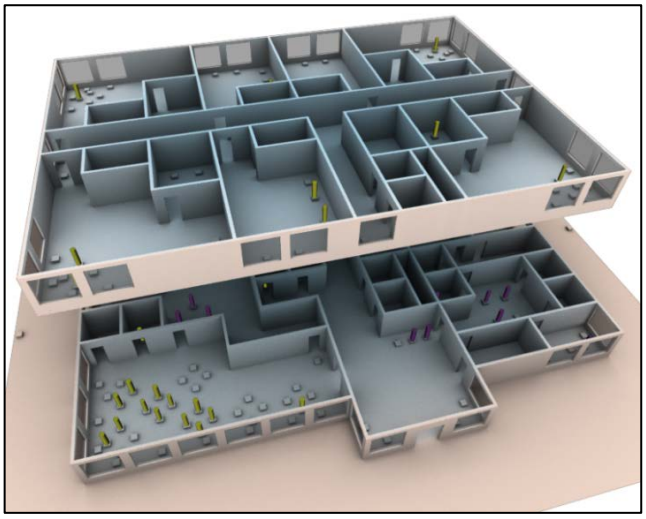

Figure 1. A snapshot of the simulation results. The cylinders represent hotel guests (yellow) and employees (purple). The color applied to the floors and walls indicate cool (blue) and warm (red) temperatures.

4. PERCEPTION OF OCCUPANT MOVEMENT

Previous work in the domain of building evacuation modeling has concentrated on visualizing relatively short time periods. Occupants move slowly and their movement is clearly communicated. However, to make valid inferences in the domain of energy use and comfort modeling, multiple time scales need to be considered, such as hours, days, and weeks. For example, if an occupant walks into a room and immediately closes a window, that might indicate a greater degree of discomfort than if the occupant remains in the room for hours and only then closes the window. To draw such contextual understanding from long simulations in a reasonable amount of time, it is necessary to speed up the playback of the simulation results. However, large *speedup* factors can make motion appear incoherent as objects may move significant distances between animation frames.

Consider a case of trying to compress a long simulation into a 10 second animation played at 24 frames per second (fps). If we want to watch the results of a 1-hour simulation, we would need a speedup factor of 360. Each animation frame would represent 15 seconds of simulated time, in the span of which an occupant can cover around 21 meters (assuming average waking speed of 1.4 meters per second). With simulated occupants covering such distances between frames, motion would appear incoherent. Refer to Figure 2 for an illustration of this problem, where two consecutive frames, images (a) and (b), show simulation results that were speeded up 360 times. Looking at the two frames, one might conclude that occupant A in the first frame is the same person as occupant C in next frame, and that occupant B is the same as occupant D. However, in the image (c) of Figure 2, speedlines are used clarify the movement of the occupants, showing that while occupant A indeed moved to location C, occupant B went down the hallway and a third occupant walked into location D.

The addition of *speedlines* to a scene is an art technique often used to convey motion in print illustration. Unlike particle traces, which are commonly used in engineering applications, speedline curves do not precisely adhere to simulation-generated paths. Instead they are smoothed to more clearly communicate the essence of a motion, ignoring small details and noise in the actual path. Another stylistic depiction is an X-ray effect to communicate hidden activity, achieved by showing speedlines with a decreased opacity when obstructed by the building geometry. See Figure 2(c) and Figure 3(b) for illustrations of this effect.

We vary line thickness along a speedline to help convey the direction of motion and the time since the occupant was present at a location. Thicker lines indicate recent occupant positions, while thinner lines indicate old positions. The maximum line thickness is set to a constant and then scaled to indicate the age associated with the position. In particular, the *scale factor*, s, at a given position along the curve is a function of Δt_{age}, the duration of animation time since an occupant was present at that position.

$$s = 1 - \frac{\Delta t_{\text{age}}}{\Delta t_{\text{fade}}}, \text{where } 0 \leq \Delta t_{\text{age}} \leq \Delta t_{\text{fade}}$$

The input parameter Δt_{fade} represents the animation time required for speedlines to fade away. This parameter stays constant throughout the visualization. For example, with a value of 0.25 seconds for Δt_{fade}, the speedline will disappear after 6 frames of 24 fps animation, after the occupant stops moving. The speedline length increases as Δt_{fade} increases.

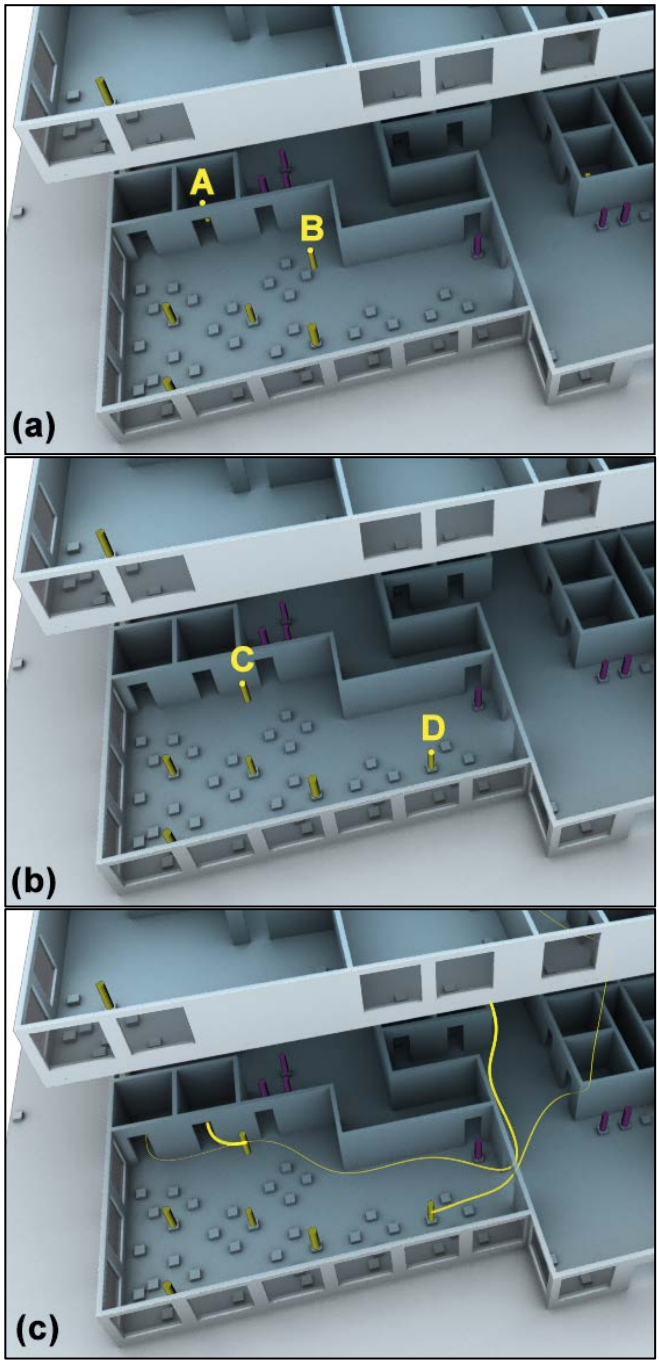

Figure 2. Two consecutive frames (a) and (b) at 360x speedup; image (c) includes speedlines to resolve the ambiguity in occupant movement.

Figure 3 demonstrates the effect of using a small Δt_{fade} in image (a), where the speedline only indicates that the occupant entered the room. The larger Δt_{fade} in (b) also communicates the origin of the trip. Note that increasing the speedup factor also increases the length of the speedlines, as occupants cover greater distances between frames. In Figure 6, a speedup of 3600 results in extremely long speedlines. Each animation frame represents 150 seconds of the simulation, enough time for occupants to move as much as 210 meters.

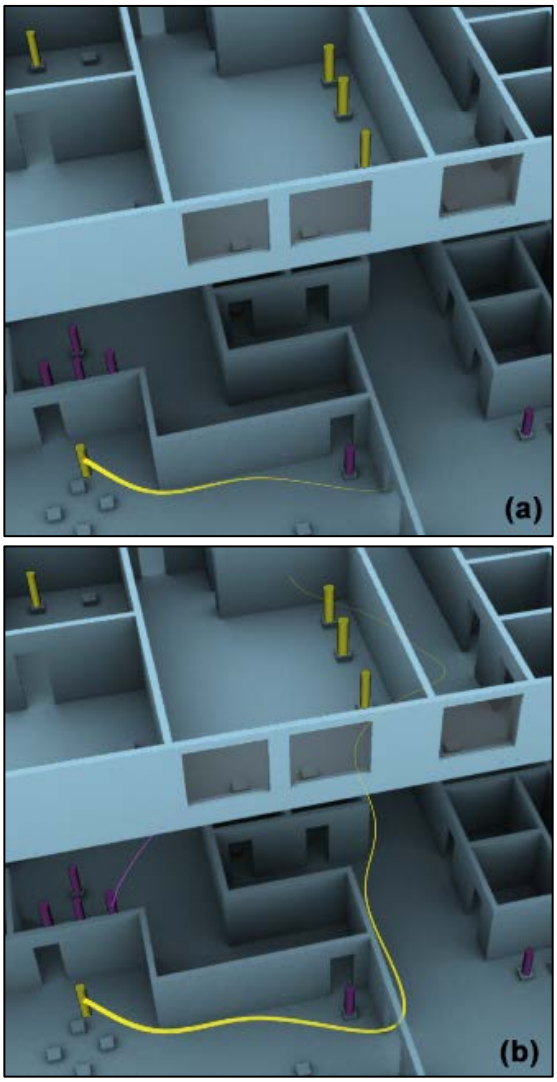

Figure 3. Speedlines, (a) short *speedline*, and (b) longer *speedline*.

The main trade off in picking the right value for Δt_{fade} is that large values will retain movement-related information longer, but increase the visual complexity of the animation. The long speedlines associated with large Δt_{fade} emphasize frequently travelled paths, potentially aiding designers in their understanding of circulation patterns. However, the longer the speedlines, the more likely they are to blend with one another, which partly conceals the motion of individual occupants. This blending of speedlines is likely to occur for complex scenarios animated with high speedup factors.

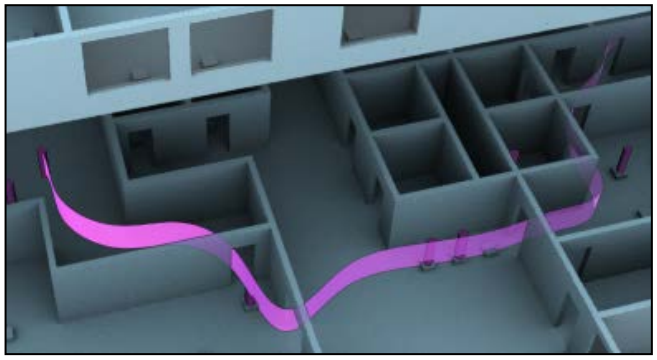

Figure 4. An example of a ribbon tracking an occupant.

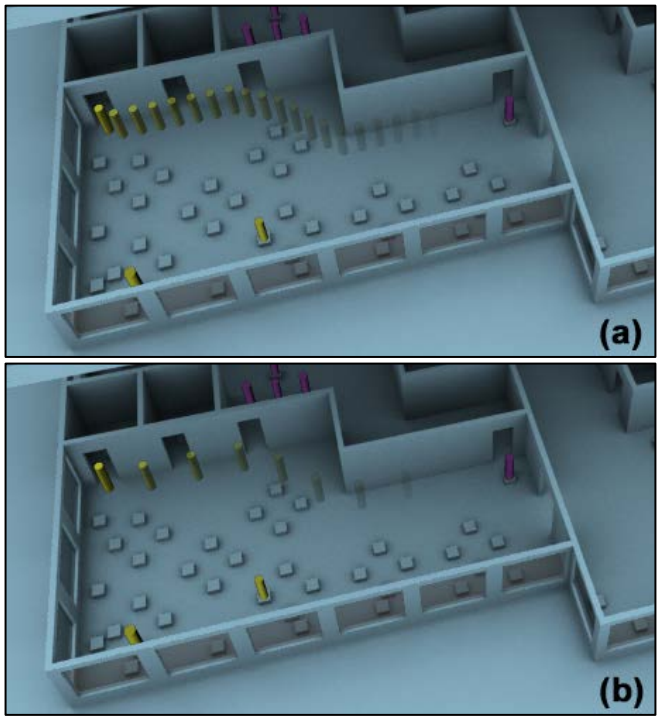

Figure 5. High density (a) and low density (b) strobe visualization.

We have extended our implementation of speedlines to flow ribbons (Joshi et al. 2005), as shown in Figure 4. A *flow ribbon* can be described as the surface between two speedline curves, one trailing the bottom of an occupant and the other trailing the top. Instead of varying thickness, surface opacity is modulated in the same fashion. Unlike speedlines, ribbons convey the relative size of an object, as well as any change in its orientation. In our case only occupant positions were modeled, but if we were to track their orientations as well, ribbons would help communicate events such as falling or lying down. Flow ribbons exhibit a strong visual relationship with 3D geometry, making it clear when occupants move through doorways.

Another artistic motion depiction we explore is *strobe images*. To achieve a strobe effect, an object is drawn several times in a given frame with different opacities, where more transparent versions indicate older positions. As shown in Figure 5, we experimented with the effect using different density levels. Strobe images can reveal subtle details of occupant interactions with the building when used with a more anthropomorphic occupant representation rather than the cylindrical geometry shown in our animations. With a strobed anthropomorphic occupant, activities such as opening windows, switching lights, or pressing elevator buttons would be apparent since the actual occupant shape and action would be represented in each image. For example, it would be easy to distinguish whether a person standing near a window is actually trying to open it, or whether they have simply stopped to enjoy the view. A disadvantage of strobe images is that they may lead viewers to overestimate the total number of simulated occupants.

5. ATTENTION TO KEY EVENTS

Visualizations that overlay multiple types of information have the potential to reveal patterns involving a diverse set of simulated elements and effects. By simultaneously observing temperature, occupant movement, and window states, a designer may become aware of a situation where a poorly designed room leads to overheating, which induces occupants to leave a window open, resulting in increased overnight heating load. There is, however, a drawback to displaying large amounts of information: a key event, such as the opening or closing of a window, may be completely overlooked. The problem is expressed in de Koning et al. (2009) as follows:

> *…it is not surprising that learners often have difficulties in focusing their attention on essential information in an animation, as objects that have high perceptual salience due to their movements easily distract them. This might especially hinder learning in situations where the thematically relevant aspects are not the most salient in an animation.*

In our visualizations of the hotel and its occupants, we observe that the opening of windows can be difficult to spot. While speedlines, flow ribbons, and strobe images seem beneficial for the perception of movement, they attract the viewer's attention and in all likelihood increase the chances of window manipulations going unnoticed. We therefore experimented with a glowing effect, similar to the treatment

of organizational structure changes in Khan et al. (2009a), to cue attention to a window slightly before it is opened. The effect is shown in Figure 6. The green glow is quite salient even in comparison with the long speedlines required to clarify movement over a long time scale.

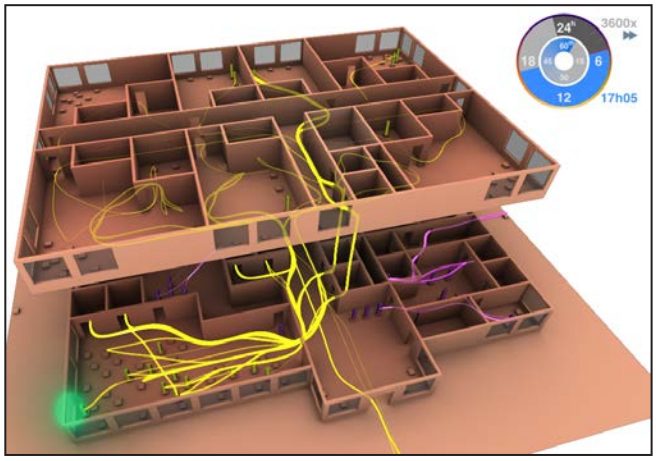

Figure 6. A glowing effect draws the viewer's attention to a window being opened in the hotel restaurant.

Note that the red color in Figure 6 indicates warm late afternoon temperatures. By contrast, the shades of blue in Section 4 reflect an earlier time of day. We are coloring building geometry based on temperature data as previously done by Hailemariam et al. (2010), with the difference that the temperature data is simulated, not measured.

The use of a short-lived glowing effect is an example of cueing in animation applied to simulation results. Previous work reviewed in de Koning et al. (2009) inspires a number of ideas for future research in this area. Another way to emphasize a key event is to slow down the animation while the event is unfolding, then speed it back up once the event has passed. An important lesson from past work is that even if cueing is successful at directing the viewer's attention, it will not necessarily result in better understanding of what the animation represents. User studies evaluating a wide range of new and existing visualization techniques could provide valuable insights into how designers observe and interpret patterns found in detailed simulations.

6. PERCEPTION OF TIME

Time plays a crucial role in simulation, and it is therefore essential that visualizations clearly communicate the temporal context associated with each event. This temporal context applies to time as represented in the simulations, as well as the progress one has made through the animation. We have designed a custom clock widget, illustrated in the top right corner of Figure 6 and in more detail in Figure 7, that consolidates time-related information pertaining to simulated events and the visualization itself.

To help the viewer associate simulated events with their associated periods of simulation time, the inner ring of the clock shows the minutes of the current hour, and the outer ring shows the hours of the day. A narrow band of color surrounds the outer ring with dark purple near midnight and light yellow near noon. This provides a non-numerical indication of the time of day to supplement the clock labels.

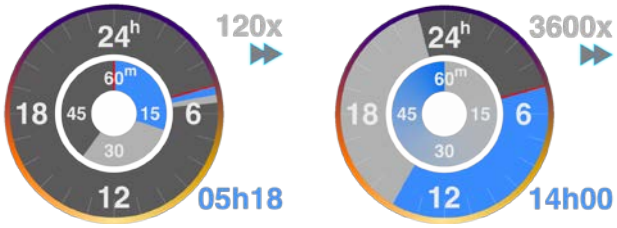

Figure 7. Clock widget at speedup rates of 120x (left) and 3600x (right).

The start time of the simulation is shown with a red line. To show the total time period covered by the simulation, sections of the rings are colored light gray while inactive periods are colored dark gray. The elapsed duration of the simulation is shown using a blue radial progress bar, which gradually fills the light gray area. If the simulation exceeds an hour, the inner radial progress bar fades away rather than forming a solid color slice, since the simulation duration is outside the range of 60 minutes. To precisely communicate the current time of the simulation, a numerical time value of both hours and minutes is shown in the bottom right corner of the widget in a blue color matching the color of the progress bar inside the clock's rings. Since the time scale is hard to perceive with large speedup factors, a numerical value of the factor is shown in the top right corner of the widget with a fast-forward symbol below it. To minimize distraction from the primary visualization, the clock is placed in the corner where it is somewhat unobtrusive yet easily referenced. The widget clearly indicates when an animation loops, as the blue sections reset to light gray.

While currently our widget only supports minutes and hours, in the future we plan to generalize it to work on larger scales such as days, weeks, months, etc. This direction of generalization motivated the decision to place the hour ring of the clock on the outside of the minute ring,

in contrast with traditional analog clocks where the hour hand is shorter than the minute hand. The principle behind placing hours on the outside is to keep transitions in spatial and temporal representations consistent: one zooms out on a projection of a 3D model to reveal larger spatial scales; one should "zoom out" on the clock widget to reveal additional rings for days of the week, weeks of the month, months of the year, and larger time scales as needed.

7. CONCLUSION

To help designers understand increasingly complex occupant simulation results, we have explored the use of several visualization techniques inspired by previous work in non-photorealistic rendering, cognitive psychology, and human-computer interaction. The results of a prototype simulation were animated at different speeds, demonstrating how speedlines, flow ribbons, strobe images and attention cues can clarify the movement of occupants and emphasize their interactions with a building. To situate events in both simulation and animation time, we designed a scalable, novel clock widget. We have demonstrated how several multiscale visualization challenges can be addressed for simulated patterns unfolding over seconds, minutes, and hours. Future research is needed to extend these techniques to days, seasons, and years. Also, user studies are necessary to quantitatively evaluate the strengths and weaknesses of each technique. This paper represents an early step towards enhancing sustainable design tools with automatically generated 3D visualizations effective for discovering subtle details in simulation results featuring multiple time scales.

References

BOURGEOIS, D. 2005. Detailed Occupancy Prediction, Occupancy-Sensing Control and Advanced Behavioural Modelling within Whole-Building Energy Simulation, Ph.D. Thesis, l'Université Laval, Canada.

DACHSELT, R., FRISCH, M. AND WEILAND, M. 2008. FacetZoom: A Continuous Multi-Scale Widget for Navigating Hierarchical Metadata. Proceedings of the SIGCHI Conference, Florence, Italy, 4 pages.

DE KONING, B.B., TABBERS H.K., RIKERS, R.M.J.P. AND PAAS, F. 2009. Towards a Framework for Attention Cueing in Instructional Animations: Guildines for Research and Design. Education Psychology Review, vol. 21, 28 pages.

GOLDSTEIN, R., TESSIER, A. & KHAN, A. 2010. Customizing the Behavior of Interacting Occupants using Personas. Proceedings of the SimBuild IBPSA-USA Conference, New York, NY, USA, 8 pages.

GOLDSTEIN, R., TESSIER, A. AND KHAN, A. 2011. Space Layout in Occupant Behavior Simulation. Proceedings of the International IBPSA Conference, Sydney, Australia, 8 pages.

HAILEMARIAM, E., GLUECK, M., ATTAR, R., TESSIER, A., MCCRAE, J. AND KHAN, A. 2010. Toward a Unified Representation System of Performance-Related Data. Proceedings of the eSim IBPSA-Canada Conference, Winnipeg, Canada, 8 pages.

HALDI, F. 2013. A Probabilistic Model to Predict Building Occupants' Diversity Towards their Interactions with the Building Envelope, Proceedings of the International IBPSA Conference, Chambery, France, 8 pages.

HALLER, M., HANL, C. AND DIEPHUIS, J. 2004. Non-photorealistic rendering techniques for motion in computer games. Computers in Entertainment, 2(4), 10 pages.

HOES, P., HENSEN, J.L.M., LOOMANS, M.G.L.C., DE VRIES, B. AND BOURGEOIS, D. 2009. User behavior in whole building simulation. Energy and Buildings, 41(3), 8 pages.

HÖFFLER, T AND LEUTNER, D 2007. Instructional animation versus static pictures: A meta-analysis. Learning and Instruction, 17(6), 722-738.

JOSHI, A. AND RHEINGANS, P. 2005. Illustration-inspired techniques for visualizing time-varying data. Proceedings of the IEEE Visualization Conference, Minneapolis, MN, USA, 8 pages.

KHAN, A., MATEJKA, J., EASTERBROOK, S. 2009a. The Role of Visualization in the Naturalization of Remote Software Immigrants. Proceedings of the Software Engineering Conference, Kaiserslautern, Germany, 6 pages.

KHAN, A., MATEJKA, J., FITZMAURICE, G., KURTENBACH, G., BURTNYKA, N. AND BUXTON, B. 2009b. Toward the Digital Design Studio: Large Display Explorations. Human–Computer Interaction, 24(1), 39 pages.

MCCRAE, J., MORDATCH, I., GLUECK, M. AND KHAN, A. 2009. Multiscale 3D Navigation. Proceedings of the ACM Symposium on Interactive 3D Graphics, 8 pages.

MCLOUGHLIN T., LARAMEE R. S., PEIKERT R., POST F. H. AND CHEN M. 2010. Over Two Decades of Integration-Based, Geometric Flow Visualization. Computer Graphics Forum, 29(6), 23 pages.

NARAHARA, T. 2007. The Space Re-Actor: walking a synthetic man through architectural space, Master's Thesis, Massachusetts Institute of Technology, Cambridge, MA, USA.

PAGE, J. 2007. Simulating Occupant Presence and Behaviour in Buildings, Ph.D. Thesis, École Polytechnique Fédérale de Lausanne, Switzerland.

RASSIA, S. 2008. The analysis of the role of office space architectural design on occupant physical activity. Proceedings of the International Passive and Low Energy Architecture (PLEA) Conference, University College Dublin, Ireland, 6 pages.

TABAK, V. 2008. User Simulation of Space Utilisation: System for Office Building Usage Simulation, Ph.D. Thesis, Technische Universiteit Eindhoven, Netherlands.

URBAN, B., GOMEZ, C. 2013. A Case for Thermostat User Models. Proceedings of the International IBPSA Conference, Chambery, France, 8 pages.

VAN WIJK, J. J. AND VAN SELOW, E. R 1999. Cluster and Calendar based Visualization of Time Series Data. Proceedings of the IEEE Symposium on Information Visualization, 5 page.

Session 4: Interactive Environments **59**

Tangible 3D Urban Simulation Table 61
Flora Salim
RMIT University

Typologies of Architectural Interaction: A Social Dimension 65
Seoug Oh, Veronica Patrick, Daniel Cardoso Llach
Design Ecologies Laboratory, The Pennsylvania State University.

Designing Fluvial Sites: Digitally Augmented Physical Hydraulic Modeling 73
Alexander Robinson
USC School of Architecture.

Tangible 3D Urban Simulation Table

Flora Salim

RMIT University
GPO Box 2476,
Melbourne, VIC 3001, Australia
flora.salim@rmit.edu.au

Keywords: Tangible Interaction, Urban Simulation, Spatial augmented Reality, Tangible Table, Wind Tunnel Simulation.

Abstract

Design models for an urban landscape could simulate how design alternatives perform with regards to volatile environmental phenomena, human movements and social interactions in the city. This paper presents a low-tech markerless approach to designing and developing a tangible 3D urban simulation table, using an ordinary table, generic building blocks and fabricated urban models, a Kinect and a projector. The digital 2D scene was projected on the table, in response to the forms and configurations of physical 3D models on the table. The installation that was developed for a public exhibition was specifically designed for visualizing wind flows and speed on an urban site. Users can get their hands on the 3D tangible building blocks to change the configuration of the urban model on the table and get a sense how it influences the wind flow around the site.

1. INTRODUCTION

Consider this scenario. In a dimly lit room, a team is gathered around a table, on which sits a collection of 3D building models of different height and volume that represent a topographic representation of an actual urban precinct. As the tangible building blocks are arranged into different configurations, patterns of wind flow emerge across the table. The wind simulation that runs on the site is projected on the table, with variable wind direction and velocity visualized as a flow of particles with various density and speed around the buildings. The team could use the 3D building blocks to explore the effect of any given building design on the site in regard to local wind conditions. Through careful manipulations performed on the set of blocks, users could find urban volumetric configurations that could potentially divert, slow down or cancel the wind in the area (Figure 1).

Different design options for new developments on a vacant land parcel in a particular urban precinct can be explored on the table. Architects and engineers could rotate the 3D tower model to see if a curved facing façade or a flat facing façade would work best against the prevailing wind, and discover the most optimal orientation and form of the new tower that would minimize local turbulence or reduce high wind pressure on pedestrianized areas around the building. Similarly, the same exercise can also be applied to discover where to best place a new bus shelter, transit hub, or a natural or artificial windbreak in an existing urban site or pedestrian areas that are inflicted with strong winds, and discover the forms and typology that would work best for the context of the site.

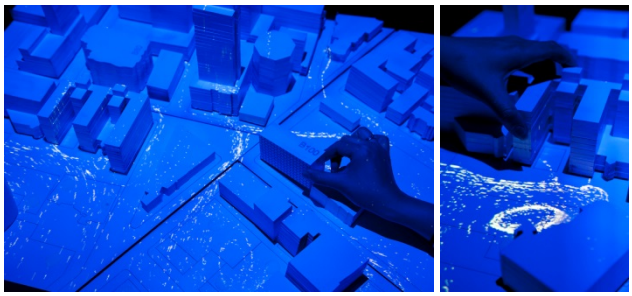

Figure 1. The low-tech tangible 3D urban wind simulation table.

Those are the example scenarios that can be explored in the tangible urban simulation table presented in this paper. The projected feedback of the contextual and real-time analysis of the geometry, size, and orientation of a group of 3D urban models on the table allow the visual testing of "what-if" urban scenarios against the real-time and historical urban context in preliminary design exercises. Using 3D scanning and spatial projection, real-time data analysis, and physics simulation, the tangible urban simulation table presented in this paper demonstrates a powerful new approach for designing and interacting with flexible and modular 3D physical building blocks, environmental, and urban data for collaborative

architectural and urban landscape design in the early design stage.

We consider this as a low-tech prototype, as the installation uses an ordinary table surface on which to place the three-dimensional building models and combines a low cost 3D depth-sensing camera (Kinect) and spatial projection of a real-time fluid simulation on the surface. Although it is a low-tech set up, the visualization content enables it to look like a hi-tech tool with its intuitive visual design and instantaneous feedback to changes on the table. Any 3D models or arbitrary objects can be used as input on the table. The installation itself is essentially an interactive digital wind tunnel with physical building blocks as input devices for collaborative design and planning exercises.

2. RELATED WORK

Tangible user interfaces emerged as tabletops in the 1990s as a media for social computing. Urp, a tag-based Luminous Table for urban planning (Underkoffler and Ishii 1999), was developed for designers and urban planners to gather around a simulated view of the entire urban planning stage and manipulate the positions and orientations of the building blocks on the table. There are two major limitations of the Urp table. First, Urp used static objects and trackers, or building blocks that have a fixed geometry and cannot be flexibly modeled in real-time. The architectural models in Urp used predetermined forms. The system relies on attaching visualised information to pre-existing models and must correspond at least in its dimensions to the simulation that will be overlaid on it (Underkoffler and Ishii 1999). This renders a system like Urp not applicable for form-finding exercises in the early stage design of new architectural design and urban development projects. Second, the wind simulation in Urp is projected at a modest eight Hertz (Underkoffler and Ishii 1999), and only takes a limited number of objects as input to the airflow simulation.

Another tangible tabletop for urban planning is ColorTable (Maquil et al. 2008), an interactive design tool based on color blocks and barcodes, representing different design elements that the user can move and organize to test different ideas in a collaborative context. The strength of the system was in its capabilities for creating a global database with different design components. However, ColorTable did not have an associated analysis process that supports architectural decision making in all stages. Users of the ColorTable tested different ideas using 2D maps, plans, and cards that represented symbolic building blocks and infrastructures. There is no facility for 3D inputs that support the creation of flexible architectural or urban landscape models. The ColorTable was set up in the MR-Tent (Wagner et al. 2009), a mixed reality environment for community participation in creating a vision for an urban project. This project was set up as a visualization and navigation tool for probing the stakeholders of a city or a potential urban project to discuss urban planning issues, mainly revolving around the development or placement of specific infrastructure and services on site. However, such a tool, useful in urban planning, is not applicable for architectural and urban landscape design since it does not cater to flexible 3D objects and materials. ColorTable relies on color-coded blocks and tokens as input devices.

3. DESIGN AND DEVELOPMENT PROCESS

The following are the four major components that need to be designed and developed for any low-tech tangible 3D urban simulation table:

1. 3D scanning and 2D/3D geometry reconstruction
2. Physical 3D models
3. Digital simulation taking 2D/3D geometry as input
4. Projection and digital data augmentation.

The key component that enables scanning and monitoring of physical objects and surfaces is Xbox Kinect, a popular and affordable vision sensor with built-in depth sensing camera. With Kinect, 3D objects can be detected and recognized, and gesture detection has never been easier to implement. Since its release at the end of 2010, Kinect has been utilized for various purposes such as for videoconference support (DeVincenzi et al. 2011), vision-based sensing in robotics (Krainin et al. 2011), and gesture-based interaction with objects in virtual environments (Santos et al. 2011). StereoBlocks demonstrated the use of Kinect to scan physical building blocks, which are used to construct virtual 3D models that are projected side-by-side on the table next to the physical objects (Jota and Benko 2011). StereoBlocks is less intuitive than the method and demonstration presented in this paper, and not appropriate for the complexity of urban models as presented in this paper. For the tangible 3D wind tunnel simulation table, the following is the design and development process.

3.1. 3D Scanning and Geometry Reconstruction

First, arbitrary foam models hand-cut manually using hot wires were made. Microsoft Kinect was used to scan the 3D models. The objects were analysed using blob detection and depth analysis maps to reconstruct the digital 3D

representation. In essence, any arbitrary models of any size and shape can be used for this purpose. Figure 2 (right) demonstrates an initial experiment using Kinect that correctly detects the objects on the table and draws bounding boxes around the objects.

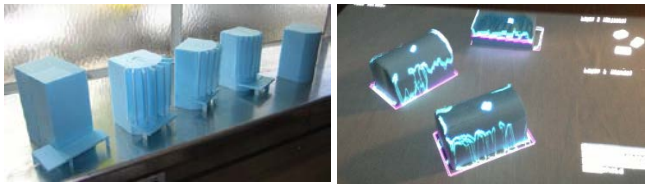

Figure 2. Arbitrary hot-wired cut foam models.

3.2. Physical 3D Urban Models

For the installation of the tangible urban wind simulation, it is essential to demonstrate that the simulation can work on a high-density urban model and still produce highly responsive feedback. Therefore, an actual city model scaled to 1:500 (Figure 3) was modeled and fabricated using a 3D laser cutter. The material chosen for this purpose was MDF (Medium Density Fibre) boards, a type of wooden material. The laser-cut MDF models were then painted in white to allow clear projections (Figure 4).

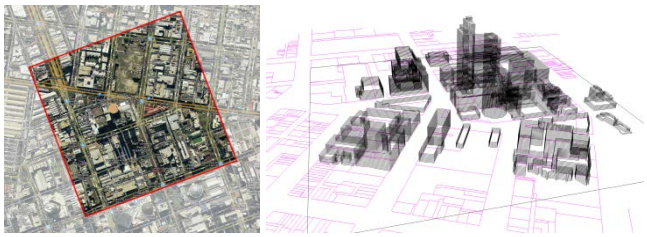

Figure 3. 3D urban model of the city.

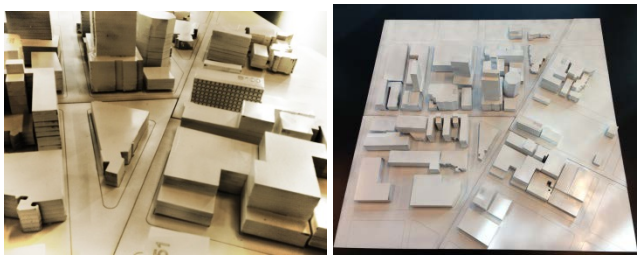

Figure 4. Laser-cut urban models.

3.3. Digital Wind Simulation

The third component is the simulated wind flow based on the digital representation of the physical objects. To simulate the motion of air, the grid method of fluid dynamics was used based on Navier-Stokes equations [7]. The space was divided into a two-dimensional grid and the fluid as air occupied its individual cells. The grid could be understood as two overlapping grids; one for storing the density of the air as a density field, and the second to store its velocity, as a vector field. Each point inside the grid had a velocity vector and a density value. The maximum density of the particles is set to the resolution of the screen. The calculation of the air flow is based on Jos Stam's simplified Navier-Stokes algorithm [7].

Real-time visualization demands fast computation, and thus degrades the precision of the analysis. This tangible tool did not employ full-fledged computational fluid dynamics, as such an analysis will require days to complete. Instead, a simplified version of the fluid analysis and visualization was implemented. The main purpose of the dynamic feedback is to give users intuitive performance feedback on their preliminary ideas of their design. In further research we will be evaluating the precision deviations, in this case by implementing the more advanced fluid dynamic methods. Therefore, even though our fluid dynamics simulation was able to operate in 3D, we used it only in 2D, as it would be necessary to sync multiple Kinect to determine the 3D shapes of the models of the buildings properly. Also, the 3D simulation would not be able to run in real time. Therefore, each building model was scanned and a 2D planar slice of the model was set as an input in the vector field of the fluid simulation. From each edge of the polygon a vector was calculated, which adjusted the vector field of the fluid dynamics. As a result, the particles representing air flow move and change velocity according to this vector and density fields, and also flow around the obstacles. The length and size of each particle is mapped to the velocity.

3.4. Projection and Digital Data Augmentation

The final step is to integrate the three and calibrate the system. The table is 1m x 1m, placed in a 3m x 3m dark curtained area. The augmentation of the digital urban simulation on the surface employs the use of an ordinary HD data projector. The Kinect and the projector need to be calibrated to scan and project on the same area of the table. For the purpose of the exhibition, we found that the table had to be suspended at chest height to provide the best matching throw distance for the projector and the scanning area for the Kinect. Having the table at chest height also allows very intimate interactions with the tangible objects and a more immersive experience for the users.

The two video processing streams (for Kinect and the projection), and the wind simulation, all run on a standard Dell Desktop PC with embedded Intel HD integrated graphics, with no discrete graphic cards. The fluid

simulation works on a low-density configuration of arbitrary 3D objects (Figure 5). It also works well for a complex and high-density urban model (Figure 6).

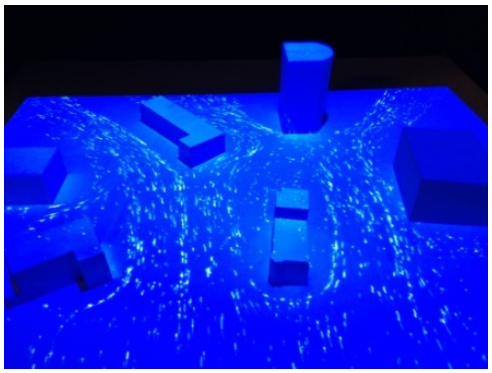

Figure 5. Wind simulation with low-density 3D objects.

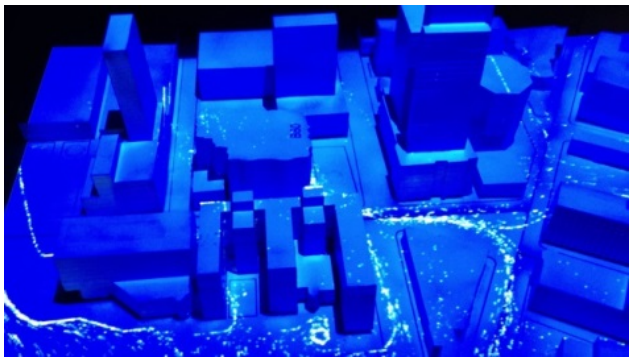

Figure 6. Wind simulation with high-density 3D urban models.

4. PRELIMINARY EVALUATION

The installation was one of the exhibits in a three-week public exhibition. The event draws attendance from architects, engineers, urban designers, urban planners, practitioners from the construction industry, students from various disciplines, and also the general public. Attendees were invited to interact with the objects on the table, construct and deconstruct the city, and perform form-finding exercises to discover wind patterns and flows, as shown on Figure 1. The following responses were recorded during the event: “Impressive”; “Extremely responsive”; an engineering professor said, “I could use this to teach wind tunnel effects to my students”, a group of engineers said, “This is a very intuitive tool, useful for early design”, a student said, “Now I know why that part of the road is very windy”.

5. CONCLUSION

This project explored the concept of interacting with a digital model through the use of tangible objects for rapid experimentation with forms and shapes. It presents an affordable opportunity to create and participate in a tangible interaction platform for collaborative urban design. By creating an interface to the digital models integrated with an environmental simulation, a real-time feedback loop can be computationally augmented on the tangible physical representation. In the early stages of design, tangible interfaces can be used to mediate expert and non-expert users in a collaborative environment and as an input device to 3D CAD software for digital modeling and further analysis. This table is envisioned to influence the design and decision making process in architecture, engineering, the construction industry, and urban and town planning exercises. Future works include evaluating the table for use in architecture and construction projects. Future versions of the table will have a series of "layers" which will allow users to view other types of analysis data. It will also employ a 3D fluid solver to improve the accuracy of the wind simulation. To do this, further research into the use of high performance computing is required.

Acknowledgements

The author would like to thank Jane Burry, Gerda Gemser, Sarah Pink, Kerry London, and Mark Burry for their support, RMIT Design Research Institute for the seed funding for the project, and Australian Research Council’s Linkage grant no. LP120200305.

References

DeVincenzi, A., Yao, L., Ishii, H., Raskar, R. 2011. Kinected conference: augmenting video imaging with calibrated depth and audio. In Proc. CSCW ’11, ACM.

Jota, R. and Benko, H. 2011. Constructing virtual 3D models with physical building blocks. In Proc. CHI EA’11, Extended Abstracts on Human factors in computing systems, ACM.

Krainin, M., Henry , P., Ren, X., and Fox, D. 2011. Manipulator and object tracking for in-hand 3D object modeling, The International Journal of Robotics Research, July 7.

Maquil V., Psik T., Wagner I. 2008. The ColorTable - A Design Story, In Proc. TEI 2008, Feb 18-21, Bonn, Germany.

Santos, E. S., Lamounier, E. A., Cardoso, A. 2011. Interaction in Augmented Reality Environments Using Kinect. In Proc. XIII Symposium on Virtual Reality (SVR ’11), IEEE Computer Society.

Stam, J. 2003. Real-Time Fluid Dynamics for Games. In Proc. the Game Developer Conference.

Underkoffler, J. and Ishii, H.. 1999. Urp: A luminous-tangible workbench for urban planning and design. In Proc. CHI 1999, ACM, 386–393.

Wagner I., Basile M., Ehrenstrasser L., Maquil V., Terrin J., Wagner M. 2009. Supporting community engagement in the city: urban planning in the MR-tent, In Proc. of Communities and Technologies, June 25 - 27, University Park, PA, USA.

Typologies of Architectural Interaction: A Social Dimension

Seoug Oh[1], Veronica Patrick[2], and Daniel Cardoso Llach [3]

Design Ecologies Laboratory
The Pennsylvania State University
121 Stuckeman Family Building
University Park PA, USA, 16802
[1]szo124@psu.edu, [2]vrp5027@psu.edu, [3]dzc10@psu.edu

Keywords: Responsive Architecture, Interaction Design, Human-Centered Design, Smart-Skin.

Abstract

Interactive architecture is concerned with exchanges between humans, environmental factors, and the built environment. These systems are commonly presented as instruments to a) maintain adequate levels of interior lighting and temperature adapting to occupants' needs, and b) reduce building energy consumption by autonomously regulating solar intake in response to environmental factors (Cardoso et al. 2011). While these approaches have yielded promising questions and applications, in this paper we are more interested in exploring interactive architecture's potential role as catalyst for social activity. First, we analyze a selection of contemporary, interactive architecture projects, proposing a set of typologies of architectural interaction driven by the kind of exchanges each project establishes with both occupants and the environment. Second, we test these typologies through a controlled experiment with a responsive artifact that we use as a platform to investigate different types of interactivity and their effects on social activity. In one study, for instance, our responsive artifact is programmed to respond solely to environmental factors. In the second study, it is programmed to respond exclusively to human input. By presenting the typologies, the prototypes, and our observations about the interactions they enable, this paper proposes a new way of thinking "socially" about interactive systems, expanding on a crucial ongoing discussion about the relationship between interactive buildings, humans, and the environment.

1. INTRODUCTION

Architecture not only provides us with shelter from the harsh external environment but can also be interpreted as an index of its social and cultural context. For instance, the plain and protruding facade of Moller house by Adolf Loos has been interpreted as a symbol of "the isolated condition of the modern-man" (Colomina 1996); others have suggested that smooth and seamless spaces reveal contemporary anxieties and an "impossibility to dwell" (Vidler 2002); some interpret the networked, patterned surfaces of contemporary architecture as a manifestation of today's fluid identities—elements existing in connection to each other yet easily shifting states between different conditions (Picon 2013). What do interactive facades tell us about the cultures that produce them? How can we ask questions of cultural meaning through the definition of interactive architectural systems?

Based on our findings, we believe that interactive architecture presents an opportunity to index key aspects of our digitally-mediated and networked society. More importantly, we hypothesize that interactive architecture can be a device to re-signify social space. In this case the concept of social is not limited to a mere interaction between human actors, but is instead understood as an environment jointly configured by humans and non-human actors—and even exclusively by non-human actors. Our research takes off from this position, directing attention to the social questions raised by interactive architecture, and (tactically) away from sustainability themes. In what follows we define typologies of interaction within contemporary interactive architectural practice, and examine the social dimension of these typologies through experiments and prototypes.

2. TYPOLOGIES OF INTERACTION

2.1. Overview: Charting the Territory

Cybernetics, "the science of control and communication, in the animal and the machine" (Wiener 1948) introduced a way to understand a mechanism based on its behavior. By analyzing a mechanism in relation to communication, a complex system consisting of a multiple elements can be understood in a relatively simple and clear manner without much consideration for the underlying logic of each component. Key to cybernetics is the distinction between a "conversation" and a "reaction." A *conversation* requires an exchange of information between two or more independently intelligent agents resulting in unscripted conclusions, whereas a *reaction* is a one-way transfer of information that generates pre-determined conclusions (Frazer 1993). We started by searching for typologies within existing interactive architecture projects using these two concepts as a framework for categorization. However, these two concepts did not adequately situate, in our view, the unique capacity of (large) architectural cybernetic systems to foster collective forms of social interaction. We then added a social "vector" to our cybernetic analytic frame.

The projects we analyzed were chosen somehow arbitrarily from numerous sources, including Interactive Architecture, The Creators Project global network and ACADIA, among others (Fox and Kemp 2009; Intel and VICE 2010; Mitchell et al. 1981). To the best of our knowledge, the projects we chose represent a wide sample of interactive architectural approaches that expose trends within the discipline. It is important to note that we did not intend to give a comprehensive picture of the field, nor to be all-inclusive. Our intent was to identify different types of interaction that have been deemed desirable end goals by practitioners of interactive architecture. While our list includes academic research projects, we privileged projects with an artistic and/or commercial bent—including built installations and commercial buildings. The sample comprises twenty-eight existing projects and twelve published papers spanning from 1997 until 2013 (see Appendix). In consideration of the kind of interaction each project incited, we placed them in a radial diagram describing what we have defined as the typologies of Reactive, Conversational, and Social interaction (See Figure 1).

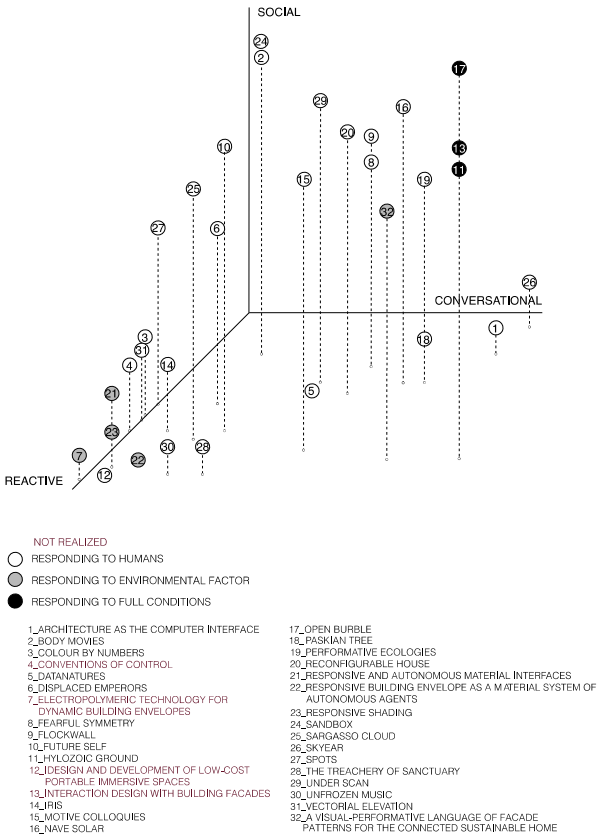

Figure 1. Typologies of interaction space. This diagram shows the categorization of selected projects placed relationally within the framework of our typologies: *reactive, conversational* and *social.* Many projects contained characteristics of multiple categories; therefore it was necessary to depict them within a 3-dimensional space.

2.2. Reactive Projects: Single Loop Systems

In our analysis, "Reactive" refers to projects that enable a "single loop" of interaction with pre-determined outcomes. "Single loop" refers to a one-directional flow of information between two or more agents. Namely, there is a clear distinction between the input and output, with the input parts dominating the output parts (Ashby 1957). This form of interaction is reactive rather than interactive (Haque 2006).

We identified a large number of projects as predominately Reactive. An example is "Electropolymeric Technology for Dynamic Building Envelopes" (#7) (Krietemeyer et al. 2011). This project explores possible variations of electroactive polymers (EAP) and their effects on reducing glare discomfort and increasing energy performance. The EAP glazing rolls up or down after receiving a small voltage, pre-determined to control solar

gain. Another example of an almost exclusively Reactive project is "Design and Development of Low-Cost Portable Immersive Spaces" (#12) (Pak et al. 2011) This project aims to develop a portable immersive space, serving as an interface to a controlled virtual environment, in which people interact using simple gestures. To successfully manipulate the space, users require knowledge of a set of pre-defined hand motions that trigger specific responses. In both examples of Reactive projects mentioned above, the interactivity consists of a one-directional mapping between an action and a response.

2.3. Conversational Projects: Coupling Systems

In our analysis, *Conversational* refers to systems where two or more agencies are coupled, mutually affecting each other. Projects in this territory do not necessarily have a single goal; instead, the interacting agencies construct a common outcome through their mutual reconfiguration.

Our definition of "Conversational" owes to Gordon Pask's Conversation Theory, which developed the concept of mutual feedback most often associated with early cybernetics. Crucial to Ashby's theory is the notion that when different mechanisms are connected in order to form a large system, the system is coupled. "Two or more whole machines can be coupled to form one machine; and any one machine can be regarded as formed by the coupling of its parts, which can themselves be thought of as small, sub-machines" (Ashby 1957). The key point of a coupled system is the emergence of new features that differ from the behaviors each mechanism displays individually, occurring in the system by virtue of the reciprocal communication, or coupling, of the different mechanisms. Pask thus emphasizes the mutual "heuristic experience" between human and machine. According to him, participants partaking in a conversation are able to develop unique understandings and experience unforeseen conclusions.

In our catalogue, one example of a predominately "Conversational" project is "SkyEar" (#26) (Haque 2004). The piece consists of ultra-bright LEDs planted within a carbon fiber net and balloon structure floating 60-100m above the ground. The color of the form changes in response to the electromagnetic environment where storms, mobile phones, radio signals and television broadcasts all provide input. The process of participants calling the structure, listening to the sky and taking part in actively changing its colors is the focus of the piece. According to its author, through the communication of agencies, "humans and devices and their shared environments coexist in a mutually constructive relationship" (Haque, 2007).

2.4. Social Projects: Collective Systems

While researching projects that could be described using the cybernetic frame, we came across a type of interaction many designers were striving for, which was not represented in the technological definitions: "Social." *Social* is a very ambiguous term, but for our purposes, we defined it as activities where two or more human entities interact with each other. Projects in this territory incite interactions involving multiple actors. In our Catalogue, the large-scale installation works of "Relational Architecture" by Rafael Lozano Hemmer stand out in this category. One such project is "Body Movies" (#2) (Lozano-Hemmer 2001). For this experiment, the artist projected a video feed onto the facade of a movie theatre in Rotterdam. These projections were then washed out by two large xenon lights and only reappeared when the shape of someone's shadow provided enough darkness. The intended game's attractiveness paled in comparison to the participant's desire to interact playfully with each other's magnified shadows. Another example, "Sandbox" (#24) (Lozano-Hemmer 2010), consists of projections between two groups of people at two different scales; thus allowing them to communicate through gestures and movement although they are not physically close to each other. Through artifacts like these, social becomes "far more subtle, passive, and subconscious" (Fox and Kemp 2009). In this territory, the way in which the artifact is set up is less important, as it is meant to be a catalyst for human-to-human interaction, not the center of attention.

2.5. A note on typology: a continuous space

We initially used a 2-D diagram to represent the typological space of interactive architecture. However, it became apparent that "reactive," "conversational," and "social" were not always exclusive attributes of interactive architecture projects, and were better understood as dimensions of a more fluid landscape of interactional strategies. Although defining the criteria for each typology was crucial, projects would rarely fit neatly into just one typology. We thus represent our typologies in a 3-D space (See Figure 1). This representation allows us to identify certain clusters of particular interest. For instance, we identify a new genre of social space characterized by interactive architecture projects located "in-between" our "social" and "conversational" typologies. These spaces are

characterized by multitudes of both human and non-human actors engaging in communication. For instance, the pavilion installation "Flockwall" (#9) (Fox 2009) contains an array of kinetic artifacts that respond to inhabitant movement with a swarm-like intelligence. This creates a collective social environment where multiple conversations flow freely between groups of humans and artifacts, defining, in our view, a new kind of public social space.

Analytical advantages of categories notwithstanding, it is important to note that no human action can be fully prescribed by the design of an interactive architecture system. The possibility for social activity to occur serendipitously exists within any of our categories. For example, projects that interact with humans are expected to encourage a passerby to engage with the artifact but those that respond to environmental factors may grasp the attention of pedestrians curious about the underlying logic of its autonomous behaviors. Additionally, projects intended to promote social activity may become dull after a certain period of time, as people who participate become tired with its reaction and no longer have the desire to play. Therefore, a measure of achieved social activity may not directly relate to design intentions.

3. HYPOTHESIS

Interactive architecture's capacity to characterize physical space inscribes new design opportunities to shape social interaction. Now that human to non-human systems have made interaction designable and increasingly affordable we suggest that qualitative aspects of social activity is designable as well. We thus hypothesize that the implementation of interactive architecture can both help trigger and *qualify* social activity within a space, within certain margins, through the interactional design of the artifact itself.

4. EXPLORATIONS

4.1. Overview

The ultimate objective of our study is to spark a discussion regarding the social dimension of interactive architecture. Based on our typological study, we designed and tested two different interactive situations, configured by a series of programmable interactive modules we also designed. By tactically changing the modules' program, we were able to observe the effects of different kinds of interactive behavior on people. In Situation 1, the modules are programmed to respond solely to environmental inputs (temperature). In Situation 2, the modules are programmed to respond solely to human motion. By observing and recording people's reactions, we try to interpret the social effects of each interactive strategy. Which situation spurred more lively social interactions? Which typological space do the resulting situations occupy?

4.2. Prototype Design

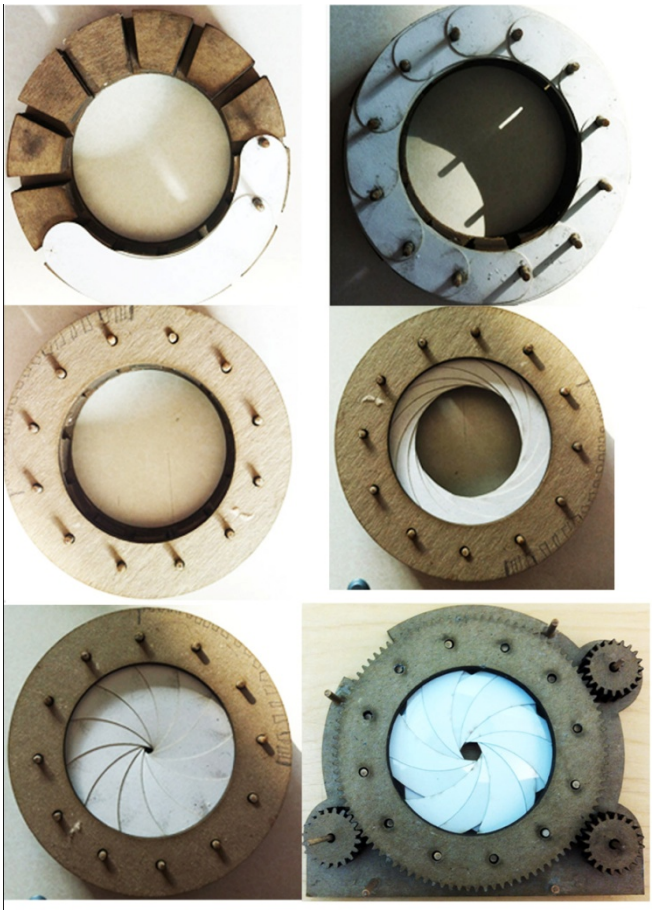

Figure 2. Iris Mechanism

A kinetic prototype was developed with simplicity of mechanism, reasonable cost of materials, and size of supporting parts as central considerations. The iris mechanism was adopted because of the emergence of a circular pattern when the twelve rounded shape components are rotated. In order to be connected to a servomotor, the center donut-shape part was designed as a gear that maintains its stability with three small, fixed gears. Superficially, the module resembles Jean Nouvel's modules for the "Institut du Monde Arabe" in Paris. The crucial difference is that this prototype was developed as a

programmable platform to explore different types of interactivity, and their effects on social activity.

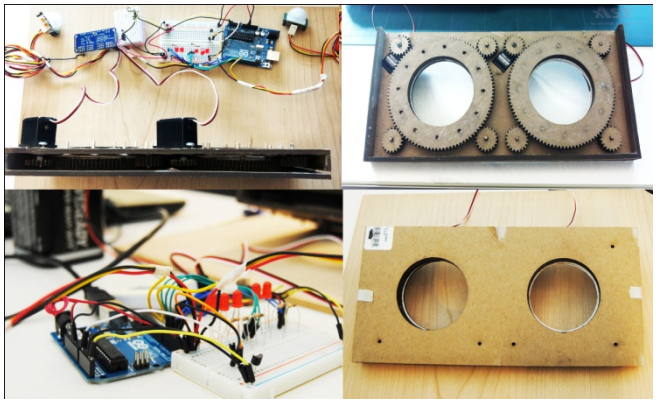

Figure 3. Robotics of the Prototype

The Arduino Uno loaded Atmel 8-bit AVR micro-controller (ATmega328) is employed to react to input data and send signals to the servomotors. A small gear that connects to a servomotor was mounted to the central iris gear on the top-left. When the prototype is connected to a servomotor, the iris rotates based on the signal from the micro-controller. For environmental-responsiveness, Analog Devices TMP35 were used to measure temperature. These devices could detect a temperature range from -40 C to +125 C through an output voltage sent from the sensor to a micro-controller. For human-responsiveness, a Microsoft Kinect, consisting of an infrared and RGB combination camera, was used to detect human presence. With the use of open source libraries, the device provided 3 RGB of data, capturing the scene and 3-dimensional positions of objects.

5. EXPERIMENT SETUP

5.1 Prototype & Location

Six units of the prototype were used for the experiments. The prototype was set a glass wall in the lobby of the Penn State Department of Architecture building, directly in front of the building's main entrance in order to be as exposed as possible to passersby.

5.2. Description of Experiments

Three experiments were designed and conducted, the first and third lasting twenty-four hours, and the second lasting six hours. In the first experiment ("Situation 2"), the prototype responded to humans in real-time and the video recorded anonymous interactions with the prototype. In the second experiment ("Situation 1"), the setting was identical, but the prototype responded to temperature. A third experiment recorded the usual movement of people in the space when there was no artifact, and was used as a baseline for the previous two experiments.

In each experiment, we recorded and observed people passing by the artifact. Moreover, we selected some of the passersby to respond to a survey about the artifact. We used the observations, the recorded video, and the survey data to understand the effects of each interactive strategy on the social situation. In this report, we present preliminary conclusions based mostly on the observations.

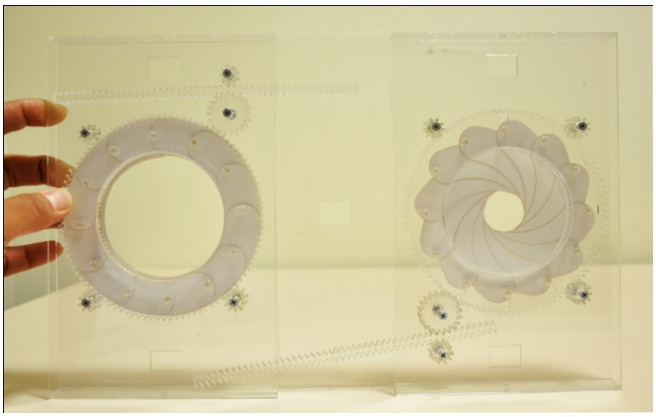

Figure 4. One of the prototype's modules.

5.3. Baseline situation

Observational results of the third situation, a baseline in which no artifact was present, showed that the use of the selected space was not significantly different from a conventional lobby, where people were hastily moving toward their destinations without stopping. The average duration of staying time was less than 1.5 seconds.

5.4. Situation 1: Environmental responsiveness

When the temperature responsive artifact was placed within the space there was not a significant difference in staying time as compared to the baseline situation. This environmentally responsive system was designed to react to temperature, updating every five minutes. Each prototype unit had five variations: full-open, 2/3 open, half-open, 1/3 open, and full-closed. These variations were determined by the temperature in a test cell. For example; when the temperature went below 15 Celsius, all six units were closed and when the temperature reached higher than 25 Celsius, all units were open. If the temperature was between 15 and 25 Celsius, the states of the units varied and were randomly determined by software.

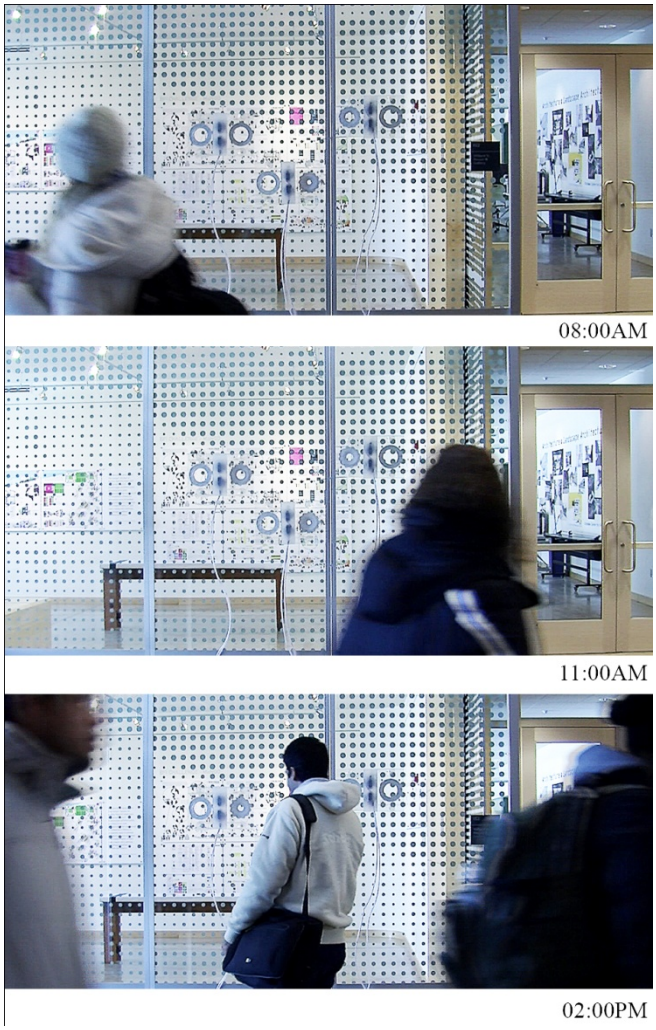

Figure 5. Situation 1: Opening variations

In this situation, the artifact caught the initial attention of nearly half of the observed population. One passerby among the fifty stopped to attempt to understand its underlying logic and several sought out a brief explanation of what the artifact was doing. It was interesting that the artifact could initiate conversations between the designers/programmers and the curious public. In the questionnaire, seventy percent responded positively to the device's intelligent intent. Synthesizing our observations, people had a low level of curiosity regarding the behaviors of the artifact. It rarely triggered serendipitous social activities but it did initiate a subtle social connection between the designers/programmers and users.

5.5. Situation 2: Human-responsiveness

In the case of human responsive artifacts, the average duration of staying time increased meaningfully from 1.4 seconds to 4.1 seconds. In the Processing environment, Depthmap with OPENNI library for Microsoft Kinect was used to detect an object. If an object was detected within a range of one meter to one and a half meters from the 3D (X, Y, Z) position of each unit, the corresponding unit changed its state from open to closed.

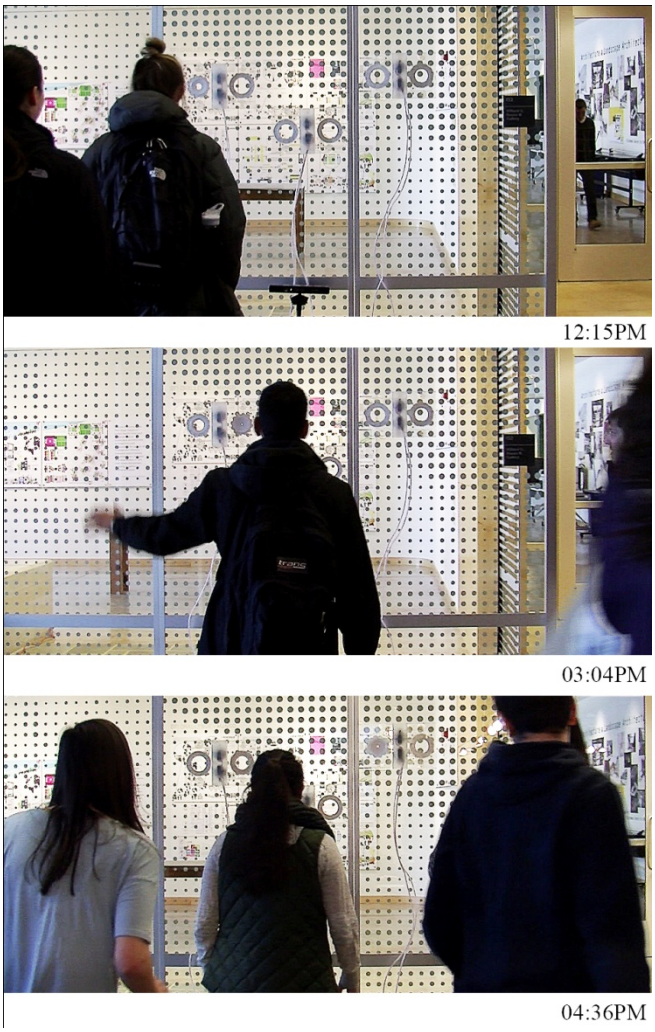

Figure 6. Situation 2: Sequence of human-responsiveness.

When the object disappeared from range, the unit returned to its open state. With this responsiveness, the users could control the unit with a hand gesture; therefore, initiating a unit to change state without a physical interface. Our intention was to initiate a playful interaction where the participant would motivate the different units to trace their continued gestures. The situation unfolded partially as expected. The human responsive artifact drew the attention of passersby and aided in transforming the lobby into a more lively and active space. While some people still passed

by without giving much attention to the artifact, most of those who passed by quickly became interested and stopped to interact with it, walking back and forth and studying the responses. The playfulness was especially noticeable when a group of people passed through the space together. Reacting with surprise, joyfulness and conversation, the group's responses, triggered by the artifact's movements, briefly reconfigured the social atmosphere.

6. CONCLUSIONS

6.1 Results

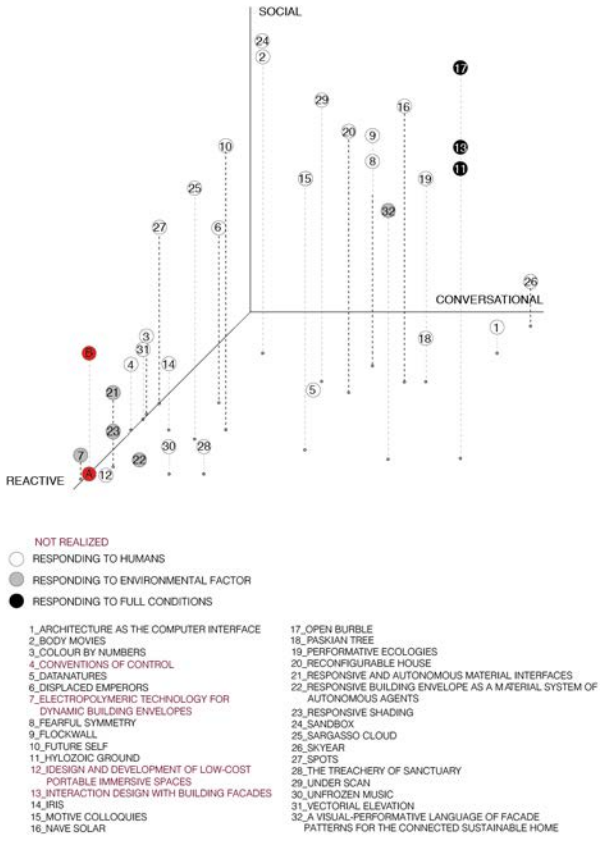

Figure 7. Typologies of interaction with experiments added in red. A: Environmentally-responsive experiment, B: Human-responsive experiment.

Following our hypothesis, the experiments showed two distinct social atmospheres in each of the two situations. In the diagram above (Figure 7) we place both situations within our typological "space."

6.2 Limitations and next steps

(1) The amount of data collected requires considerable additional work. In addition to our micro-ethnographic observations, we collected several hours of video, which may hold clues to a better understand of the social situations we generated. In future prototypes, we will tune the experiment and data capture techniques to better address questions about the social situations.

(2) As shown in Figure 7, the situations our devices created fall within the "reactive" category—and rank relatively low in the "social" dimension. In future prototypes, we will seek a "conversational" interaction model. Following Ashby's example, this may require shifting to a decentralized system, and relying on the sub-system's components feedback. A possible scenario would combine the experiments into one artifact designed to concurrently respond to temperature fluctuation and human interaction. Within this setup, the artifact will have an agenda independent of humans, but also have the capacity to interact with people when confronted. We hypothesize that this design setup, centered on input negotiation, will initiate longer interactions because the artifact's operating logic will not be immediately obvious.

6.3 Contributions

The key contributions of this paper are (1) a conceptual and analytical framework for addressing new forms of social activity emerging around interactive architectures, outlining a role for design, and (2) an experimental template, consistent with this conceptual framework, to explore the social dimension of interactive artifacts.

Acknowledgments

A Collaborative Design Research Grant awarded to Dr. Cardoso Llach by the Stuckeman School of Architecture and Landscape Architecture at The Pennsylvania State University funded the research in this report.

References

ASHBY, W. R. 19576. An Introduction to Cybernetics. Chapman & Hall Ltd.

BEILHARZ, K. 2005. "Architecture as the Computer Interface: 4D Gestural Interaction with Socio-spatial Sonification". Proceedings of 23nd eCAADe conference, 763-770.

BEESLEY, P., 2009 "SARGASSO CLOUD". http://philipbeesleyarchitect.com/sculptures/0924Opwijk_Pluto/index.php

BEAMAN, M. L., BADER, S., 2010. "Responsive Shading | Intelligent Façade Systems". Proceedings of the 30th Annual Conference of the Association for Computer Aided Design in Architecture (ACADIA), 267-270

BEESLEY, P., 2010. Hylozoic Ground: Liminal Responsive Architecture Philip Beesley ed. Ohrstedt, P. and Isaacs, H. Riverside Architectural Press

CARDOSO, D., MICHAUD, D., AND SASS. L., 2007. "Soft Façade Steps into the Definition of a Responsive Facade for High-Rise Buildings" Proceedings of 25th eCAADe Conference, 567–573

CARDOSO, D., ARGUN A., ROCHA,C. A., AND GONZÁLEZ, J., 2009. "Drawing Transparencies: 'Responsible Responsiveness' in Spaces Through Organic Electrochromism". Proceedings of 27th eCAADe Conference,83-88

COLOMINA, B. 1996. Privacy and Publicity: Modern Architecture as Mass Media. The MIT Press.

DOUMPIOTI, C. 2009. "Responsive and Autonomous Material Interfaces". Proceedings of the 31st Annual Conference of the Association for Computer Aided Design in Architecture (ACADIA), 318-325

EDIER, J., EDIER, T. 2005. SPOTS(Building), Berlin, Germany

FOX, M., Kemp, M. 2009. Interactive Architecture. Princeton Architectural Press.

FOX, M. 2009. "Flockwall: A Full-Scale Spatial Environment with Discrete Collaborative Modules". Proceedings of the 29th Annual Conference of the Association for Computer Aided Design in Architecture (ACADIA), 90-97

FOX, M. 2012. "Conventions of Controls: A Catalog of Gestures for Remotely Interacting with Dynamic Architectural Space". Proceedings of the 32nd Annual Conference of the Association for Computer Aided Design in Architecture (ACADIA), 429-438

FRAZER, J., 1993. " The Architectural Relevance of Cybernetics". Systems Research, Vol 10, No 3.

GILMORE, A. 2008. "Paskian Tree". http://garymcginty.com/Paskian-Tree

GLYNN. R., 2008. "Performative Ecologies". http://vida.fundaciontelefonica.com/en/project/performative-ecologies/

GLYNN, R.2010. "Fearful Symmetry". www.ruairiglynn.co.uk/portfolio/fsymmetry/

GLYNN. R. 2011. "Motive Colloquies". www.motivecolloquies.com

HAN C. M., RYU S.W., 2012 "IRIS", Exhibited in Seoul Art Space, Korea

HAQUE, U. 2006. "Architecture, interaction, systems", AU:Arquitetura &Urbanismo. 147 .68-71

HAQUE, U. 2006. "Sky Ear". http://www.haque.co.uk/skyear.php

HAQUE, U. 2006. "Open Burble". Exhibited in the Singapore Biennale 2006

HAQUE, U. 2006. "Reconfigurable House". http://www.haque.co.uk/reconfigurablehouse.php

HAQUE, U. 2006. "Sky Ear". http://www.haque.co.uk/skyear.php

HAQUE, U. 2007. "The Architectural Relevance of Gordon Pask", Architectural Design.

HOOKER, B., KITCHEN, S. 2006 "DATA NATURE", Exhibited in ISEA2006 Symposium + ZERO1

KOLODZIEJ P., RAK, J. 2013 "Responsive Building Envelope as a material System of Autonomous Agents", Proceedings of the 18th International Conference on Computer-Aided Architectural Design Research in Asia (CAADRIA 2013), 945–954.

KOTSOPOULOS, S. D., CASALEGNO, F., CARRA, G., GRAYBIL, W.,AND HSIUNG, B. 2012. " A visual – performative language of façade patterns for the Connected Sustainable Home". Proceedings of the Symposium on Simulation for Architecture and Urban Design. No. 5

KRIETEMEYER, A. E., DYSON, A. H. 2011. "Electropolymeric Technology for Dynamic Building Envelopes". Proceeding of ACADIA Regional Conference, 75-83

KRIKORTZ, E., LAVEN M. AND BROMS, L. 2006."Colour by Numbers". http://electroland.net/projects/rgb/8

LOZANO-HEMMER, R., 1999. "Vectorial Elevation". http://www.lozano-hemmer.com/vectorial_elevation.php

LOZANO-HEMMER, R. 2001. "Body Movies". http://www.lozano-hemmer.com/body_movies.php

LOZANO-HEMMER, R., 2005. "Under Scan". http://www.lozano-hemmer.com/under_scan.php

LOZANO-HEMMER, R. 2010. "Sandbox". http://www.lozano-hemmer.com/sandbox.php

LOZANO-HEMMER, R. 2011. "Nave Solar". http://www.lozanohemmer.com/nave_solar.php

MILK, C., 2012. "The Treachery of Sanctuary". http://milk.co/treachery

MITCHELL, W. J., SEVTSUK A. 2008. "Unfrozen Music: Designing & Programming Digital Water Walls." In Digital Water Pavilion at Zaragoza's Milla Digital and Expo 2008

PAK, E., VROUWE I. AND BERBEKE J. 2011. "Design and Development of Low-cost Portable Immersive Spaces". Proceedings of the 31th Annual Conference of the Association for Computer Aided Design in Architecture (ACADIA), 260-267

PICON, A. 2013. Ornament: The Politics of Architecture and Subjectivity. The MIT Press.

TELHAN, O., CASALEGNO, F., PARK, J., KOTSOPOULOS, S., AND YU, C., 2010. "Interaction Design with Building Facades". Proceedings of the fourth international conference on Tangible, embedded, and embodied interaction, 291-294

VIDLER, A. 2002. Warped Space: Art, Architecture, and Anxiety in Modern Culture. The MIT Press.

WIENER, B. 1948. Cybernetics: Or Control and Communication in the Animal and the Machine. The MIT Press.

WOOD, S., ORTKRASS, F. AND KOCH, H. 2012. "Future Self". http://random-international.com/work/future-self/

Designing Fluvial Sites: Digitally Augmented Physical Hydraulic Modeling

Alexander Robinson

USC School of Architecture
Watt Hall, Suite 204
Los Angeles, CA 90089
alexander.robinson@gmail.com

Figure 1. Video frame showing sediment analysis in hydraulic physical model.

Keywords: Physical Modeling, Time-Lapse, Augmented Video, Feedback, Landscape Architecture, Civil Engineering, Fluvial, River, Flume, Hydraulic Modeling

Abstract

This video presents an urban river design methodology that employs high-resolution hydraulic physical models. The video augments the process with metric and spatial performance analysis to enhance the methodology and facilitate iterative design for multiple critical functions. Overall, the approach prototypes an enhanced methodological common ground between fundamental civil engineering and landscape architecture design tools.

1. OVERVIEW

For a collaborative studio between USC and Los Angeles engineering entities, the Landscape Morphologies Lab developed a custom hydrological model to develop landscape design alternatives for the Los Angeles River channel responsive to critical flood management and habitat goals.

An investigation of computational civil engineering river modeling systems (such as HEC-RAS) concluded that they cannot engage at the scale and morphology of landscape site design, and a physical model was chosen as the means to bridge between these two often-disparate methodological worlds, as well as to provide numerous additional advantages.

The physical model became the foundation for a design environment that enabled the development of landscape program and form optimized to perform within the complex and varied hydrological conditions of the River. As a scaled physical representation of form and hydrology (with limited vertical distortion) the model allowed the assessment of multiple parameters, including flood protection, sediment scouring (vegetation/habitat survival), and flow dispersal—as well as aspects of experiential value, urban programs and interfaces, and aesthetic and cultural values. While cumbersome to construct and operate, physical modeling's dynamic high resolution representation has known advantages for both iterative design development and public

presentation. Furthermore, with the growing availability of precision milling machines this has the potential to become a low-expertise means to validate speculative designs that were previously easily dismissible within performance paradigms dominated by engineering parameters.

While the use of hydraulic models within landscape architecture design is not unprecedented, the video presents a digitally augmented version of the process that proposes expanded potentials that strengthen and solidify the advantages of the tool. In its most elemental augmentation the video associates a presentation of the complex spatial hydraulic performances with a metric of flow conditions relative to "designed" rain events. Flood moments and other specific behaviors are spatially identified within this metric performance context. Specialized digital augmentation, facilitated through the color processing of video, is used to help isolate and visualize dynamic high-resolution spatial processes (scouring and flow dispersion) within this framework. In this project these augmentations were done in post-processing analysis, but in future manifestations could be integrated into real-time modeling and iterative design development. These methods seek to augment rather than overly reduce the rich spatial data-set of physical modeling and focus the feedback towards appropriately complex, multi-performative solutions.

Acknowledgements

Sandra Wong, Chuan Ding, Tina Chee, Los Angeles Bureau of Engineering (Deborah Weintraub, Carol Armstrong, Kent Welling, Meghan Whalen), USC MLA Studio Students, Los Angeles Department of Water and Power, United States Army Corps of Engineers (Charles Dywer, Alison Lind, Erin Jones), USC Viterbi School of Engineering, Coastal Enterprises.

Session 5: Design Search and Optimization **75**

Parameters Tell the Design Story: Ideation and Abstraction in Design Optimization 77
Erin Bradner, Francesco Iorio, Mark Davis
Autodesk Research.

Genetic Based Form Exploration of Mid-Rise Structures Using Cell Morphologies 85
Ornid Oliyan Torghabehi, Peter von Buelow
Taubman College of Architecture and Urban Planning, University of Michigan.

Design Agency: Prototyping Multi-Agent System Simulation for Design Search and Exploration 91
David Jason Gerber, Rodrigo Shiordia, Sreerag Veetil and Arjun Mahesh
School of Architecture, University of Southern California.

Parameters Tell the Design Story: Ideation and Abstraction in Design Optimization

Erin Bradner[1], Francesco Iorio[2], and Mark Davis[1]

[1]Autodesk Research
One Market, Suite 200
San Francisco, CA, 94105 USA
{erin.bradner, mark.davis}@autodesk.com

[2]Autodesk Research
210 King E, Suite 500
Toronto, ON M5A 1J7, Canada
francesco.iorio@autodesk.com

Keywords: Design Optimization, Optioneering, Ideation, Architectural Design, Engineering Design, Qualitative Research.

Abstract

We report qualitative findings from interviews and observations detailing how professionals generate and evaluate design ideas using design optimization tools. We interviewed 18 architects and manufacturing design professionals. We frame our findings using the Geneplore model of creative cognition and classify examples of ideation and abstract design thinking arising from optimization workflows. Contrary to our expectations, we found that the computed optimum was often used as the starting point for design exploration, not the end product. We also found that parametric models, plus their associated parameters and simulations, serve as an alternate, highly valued form of design documentation distinct from engineering schematics.

1. INTRODUCTION

We focus our research on optimization in a professional design practice. We select this focus because computational power that was once restricted to large government entities has become increasingly accessible to private entities (Thibodeau, 2013). Meanwhile, the professional use of parametric modeling has provided adaptive structures against which iterative simulations can be run. We've observed that computationally intense, heuristic searches of design spaces are becoming more commonplace in professional practice than in the past.

The proprietary nature of professional design processes, and their resulting designs, led us to choose an ethnographic approach to our research. While the use of simulation tools has begun to be systematically documented in the literature (e.g. Tsigkari et al. 2013), to our knowledge there are no published, comparative accounts of goal-driven design and optimization used professionally. The qualitative findings reported here begin to fill this gap.

As software designers and high-performance computing experts, the high-level objective of our research is to expose the opportunity for new or improved computing architectures and user interfaces for generating, exploring and describing design spaces via optimization. In this study we advance toward that objective by first detailing how professional designers use design optimization to ideate – i.e., to generate and then explore solutions, to discover new and unexpected ideas, and to focus or expand their understanding through data visualization. We then articulate the multiple levels of abstraction engendered by optimization workflows, including: problem definition, evaluation, coding and documentation.

2. DESIGN OPTIMIZATION

Design optimization tools are creation tools that use parametric modeling, performance simulation and mathematical optimization to systematically generate and evaluate design alternatives (Holtzer et al. 2007). Design optimization, also known as design optioneering (Gerber et al. 2012) and computational design (Arieff 2013), is a departure from traditional architecture and engineering practice. Typically, architects generate a relatively small set of design alternatives that represent specific points in a multi-dimensional design space (Flager and Haymaker 2007). In architecture, this small set of design alternatives may be communicated in the form of two or three laser physical cut scale models or a few dozen digital photo-realistic visualizations. Even with the support of state-of-the-art computer-aided design tools (CAD), individual

designs are iterated relatively slowly and with considerable design effort. (Ibid.)

Conversely, architects and engineers using design optimization practices generate orders of magnitude more design alternatives by specifying design objectives in the form of design parameters and parameter ranges (Tsigkari et al. 2013). They use stochastic search methods, such as genetic algorithms, to automatically and iteratively compute large sets of design alternatives (Holzer et al. 2007). The designs that best fit the architects or engineer's predefined acceptance criteria survive multiple generations to spawn successive generations of unique, new designs.

Contrasting with traditional design practices, optimized designs are computed parametrically and bred algorithmically. The numerous design alternatives that are produced are often represented by a multi-dimensional plot of solutions and might be coupled with a matrix of thumbnails of rendered designs, as in Figure 1. Researchers investigating the approach argue that design optimization enables designers to "more efficiently, and with more certainty, explore complex and tightly coupled design solution spaces" (Ibid.) than traditional design practices.

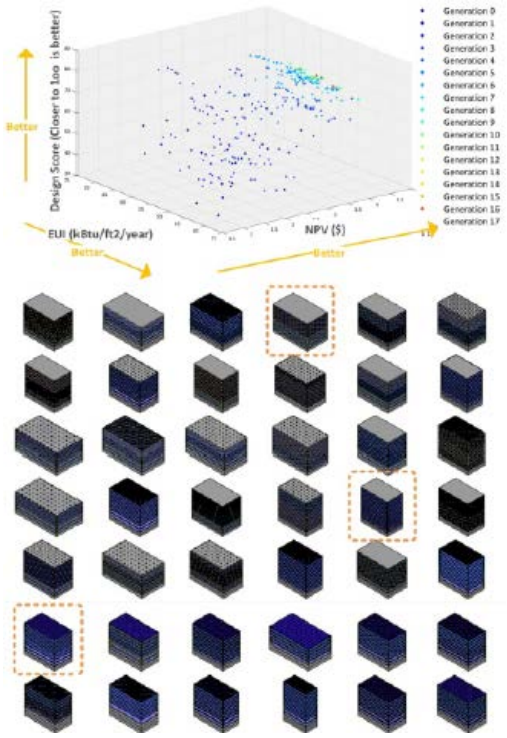

Figure 1. Sample Design Optioneering Results from (Gerber et al 2012).

2.1. Design Optimization as Creativity Support

Design optimization tools are an under-researched class of creativity support tools. Professional engineers and architects perform what we dub *constrained creativity:* their creative ideas must perform an intended function, and satisfy specific performance criteria (Shah et al. 2003). These professionals concern themselves with how to generate and explore ideas that are optimized against multiple, competing objectives, variables or constraints. In building design, for example, it is necessary to simultaneously consider multiple complex objectives including site utilization, structural design, building form, energy use, buildability, and operating costs.

To the extent that design optimization tools enable users to be "not only more productive but also more innovative" (Shneiderman et al. 2006), they fall into the application category of creativity support tools. Creative activities that lead to innovation include idea generation, easy exploration, rapid experimentation and fortuitous combination. (Ibid.) Designers using design optimization tools combine ideas through the algorithmic generation of design alternatives, they experiment through adjusting design parameters, and they explore through examining data visualizations of solution sets. Optimization tools do not simply automate idea generation. They support the creative process of idea generation, exploration and refinement.

2.2. Design Optimization and Creative Cognition

Engineering and architectural design are inherently generative disciplines. The set of design algorithmically computed alternatives for any given real-world design task is vast. Flager et al. calculate that for the one room, steel-frame building used in their energy and structural optimization study there were $55x10^6$ possible solutions (Flager et al. 2009). Cognitive limitations prevent humans from imagining even a small fraction of the possible alternatives in a problem with high dimensionality and millions of solutions. Not even the most skilled designer can handle this level of mental complexity. Variable interactions are particularly difficult to imagine—how do window size, glazing type and building orientation interact to produce the most energy efficient building? Furthermore, time constraints prevent designers from exhaustively exploring the solution set for top performing solutions.

In our qualitative research we observed that both architects and engineers explore a wide range of design parameters and constraints by applying iterative design techniques to "solve" for their designs. Geneplore is a heuristic model of creative cognition (Ward et al. 1996) that we found particularly useful in framing the design

processes we observed. We will briefly describe this model now. Figure 2 shows the basic structure of the model.

The Geneplore model involves three fundamental cognitive processes: generate concepts, explore and interpret concepts, and evaluate the problem to focus or expand the concept. These processes map nicely to the design optimization process in architecture and engineering whereby designers use goals and parameters to abstract the design problem, then generate concepts. Together with the design optimization system, they explore the strengths and weaknesses of the candidate solutions, and then use insights gained from both the generation and exploration activities to refactor the design problem. Meanwhile, design constraints, such as building height, are introduced which reshape the problem definition and also reshape how concepts are interpreted.

A key contribution of the Geneplore model is the notion of a preinventive structure. The term preinventive is used to denote a germ of an idea, a "half-baked" sketch, or a design hunch that may hold promise. Patterns, 3D models and conceptual combinations (Ibid.) that prefigure creative concepts are all examples of preinventive structures.

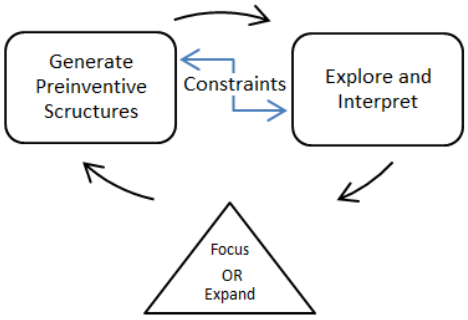

Figure 2. Geneplore Model from (Ward et al. 1996).

We acknowledge here that it is unusual to map a cognitive model like Geneplore onto a system model such as design optimization. Nevertheless, we were compelled to do so because we found ourselves drawing heavily on the Geneplore model to inform the analysis of our interview findings. We present our interview study and data analysis next. We contend that that preinventive problem statements, conceptual combinations and constraints are the primitives on which design optimization operates. We will also explain that idea generation, exploration, and adjusting the problem focus – the three pillars of Genepolore – are the three most common activities performed by users of design optimization tools.

3. INTERVIEW STUDY

We interviewed 18 design professionals in the fields of architecture (15) and manufacturing/fabrication (3). Interview duration ranged between 1.5 and 3 hours. The majority of our interviews were conducted at the participant's place of work, though 5 (28%) were conducted over the phone with screen sharing. Interviews were recorded (audio only) and transcribed. Due to the proprietary nature of the designs produced by the workplaces we visited, photos were prohibited and we weren't allowed to take away design artifacts. We coded the interviews and observations, applying a grounded theory approach (Strauss and Corbin 1998). Here we present a *thick description* of the workflows that professionals follow when conducting design optimization.

We knew enough about design optimization tools at the outset of the study to reject the hypothesis that it is used solely to conclude the design process by selecting the winning design from a set of all plausible alternatives. Through prior contact with architects and engineers we learned that it was being used by many at the start of the design process—at a stage called design conceptualization. This puzzled us. How was a tool that was designed to computationally *solve* design problems being used to *question* and *explore* design problems? We wanted to understand how and why an engineering technique that emerged from NASA (Schmit and Thornton 1964) to compute the single highest-performing design for an airfoil was being used by architects to compute the quality of penthouse views in design alternatives for a building in Bangalore (Tsigkari et al. 2013).

3.1. Analysis

In the analysis below we first describe the ideation process we observed. We briefly detail how professional designers use design optimization to generate and then explore solutions, to discover new, and sometimes unexpected, ideas. We also describe how they focus or expand their understanding through data visualization. We then articulate the multiple levels of abstraction: problem definition, evaluation, coding and documentation. Design insight and improved design quality are two examples of the value gained from design optimization. Yet abstractions are also the primary source of the user experience challenges, such as sufficiently understanding statistical correlations between design variables in order to reduce or expand the dimensionality of the design problem.

3.2. Ideation

Design ideas from architecture and engineering are the product of creative ideation whereby ideas are generated and evaluated for suitability using qualitative and quantitative evaluation criteria (Shah et al 2003). As indicated by the Geneplore model (Ward et al. 1996), there are two distinct activities: generation and evaluation. The traditional ideation process is iterative (Flager and Haymaker 2007). When design optimization techniques are applied, the design process becomes less iterative yet more design candidates, by several orders of magnitude, are produced. One participant described the difference in the two processes in these words:

"The typical design workflow is to design then throw to the analyst. Redesign. And then keep playing catch. It's inefficient. [Design optimization] captures the criteria that are important to you then have the cloud process all the permutations."

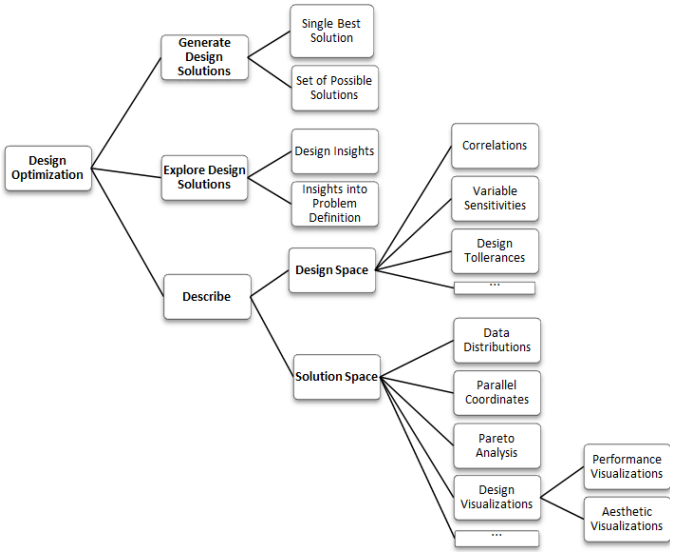

Figure 3. Uses of Design Optimization.

The starting point in the design optimization process thus shifts from specifying geometry in a CAD system:

design → evaluate → select or redesign

…to defining the design problem:

define → generate + explore → select or redefine.

Here we'll outline the activities of generating, exploring, describing, and selecting solutions, as summarized in Figure 3.

3.2.1. Generate Solutions

Architects and engineers often cannot compute nor comprehend the effects of combining multiple variables in a complex system. Design optimization tools procedurally generate design solutions from a machine-readable definition of the design constraints and parameters. Typically, the design optimization system returns a large number (100s to 1000s) of design solutions. One study participant explained this automated idea-generating process thusly:

"Good design has inspiration to it...if you have that vision you can encode it and parameterize it and explore it further. Now we have a rich flora of options."

Examples of designs that our participants optimized include high-rise buildings, hospital patient care wards, an engine manifold, and installation art. The elements of the design that were optimized include, but are not limited to: aesthetic form, structural form, mechanical performance, human performance (nurse walking distance) and building energy efficiency. *Liters per second* is an example of a design parameter from the engine manifold example. Engineering constraints are such things as "*no more than 2 bars of pressure drop."* An architectural constraint might be *"must maintain an average of 40% natural light."*

3.2.2. Explore Solutions

We appropriate the term *explore* from the Geneplore model of creative cognition to describe the way users purposefully adjust their parameter ranges and review the resulting solution sets. One user referred to this as an act of discovery: *"The key is the discovery phase. As you adjust ranges, you discover options you may not have expected."* Surprisingly to us, both architects and engineers in our study said that the computed optimum was often used as the starting point for this exploration. In one case, the structurally optimal alternative design for a high-rise building was used to seed the exploration process for its aesthetic design. The structural engineer from this group explained that *"the optimum is a way to talk about form"* indicating that the solution they chose from the set of high-performing solutions in their structural optimization served as the conceptual sketch on which the aesthetic designers could iterate.

3.2.3. Describe the Solution Space

The solution space is the set of all solutions computed by the design optimization algorithm. We observed two primary ways that design optimization describes the

solution space for users. These are visualizations and data plots. Visualizations can be further classified into performance visualizations (a.k.a. simulations) and aesthetic visualizations. A heat map showing regions of stress on a 3D model of a metal bracket under a simulated load is an example of a performance visualization. Our study participants explained that they use visualizations to develop their understanding of the impact of their design choices on aspects of performance. In one case, a mechanical engineer optimizing the design of a manifold attributed a major design insight to a computation fluid dynamic visualization he reviewed:

"[the visualization] gave us the insight to open the diameter… the diameter of the opening could not be expanded but the diameter of the shaft cold be flared to increase flow."

Aesthetic visualizations are also 3D renderings of design alternatives. When used by architects, these visualizations allow systematic exploration of building form. These visualizations are important since, as one structural engineer put it: *"slight variations to form, to a designer's eye, are either elegant or fat."*

Data plots, commonly in the form of scatter plots, are another type of data visualization we observed being used. Respondents expressed a range of opinions about the utility of different types of plots. One study participant sung the praises of parallel coordinate charts while another pledged his allegiance to Pareto plots. A manager said this about the computational designers he manages and their discussions of different plot types: *"they talk about tradeoffs in a spiritual way."* We suspected that different plot types allowed certain designers to extract more information about design tradeoffs more quickly than others. We theorized that there was an interaction between the sophistication of users' statistical knowledge and the utility they assign to the different types of plots.

3.2.4. Describe the Design Space

The term design space describes the mathematical definition of the design. It includes the design variables, and constraints; the ranges or discrete values assigned to those variables; and any other bounding criteria that can be expressed mathematically. Study participants used statistical analyses such as correlations to examine the interaction between variables. They actively sought these statistical descriptions of the design space because *"understanding dependencies between different systems [variable types] is very challenging"* and because statistical analysis gives them insights to add or remove variables when warranted. For example, they remove variables found to be highly correlated to reduce the "dimensionality" of their problem space; they split variables based on variable sensitivities; and they adjust parameter ranges up and/or down to account for design tolerances.

3.2.5. Select Solutions

Something we found counterintuitive was that many participants in our study selected the highest performing solution from a solution set to initiate their design ideation process, rather than to conclude it. This remained befuddling until we learned that our participants were using computational design more frequently in the earliest, most conceptual phase of design than in any other phase. They considered the optimum to be the computational equivalent of a back-of-the-napkin sketch. Borrowing again from the Geneplore model of creative cognition, the computed optimum is the pre-inventive structure that seeds the ideation process: *"instead of starting with nothing, you start with something…your optimum gives you a starting hunch."*

That said, it was not only the single highest solution that was important and useful, but often the full set of high performing solutions. Our study participants reported consulting Pareto plots iteratively in the conceptual design phase to rapidly identify and select "interesting" solutions. Pareto plots are a type of scatter plots commonly used to distinguish high-performing solutions in the set of all feasible solutions. The Pareto set is composed exclusively of the high performers: for any given solution in the Pareto set, it is impossible to increase performance along one axis without decreasing performance along another axis. A mechanical designer qualified his interest in identifying the highest performing designs during the conceptual design phase by explaining that he is looking to determine "*what direction the performance is trending."* He iteratively generates high performing solutions using visualizations such as Pareto plots to explore how adjusting the parameters by hand affects the overall quality of the resulting solutions.

3.3. Abstraction

To define a design problem requires abstracting the problem into mathematical descriptions such that the design optimization tool can compute alternatives. An empirical study of engineers has shown that the level of abstraction and precision in a problem definition affects the quality and

quantity of ideas generated (Fricke 1999). Problems defined with low precision produce few and poor solutions because engineers fixate on concrete solutions too early. Conversely, too many solutions also produce poor solutions because managing too many solutions diminishes the engineers' ability to identify, evaluate and modify the best solutions. Successful designers balance their search for solutions. (Ibid.)

We did not evaluate the quality of design solutions our study participants produced by design optimization tools; however, our interviews with architects and engineers suggest that design optimization tools maximize the positive effects of precision in problem definition while minimizing the negative effect of large solution sets. Furthermore, we suspect that the demands of abstracting the problem into a precise definition, which our participants stress is nontrivial, improve the designers' ability to evaluate solutions. We discuss multiple levels of abstraction in the design optimization workflow next.

3.3.1. Problem Definition as Abstraction

"Think about the underlying logic and how you can transform it."

Using design optimization tools necessitates abstraction. Users must precisely define the problem space across multiple dimensions. One participant succinctly summarized his design problem for an office tower this way:

"I work to balance aesthetics and sustainability. We wanted a cohesive skin. [goal] The client wanted 40% natural light. [constraint]"

Our participants defined between 12 and 60 design parameters for the range of projects they worked on. They explained that it was not sufficient to simply describe the building or object geometry in the problem definition; rather, they needed to extract the underlying logic of their design problem. They routinely need to abstract variables so they can *"optimize things that aren't the same"* such as energy efficiency and structural efficiency. Designers also report that they often look at multiple competing criteria at the same time, such as daylight exposure, and view quality from windows in a building. Abstracting design goals and parameters into quantifiable representations is the first level of abstraction that design optimization demands from users.

3.3.2. Code as Abstraction

"You need to write the rules correctly."

The second level of abstraction required by design optimization is programming. Most, but not all, of the design optimization problems that our study participants work on require that they script algorithms to procedurally generate solutions. In the case of hospital design, the design goals and parameters interact according to a specific logic embedded in the optimization code, since hospital design is subject to rigorous building codes and regulation.

One participant explained the challenge of converting building code to software code in these words: *"you need to write the rules correctly for what you are trying to check."* In one architectural case 5000 lines of code produced 2000 design alternatives, each satisfying rules for solar gain, cost, buildability and acoustics.

When architects abstract designs into rules and make observations such as *"you need to write the rules correctly"* they begin to sound more like software programmers than architects. One of our interview participants rejected design optimization precisely because of this level of abstraction it demands. His view is that design optimization transforms the practice of architecture away from the "rational" or concrete practice of creating CAD drawings to a more abstract practice:

"Revit [a CAD tool] is rational. When you're working in Revit, your goal is set: I'm designing a building. I'm producing construction documents. In Grasshopper [a design optimization tool] there is no proscribed approach nor outcome. I can design a tree or a car."

This study participant asserted that when architects use design optimization to produce *"1200 variations, you're not being an architect any more. You are a computer programmer. A bus driver."* This comment implies that the level of abstraction inherent in the coding aspect of design optimization fundamentally alters architecture from a practice of documenting design into CAD, to a practice of abstracting rules into software.

3.3.3. Evaluation as Abstraction

"Then they start to push each other around."

Sound decisions about tradeoffs in multi-objective design problems require sophisticated statistical thinking. As we stated earlier, even skilled designers often struggle to comprehend the effects of combining multiple variables in a

complex system. A particularly germane example from our data came from an interview with a structural engineer. He told us of output from design optimization that combined structural strategies in an interesting and unexpected configuration. Design optimization had produced a design wherein the widest section of the building he was designing had a tied fan structure with cross-bearings tapering as they went up, while two narrower sections used two different structural strategies: suspension and truss. When we asked for his reaction to the configuration he replied: *"you have these strategies in your mind, but you may not know how they will interact."* The abstractions in this example are the structural strategies. The design optimization system has no formal definition of a tied fan, suspension or truss. It simply computes the thickness and position of the beams. The designer abstracts what he sees in the output into structural strategies.

Our transcript from an interview with an architect/artist who designs and fabricates installation art is replete with abstract criteria that he used to evaluate the results from his optimizations. Examples of these criteria are: minimal surfaces, the absence of double curvature, and "*mathematical purity*". To visualize the design optimization process he output the calculations directly to a 3D model and watched the model transform as the problem was being solved. At the start, the design was very angular but once the design optimization ran, the geometric elements started to *"push each other around to find equilibrium."*

These two examples imply that evaluations may be concrete, such as the percent of solutions that meet or exceed 40% natural light, or they may be abstract, such as a structural engineering strategy or a mathematical purity.

3.3.4. Documentation as Abstraction – *"Not a perfect translation of genotype to phenotype."*

We were surprised to learn the extent to which architects abstracted their designs. One participant stressed that the *"parameters need to tell the design story."* An architectural firm we interviewed described the process by which they encoded the expression of architectural forms and performance parameters into an "architectural genome." Another architectural firm referred to the "master files" that they produced using their design optimization practice. These types of files, genomes and master files, are the symbolic description of the design problem. These files are the design story as told by the parameters. This type of documentation is a fundamental departure from the set of elevations and floor plans in traditional design. The obvious analogy, used by our participants, is that the master file is a genotype and the set of CAD drawings is a phenotype. One study participant cautioned us that there is *"not a perfect translation of genotype to phenotype"* implying that design optimization does not replace the expertise of the architects.

Design optimization requires that professionals abstract the design problem far more systematically and comprehensively than in traditional, iterative design processes. As a result of this obligatory abstraction, design optimization has enabled design professionals to generate and explore more mathematically complex design alternatives than they would otherwise. This process of ideation through abstraction appears to be the creative engine of design optimization. That said, abstract thinking is difficult even for trained professionals. One participant reported that plots of solution sets that are output from design optimization are more difficult for him to evaluate than CAD models: *"A [CAD model] is something you can respond to…I like that. I don't like that."* This was echoed by another respondent:

"the usability of the output is not there… even the visual examples are hard to digest for us, much less for the clients who don't have the expertise."

We were surprised to find this pattern in our interviews: user interfaces for data exploration in design optimization produce a poor user experience. This finding led us to wonder what attributes of these plots contributed to the poor user experience. At a cognitive level, we also wanted to learn how architects and engineers conceptualize the statistical analyses in design optimization, yet we have no data in our interviews on this topic. In a future study we plan to develop a framework describing how architects and engineers use data visualizations and apply that to prototype user interfaces for exploring solution spaces.

4. CONCLUSION

This research describes the use of design optimization tools across multiple professional disciplines including architecture and engineering. It leverages a creative cognition model of ideation (Ward et al 1996) to frame the activities we observed, including: generating design solutions, evaluating design solutions and describing both the problem and solution space. It examines an understudied creativity support tool, design optimization, and it articulates the role ideation and abstraction play in design optimization. One key finding is that that

professionals use design optimization to gain understanding about the design space, not simply to generate the highest performing solution. Professionals reported that the computed optimum was often used as the starting point for design exploration, not the end product. A second key finding is that in some design organizations parametric models plus their associated parameters and simulations are serving as an alternate, highly valued form of design documentation distinct from engineering schematics. Much like a genome encodes a genotype, a parametric model and associated simulations encodes the expression of form and performance across any given set of parameters. The parameters tell the design story.

A next step for our research is to develop user interface design principles and prototypes that remove abstraction between solution sets and individual design solutions. User interfaces should enable users to easily pivot between exploring a solution set and examining a specific solution. They should also map decision-making criteria, such as parameter values and variable interactions, directly onto 3D models of individual designs. For any given design there are numerous nearby variations that are generated by incrementing up or down a variable range. We are exploring various user interfaces to present the detail of individual solutions while preserving the context of nearby solutions.

There are two distinct but related reasons why design optimization is important to the research community. First, this class of tool suffers from poor user experience (Maile 2007). Our professional users reported this in interviews, and expert academic users report "the lack of user-friendly, mature and comprehensive user interfaces limits the usage in practice." (Ibid.) Poor user experience is due in part from a dearth of user experience research in the field of design optimization (Flager and Haymaker 2007). With this study, we hope to ameliorate the lack of research in this area.

Secondly, this research is important because users of design optimization are making buildings more structurally sound with less building material, they are making automobile engines more efficient, and they are improving the quality of care in hospitals by making them more comfortable places to work. Design optimization tools are used for sustainable design, yet are built on stratified layers of abstraction that we believe place considerable cognitive demands on the user. Abstractions exist when the design problems are defined, coded, and interpreted through data visualizations. Our findings suggest that the abstractions inherent in the workflows may conceptually distance designers from their designs, or lead them to make important design decisions based on incomplete information. This research may give tool developers, ourselves included, insight into how to amplify, focus and/or minimize these multiple levels of abstraction when designing optimization software.

Acknowledgements

We thank Michael Bergin for his coaching on design optimization techniques.

References

ARIEFF, A. 2013. New Forms that Function Better. MIT Technology Review http://www.technologyreview.com/review/517596/new-forms-that-function-better/

FLAGER, F. AND HAYMAKER, J. 2007. A Comparison of Multidisciplinary Design, Analysis and Optimization Processes in the Building Construction and Aerospace Industries. In *Proc. of the 24th International Conference on Information Technology in Construction.*

FLAGER F, WELLE B, BANSAL P, SOREMEKUN G, HAYMAKER J. 2009. Multidisciplinary process integration and design optimization of a classroom building. *Journal of Information Technology in Construction*, Vol. 14. 595-612.

FRICKE G. 1999. Successful approaches in dealing with differently precise design problems. *Design Studies*, Vol. 20, 5. 417-429.

GERBER, D. J., LIN, S.-H., PAN, B. AND SOLMAZ, A. S. 2012. Design optioneering: multi-disciplinary design optimization through parameterization, domain integration and automation of a genetic algorithm. In *Proc. Symposium on Simulation for Architecture and Urban Design*, Society for Computer Simulation International.

HOLZER, D., HOUGH, R. AND BURRY, M. 2007. Parametric Design and Structural Optimisation for Early Design Exploration. International, *Journal of Architectural Computing*, Vol. 5, 4. 625-643.

MAILE, T., FISCHER, M., BAZJANAC, V. 2007. Building energy performance simulation tools – a life-cycle and interoperable perspective. *Working Paper*. Center for Integrated Facility Engineering, Stanford University.

SCHMIT, L. A. AND THORNTON, W. A. 1964. Synthesis of an Airfoil at Supersonic Mach Number. National Aeronautics and Space Administration, *NASA Contract Report CR-144*.

SHAH, J., VERGAS-HERNANDEZ, N., SMITH, S. 2003. Metrics for measuring ideation effectiveness. *Design Studies* Vol. 24. 111-134.

SHNEIDERMAN, B., HEWETT, T., FISCHER, G., JENNINGS, P. 2006. et al. Creativity Support Tools: Report from a US National Science Foundation Sponsored Workshop. *International Journal of Human Computer Interaction*, 20, 2. 61-77.

STRAUSS, A. AND CORBIN, J. 1998. *Basics of qualitative research: Techniques and procedures for developing grounded theory*. Thousand Oaks, CA: Sage.

THIBODEAU, T. 2013. U.S. makes a Top 10 supercomputer available to anyone who can 'boost' America. In www.computerworld.com.

TSIGKARI, M., CHRONIS, A., CONRAD JOYCE, S., DAVIS, A., FENG, S., AISH, F. 2013. Integrated Design in the Simulation Process In *Proc. of Symposium on Simulation for Architecture and Urban Design*.

WARD, T., SMITH, S., FINKE, R. 1996. *Creative Cognition: Theory, Research, and Applications*. Bradford Books. 189-21.

Genetic Based Form Exploration of Mid-Rise Structures Using Cell Morphologies

Omid Oliyan Torghabehi and Peter von Buelow

University of Michigan
Taubman College of Architecture and Urban Planning
2000 Bonisteel Blvd.,
Ann Arbor, MI 48109-2069
oliyan@umich.edu, pvbuelow@umich.edu

Keywords: Genetic Algorithm, Form Exploration, Cell Morphology, Associative Modeling, Seismic Design.

Abstract

This research explores well-performing forms of mid-rise buildings which use cellular morphologies as perimeter bracing of the structure. The study is based on structural performance under earthquake loading. The geometry of the structure is created by parametric modeling following the principles of cellular space division. Optimization software is employed as a genetic based tool for exploration of design alternatives. The software combines parametric modeling, finite element performance simulation, and a genetic algorithm coupled with database storage. Externally braced frame structures consist of a braced load bearing system in the perimeter of the structure.

In this study a parametric, vertical, spatially framed system is developed based on cellular morphology. The parametric model is used in a performance-oriented process of form generation guided by a genetic algorithm (GA). Using the database to store all of the evaluated design alternatives ,then exploration of desired solutions will be performed through data mining. A palette of well performing design alternatives is generated as the exploration result.

1. INTRODUCTION

The natural world has always been an influential source of inspiration for architects and engineers. Natural inspiration has contributed to the quality of design in different areas, including visual and conceptual design. With common access to digital and computational tools during the design process, inspiration from nature has contributed to design at the level of computation (Roudavski 2009). With the advent of numerical simulation software and a growing tendency for engineers and designers to take advantage of simulation tools in the design process to evaluate the performance of different design solutions, the performance-based form finding process has emerged and evolved to be an effective design process.

Inspired by patterns of cellular division, we chose Voronoi patterns for a form exploration process to generate peripheral bracing systems for midrise towers. Voronoi patterns appear everywhere in nature. At the microscopic level they exist in the basic principles of cell division. At the macroscopic level the patterning of giraffe skin and turtle shells have the same principles. Technically, for a set of points a plane is divided into Voronoi cells in a way that each cell belongs to a specific point and every point in that cell is closer to that site than any other (Dimcic 2012).

Genetic Algorithms (GAs) are widely used in computational form finding processes. Due to their stochastic nature, GAs can effectively search the design space of highly nonlinear problems (von Buelow et al. 2012, Dimcic 2012, Baldock and Shea 2006, Kicinger et al. 2005). Moreover, design evolutions can be used as an aid in stimulating the designer creativity. The advantage of such an evolutionary approach is the creation of diverse sections of the state space that meets performance targets and increases the possibility for discovering a variety of potential solutions by providing a larger search space for designers to interact (Malkavi 2006).

Genetic Algorithms are used in this research as the optimization engine in the process of form exploration. ParaGen, a genetic based method, combines associative parametric software with simulation and analysis tools such

as Finite Element Analysis (FEA) software to build a database of well performing solutions. This database can then be mined, both visually and through performance values, to explore suitable design alternatives. The goal is to develop a palette of well performing solutions through detailed form exploration (Figure 1). The ParaGen method and details of its utilization can be found in (von Buelow, 2012). This paper shows the method applied to the more complex performance optimization of a Voronoi mesh support structure subjected to earthquake loading.

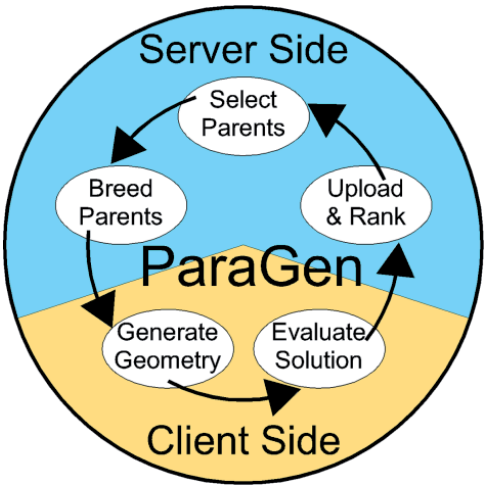

Figure 1. Form exploration cycle in ParaGen.

2. GEOMETRY DEFINITION

The first step in setting up a form finding process is to define a consistent parametric model with well-defined geometric boundary conditions. This paper explores the form finding of a 15-story tower with radial floors on each story. The floor-to-floor height of each story is taken as 3.5 m. On each floor, a rigid concrete slab distributes and transfers the gravity dead and live loads to a radial network of steel wide-flange beams (Figure 2). These beams transfer gravity loads to a central column and the cellular steel skin and also they create semi-rigid diaphragms for story levels. The cellular skin is also the main load bearing system for earthquake loading. In order to design the cellular skin frame for seismic loading, the tower is analyzed for self-weight and seismic loads induced by story mass at each level of the tower.

In order to define the solution space for the structure in this research, a parametric model is set up. Generative Components (GC), by Bentley Systems, is used to create the parametric model of the structure. The basic rules and parameters determine the geometry of the model and the range of possible forms. The degree of freedom in overall geometry and the patterning resolution of the skin is controlled by defining a certain number of variables and rules in the parametric software.

The overall geometry of the structure is created by a multi-section B-spline surface constructed with fifteen circles placed on horizontal planes distanced 3.5 m in the vertical direction. These circles are also used to create story beams. The radius of each circle is a parameter that can vary from 7 m to 20 m.

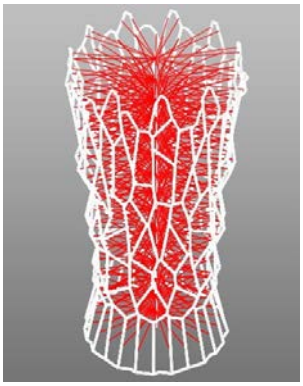

Figure 2. Geometry definition.

In order to create the skin pattern for the structure, Voronoi seeds are laid out on a plane at the bottom of the tower according to ten concentric circles evenly spaced from the base story circle to the top overall height of the tower, which is 52.5 m. Voronoi seeds are created based on ten parameters defining the number of points that will be placed evenly on each of the ten circles. These parameters control the density and the configuration of the Voronoi seeds in the plane.

Using the procedure described above, seeds are distributed in the XY Plane using a GC script transaction. A

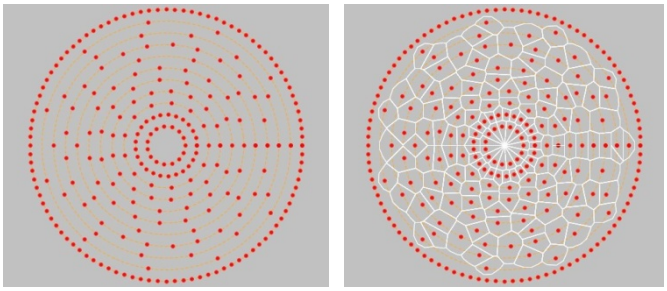

Figure 3. Voronoi pattern creation.

plugin called rcQhull is used to generate a 2D Voronoi diagram based on the distributed seeds (Figure 3). The fitness of the patterning of the peripheral skin is directly proportional to the number of seeds. Subsequently, the vertices of the Voronoi diagrams are projected onto the B-spline surface of the towers and the polygons are regenerated on the tower skin using the mapped vertices.

In order to create the story beams, the structure was cut by horizontal planes at each floor level. Radial floor beams were created from the center to the intersection of the planes and the structure (Figure 4).

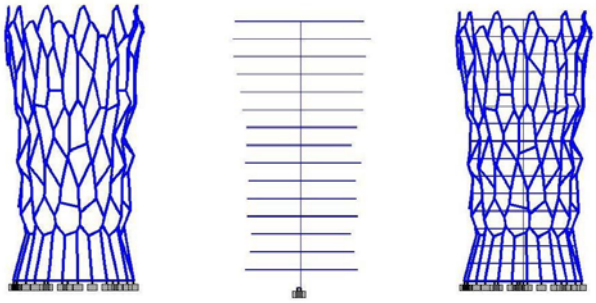

Figure 4. Structural system geometry.

3. STRUCTURAL LOADING

The structure is designed to resist dead, live, self-weight and seismic loading conditions. Dead and live loads are applied to the story beams, which transfer the loads to skin members. Commercial finite element software STAAD.Pro, from Bentley Systems, was used to carry out structural analysis and design of the structure. Steel HSS pipe sections were used for skin frame and W sections were used for story beams and the central column. All connections in the outer shell are considered rigid, with simple connections between the floor beams and the shell. The simple connection will transfer the gravity loads without induction of moments to the skin frame at the point of connection. Using Colorado as the project site, the seismic parameters are tabulated in Table 1 based on the IBC 2006 building code for that state.

Ss	2.142 g	**Soil Class**	4
S1	1.099 g	**Fa**	1.0
TL	10	**Fv**	1.5
I	1	**CT**	0.035
Rx	4	**X**	0.75
Ry	4		

Table 1. Seismic parameters IBC 2006.

The structure is analyzed under gravity and seismic loadings and designed based on AISC-ASD building code. The FEA is iterated to get convergence of member sizes.

4. FORM EXPLORATION

ParaGen is used for the form exploration. ParaGen combines selected programs under the framework of a genetic algorithm (GA). ParaGen combines currently available associative parametric software such as Generative Components with analysis tools to explore a range of well performing design solutions. The entire cycle runs on a Windows cluster synchronized over the internet by a web server (von Buelow, 2012). Through the use of multiple objectives, the cluster searches the solution space to fill a database of well performing solutions.

Using multiple objectives as fitness functions for the GA, ParaGen uses a Non-Destructive Dynamic Population GA (NDDP GA) to fill a database with successive generations of solutions (von Buelow, 2013). Through

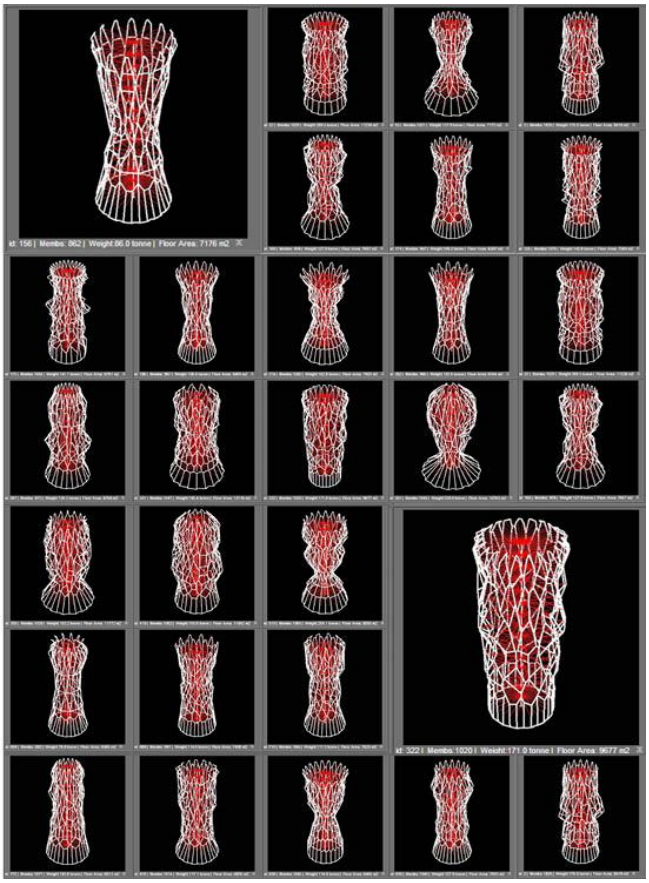

Figure 5. Sample of initial, randomly generated solutions

selection breeding and mutation, the form exploration process effectively explores the solution space for structurally well performing light-weight systems. The online database created by ParaGen can be searched using structured queries based on both performance values and geometry such as base shear, maximum deflection, total weight, and number of members, among others. The designer can use this data to sort and explore the solutions for desired combined performance.

Through selective breeding, the GA successively explores more "fit" areas of the solution space. The resulting solutions are not only optimized for explicit objectives, but can also be searched by the designer to interactively explore the design solutions and even combine desired solutions through manual breeding.

The process begins with the random generation of solutions. After a sufficient number of solutions with performance values have been loaded into the database, the GA begins to use a series of fitness functions based on database queries to build the breeding populations (see Figure 5).

Multi-objective exploration is carried out through selective breeding of parents picked from sorted sets with multiple fitness criteria like deflection, minimal weight, maximized floor area, and maximized modal frequency.

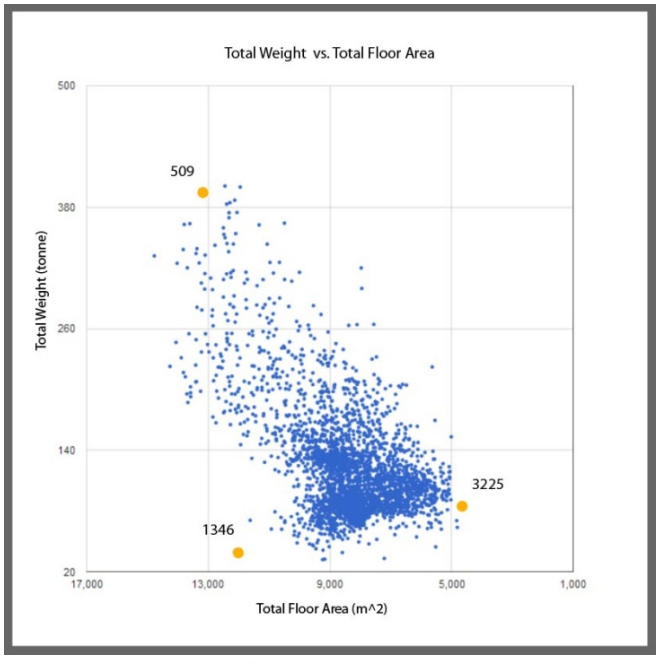

Figure 6. Pareto front for first modal frequency vs. total weight.

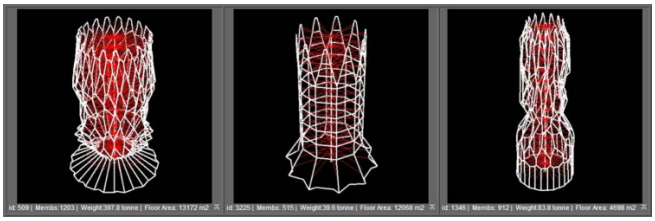

Figure 7. Three solutions chosen from Figure 6: 509, 3225 and 1346 (from top left to bottom right.)

As with many design problems, there are conflicting objectives that have to be balanced to find the most desirable solutions. For example, although due to gravity loadings the optimal structure tends to move toward a more slender tower, the lateral seismic loading requires bigger lateral dimensions that increase member length and consequently increase overall weight. ParaGen has built-in capabilities for graphing Pareto fronts and parallel coordinates graphs for the exploration of multiple objectives. Figure 6 shows a graph of the Pareto front resulting from a comparison of Total Weight (in tonnes = 1000 kg) vs. Total Floor area. By clicking on the plot dots, the tower thumbnails can be displayed for comparison. In this way, trade-offs can be explored along the Pareto front. In this research 3400 solutions were generated through the process of form exploration. Figure 7 shows images of the solutions for three points selected from the plot.

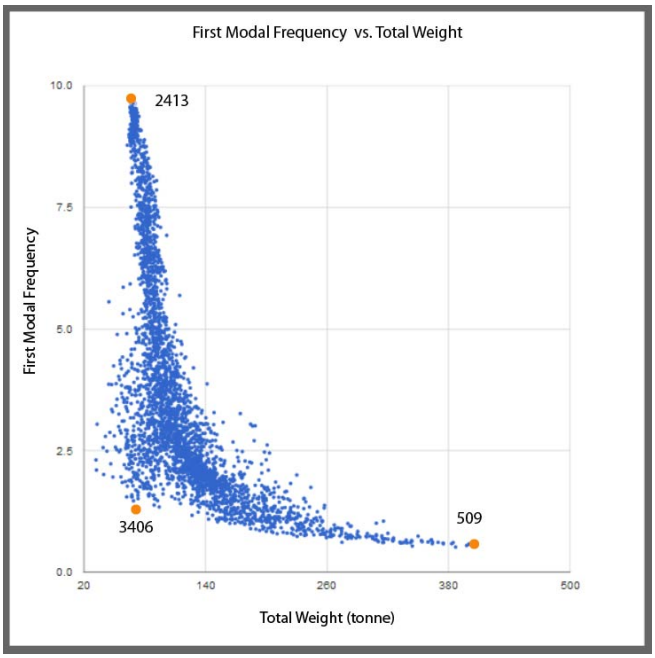

Figure 8. Pareto graph of weight vs. first modal frequency.

Figure 8 shows a graph of two performance values: Modal Frequency vs. Total Weight. Since the diameter of the tower was allowed to vary, the least-weight solutions have a smaller diameter. Interestingly the heavier towers are actually less stiff since the radius of the plan section is greater. Stiffer structures have the cone shaped overall geometry which increases lateral stiffness. Three solutions chosen along the Pareto front are shown in Figure 9.

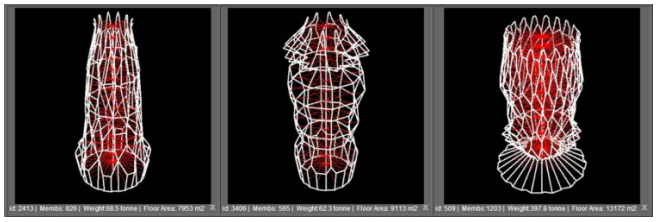

Figure 9. Three solutions chosen from Figure 8: 509, 3406 and 2413. (from top left to bottom right)

Because all geometric properties, as well as the performance values found in the analysis, are stored in the solution database and linked to several graphic images, exploration of the forms is interactive and controlled through ParaGen's web interface. Any area of the solution space can be described through a bracketing of the geometric and performance values in the menu at the top of the web page. Figure 10 shows the search control settings and Figure 11 shows the resulting solution set. By changing the search parameters, different areas of the solution space can be made visible. Figure 12 shows an alternate representation of these solutions, depicting the actual member section dimensions determined by the FEA in STAAD.Pro.

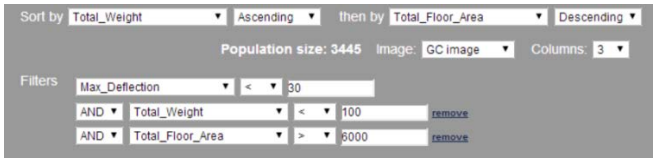

Figure 10. Sample of interface for final generation of forms.

5. DISCUSSION AND CONCLUSION

The main purpose of this paper is to illustrate the application of the genetic based form finding process in exploring cell morphologies as a seismic load bearing system in midrise towers. In this example ParaGen combines associative modeling software with finite element analysis software and a genetic algorithm. The parametric model creates the complex morphology of the tower skin based on Voronoi patterns using a small number of parameters. This associative model is very flexible so the GA can be used effectively to explore the design space using the various fitness functions supplied.

In this example, the complexity of generated Voronoi forms is architecturally desirable, and the flexibility of the parameters in controlling overall geometry through radius of the stories as well as local geometry through resolution of Voronoi patterns makes ParaGen an effective method to explore the innovative forms.

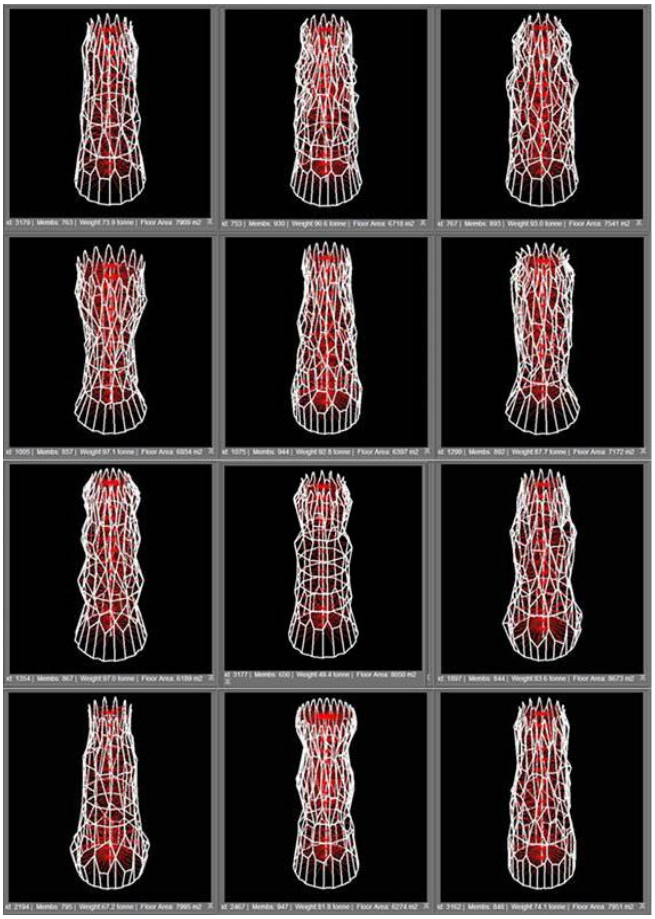

Figure 11. Solutions found with settings from Figure 10.

Through the process of parametric model generation, it was observed that in some models long columnar members would emerge at the bottom level. This would reduce the lateral stiffness of the lower level which can induce the soft story effect. This situation was partially covered with GA in the exploration process by increasing the Voronoi seeds at the bottom story to decrease the length of columnar members. Moreover, during the multi-objective breeding in the final generations based on minimized weight, minimized

base shear and maximized floor area structures, regular patterns took over the population, which implies their better performance mainly due to continuous load path (see Figure 12).

Although the initial generation and analysis of more than 3000 solutions took approximately two weeks to run on a cluster of 10 machines, the subsequent exploration of the solution database created is near instantaneous and certainly interactive. Of course any number of machines can be added to a cluster for faster processing times. All that is required is the software to be used in the generation and analysis phases, and an internet connection to access the server and database. As a result, the ParaGen method can be used to advantage in exploring complex problems with multiple performance objectives and large geometric variability.

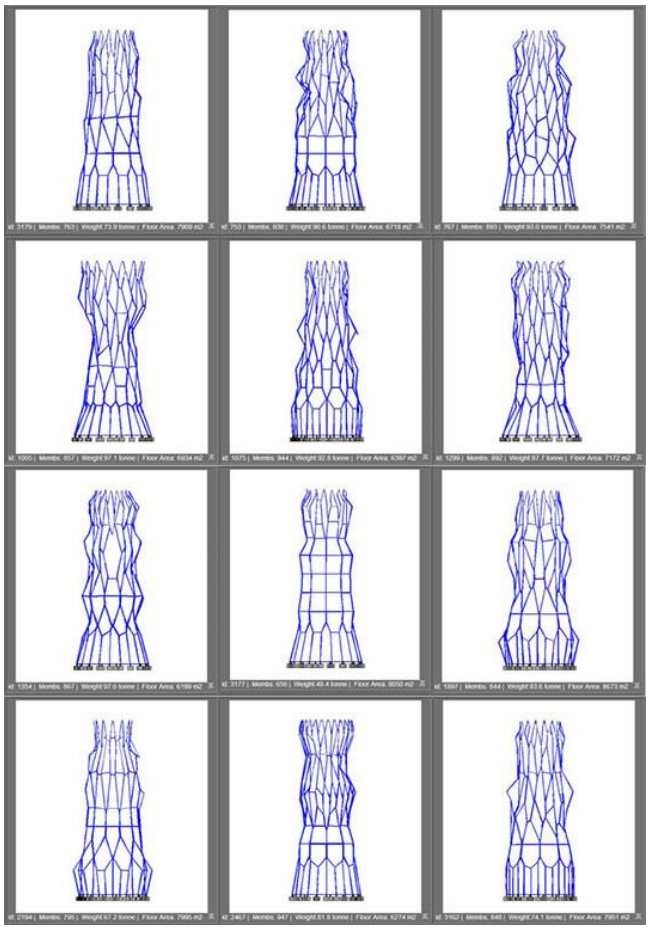

Figure 12. Solutions found with settings from Figure 10. Actual member section dimensions were determined by the FEA in STAAD.Pro.

References

ROUDAVSKI S., Towards Morphogenesis in Architecture. 2009. *International Journal of Architectural Computing*, Vol. 7, No. 3. pp. 345-374.

DIMCIC, M., KNIPPERS, J., 2012. Integration of FEM, NURBS and Genetic Algorithms in Free-Form Grid Shell Design. *Computational Design Modeling*. Pp 97-103.

TURRIN, M., VON BUELOW, P., Stouffs, R. 2011. Design explorations of performance driven geometry in architectural design using parametric modeling and genetic algorithms, Advanced Engineering Informatics. *Elsevier*, Vol. 25, No. 4, pp. 656-675.

BALDOCK, R., SHEA, K. 2006. Structural Topology Optimization of BracedSteel Frameworks Using GeneticProgramming. *Intelligent Computing in Engineering and Architecture*. Vol 4200. pp. 54-61.

KICINGER, R., ARCISZEWSKI, T., DEJONG, K. 2005 Evolutionary designing of steel structures in tall building. *ASCE J. Comp. Civ. Engrg*.

MALKAWI, A. 2006. Performance simulation: research and tools. *Proceedings of Performative Architecture*. 87-95.

VON BUELOW P. 2012. ParaGen: Performative Exploration of Generative Systems. *J.IASS*, Vol. No.4. pp. 271-284.

VON BUELOW P. 2013. Techniques for More Productive Genetic Design: Exploration with GAs using Non-Destructive Dynamic Populations. in *Adaptive Architecture*. Proceedings of ACADIA

Design Agency: Prototyping Multi-Agent System Simulation for Design Search and Exploration

David Jason Gerber, Rodrigo Shiordia, Sreerag Veetil and Arjun Mahesh

University of Southern California
School of Architecture,
Watt Hall 204, Los Angeles, CA 90089
dgerber@usc.edu

Keywords: Parametric Design, Generative Design, Multi-Objective Optimization (MOO), Multidisciplinary Design Optimization (MDO), Multi-Agent Systems.

Abstract

This work presents prototypes of multi-agent system simulation for design search and exploration. We describe an experimental approach in part based on a previously established multidisciplinary design optimization (MDO) framework. Here the work further explores the potential impact of MDO in conjunction with multi-agent systems on the early stages of design. Specifically, this paper addresses the potential of introducing agent-based computing techniques into the multidisciplinary architectural design optimization and search workflow to tackle geometrically complex design problems and to facilitate early stage design exploration. To address these interests, a series of prototyped workflows were studied inclusive of environmental performance and structural performance metrics and benchmarks. This paper presents a novel methodology for using simulation data in conjunction with multi-agent systems as a way for reinforming form and enhancing performance in a generative design environment. The methodology is based on the use of swarm algorithms and their integration with data generated by simulation software. The interaction between these two domains, the simulation data and swarm algorithms, generates the final output as a modified geometry that is then evaluated by comparison for enhanced design performance.

1. INTRODUCTION & OBJECTIVE

Computer-Aided Design and Engineering (CAD/CAE) and heuristic simulation tools enable architects and engineers to 'design-in' higher performance for their buildings by simulating spatial, material, environmental and structural systems with greater certainty. This work situates itself amongst a body of research that studies the applicability of multi-agent systems for use in design as generative bottom-up strategies for form finding and optimization and search for design domains. Figure 1 illustrates two experimental agent-based swarm tectonic projects that, on the one hand, engender contemporary aesthetics and, on the other, demonstrate by comparison how these projects can be researched through a discourse of performance and design exploration and search. The top example is an experiment without the incorporation of the simulation data set and the bottom example is a project where the agents are directed through the analytical data, forming informed paths.

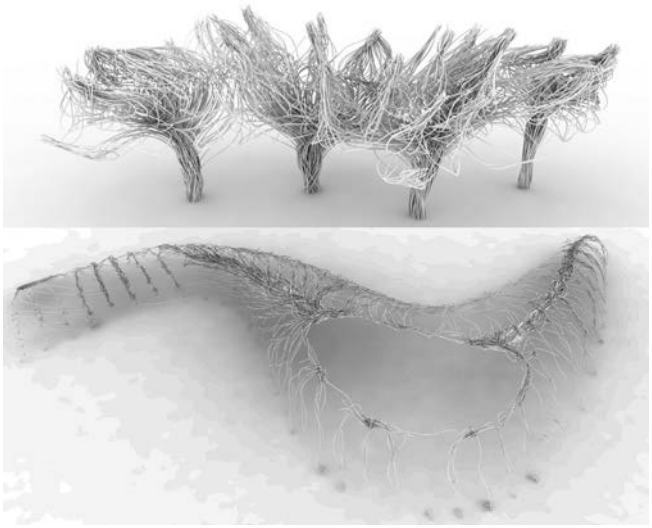

Figure 1. Image of experimental "nest" projects: in the above case originating from simple surface conditions and swarm logics; and in the case below via incorporation of analytical simulation data of performance metrics.

The research objectives presented in this paper are first to determine whether the multi-agent based approaches

provide a viable model for engaging with data from simulation, and second to validate some initial results as providing improvements in a performance metric and for design search and exploration and prototyping. While the performative aspect of the final output is analyzed, there is also an interest in analyzing the successes and failures of the entire workflow in reference to its applicability in contemporary design practice.

2. BACKGROUND & REVIEW

The work is backgrounded through a set of precedents that both trace a brief history and more importantly reflect on current examples of where the work can be understood as potentially novel. Simulation software is now commonplace in the design field, with most design suites now including many different models for simulating sun, lighting, structural performance, fluid flows, etc. As these models become easier to use and cheaper in terms of computation, they should be integrated into the generative design process (Weinstock and Stathopoulos 2006). While most designers engage with the information from simulations as a form of validation or as an aid in the decision making process, there are numerous precedents that have used the information from simulation as a platform and a driver in the generative process (Miranda and Coates 2000; Ireland 2009; Snooks 2012). The data generated by a simulation becomes a stage in the workflow, as opposed to a final validation of the design solution (Doumpioti 2010). Here the work uses a simulation of multi-agent systems as a means to explore the benefits of bottom-up design strategies to accomplish the aesthetic and performance objectives. One example of a bottom-up approach where multiple entities make decisions based on local information is a flocking system (Reynolds 1987). This system has become more and more accessible to designers and it represents a model for the generation of systems that generate geometry from many local interactions, both between elements in a system and between these and their environment (Aranda and Lasch 2006). The process of modifying this basic model for specific objectives becomes the domain of the computational designer, where behavior is crafted for specific purposes based on a material system and geometric constraints. These types of systems have been applied to design problems of varying scales ranging from urban design (Popov 2011; Bus 2012), to surface panelization (Baharlou and Menges 2013), to name but a few. Critical to our starting point are MDO frameworks and the use of parallel computing and optimization for our current research trajectory (Gerber et al. 2012; Lin and Gerber 2014). Included in these frameworks is the reliance on and use of simulation and analysis packages for informing and the formal result as well as for deciphering performance enhancements (Gerber and Lin 2013). Through the Pareto Optimization that we have pursued across multi-objective design search spaces we realized the level of topologic extensibility as well as the modeling of ever more diverse and competing objectives (design agencies) requires experimenting with multi-agent systems first through swarm-like scripts and then secondly through the incorporation of high fidelity performance analysis engines. Some work has attempted to do similar data-driven agents through integration of a data field with a swarming algorithm explored for material organization and formation objectives (Tsiliakos 2012). Other work by Schumacher explores the realm of reconfigurable architecture through the simulation of social agencies (Schumacher 2011).

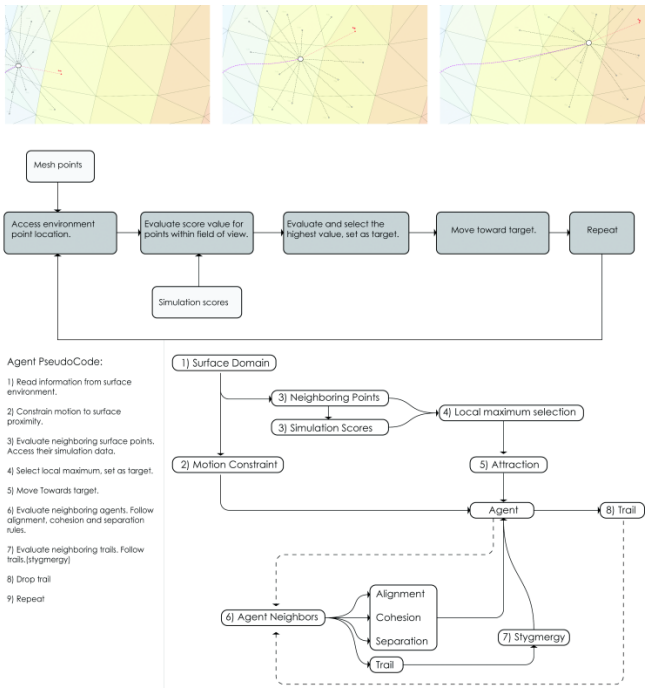

Figure 2. Pseudo code and algorithm design for the multi-agent based simulation incorporating analytical data. Image shows the algorithm for each agent; the process updating; the result of the agent's motion through the surface domain, from its start point, to a local maximum (a point where the neighboring point's scores are lower) and termination.

3. RESEARCH METHOD

The methodology of the research has been to work in an incremental fashion with the end goal of being able to measure improvements in design outcomes in formal terms, in design optimization and performance terms and finally in terms of design process. The work is reliant on three categories of simulation in the overall design computation workflow: 1) simulating design typologies through the use of an associative parametric geometry modeler; 2) simulating swarm logic through agents and a multi-agent system (MAS); and 3) the simulation of solar radiation and structural finite element modeling (FEM) and analysis for informing the probabilistic behavior of the agents and analyzing the resultant outputs.

As a first step, the design of the experiment(s) begins with undirected agents, meaning simple swarms that are only bounded by the surface condition or proximity and pseudo gravity or initial inertia and direction. As a second step, these initial design surfaces are then run through an analytical workflow for determining the initial solar radiation or structural performance, for example. The third step is to relate the values of the analyses to the design surface, now a mesh where each tessellation has an associated value that further influences the agent's behavior. The fourth step then exports the results of the agent-based swarm for post analysis in terms of improved solar radiation and also improved material distribution as a means to analyze structural optimization. A last step includes the rapid prototyping in multi-material 3D printers for design prototype evaluation. (See Figure 5)

3.1. Design Surfaces and Constrained "Nests"

The initial design type has been to use a series of parametrically defined design surfaces that exhibit complex curvature and incorporate holes for topologic complexity. It is important to note the surface openings purposefully add a second level of complexity for a human designer to predict performance outcomes. Intrinsic to our line of inquiry is one that is in part predicated on previous design computing and cognition research that suggests that the human designer is limited by issues of problem scale and coupling. Our observations, simplified, are that the human designer should be given more automation in order to aid in the management and production of ever more complex geometries while maintaining or enhancing their performance characteristics (Flager et al. 2014). Figure 1 illustrates two of a large series of initial surface experiments that visualize the undirected and directed (i.e. simulation data incorporated) surface types discussed throughout this research paper. These initial surfaces are defined through Rhino Grasshopper as a simple parametric model from which we explore an extensive solution space. From this surface model we export a mesh for importing into a 3D Java based environment where we program our agents and simulate the multi-agent system behavior. Taking a surface mesh as input, a multi-agent system is initiated by spawning the agents, one for every vertex of the input geometry. Each face's center is attracting the agents towards it, keeping the agents purposefully close to the surface as an initial condition. Once the simulation has been run the output geometry is extracted from each agent's trajectory captured at a given point in time. We then use a number of surface and mesh operations in Rhino to isosurface and/or pipe the agent trajectories into architecturally recognizable geometry and systems, both for structural definition but as well for shading characteristics. By managing the input mesh's vertices through count and pattern, the spawning points are controlled and different densities emerge, making the output a field of trajectories which engender varying degrees of performance for our multi-objective design search space.

3.2. Shells as "Fields of Intensities"

After having explored an extensive set of design surface types and undirected swarm scripts and their varied parameterizations of the values within these scripts, we then chose a sub-set for further simulation and data analysis. The selection of the sub-set was based on keeping our initial design surface density and complexity relatively simple from a computational overhead and post analysis point of view.

This incremental step of the research focused on developing a methodology to explore the architectural shell. An important theoretical concept to our work in contemporary architectural design is that of the shell as an architectonic entity that is both form and structure, and that can be understood as a field (Allen 1997). Our surface shells can therefore be understood conceptually and then computationally as fields of intensities, which then allow for empirical influence over our multi-agent systems approach during simulation but as well for post analysis. Our shells as fields of intensities can then be abstracted as a collection of points in space with varying values per vertex in a current iteration. One value represents the amount of light and solar radiation that a particular point receives, and/or it represents

the amount of stress relative to the whole shell at that point of the geometry. As such, this collection of points and their associated values is a field of intensities (real numbers) where the specific performance of a location (coordinate values) bears a relationship with the whole shell in a particular location relative to the sun. The different values can then be selected for influencing the behavior of the individual agent recursively within the entire population of agents based on specific design parameters written into the agent classes as objectives. Our multi-agent based design objectives include that of minimization of structural weight and or maximization of solar shading. The integration of this multi-objective data field with a swarm algorithm is then tested for viability as a model for material organization and formation.

3.3. Workflow Tools and Algorithms

The workflow has been built around a series of open source simulation environments and an easy-to-use associative parametric design and visual programming environment, Grasshopper/Rhinoceros, and a series of plug-ins for integrating performance simulations and generating data that can then be read by a custom agent based swarm algorithm programmed in the Processing 2.0 environment and language. The specific Grasshopper plug-ins incorporated to date include Karamba, used for running stress simulation of a shell structure, and Ladybug, used to run a Radiance based simulation. The simulation data is exported as text files that can be read by the agents in our Processing sketch that read the surface vertices and coupled data values. The agents are then spawned and programmed to make movement and trajectory decisions based on the local information, including the intensity values from the simulation, proximity to neighbors, and trails left by other agents.

The multi-agent system is based on simple flocking behaviors described by Craig Reynolds. Each agent has the capacity to read the data from the simulation, which is paired with its corresponding point in a mesh object. Thus, the agent's environment is a collection of points to which it is constrained, and each point is assigned an intensity score based on the data from the simulation. The agent's trajectories then become a generative geometry for material organization and material re-organization. This happens in a collective recursion. The agent-based trails are exported again as a text file into the Grasshopper/Rhinoceros environment, and they are re-meshed as part of the initial geometry, inscribing a pattern onto the surface.

Figure 3 Images show shell stress (top) and solar radiation (bottom) simulated and evaluated on a user-defined surface, and the resultant trajectories of a multi-agent system that searches for local maxima in the field of values. Each agent reads this information and reacts to it, collectively finding points of greater intensity on the surface.

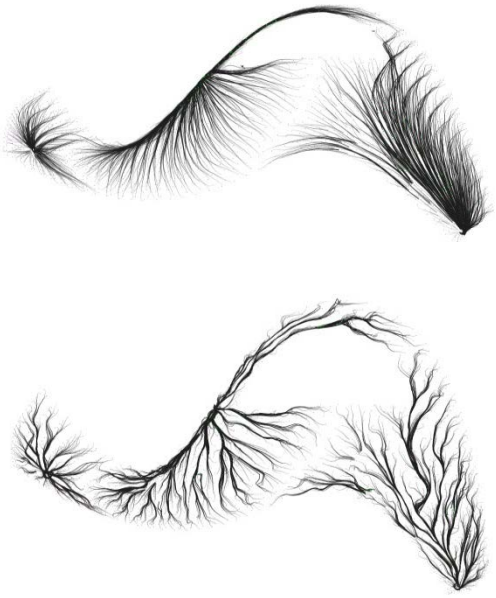

Figure 4. Images illustrate the system without trail following (above) and with the addition of the trail following behavior to the agents (below).

3.4. Stygmergy and Performance

Another increment and thrust of the inquiry into the multi-agent based simulation has been to augment the

scripts to incorporate another layer of information that can be read by the agents, specifically that of the trail positions of all other proximate agents. This process mimics natural systems such as pheromone trail following in ant societies and is known as Stygmergy. Stygmergy has been explored previously and provides a way for path optimization in an agent system (Ireland 2010). This behavior was introduced to prevent the homogenization of the system as can be seen in the top version of Figure 4, and to reduce the amount of redundant material deposited in the surface when the paths are re-meshed, seen in the bottom of Figure 4. This actually means that the paths tend to converge as the agents are attracted to other trails. This self-organizing aggregation has a great effect on the outcomes for each objective, but as well for the shells as a whole. The initial runs did not include stygmergy but once implemented we are able to form find inclusive multiple levels of collective intelligence and analysis for the post analysis. This stygmergic method provides a solution for situations where the addition of material would just result in a global thickening of the surface and reduce overall efficiencies in terms of structure and material deposition.

3.5. Post-Analysis and Prototyping

The scripts are then run and the paths are then iso-surfaced back onto the surface for post analysis. The "embossed" pattern was hypothesized to enhance the performance of the design surface type in the criteria that it was initially analyzed for either solar radiance and or for structural performance. We theorized an addition of material based on the accumulated stygmergic agent paths would affect structural performance through a thickening of the trajectories as primary paths of stress, and an overall thinning of the shell structure, predicted to provide lines of increased resistance allowing for a reduced thickness elsewhere. In the case of the solar radiance performance, we theorized the accumulated paths of thickened geometry would provide a material barrier for shading, lowering incidence of solar gain on the underlying surface and volume of air. Figure 5 shows the full sequence of steps taken from initial surface through to final physical prototyping. From the top one can see the original analysis of the surface, then the agent paths, projected to an offset version of the surface, and then the analysis of the surface with the simulation data included. Discussed in the analysis is how the global average was reduced by simple material deposition and measured through an FEM based analysis.

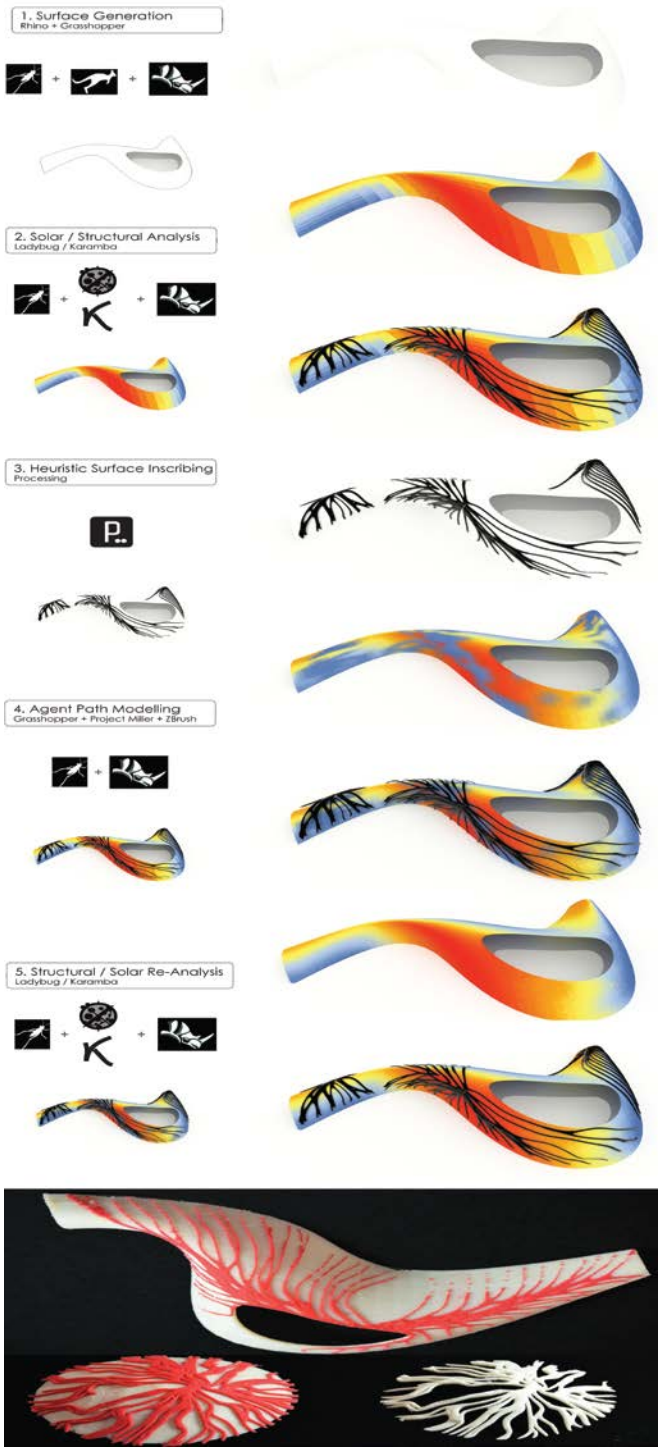

Figure 5. Detailed steps and workflow through to 3D multi-material rapid prototyping. The image illustrates the complete workflow, which progresses from a generation of a surface, its simulation-based analysis and resulting data, the result from the data-influenced multi-agent system, stygmergy, and the final post-analysis.

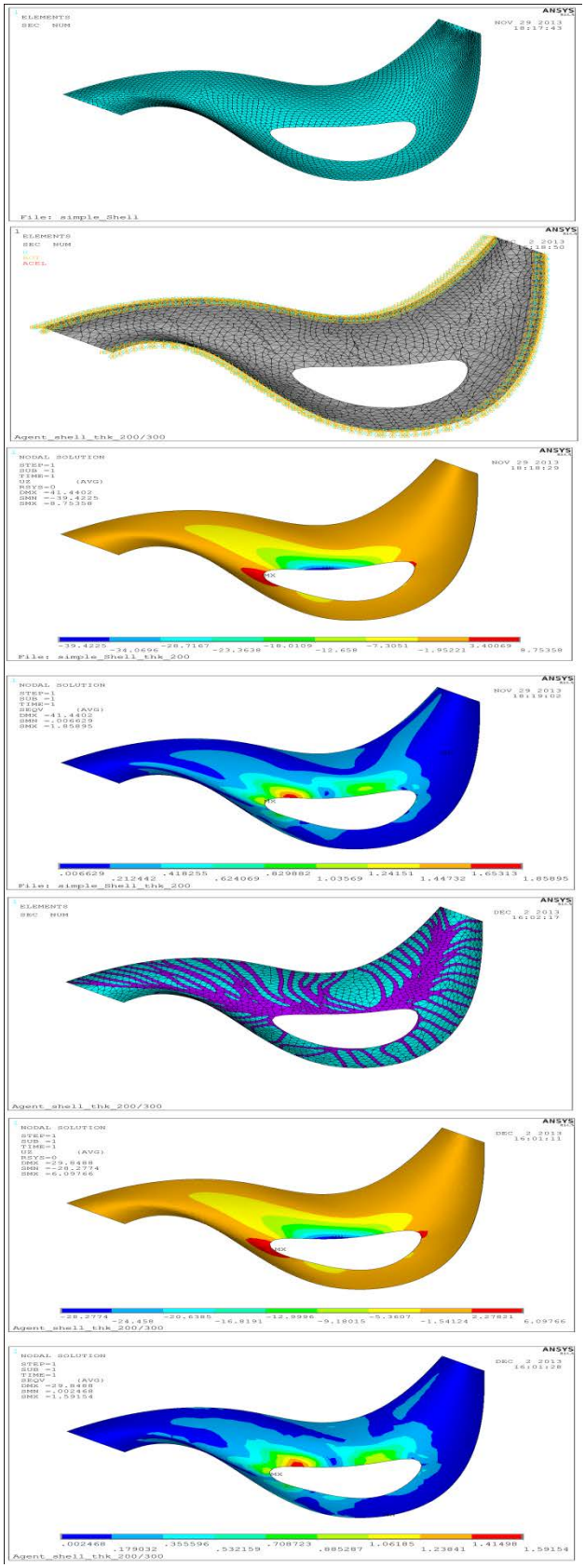

Figure 6. The image shows the sequence of ANSYS based post analysis of the multi-agent based form finding and its structural efficiency improvement for the shell topology. It illustrates the analysis of the shell without agent paths and the re-analysis of the shell with the paths. There is a measurable and visualized difference from step 4 to step 7.

4. ANALYSIS

A final line of inquiry was to post analyze the results with a high degree of accuracy and within a standalone FEM analysis environment, that of ANSYS. The research objective included an effort to provide for an empirical analysis of the results of the multi-agent based trajectories and the stygmergy accumulation and optimization. One shell was compared from its initial state to that of the data driven trajectory state. The Finite Element Model (FEM) used Static Stress with Linear Material Models as its analytical approach. This allows a model to be analyzed with multiple loads, while solving the equations at one time in parallel. However, load case multipliers that were considered for this particular analysis do not include any live or surface loads. For the time being we simply looked at dead load optimizations. For the initial post analysis only acceleration due to gravity was included in the analysis. The acceleration direction multiplier is multiplied by the acceleration *Due To Body Force* that is then multiplied by the acceleration load case multiplier, g = 9.81 m/s^2 (in Z direction). Furthermore, only Von Mises stress is analyzed, for it reflects structural stress cases that are material specific, as explained below. The displacement and structural behavior of the mesh is solely the resultant of the Von Mises stress in its current analysis. For FEM simulation purposes, a material was necessary, so a standard timber with isotropy behavior (same resistance and stiffness in each direction) was chosen. This allowed for our analysis of the timber to be modeled and studied with an elastic nature. Furthermore, in terms of future research interests our choice of timber represents many products from different manufactures similar in form to Cross Laminated Timber (CLT) panels and boards. These CLT panels are standard thin timber boards glued together with the main fiber crossed from one board to the other. In this way they achieve the isotropy of the "composite material". For this reason Von Mises stress is applicable. Here, as with the original parametric geometry model, we conceived future material parameterizations, especially those considered elastic in nature, to be included in the future study.

In the sequence of images in Figure 6 the bottom curves of the mesh have been constrained as a fixed boundary for the analysis and no other constraints are induced in the mesh. The following values are the basic characteristics used for defining the simulated material property: E = 10000 MPa, Poisson ratio = 0.2 and Density = 500 kg/m^3 = 5.0e-07 N/mm^3.

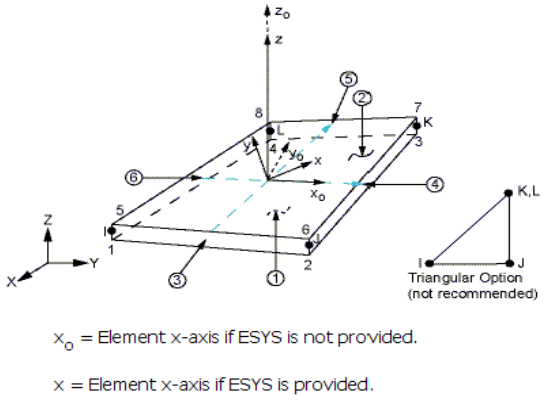

Figure 7. The geometry, node locations, and the element coordinate system for the FEM (shell element 181 of ANSYS) used for the analyses. The element is defined by shell section information and by four nodes (I, J, K, and L) as shown.

The shell element 181 of ANSYS has been utilized for the analysis. SHELL181 is suitable for analyzing thin to moderately thick shell structures. It is a four-noded element with six degrees of freedom at each node: translations in the x, y, and z directions, and rotations about the x, y, and z axes. SHELL181 is considered well suited for linear, large rotation, and/or large strain nonlinear applications. Changes in shell thickness are accounted for in the nonlinear analyses. In the element domain, both full and reduced integration schemes are supported and SHELL181 accounts for follower effects of distributed pressures. Element formulation is based on logarithmic strain and true stress measures. Element kinematics allow for finite membrane strains (stretching). However, the curvature changes within an increment are assumed to be small for our initial analyses. Our chosen method to run the analysis and comparisons was to vary the shell thicknesses within a limited range. The analysis maintained the range of thickness between 200 to 300 mm. The original mesh has been modeled for three values of thicknesses and yielded the results illustrated in Table 1.

Thickness	Deformation (mm)	Stress Von Mises (MPa)	Volume (m^3)
250	-30.20	1.71	1069.2
300	-24.27	1.60	1282.5
200	-39.42	1.86	855.4

Table 1: Enumerates the FEM thickness, deformation, Von Mises stress and Volumes for the experimental ranges tested across the shell structure.

The original mesh is then solved through the FEM simulation for the deformation; Von Mises and then overall shell volumes are calculated. Then a new shell model is solved with the additional material allocated along the ribbed areas of maximum stress generated by the multi-agent based results. Then two groups of meshes with varying thickness are modeled and combined, where group 1 is the original shell having a 200 mm thickness and group 2 is the multi-agent stygmergic paths turned into the ribbed area of maximum stress, having a 300mm thickness. We then analyzed the combined case and benchmarked it against the shell-only minimum thickness case. Results yield the following values as seen in Table 2.

Thickness	Deformation (mm)	Stress Von Mises (MPa)	Volume (m^3)
200 (300 rib)	-28.28	1.60	1026.3

Table 2: Enumeration of the shell with the multi-agent driven path (ribs) thickness performance enhancements and ranges. Of particular importance is to note overall volume reduction while still maintaining a minimum Von Mises stress and non-extreme deformation calculation (or understood to be within allowable range).

The results shown in Table 2 highlight the improved behavior understood to be achieved through the minimization of overall structural volume when inclusive of the ribs on the shell. Most importantly, the post analysis demonstrates that for an equal Von Mises (1.60 MPa) we do achieve a specific volume minimization of 256.2 m^3. Furthermore the results are within the allowable ranges of Von Mises stress and displacement, indicating that there is a volume advantage and hence material savings in the multi-agent based approach.

5. CONCLUSION

The work presented here is a set of initial experiments designed to begin to test and evaluate a set of workflows that can integrate existing lines of design exploration and search through MDO with those of the bottom-up strategies and self organizing methods for optimization through the multi-agent system. Our general notion of 'Design Agency'

is becoming a field where numerous researchers and practitioners have begun to explore the possibilities for its effect on architectural modes of production and artifact. Design Agency, and the use of multi-agent systems, albeit in its infancy is also explored for the potential impacts upon form finding through performance empirically. To date the research has been explored with three overarching objectives: 1) determining whether the multi-agent based approaches provide a viable model for engaging with data from simulation; 2) validating initial results as providing improvements in a performance metric; and 3) improving design search, exploration and prototyping. While we have endeavored to measure the success and failures across all three of these lines of inquiry the focus here has been to measure empirical outcomes first, as is seen in the case of the material minimization presented in the last section. We have achieved this over a short time frame and expect to extend the research through a more rigorous literature review and survey, a series of tool and workflow developments, experimenting across a variety of architectural types and topologies, while working within a tightly coupled multidisciplinary research team incorporative of computer science, engineering and quantitative social science. Next steps include developing new analytical engines and design workflows through creating a society or set of agents that in a competitive and diverse coordination further optimize while extending design exploration, search, and prototyping opportunities.

Acknowledgements

This material is supported by the National Science Foundation under Grant No. 1231001. Any opinions, findings, and conclusions or recommendations expressed in this material are those of the author(s) and do not necessarily reflect the views of the National Science Foundation. We thank and the USC School of Architecture and Felice Allievi from Degree of Freedom Engineers.

References

ALLEN, S. 1997. "From object to field." Architectural design 67(5-6): 24-31.

ARANDA, B. and LASCH, C. 2006. Flocking. Tooling. New York, Princeton Architectural Press. 27.

BAHARLOU, E. and MENGES, A. 2013 of Conference. Generative Agent-Based Design Computation. Computation and Performance – Proceedings of the 31st eCAADe Conference Faculty of Architecture, Delft University of Technology, Delft, The Netherlands.

BUS, P. 2012 of Conference. Emergence as a Design Strategy in Urban Development: Using Agent-Oriented Modelling in Simulation of Reconfiguration of the Urban Structure. Digital Physicality - Proceedings of the 30th eCAADe Conference, Czech Technical University in Prague, Faculty of Architecture (Czech Republic).

DOUMPIOTI, C. 2010 of Conference. Fibre composite systems: stress as growth-promoting agent. Proceedings of the 15th International Conference on Computer Aided Architectural Design Research in Asia.

FLAGER, F., GERBER, D. J. and KALLMAN, B. 2014. "Measuring the impact of scale and coupling on solution quality for building design problems." Design Studies 35(2): 180-199.

GERBER, D. J. and LIN, S.-H. E. 2013. "Designing in complexity: Simulation, integration, and multidisciplinary design optimization for architecture." Simulation Published online before print April 9, 2013.

GERBER, D. J., LIN, S.-H. E., PAN, B. P. and SOLMAZ, A. S. 2012. Design optioneering: Multi-disciplinary design optimization through parameterization, domain integration and automation of a genetic algorithm. SimAUD 2012, Orlando, FL, USA.

IRELAND, T. 2009 of Conference. Emergent space diagrams: The application of swarm intelligence to the problem of automatic plan generation. T. Tidafi and T. Dorta (eds) Joining Languages, Cultures and Visions: CAADFutures 2009, PUM.

IRELAND, T. 2010 of Conference. Stigmergic Planning. ACADIA 10: LIFE in:formation, On Responsive Information and Variations in Architecture - Proceedings of the 30th Annual Conference of the Association for Computer Aided Design in Architecture, New York ACADIA.

LIN, S.-H. E. and GERBER, D. J. 2014. "Designing-in performance: A framework for evolutionary energy performance feedback in early stage design." Automation in Construction 38: 59-73.

MIRANDA, P. and COATES, P. 2000 of Conference. Swarm modelling. The use of Swarm Intelligence to generate architectural form. 3th International Conference on Generative Art, Politecnico di Milano University, Milan, Italy.

POPOV, N. 2011. Generative sub-division morphogenesis with Cellular Automata and Agent-Based Modelling.

REYNOLDS, C. W. 1987 of Conference. Flocks, Herds, and Schools: A Distributed Behavioral Model, in Computer Graphics. SIGGRAPH '87.

SCHUMACHER, P. 2011. The autopoiesis of architecture. Chichester, J. Wiley.

SNOOKS, R. (2012). "Snooks, Roland. Fibrous Assemblages and Behavioral Composites, The Funambulist. Accessed July 25th, 2013, from http://thefunambulist.net/2012/04/20/guest-writers-essays-25-fibrous-assemblages-and-behavioral-composites-by-roland-snooks/.

TSILIAKOS, M. 2012 of Conference. Swarm Materiality: A multi-agent approach to stress driven material organization. Digital Physicality - Proceedings of the 30th eCAADe Conference.

WEINSTOCK, M. and STATHOPOULOS, N. 2006. "Advanced simulation in design." Architectural Design 76(2): 54-59.

Session 6: Fabrication and Design **99**

Visual Robot Programming — Linking Design, Simulation, and Fabrication **101**
Johannes Braumann, Sigrid Brell-Cokcan
Association for Robots in Architecture.

A Freeform Surface Fabrication Method with 2D Cutting **109**
Andres Sevtsuk, Raul Kalvo
City Form Lab, Singapore University of Technology and Design.

Design-Friendly Strategies for Computational Form-Finding of Curve-Folded Geometries: A Case Study **117**
Shajay Bhooshan, Mustafa El-Sayed, Suryansh Chandra.
Zaha Hadid Architects.

Visual Robot Programming – Linking Design, Simulation, and Fabrication

Johannes Braumann and Sigrid Brell-Cokcan

Association for Robots in Architecture
Gfrornergasse 6/15
Vienna, Austria, A-1060
johannes@robotsinarchitecture.org

Keywords: Visual Programming, Robotic Fabrication, Parametric Simulation, Design Feedback.

Abstract

In the creative industry, architects and designers have to realize complex, prototypical projects without the profit margins or the economy of scale of other industries. One of the core enablers of such processes are fluid and efficient workflows that allow a maximum of flexibility throughout the design process. However, rather than fully automating the design process, approaches are required that allow quick and intuitive changes of key parameters. Using visual programming tools, architects and designers are now able to create their own *virtual simulation environments*, where they can change key parameters with the push of a slider, and observe the results on their designs in real time. This research shows approaches on how parametric environments can be extended beyond simple design iterations to directly link the design with robotic fabrication. Due to their inherent multifunctionality, robotic arms are of special interest to the creative industry and can profit from the similar versatility of visual programming environments.

1. INTRODUCTION

In architecture and design, problem-solving through trial and error has a long history (refer to Cross et al., 1981) as, unlike other disciplines, many architectural problems are of an aesthetic, subjective nature—coupled with technical relevance—and often cannot be mathematically described. Without an accurate definition, such problems are impossible to be solved numerically via calculations and formulas. Therefore—through numerous prototypes, renderings, drawings, etc.—designers create various design iterations and constantly evaluate and improve upon them. A crucial part of this optimization process is the constant feedback that supports the designer's decision-making.

Today, a significant part of the technical feedback in the construction industry is generated by software such as Building Information Modelling (BIM) suites that are capable of immediately calculating a building's performance and even evaluating if a building conforms to zoning and construction laws.

In the area of design, we currently observe a trend towards using accessible visual programming environments such as Grasshopper and Dynamo for solving architectural and aesthetic problems. Designers use this parametric environment not only for rapidly generating design iterations with the push of a slider, but also for integrating custom simulation functions that graphically support their decision making. While programming has been an important tool in architecture for a long time, the immediacy of feedback makes visual programming especially appealing – it is not necessary to compile code, but changes to the parametric definition are reflected instantly in the viewport, allowing the designer to deduct an immediate relationship between cause and effect, thereby enabling an intuitive approach to problem solving through interaction. Using such tools, the trial-and-error process becomes much faster than the manual generation of design variants, highlighting the advantages of dynamic workflows that allow a constant evaluation of the output through simulation.

However, an aspect that is frequently missing in these workflows is the actual fabrication: While much time and effort is put into the creation of intelligent, parametric objects, all this intelligence is lost when objects are saved as generic 3D geometry to be processed by Computer Aided Manufacturing (CAM) software (Brell-Cokcan and Braumann, 2010). This interrupts the workflow, as changes to the parametric design cannot directly propagate to the CAM environment.

This research focuses on virtually integrating machines such as robotic arms into a visual programming environment and thus linking them via simulation to a fluid design-to-fabrication workflow. While doing so has the potential of greatly optimizing Computer Aided Design (CAD) to CAM workflows, it also offers benefits over traditional robot programming, enabling completely new ways of interacting with a machine as a design tool.

2. ROBOTIC FABRICATION AND SIMULATION

2.1. Robots in the Creative Industry

One of the main aspects that sets the creative industry apart from other industries is that architects and designers deal mostly with prototypes and mass customization, as opposed to mass fabrication. As such, the challenge for utilizing robotic fabrication in the creative industry is not so much the hardware, but rather the programming. Even though new mathematically elaborate solutions are capable of reducing the amount of geometric complexity in buildings (Pottmann et al., 2007), architects and designers still have to find solutions that enable them to automatically create machine code for a large number of self-similar objects, a process that is referred to as *mass customization*. When using Computer Numerical Control (CNC) machines (e.g., for milling), the process is relatively straightforward, as the workspace of the machine is clearly defined and each point can only be approached in a single way. The complexity increases exponentially when multi-axis robots are involved, as their many degrees of freedom provide robotic arms with no less than eight ways of approaching the same end-effector position (Figure 1).

Even with high-end commercial software such as RobotMaster, there is currently no fully automated strategy for defining the best robotic movement strategy. Therefore, it is crucial to *simulate* the full kinematics of industrial robots in order to prevent collisions and other problems.

2.2. Towards Visual Robot Programming

The programming and simulation of robotic arms is tightly linked, as they greatly influence each other. We currently see three different strategies and environments for programming and simulating complex robotic tasks:

Teaching, also referred to as *online programming*, is the most basic way of programming a robot by moving the actual machine and then saving its position. Therefore, the movements of the robot are basically simulated during the programming. However, teaching is very time consuming and not suitable for subtractive fabrication.

Adapting CAD-CAM strategies for robotic use: CAM software is used for generating toolpaths and is coupled with robot simulation/code generation software. While it offers existing CAM users an easy way to transition to robots, the problem is that such workflows are limited to a few established fabrication strategies such as milling. Furthermore a loss of information and parametric intelligence occurs when data is sent from CAD via CAM to the robot postprocessor.

Generic robot environments are used for a multitude of applications in the greater field of robotic research, e.g. service robotics. These environments are often based on open source software (e.g. ROS, V-REP) and can be expanded by the user. Inside such software, the user can simulate a wide range of properties, from physics, to machine vision, and even subtractive fabrication (Rohmer et al., 2013). The simulation is only performed within its own environment and not linked to parametric design data.

We consider *visual robot programming* (Figure 2) as a middle way that offers many of the advantages of other programming strategies, while being tightly integrated into a designer-centric, accessible parametric CAD environment: New modules containing additional functionality (Davis and Peters, 2013) can be easily coupled with the robot-specific components, and any changes to the robotic programming are immediately reflected in the integrated kinematic simulation (see Sections 3 and 4.2). This enables the development of new fabrication strategies that go beyond subtractive fabrication, such as the simulation-based parametric shaping of carbon-fiber elements in Section 4.

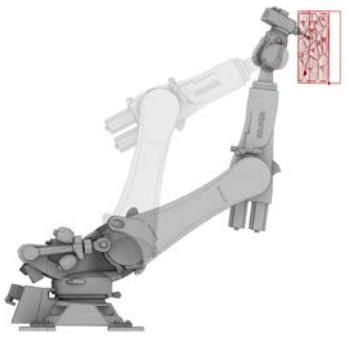

Figure 1. Two out of eight possible kinematic configurations for a six-axis robot to reach a given position in space.

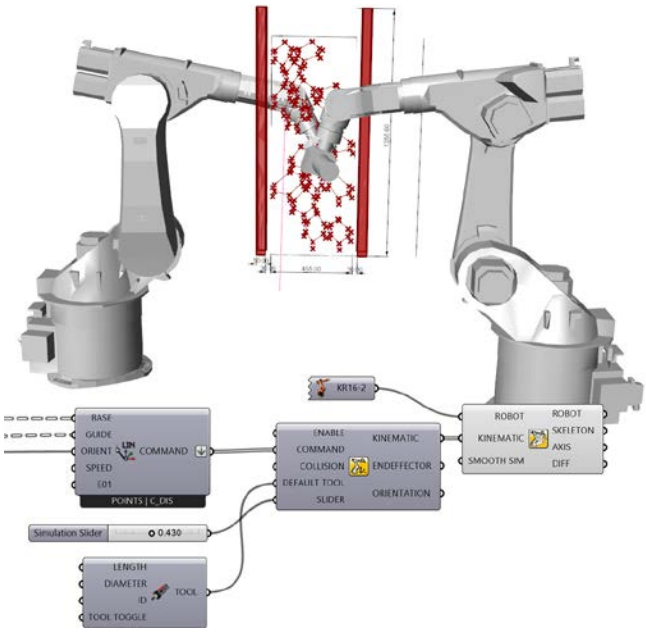

Figure 2. Visual programming using Grasshopper and KUKA|prc for design preview and fabrication simulation. Above, the stock-model placement is optimized through the parallel simulation of two lateral milling tasks.

3. VISUAL ROBOT PROGRAMMING CASE STUDY: ROBOTIC SPRAY-PAINTING

A project that showcases how visual programming can enable the quick and intuitive prototyping of complex robotic workflows was commissioned by the beverage company Absolut to promote their limited edition *Originality* series. Each bottle in this limited edition is made unique by the trail of a drop of cobalt-blue dye, being applied when the bottle is still hot (Figure 3, left). To reflect this individuality in a robotic installation, we had to move away from the industry-standard idea of robotic mass production, instead focusing on mass-customization to create a parametric design that could be applied each time with a different, unique result. However, as the installation was expected to travel to various destinations, any interface would have to be extremely accessible to allow people without special programming skills to control the robot.

3.1. Robotic Spray-painting

Several approaches were conceptually developed, but finally the idea emerged of mass-customized, spray-painted T-shirts showing a robotically abstracted black and white portrait of its owner and a streak of blue paint, similar to the Absolut bottle. Before starting with the in-depth programming, we invited the Viennese graffiti artist Skirl to collaborate with us on the spray-painting aspects of the installation. This feedback proved to be vital to the project, as it turned out that fine lines on a fabric require high air pressure, fast speed, and a very short distance of less than 6mm between the nozzle of the spray gun and the fabric itself. Therefore a KUKA Agilus robot was chosen as the robotic platform, offering a very high speed coupled with a sufficiently high accuracy and internal valves to control the airflow. Unfortunately, safety concerns due to the robot's high speed forced us to reconsider the idea of spray painting directly onto people and to switch to a 3D-scanned, static torso of a mannequin as the T-shirt mount. To apply the paint, two regular high-accuracy spray-guns with different colors were mounted at a 60 degree angle onto the robot via a custom-made holder, 3D-printed in black nylon plastic via selective laser sintering (Figure 3, right).

Figure 3. (Left) Mass-customized Originality bottle. (Right) Robotic setup with a black KUKA Agilus robot, 3D-printed spray-gun-holder.

3.2. Spray-painting Strategy

Using the visual robot programming tool KUKA|prc (Braumann and Brell-Cokcan, 2011) we rapidly prototyped spray-painting strategies, optimizing the process to take advantage of the special properties of robotic arms such as precision and speed. For example, tight corners are problematic as the robot is forced to slow down, leading to visible changes to the paint finish on the T-shirt - unlike a human, the robot is not equipped to analyze the spray-finish in real time. Where it greatly surpasses human labor is in regards to precision: based on the accurate 3D scan of the torso, the robot can keep a constant distance and orientation towards the textile surface.

For the final spray-painting workflow (Figure 4), a portrait is taken in front of a blue screen and transferred via a wireless connection into the Grasshopper environment.

Using custom-designed software modules, the blue background is removed and the remaining image separated into black and white areas, which in turn are converted from a raster graphic into vector outlines. An angled hatching is then drawn inside the outlines and projected onto the digital torso model.

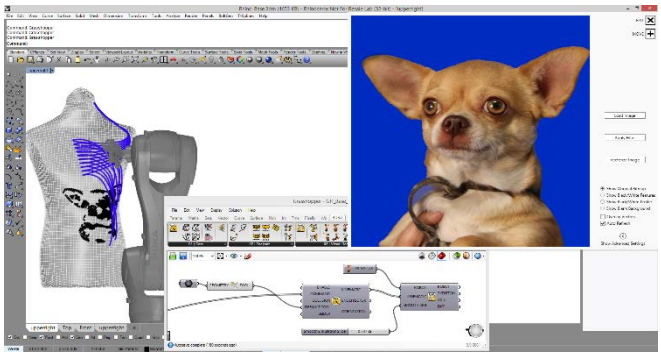

Figure 4. Visual programming environment: Custom interface for image processing, coupled with a design preview and kinematics simulation.

3.3. Interface

Finally, we achieved an elaborate fabrication strategy that contained both our knowledge of robotic fabrication as well as the graffiti artist's spray-painting technique. The remaining challenge was therefore to create an interface that would make this knowledge easily available to the operator of the installation. For the image editing, a simple user interface was set up that allows the user to select the background color with an eyedropper tool and the black/white threshold via a slider, both controls updating the resulting image in real time. All fabrication parameters, as well as the kinematic preview and the spray-painting simulation itself take place in the visual programming environment. Even without advanced knowledge, clearly labeled sliders are much easier to adjust than "hard" changes in programming code. Additional parameters such as the geometry of the blue streak, can be intuitively adjusted from within the CAD environment itself, by dragging the control point that affects the array of curves.

3.4. Project Conclusion

This fluent process, coupled with the immediate simulation feedback, enables the operator to directly interact with the client as part of the design process and to respond to the client's requests, as the individual perception of personal characteristics can differ greatly (Figure 5).

Figure 5. Robotic interpretation of a portrait using spray painting.

The Absolut Originality project was developed in less than a month, building upon the existing KUKA|prc framework. Due to Grasshopper's accessible approach towards programming, it was not necessary to develop a full interface that exposes all possible functions, but to focus on the core functionality. All other parameters could be adjusted via number sliders within Grasshopper or by directly manipulating the CAD environment. Generating the spray-painting control-data file from an image takes less than a second, while the cycle time of the physical fabrication itself was measured at between four and eight minutes, depending on the size and complexity of the image.

4. SIMULATION FOR ROBOTIC FABRICATION

In addition to streamlining existing processes, visual programming can also be used to solve completely new problems in the creative industry that are outside the scope of industry-standard commercial applications.

In the creative industry advances are not only made in the area of (robotic) fabrication, but also in the development of new materials that are custom-tailored to the needs of designers and architects. One such material is splineTEX, a composite material under development at the Austrian technology-startup superTEX that enables the construction of spatial, low-weight, high-performance elements resembling digital wireframe structures (Figure 6).

Figure 6. Manual shaping of carbon-fiber tubular structures.

The material is available as long tubes with an interior carbon fiber mesh. In its base state, it is soft and flexible and can be manually shaped. Once brought into its desired shape, a special epoxy is pumped through the carbon-fiber layer, thus hardening it and creating an extremely rigid, but lightweight, tube. Programming and simulating such a process, with a goal towards converting it into a repeatable and controllable fabrication strategy, is a major challenge, as no comparable processes or commercial solutions exist. The prototyping of new software solutions for such applications is greatly facilitated by the modular structure of visual programming environments. Instead of having to understand the syntax of imported libraries, additional functionality can be rapidly integrated via modules, containing, for example, evolutionary solvers and other complex algorithms.

4.1. Non-standard Fabrication of the Wireframe Pavilion

Closest to the forming of splineTEX is the 2D and 3D bending of steel rods. In 2004, the design studio "Wireframe Will Work" (Figure 7) was led by one of the authors at Die Angewandte in Vienna and in a similar way aimed to transform the aesthetics of digital wireframe structures into a physical object. Compared to today, the range of available software and machines was limited, with no commercially available machine capable of bending metal three-dimensionally. The state of the art would have required the manual processing of more than 9000 individual radii at a prohibitive cost. By analyzing the bending machine's data stream, it was possible to reverse-engineer the commands and to automatically create the machine code for bending each individual element, which was then saved onto a floppy disk that could be read by the CNC machine. This enabled the fabrication of all parts of the Wireframe pavilion within just a single day, as opposed to manual fabrication, which would have taken weeks. The process of and specific pre-processor for bending rebar steel in three dimensions was later registered at the patent office. (Brell-Cokcan and Comploi 2006)

A similar process of bending steel with a robot was utilized for the Wave pavilion project (MacDowell and Tomova, 2011) and an installation for the Australian Biennale pavilion in 2012 (Pigram et al., 2012).

Figure 7. Wireframe Will Work project using CNC-bent steel rods. CNC bending machine (left), pavilion (right).

What sets rebar steel apart from splineTEX is that the bending machine causes a nearly fully plastic deformation of the steel, with only a slight amount of bouncing back, which enables a precise and repeatable control over the entire process. Therefore, once a segment of the rebar steel is bent, it will retain that shape. In contrast, the carbon-fiber elements stay fully flexible until they are hardened, making process control a significant challenge.

Where the rebar steel project required just a mathematical transformation of the geometric properties of the element into machine code, the robotic processing of flexible carbon fiber elements can potentially greatly benefit from simulating its material properties.

4.2. Towards Predicting Material Behavior through Simulation

Eight years later, a design studio at TU Vienna led by the authors explored new ways of working with ultra-light materials: splineTEX allowed the students to create large, spatial structures that can be formed freely without depending on heavy equipment. A prototype was developed to be exhibited at the Rob|Arch conference in Vienna (Figure 8).

Figure 8. splineTEX pavilion prototype exhibited at Rob|Arch in Vienna.

While the initial free shaping and prototyping was exceedingly intuitive and easy, producing the final design according to CAD data proved to be more complicated than expected. As the 3D design was entirely drawn digitally, it did not take the material properties of the carbon-fiber tubes into account. Therefore, many jigs, tripods, and weights were required to force the material into shape. After the shaping the individual tubes, robotic arms verified the accuracy of the shaping process. A bidirectional workflow had the robot tracing the CAD data while sending the offset value via Ethernet in real time to an external computer. Analysis of this data suggested that significant deviations occurred at areas that were not held by the jigs.

Based on our findings from the students' project, a custom physics solver was developed and provided with empirical data that was previously gathered by taking hundreds of photos of splines held at different positions and at different angles. The physics solver uses a particle-based approach, which divides the spline into a number of individual particles (refer also to research at ICD Stuttgart, Fleischmann and Menges, 2012 and Robofold). This simulation data is then embedded into the parametric model, along with the virtual robot models. Using the evolutionary solver Galapagos, it is evaluated at which point and angle each robot should hold the tubes to best approximate a given freeform curve with a fixed start and end of the curve geometry. The robot component will then simultaneously output the toolpath for each KUKA robot (Figure 9).

While the optimization and simulation of the shaping process was quick and efficient, the final output did not have the repetability that would have been required for an

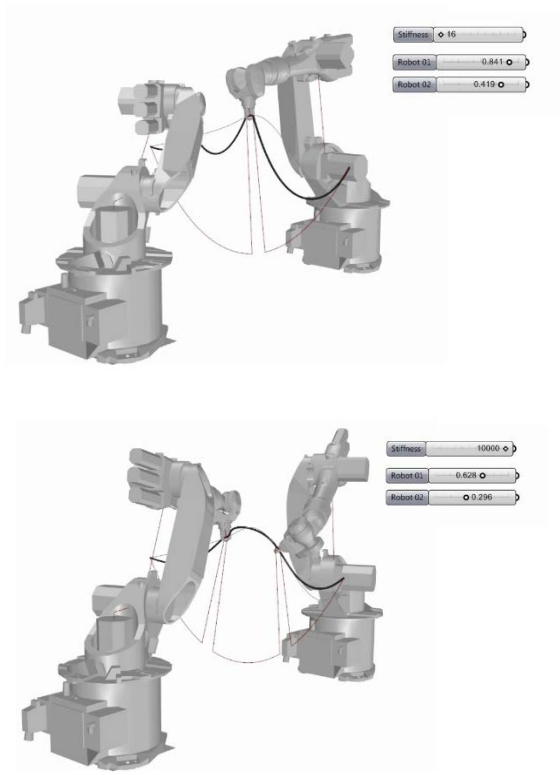

Figure 9. splineTEX form-finding and robot simulation via a physics solver and KUKA|prc. Initial spline orientation is fixed at the ends and manipulated with robots. 5mm elements (top), 20mm (bottom).

industrial process, as even a slight deviation of material or robot position would result in a different result. This was especially evident in three-dimensionally formed curves, while two-dimensional curves were much closer to the simulation. Evaluation of the results showed the material's multi-layered interior as the main cause of these deviations: as the layers interact with each other, the simplified model of the physics solver can no longer accurately predict the performance of the material. More complex simulation algorithms that also consider the twisting of multi-layered material were outside the scope of this project.

The encapsulation of complex functionality into accessible components enabled us to quickly demonstrate the shaping process through the physics solver module Kangaroo, which we then replaced with our own physics implementation that was optimized for our special use-case and multi-core environment. In turn, a new physics solver with improved capabilities could again just as easily be integrated into the network of nodes, increasing the

simulation fidelity without having to change the modules pertaining to the robot control.

5. ROBOTICALLY FABRICATED AUTOMOTIVE CHASSIS

In a later industrial research project, the focus lay on developing a system that would significantly improve the repeatability of the shaping process. When a large, German automotive OEM approached superTEX with a request to prototype the industrial fabrication of a scaled car chassis consisting of three-dimensionally formed carbon-fiber elements (Figure 10), the idea of serially winding splineTEX elements emerged.

Figure 10. Robotically fabricated carbon-fiber automotive chassis scale prototype.

5.1. Winding of Tube-like Elements

One of the limitations of any composite material is that it takes time to dry and harden. The strategy outlined in Section 4.2 would require the robots to remain stationary until the epoxy resin has hardened, which - depending on the diameter of the spline - can take many hours, thereby significantly increasing cycle time.

The main idea behind winding is therefore that multiple elements can be produced at the same time, using a mold that is mounted on the robot's flange. This strategy fits well into the idea of multifunctional robotic arms, as a single machine can fabricate many different forms, just by changing its modular "mold" end effector. In the prototypical application the mold was provided as a scaled static shape, so that our work concentrated on the development of an efficient workflow from design to fabrication. While there are several commercial software packages available for winding carbon fiber around parts in an optimized fashion, they are complex, expensive, and not optimized for larger-scale filaments. In the scope of a scaled prototype, it was decided to develop a new workflow, capable of generating and simulating parametric winding toolpaths for any possible geometry.

5.2. A Parametric Winding Process

Generally, a simple winding process around a cylindrical shape would require at least two degrees of freedom: one axis rotates the form, while the other axis adjusts its height. While such a process would basically also be possible with the car chassis element, the use of a six-axis robotic arm opens up the possibility of freely placing and orienting the form in three-dimensional space, a task that would commonly be assigned to a robot in any case. Furthermore, robotic arms are immediately available, while the construction of specialized machines is both expensive as well as time consuming. Initial winding experiments showed that the material behavior of a thick, multi-layered element such as splineTEX requires special strategies to ensure a tight and repeatable winding pattern. Ideally, the spline would always be exactly tangential to the desired winding path, with a winding speed being parametrically constrained to the mold's radii. Otherwise the tubes may slip, resulting in inaccuracies. Within the visual programming environment the definition of the base winding form influences the simultaneously calculated parametric winding speed, resulting in the desired fabrication strategy. By using an inverse transformation, the complete winding path is then converted into movement commands for the robotic arm, ensuring that the tangent of the winding path is at all positions facing the centerline of the tube-like element (Figure 11).

Figure 11. Parametrically linked robot and material simulation for winding.

5.3. Results and Outlook

A fluent workflow allows the user to input any "windable" form into the parametric environment, set the material properties and gain a full simulation of the winding process, as well as the machine code that contains the robot's movement commands. Especially notable is that this functionality could be implemented as part of a prototypical fabrication process, as opposed to a multi-year research project. Similar to the spray-painting case study, visual programming enabled this industrial project to quickly reach a stage where the programming is robust and accessible enough to be handed over to a non-expert user that would just enter new values, check the simulation, and send files to the robot. While a single robot is capable of winding complex forms, a significant potential lies in the use of multiple, cooperating robots, especially in regards to splineTEX-plast. This iteration of splineTEX contains a metal layer, which allows it to be plastically deformed. However, plast elements are too stiff to be wound like regular splineTEX, requiring an additional robot to plastically bend the spline around the form or in 3D-space. By intelligently re-using modules and structures, the change from a flexible to a plastically deformable material could be quickly implemented in a new fabrication workflow.

6. CONCLUSION

Visual programming allows the designer to work in a near-real-time environment, fluently linking design with simulation. Due to its graphic design, Grasshopper has the potential of acting as its own graphical user interface, allowing direct interaction with both code and geometry, as demonstrated in the industry projects. Multifunctional parametric programming environments, coupled with machine-specific components, can serve as highly valuable interfaces for prototypical applications, encompassing not only the design, but also material simulation and NC code generation. Similarly, on the hardware side such flexibility is enabled by robotic arms, whose potential by far exceeds that of previous CNC machines. With the development of new materials such as splineTEX, we are entering entirely new fields of fabrication where no commercial software or specialized machines exist and new approaches to programming both design and fabrication are required.

Applied projects such as the carbon-tube based car chassis demonstrate that the industry is highly interested in architectural processes that have the potential to change the way industrial fabrication is performed, be it the development of new materials, or of new design-to-production workflows that incorporate material simulation. Where architects and designers have previously tried to emulate the efficient processes seen in industry applications, new software and hardware tools now enable them to create their own streamlined, simulation-based industrial processes that are even being adapted by the industry itself.

Acknowledgements

This research has been supported by the Austrian Academy of Sciences (grant 273458) and the Austrian Science Fund (project AR 238-G21). Figure 1 shows a project by Guido Maciocci. The splineTEX-pavilion studio was co-taught with Vera Kumer; Marko Tomicic designed the realized prototype.

References

BRAUMANN J. AND BRELL-COKCAN, S. 2011. Parametric Robot Control: Integrated CAD/CAM for Architectural Design. Proceedings of the 31st Annual Conference of the ACADIA, Calgary. 242-251.

BRELL-COKCAN S. AND BRAUMANN, J. 2010. A New Parametric Design Tool for Robot Milling. Proceedings of the 30th Annual Conference of the ACADIA, New York. 357-363.

BRELL-COKCAN S. AND COMPLOI D. 2006. Method for controlling bending machines WO 2006055998 A1.

CROSS, N., NAUGHTON, J., AND WALKER, D. 1981. Design Method and Scientific Method. Design Studies 2 (4). 195-201.

DAVIS, D. AND PETERS, B. 2013. Design Ecosystems: Customising the Architectural Design Enviroment with Software Plug-ins. Architectural Design 83 (2). 124–131.

FLEISCHMANN, M. AND MENGES, A. 2012. Physics-Based Modeling as an Alternative Approach to Geometrical Constrain-Modeling for the Design of Elastically-Deformable Material Systems. Proceedings of the 30th eCAADe Conference, Prague. 565–576.

MACDOWELL, P. AND TOMOVA, D. 2011. Robotic Rod-bending: Digital Drawing in Physical Space. Proceedings of the 31st Annual Conference of the ACADIA, Calgary. 132–137.

PIGRAM, D., MAXWELL, I., MCGEE, W., HAGENHOFER-DANIELL, B., AND VASEY, L. 2012. Protocols, Pathways, and Production. Proceedings of the First International Conference on Robotic Fabrication in Architecture, Art, and Design - Rob|Arch, Vienna. 143–145.

POTTMANN, H., ASPERL, A., HOFER, M., AND KILIAN A. 2007. Architectural Geometry. Exton, Bentley Institute Press.

ROHMER, E., SINGH S.P.N., AND FREESE, M. 2013. V-REP: a Versatile and Scalable Robot Simulation Framework. IEEE/RSJ International Conference on Intelligent Robots and Systems, Tokyo. 1321-1326.

A Freeform Surface Fabrication Method with 2D Cutting

Andres Sevtsuk[1] and Raul Kalvo[2]

City Form Lab, Singapore University of Technology and Design
20 Dover Drive,
Singapore 138682
[1]asevtsuk@alum.mit.edu, [2]raul@inphysica.com

Keywords: Gridshell, Fabrication, Free-Form Surface, Furnicular Structures, Computation, RhinoPython.

Abstract

We introduce a method for creating free-form architectural structures out of 2D domain line networks. The resulting structure combines principles of thin shell and single-layer grid structures. The innovation lies in a three-dimensional geometrical arrangement, where all structural elements can be cut out of flat panels. The advantage of the proposed method is that structural support systems can be created for a wide variety of line networks using simple cutting technology (e.g. saws, laser-cutters, 3-axis CNC routers), making the construction of geometrically complex structures accessible to a wider audience at a significantly lower cost. We illustrate theoretical possibilities of the approach and demonstrate a full-scale application on a 200 square-meter pavilion built from plywood panels and clad with sheet-metal tiles at the Singapore University of Technology and Design. An analogous approach can be used with a high degree of flexibility to fabricate complex structures of different shapes and patterns for various building applications.

1. INTRODUCTION

Gridshells are part of a larger family of thin-shell structures that have a long history of structural investigation (Mungan and Abel. 2012, Schlaich 2002). Along with funicular vaults, monoliths and membrane shells, their effective structural properties have made gridshells an attractive solution for constructing bridges, hangars, domes, and pavilions that require uninterrupted covered space. Gridshells save material by using double-curved forms that follow the lines of structural thrust, thereby achieving economical, efficient and elegant structures. The geometric forms of membrane and funicular shell structures are dictated by the distribution of forces, where tensile structures work fully in tension and funicular shells fully in compression. Whereas tensile structures almost always form anticlastic surfaces (Pronk and Diminicus 2013), with exception of peneumatic shells, which are synclastic, then funicular shells form dominantly synclastic surfaces.

Gridshells and monolithic shells provide much more freedom since they can combine tension and compression into one surface. By definition, gridshells are double-curved structures (Douthe 2006). This geometrical aspect gives gridshells more global stability and reduces material usage in comparison to structures that work predominantly in bending (e.g. wall-ceiling or column-beam structures). In the context of this paper, we widen the definition of gridshells, treating them as 2D domain structures on a surface, where the surface can belong to any curvature type. We can also call our method a single-layer grid structure (Liu 2007), since every edge and every module (loop) forms an individual building block that can be fabricated separately. The advantages that result from the latter have been covered well by Canerapo (2014), and include benefits in fabrication, modularity, customization and material.

The use of double-curved forms introduces considerable challenges for the design and fabrication of such structures. Freeform gridshells tend to produce variable and complex joints between load-bearing beams. In the case of perfectly spherical shapes, such as the Bucky Ball, the convergence angles of all edges of the gridshell are identical, and the joints therefore economical to fabricate. But thrust lines of efficient spanning forms are not spherical; rather, they follow parabolic or otherwise variable curvature, requiring unique joints at every node of the gridshell. There are a number of existing ways of achieving variable curvature in such structures. The most commonly used method achieves the curvature of the gridshell through a large number of uniquely angled joints (i.e. MERO-Type), shown on the top

left of Figure 1. Constructing such joints is costly, however, requiring strong materials (e.g., steel) and advanced machinery capable of milling custom three-dimensional elements (Bo, Pottman et al. 2011).

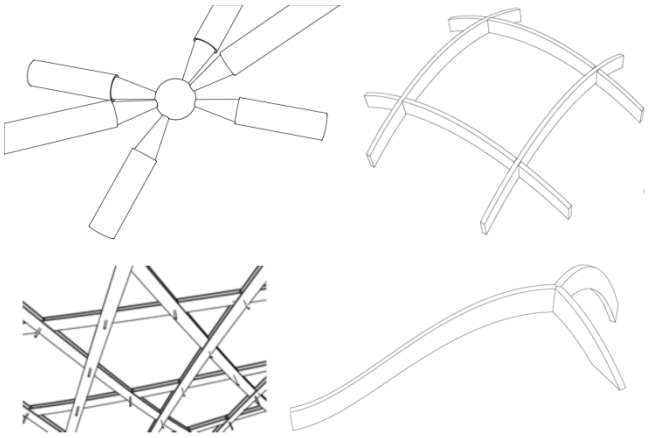

Figure 1. Top left: curvature of a gridshell achieved through custom 3-dimensional nodes. Top right: A rectangular lattice gridshell with perpendicular beams. Bottom left: Overlapping lattice gridshell with pin or tie joints. Bottom right: gridshell with 3D intersection joints.

A second approach subdivides a complex curved form into a grid of structural axes. A lattice of beams follow the axes and connect structurally at intersections (Figure 1, top right). If the members at joints meet at perpendicular angles, then this approach allows curved 3D gridshells to be achieved from 2D elements, using simple and economical joints (Sass 2005). With oblique angles—in the case of a triangulated lattice, for instance—the beams do not meet perpendicularly and their construction therefore requires 3D fabrication. In such a case, it is often more economical to tie the joints or connect them through the intersecting members with a pivoting fastener (e.g., a vertical bolt), without disrupting the continuity of the members (Figure 1, bottom left). Tie joints also allow non-orthogonal angles between beams, but the continuity of the members restricts the kinds of line networks that can be used in this method (Harris, Romer et al. 2003). The method is not suitable to line networks composed of discontinuous axes, for instance hexagonal line networks. There are also important constraints in the erection of such gridshells. Gridshells using the tied lattice structure are typically connected into a flat grid on the ground, and then gradually erected into shape by pushing in the supporting edges on site. This requires space and supporting ground, setting constraints on where such structures can be built.

A fourth approach achieves the gridshell curvature through curved structural beams, keeping all joints identical and standard (Figure 1, bottom right). Albeit repetitive, these joints too require 3D fabrication, which can be costly and restrictive (Bo, and Pottmann 2011). Only under rare curvature conditions and perpendicular line-networks can the elements of such structures be limited to two-dimensional cutting.

This paper introduces a method that allows gridshells to be structured from a curved line network that may be regular or irregular using arbitrary n-gons while keeping all structural elements and joints planar, allowing them to be fully fabricated on 3-axis cutting machines. The key benefit of the approach is that it offers great freedom in form and in the structural line-network design, while ensuring that all joints and beams can be fabricated economically from two-dimensional sheet material. An additional benefit is that the structure can be entirely prefabricated and assembled in modular components on site without large space constraints and without high-precision work on site.

To achieve this, two key innovations are necessary. First, the structure needs to be composed of two parallel walls around each network edge, and second, the adjoining non-parallel walls in each network loop need to be extruded at particular angles, such that straight intersection lines are achieved on the interior planes of n-gons. Both conditions are necessary to guarantee 2D fabrication.

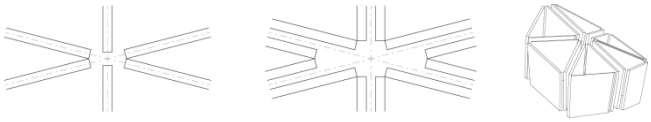

Figure 2. Left: The proposed method is not feasible with single-walls on free-form line networks without creating gaps between neighbouring elements or modifying the input line network. Middle and Right: A continuous gridshell structure is achieved through a double-walled structure around each network edge, where the planes are extruded at such angles that straight intersection lines are achieved within all interior planes of the gridshell's loops.

An analogous gridshell that can be fabricated with strictly two-dimensional cutting is not feasible with a single-wall structure without creating gaps between elements or modifying the input line-network, as illustrated in Figure 2. The figure shows in plan and axonometry how a continuous gridshell is achieved through a double-walled structure around each network edge, where the planes are extruded at such angles that straight intersection lines are achieved within all interior planes of the gridshell's loops. In the case

of a single-walled solution (left), the pairs of panels on the left and right of the node cannot move any closer to the node along their own axes without starting to intersect. The single-walled solution therefore does not allow us to achieve straight intersection lines between all adjacent panels around a node with flat-bed cutting.

The joints are connected along a linear intersection line between two neighboring planes of gridshell beams, allowing any angles to be joined through a linear fastener (e.g. weld, fold, hinge etc.) as long as fasteners can fit between the planes. The vertical depth of the walls becomes a structural variable that can be increased for stronger linear connections. The proposed solution allows a wide variety of curved line networks to be turned into a gridshell structure in an economical way.

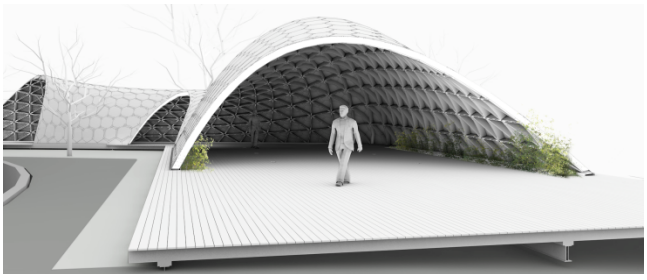

Figure 3. Rendering of the SUTD library pavilion.

We have implemented the approach in RhinoPython scripts and illustrate their implementation on a pavilion project at SUTD, manufactured from flat plywood sheets using off-the-shelf door hinges as linear fasteners (Figure 3). A similar method can be used to develop gridshells of different form, pattern, and material elsewhere.

2. USER INPUTS

The computation of a single-layer grid structure in our RhinoPython algorithm starts with two user inputs—an input line network and a NURBS surface. We call any curves, poly-curves, and polylines as lines since we only use the start and end points of any given curve. There can be alternative user inputs for line networks, for instance manifold n-gons, quads or triangular meshes. Requiring an input surface offers and easy way of obtaining normal vectors at the gridshell's nodes. Users can assign multiple different surfaces to different lines or assign the vectors manually to each edge. Since the input surface is only used to obtain an approximate normal at each node, it is not critical to keep the input surface close to the line network.

A designer can start by modeling the desired surface of the structure, subsequently adding the line network onto the surface (Figure 4). The line network can be directly drawn in Rhino, generated using a Rhino3D plugin called Rhino Paneling Tools (Issa 2012), or modeled with third party tools like Netgen (Schöberl 1997). The form of the line network can be optimized using form finding tools like RhinoVault (Rippmen et al. 2012), Kangaroo (Piker 2013), or imported from other software packages. Line networks also offer a convenient geometric base for exchanging information between different analytic software environments, including finite element analysis (FEA) software for structural analysis.

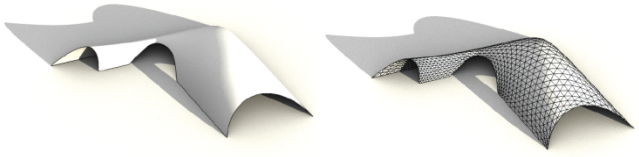

Figure 4. Left: a guiding surface. Right: Surface covered with a curved line network that defines the axes of the gridshell.

The first important step in analysing the input line network is to detect which combinations of edges form closed loops. If three or more edges in the line network form a cycle, then they are detected as loops (Figure 5). It is critical to know the loops in the line network in order to find the different extrusion angles for structural walls, as explained below. The input surface is used to obtain the initial normal vectors at every network node.

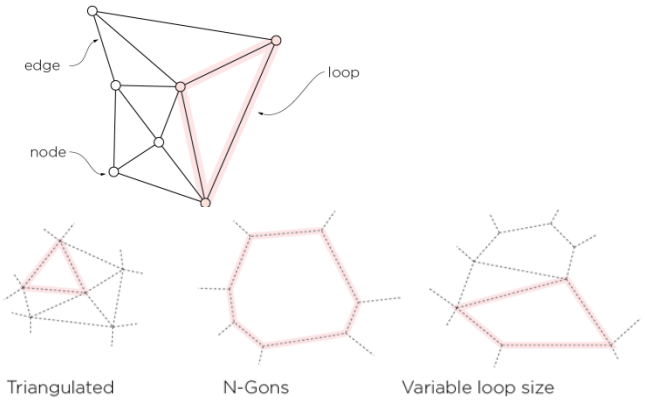

Figure 5. A network consists of nodes, edges and loops. Different network topologies can be used as input geometry.

The algorithm is able to detect loops in complex networks. Loops can be detected on regular or irregular polygons of any size (n-gons) and shape (Figure 5). The loop detection procedure is described in Figure 6. It is

important that before loop detection starts, the nodes should already have normal vectors attached to them. This is because if the angle between two adjacent node vectors is larger than 90 degrees, it is not possible to detect correct loops, as edges cannot be ordered in a counter-clockwise sequence. After loop detection is performed on every node in the network, all loops are cleaned and only unique loops are saved. The general aim of loop detection is to find a valid 2-manifold mesh structure (Botsch 2010). It is certainly possible to use a mesh as an input directly (which already has predefined loops), but many types of software used for architectural modeling do not support n-gon meshes; typical mesh strucures are quads and triangles. We achieve greater flexibility when working with lines.

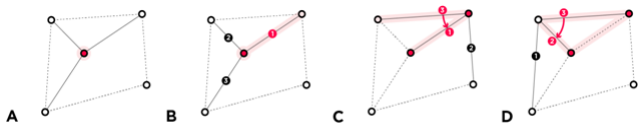

Figure 6. Process of loop detection. A. Selection of node. B. Ordering all edges in a counter-clockwise sequence and picking one of the edges as the starting point. C. Walking along the chosen edge and finding its neighboring edge that shares the smallest angle with it. D. Repeating step C as long as the walk arrives back to the starting node to form a loop, or until the node-count quota for the search is exhausted.

We have also investigated graph-based loop detection (Johnson 1975) but problems emerge in loops with a geometrically small area that have a longer perimeter than loops with a geometrically larger area, but shorter perimeter. The elegance of graph-based loop detection is that there is no need for geometrical information about each edge and loop detection is therefore computationally less intensive.

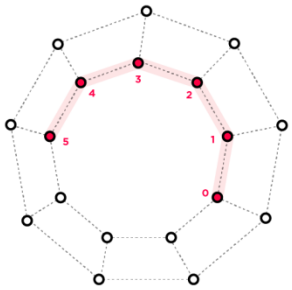

Figure 7. Search quota is the number of nodes visited before loop detection is stopped.

For better user control, we have added a search quota (maximum number of steps) that is used for loop detection. Figure 7 illustrates loop detection with quota of "5". Loops longer than 5 steps are not counted as loops and instead categorized as "naked". The script also makes it possible to set an edge naked explicitly. This provides an easy way of keeping certain edges of the network (e.g., edges of arches, ground support edge) naked for architectural reasons.

The algorithm also allows additional information to be stored about the line network. Lines can be named in model space in order to store information about special conditions and constraints they should follow during the computation process. For instance, we have reserved the name "horizontal" for lines whose normals need to be kept parallel to the ground plane. Depending on need, naming conventions can be used for many other purposes and each node can be given a custom user-defined normal vector that differs from the input surface for greater control. This can allow, for instance, the designer to introduce structural load analysis results as inputs to the node normal directions. Figure 8 illustrates how different parts of an input network can carry different names and meanings for the algorithm. Over time, we plan to introduce more user input options and potentially integrate the algorithm with engineering software for load calculations and form finding. It is possible to assign every edge a different material, height and thickness.

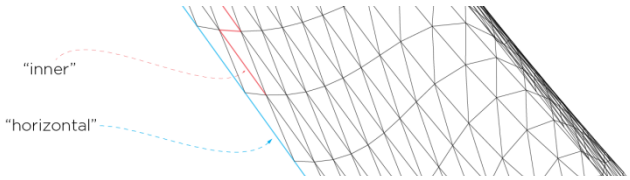

Figure 8. Different lines in the network can carry names and information about these lines. Lines that are called "horizontal" in the figure are always extruded parallel to the ground plane in the algorithm.

3. FINDING THE GEOMETRY OF STRUCTURAL PANELS

When loops have been detected and particular constraints set with naming conventions, then the central challenge of computing structural panels begins. These panels are eventually cut out of sheet material on a two-dimensional router. The structure forms double-walled panels around each input network line. Facing panels of two adjacent loops need to be parallel to each other and panels in the same loop that share a corner need to share a straight intersection edge, where a linear fastener can be placed, or where the walls can be folded. To achieve this, we need to find edge normals (e), loop-edge vectors (d), loop-edge planes (F), and loop-node vectors (l) that define the intersection lines between two adjacent panels, as shown in Figure 9.

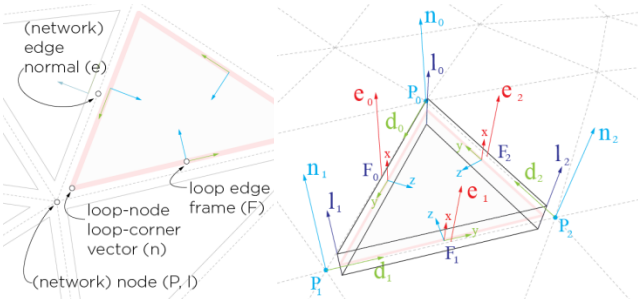

Figure 9. Illustration of node normals, loop-node normals, and edge normals.

First, node normals (n) are located at the intersection points (P) of the original input line network. The vectors of node normals are found by computing the normals at the locations of points (P). Second, the node normals at the opposite ends of each original network edge are used to derive the corresponding edge normal (e). Each edge normal is found as the average of its two endpoints' normals: $e_i = (n_i + n_{i+1})/2$. Next we need to construct a loop-edge plane (F) from the original edge normal (e) and the loop-edge vector (d) so that $F_i.x = e_i$ and $F_i.y = d_i$. The normal vector of this plane ($F_i.z$) is used to offset the loop plane inside, by at least the thickness of the construction material. An additional gap can also be created between the parallel panels in order to leave space for fasteners on both sides of the structural planes**.**

The loop-node vector (l) is calculated as the intersection line of two adjacent loop-edge planes ($l_i = F_i$ intersection with F_{i-1}). Every loop-node vector (l) is in the same plane with both of its neighbouring loop-edge vectors (l_i is coplanar with l_{i-1} and l_{i+1}). These vectors **(**l_i and l_{i+1}) and the loop-edge plane (F_i) are used to construct a structural panel, which represents the inner material surface of each loop. The surfaces are extruded outwards from each loop to achieve a desired material thickness. Since all structural panels share an inner edge with their neighbouring edges (along vector l), they can be joined to each other using linear fasteners that follow the vector (l) on the inner surface of a loop (Figure 11).

Both the desired vertical depth, which is an approximation since depth on both ends of the panels is different due to their trapezoidal shape that generates the gridshell's curvature, and the offset distance between two parallel panels are design variables that a user can control. User input for the depth of the shell sets the depth at the lower end of the trapezoid. Since the paths of forces in gridshells are generally designed to follow through the midpoints of structural elements, then the loop edges need to be extruded vertically in both directions above and below their original axis in the input line network. Our algorithm allows the user to decide where to set the centre lines relative to the structural depth of the gridshell. Once the height of each trapezoidal panel is computed, the trapezoids are offset towards the centre of each loop to form the inner surfaces of the structural loops. The choice of panel thickness and gap size can limit the geometry of line networks that can be used, as explained in Section 3 above.

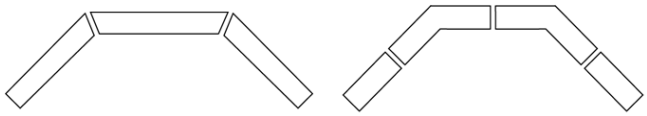

Figure 10. Left: curvature achieved through angled joints. Right: curvature achieved through angled panels.

The gridshell's curvature can be achieved in one of two ways, depending on user preference. First, if the top and bottom edges of the panels are kept parallel, the curvature can be achieved at angles between neighbouring panels (Figure 10, top). The benefit here is that edge members can be cut from constant-width boards using automated and rotating saw mills, for instance. The downside, however, is that the resulting inside and outside surfaces of the gridshell obtain complex angles at joints, where significant forces transcend. It can be hard to transfer significant forces through such angeled joints, requiring additional enforcement for load paths (this was the case in the pavilion, discussed below) or reducing the gap size to zero, such that adjacent modules touch each other at nodes. The second option is to keep panels at intersection points flat, achieving the shell's curvature instead by curving or angling individual panels themselves (Figure 9, bottom). This allows the inner and outer surfaces of the gridshell to remain flat around joints, which can be covered by flat panels, which can be used structurally, to transfer loads between edges around a node. Each panel can be fastened into the spacer blocks or edges at the opposite ends of every node to carry the forces across the node via a flat surface. We adopted this latter approach for the SUTD library pavilion.

4. ADJUSTMENTS

User inputs to the script may produce a few important constraints on the feasibility of the structure. The most important constraint concerns assigning a zero thickness to the gridshell's panels and a zero distance to the gaps

between parallel panels, which can easily produce unwanted intersections between adjacent loops. It is still possible to use the algorithm successfully with zero wall thickness and zero gap size between parallel walls, but the geometry of the network and the normal vectors at nodes are then constrained to limited solutions. This is a widely studied problem (Glymph et al. 2004, Pottman et al. 2007, and Liu et al. 2006), where the easiest solution involves keeping all node normals pointing towards a single convergence point. There is a way to ignore the normal convergence point constraint by limiting the line network to a valence of three (every node has a maximum of three edges connected to it, as in a hexagonal line network for instance). There is also a solution with a valence of four, where two diagonal edges are co-planar. But precision is critical here—when two adjacent edges are *almost* co-linear and their normals *almost* co-planar, then the intersection between them is not suitable for the structure since loop-node normals (Figure 9) deviate too much from node normals. It is therefore recommended that adjacent lines should have a smaller angle than 180 degrees. Note that the above geometric constraints only concern the zero panel and gap distance scenario and can be resolved by increasing the panel and gap thicknesses. However, there is also a constraint with panel thicknesses—if panel thickness is larger than the length of one of its adjacent edges, then an error occurs. The current state of the algorithm assumes that all these constraints are addressed by the user; they are not automatically detected.

The above method of lattice generation is suitable to most types of input line networks. Occasionally, however, the input network may contain sharp curvature peaks or concavity areas, which tend to produce sudden changes in the direction of surface normals. Sudden changes between neighbouring node vectors can produce colliding corner conditions for panels (Figure 11).

In order to avoid such collisions and sharp angular changes in nodes, the underlying node normals can be relaxed. The process of relaxation adjusts the node normal such that rapid angular changes are dispersed via Laplacian smoothing across multiple neighbouring nodes, reducing sudden normal changes in any one node (Cannan, Joseph et al. 1999). Relaxation provides better and smoother transition between node normals. Figure 11 (left) illustrates the before and after relaxation results on an arch with a relatively sharp peak. Grey normal vectors in the figure indicate initial stage node vectors; blue, the relaxed vectors. Note that "horizontal" edges are constrained to remain parallel to ground. Collisions can also be reduced by decreasing the height of structural panels, increasing panel thickness, and increasing the gap between parallel panels.

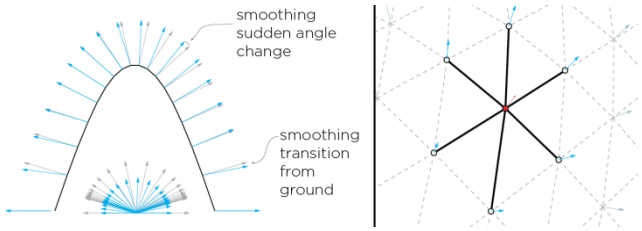

Figure 11. Left: Normal relaxation. Gray vectors show initial stage, blue the relaxed stage. Right: Normal in red, neighbouring normals in blue.

5. FABRICATION

Once the edge surfaces are extruded and populated through the structure, a double curved surface can be formed from flat edge panels. A few important steps, specific to the fastening solution chosen by the user, need to be addressed before fabricating the structure. In the SUTD pavilion case, hinges had to be fitted to the inside corners of each loop and adjacent loops had to be fixed to each other through a shared parallel plane with bolts through spacer blocks. In order to achieve this, connection holes for both hinges and bolts had to be found on every edge surface in three-dimensional space (Fgure 12).

We introduced a *hinge class* in the algorithm that takes several user inputs to determine the dimensions and hole patterns of hinges specified by the user. Depending on the pivot radius of the hinge, for instance, an additional gap may be needed in the inner corners of each loop to fit the hinge (Figure 12). The user input automatically populates line drawings on all panels for fixing the hinges between adjacent edges. We also included a *bolting class* in the algorithm to determine the exact locations for bolts in the parallel walls of two adjacent loops. The *bolting class* takes variables, such as desired number of bolts, distances from edges and bolt diameters, and automatically populates bolt holes onto all necessary panels. Solving for these hole locations algorithmically allows the user to detect any potential issues in the model and greatly improves on-site fabrication precision. All holes are predrilled during the CNC cutting process, and little error is left for fabrication on site. This reduces the site work to just an assembly process where no additional cutting or drilling is required in situ, allowing the structure to be assembled without highly specialized labor.

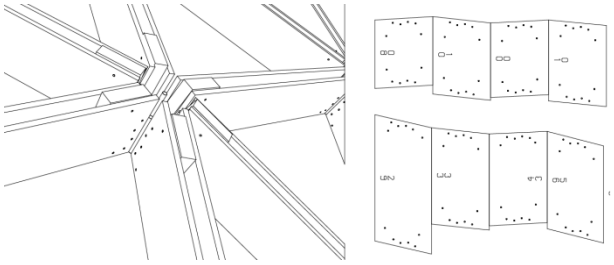

Figure 12. Left: layouts of panels with hinge- and bolt-holes. Right: same elements assembled together.

Next, after the fixtures and their desired holes have been computed, then all edge surfaces of the structure need to be flattened and fitted onto standard material sheets for two-dimensional cutting. The algorithm performs the flattening process by taking the outline of each edge surface, rotating it parallel to the ground plane, and packing numerous outlines as densely as possible to specified sizes of sheet material. In case of plywood or sheet metal, for instance, the flattening and packing can be fit onto standard 4x8 foot sheets. The packing procedure allows the user to specify the desired minimum distance between any two outlines on the layout, which helps the designer account for the size of the drill-head or laser-beam in cutting the elements. This packing procedure is further described by Dritsas, Kalvo and Sevtsuk (2013).

For outdoor use, the gridshells can also be clad with panelling tiles to prevent water, light or heat from entering the inside of the shell. Flat panelling approaches have been widely discussed elsewhere (Schiftner, 2010; Issa 2012) and for the sake of brevity we refrain from discussing them at length here. From a structural perspective, we should mention, however, that relatively strong cladding materials (e.g. rolled steel) can also be used structurally to distribute loads between gridshell panels around every node. The cladding tiles can be fixed directly to the underlying edge surfaces or spacer blocks between them, generating straight force paths through the metal cladding sheet from one edge to another. This approach was used with rolled steel cladding on the SUTD gridshell.

6. DISCUSSION

The method we introduce allows a designer to generate free-form gridshell structures from two-dimensional elements that can be cut using regular flatbed routers or laser-cutters. This approach has been implemented on a gridshell pavilion at SUTD (Figure 13). The pavilion uses 12mm plywood elements as structural edges, with a vertical depth of 200mm. Neighbouring panels are fixed with an off-the-shelf 4-inch door hinge, forming triangular loops. Two adjacent loops are fixed to each other via a parallel plane that is offset 25mm to fit a flat spacer block between the two walls. The structure is covered with 2mm rolled steel cladding tiles, which form an overlapping hexagonal "fish skin" over every node (Figure 14). The cladding sheets are screwed directly into spacer blocks between plywood walls, thereby distributing the axial loads from edge to edge via the sheet metal tiles. All plywood elements and spacer blocks are flat, cut on standard flatbed CNC routers.

Figure 13. SUTD pavilion interior view.

Figure 14. Exterior view of the cladding on the SUTD pavilion

The same algorithm can be used to generate gridshell lattices for different surfaces and different line networks. Figure 15 illustrates four different lattice patterns on an identical (anticlastic) surface. Figure 16 demonstrates the application of the algorithm on different types of surfaces using three types of line networks on each.

Beyond allowing complex double-curved gridshells to be constructed out of flat material elements, the proposed approach also offers an additional benefit—it allows the

design of the structure to be modified and fine-tuned until a very late stage in the design process.

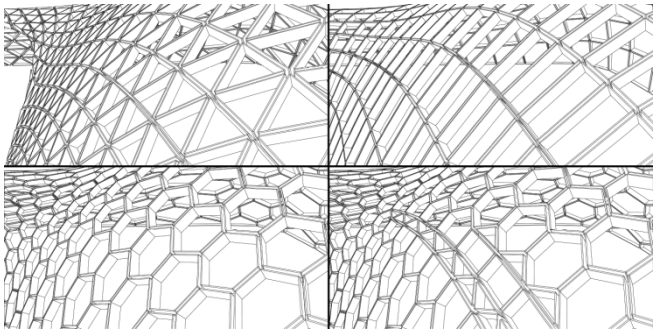

Figure 15. Regular and irregular lattice patterns on an identical surface. The algorithm can generate the three-dimensional geometries of all edge walls, while allowing each wall to be cut on a two-dimensional router.

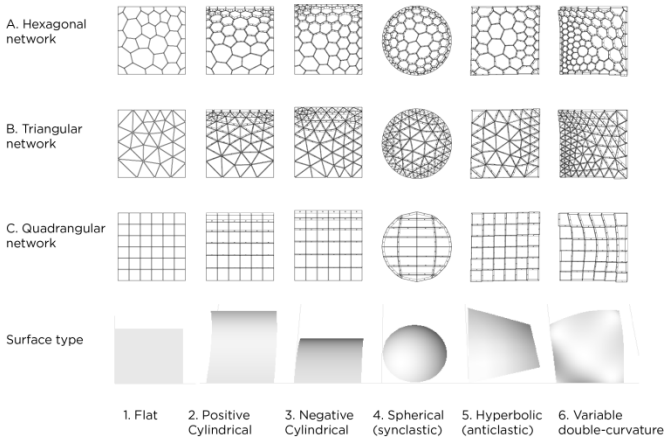

Figure 16. The panelling method applied on different curved surfaces using triangular, hexagonal and quandrangular input line networks.

A designer can simply change the geometry of the underlying line network or update the input parameters for material thickness, offset spacing, vertical depth or hinge and bolt dimensions, and the entire gridshell lattice can be regenerated instantaneously, complete with 2D fabrication layouts. Constructing the algorithms on custom scripts from multiple different classes, each of which have a set of input parameters, makes adjustments considerably easier than a large parametric or BIM model, where all parts share a long dependency chain, would allow. The process thus offers considerable flexibility and freedom for design. It can be used to develop gridshell structures of different form, material or pattern in a fast feedback loop between a designer and the algorithm.

We plan to release the software for public use by summer 2014, downloadable from the City Form Lab website (http://cityform.mit.edu).

REFERENCES

ABEL, J. 2012. "Toward Lightness In Concrete: Some 20th Century Shells and Bridges". Journal of the International Association for Shell and Spatial Structures (J. IASS). Vol. 5.

BO, P., POTTMANN. H., K.M., W.W., W.J. 2011. Circular Arc Structures in *ACM Trans. Graphics.*

Botsch, M., Kobbelt, L., Pauly, M., Alliez, P., L´evy, B. 2010. "POLYGON MESH PROCESSING". A K PRETERS, LTD. PP. 11-12.

DOUTHE, C., BAVEREL, O., AND CARON, J. F. 2006. Form-finding of a gridshell in composite materials. Journal of the International Association for Shell and Spatial Structures, 47(150):53. 14.

Dritsas, S, Kalvo, R, and Sevtsuk, A, 2013. "*PACKING OPTIMIZATION FOR DIGITAL FABRICATION*", IN ECAADE PROCEEDINGS 2013, TU DELFT (DELFT, NETHERLANDS).

HARRIS, R, ROMER, J, KELLY, O, AND JOHNSON, S, 2003. "Design and construction of the Downland Gridshelle", *Building Research & Information*, **31**(6) 427–454.

ISSA, R., 2012. Paneling Tools for Rhinoceros 5, http://wiki.mcneel.com/_media/labs/panelingtools.pdf (accessed 1 December 2013).

Liu, Y., Pottmann, H., Wallner, J. Yang, Y-L, Wang, W. 2006. "GEOMETRIC MODELING WITH CONICAL MESHES AND DEVELOPABLE SURFACES". ACM TRANS. GRAPHICS. 681–689.

Liu, X-L., 2007. "Development of grid structures in China". Journal of the International Association for Shell and Spatial Structures, 53: 101-102.

PIKER, D. 2013. "Kangaroo: Form Finding with Computational Physics". Architectureal Design. Special Issue: Computation Works: The Building of Algorithmic Thought. Volume 83, Issue 2, pages 136–137.

Pronk, A., Diminicus, M., 2013. "84 WAYS TO MANIPULATE A MEMBRANE". JOURNAL OF THE INTERNATIONAL ASSOCIATION FOR SHELL AND SPATIAL STRUCTURES, 612: 257–270.

Pottman, H., Brell-Cokcan, S., Wallner, J. 2007. "DISCRETE SURFACES FOR ARCHITECTURAL DESIGN". CURVE AND SURFACE DESIGN: AVIGNON 2006. PATRICK CHENIN, TOM LYCHE, AND LARRY L. SCHUMAKER (EDS.), PP. 213-234.

Sass, L, 2005. "A wood frame grammar: A generative system for digital fabrication", *International Journal of Architectural Computing* **Vol. 4**(No. 1) 51–67.

Schöberl, J. 1997. NETGEN - AN ADVANCING FRONT 2D/3D-MESH GENERATOR BASED ON ABSTRACT RULES. COMPUTATION AND VISUALIZATION IN SCIENCE. 1:41-52.

SCHIFTNER, A., BALZER, J. 2010. Statics-Sensitive Layout of Planar Quadrilateral Meshes in C. Cristiano, Hesselgren, L., P.M, P.H., W.J. Advances in Architectural Geometry, Springer, Wien, New York, 221–236.

SCHLAICH, J. 2002. "On Some Recent Lightweight Structures", Journal of the International Association for Shell and Spatial Structures (J. IASS). Vol. 43 (2002) No. 2 August n. 139.

Design-Friendly Strategies for Computational Form-Finding of Curved-Folded Geometries: A Case Study

Shajay Bhooshan, Mustafa El-Sayed, and Suryansh Chandra

Zaha Hadid Architects
10 Bowling Green Lane
London, UK EC1R 0BQ
{shajay.bhooshan, mostafa.elsayed, suryansh.chandra}@zaha-hadid.com

Figure 1: The completed sculpture at the 2012 Venice Biennale

Keywords: Curved Crease Folding, Material Behaviour Simulation, Design Workflows & Digital Tools, Robotic Simulation & Fabrication, Multi-Constrained Solution Space, Solvers & Visual Feedback.

Abstract

The built-prototype described in this paper explores synergies between contemporary architecture, engineering and robotic fabrication technologies. The fabrication technology and process used is a scaled and numerically controlled version of the 'scoring-paper and manual folding' method used to find feasible geometries. The essential contribution of the paper is a case-study of a digital-design strategy that enabled multi-displinary and novel solutions to address the difficulties in the design and manufacture of architecture-scale assemblies of curve-crease-folded panels.

1. INTRODUCTION

The research and built-prototype described in this paper explores synergies between contemporary architecture, engineering and robotic fabrication technologies. The fabrication technology and process used is a scaled and numerically controlled version of the 'scoring-paper and manual folding' method used to find feasible geometries. The iterative and collaborative effort between the Zaha Hadid Architects, Buro Happold Engineers and RoboFold spanned from initial studies in paper, scaled studies in aluminum, 3 sets of mock-ups, to fabrication of the actual sculpture and its assembly at the 2012 Venice Biennale (Figure 1). The research operates

against the backdrop of the exciting potentials that the field of curved crease folding offers in the development of curved surfaces that can be manufactured from sheet material. The two main areas of difficulties that arose in the design and production of the self-supporting prototype —developing an intuitive design strategy and production of information adhering to manufacturing constraints— are described. The essential contribution of the paper is a case study of a digital-design strategy that enabled collaborative and novel solutions to address these difficulties. We conclude, on the basis of such a case study, with speculation on the possible features of a physically-based form-finding method for curve-crease geometries that could negotiate the multiple objectives of ease of use in exploratory design, and manufacturing constraints of their architectural-scale assemblies.

Design exploration and computational methods

There are several seminal design and art precedents within this field - Richard Sweeney (Sweeney, R., 2013), David Huffman (Huffman, D., 1996), Erik Demaine (Demaine, E., 2010), etc. Most of the precedents, projects and available literature on design methods highlight the difficulty in developing an intuitive, exploratory digital-design method to generate feasible geometries. Our initial survey of methods included both the simple and common method—the method of reflection (Mitani and Igarashi, 2011)—and the involved Planar-Quad-meshes and optimization-based method. (Kilian et al., 2008) Most methods, including the two above, presented difficulties towards incorporation within an intuitive and parametric early-stage-digital-design method, with the first one proving difficult to explore variety of generalized solutions free of prior assumptions, and the second one being elaborate involving scanning of physical paper models, proprietary optimization algorithms, etc. For an extensive overview on the precedents and computational methods related to curved crease folding, we refer the reader to a survey (Demaine et al., 2011). Further, we were particularly interested in the recent developments of physically-based interactive tools that operate on user-specified coarse linear piecewise complexes that are iteratively refined to produce feasible solutions via sub-division and energy minimization methods (Solomon et al., 2012).

2. PROJECT WORKFLOW

In order to find a strategy with a progressive error-reducing process of convergence that takes into account solutions that satisfy evolving design, structural and manufacturing constraints, an intuitive, multi-stage and multi-resolution workflow that also prioritized computational speed and user interaction was developed, as opposed to a single-stage involving the search for an exact solution (Figure 2).

Base mesh generation & planarity constraint

The initial stage of the workflow is the design of a predominantly quad faced, low-resolution mesh (*low-poly*), which was the primary vehicle for the expression of design intent. Through the relatively straight forward process of shaping this *low-poly* we are able to explore and formalize both the underlying formal and topological conditions driven primarily by design and contextual constraints, as well as incorporating the assumed major structural behaviour into this early stage of the design.

In addition to these advantages, working with a relatively low resolution mesh also acts as the first step in the sequence of error distribution and reduction; this is done by ensuring that one of the two primary directions of the mesh face flow (Figure 3b) is shaped by no more than 3 vertices, thereby guaranteeing the formation of planar arcs in those directions. The planarity of these arcs aids in the aim of creating a mesh whose faces fall within a certain neighbourhood of accuracy in regards to the individual planarity of each face.

Subsequently, this *low-poly* is converted into a high resolution mesh with an inherited underlying quad structure using a sub-division scheme: the modified Catmull-Clark subdivision scheme in-built into Autodesk Maya (Stam, J., 1998). This high-resolution quad grid also inherits the underlying assumed planarity of the faces, which essentially reduces the need for further optimization processes that could have potentially disruptive effects on the design intention of the geometry. This high resolution mesh is then used as the base surface for the next stages in the workflow, therefore transferring its ‘planarity’ advantages to the geometries generated off of it.

Since the design was to be materialized through a series of thin curve fold metal panels, much of the

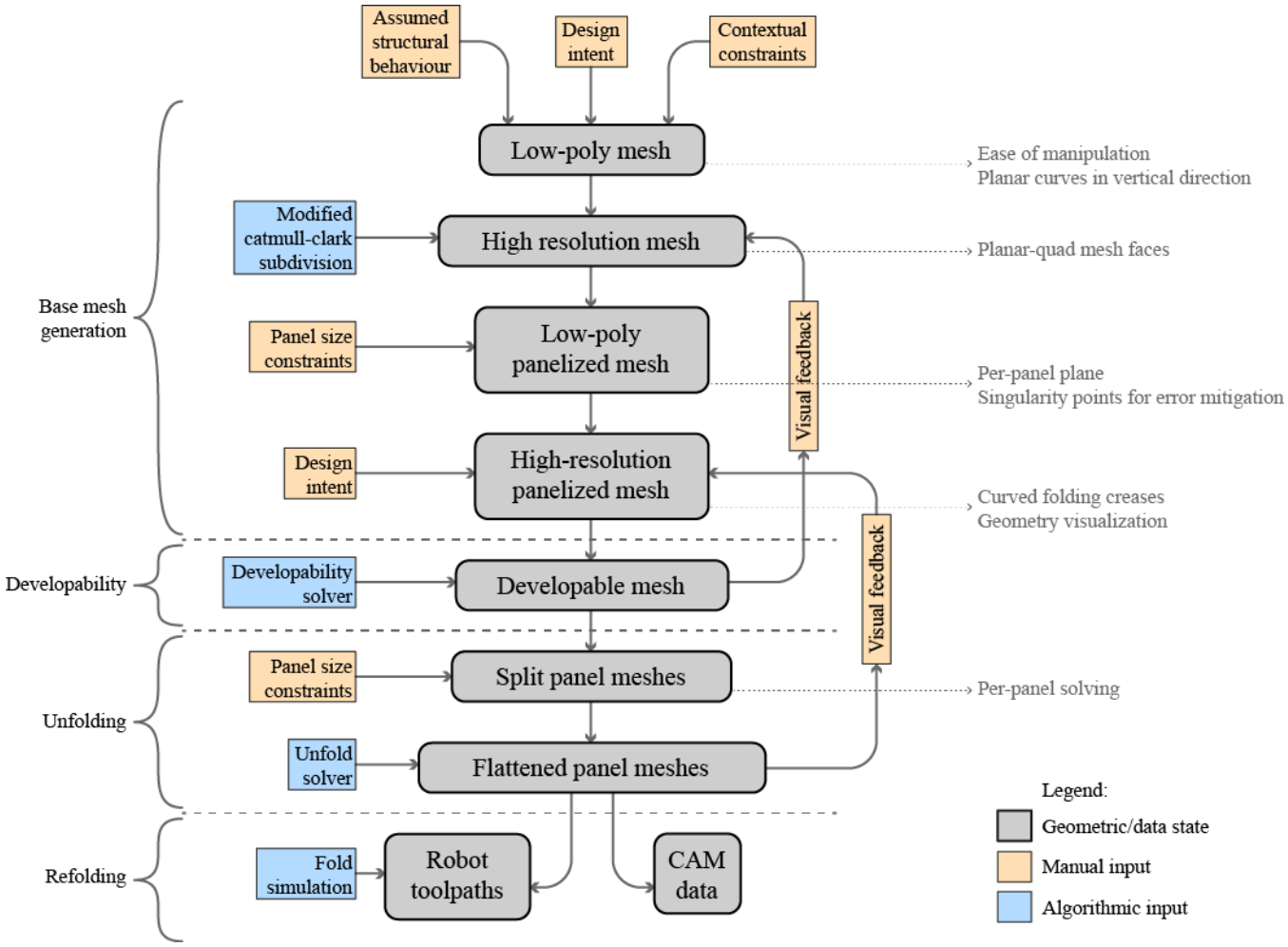

Figure 2: Project Workflow.

accuracy or error reduction would reside in the design and generation of the panel geometries themselves, as well as the topological conditions present between the panels populated on the mesh. With this in mind, a series of degree-three curves were extracted from the high resolution mesh using the aforementioned underlying planar arc information present in either primary direction of the mesh. These arcs were used to generate the boundary information for the panel geometries on the surface. The first step was to incrementally traverse the parametrized curve lengths of neighbouring arcs to generate a series of degree-one curves that describe the straight fold lines of the panel geometry. The generation of these curves in this method again ensures the planarity of each panel due to each panel section being informed by a curve segment defined by only three points; therefore effectively defining the plane that is symmetrically tessellated into a panel, therefore ensuring faceted geometry that is in a viable neighbourhood of physical feasibility.

It is important to note that this method of defining the plane of each panel independently, and using the inherent tangential continuity and "topological generality" (Xie and Qin 2002) of the base subdivision surface to create visual continuity between the panels, induces a series of conical elements with their apex at the vertex between two panels or essentially at a point on the line at which the two respective planes met. This point of geometric rupture will be hereafter referred to as the singularity point, with the amount of singularity points present having a relationship of $n/2$ to the geometry with n being the number of panels used to populate the surface.

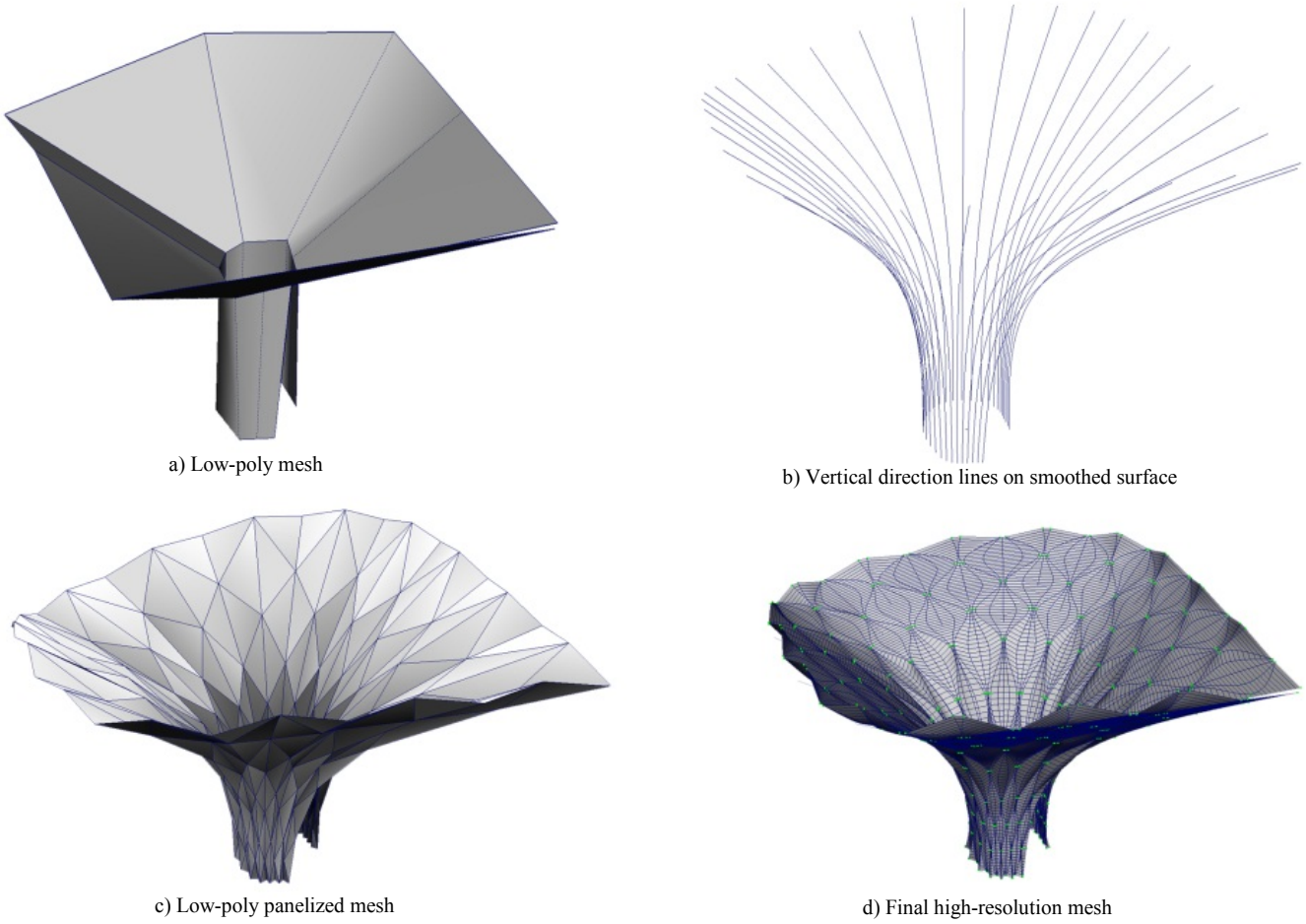

a) Low-poly mesh

b) Vertical direction lines on smoothed surface

c) Low-poly panelized mesh

d) Final high-resolution mesh

Figure 3: Individual steps of generation workflow.

The geometric rupture along the singularity points allows for each panel to now be further refined in an independent fashion to transition from geometries of straight folds to higher resolution geometries of curved fold lines. This is a relatively simple step that involves converting the straight line segments that describe each panel into curvilinear line segments that define the new tessellated panel geometry.

Developability constraint

These singularities became the point of departure for the next stage of the workflow, which builds upon the error reduction strategy of the previous stages. Acknowledging that the conical singularities would cause errors in the folding behaviour of the now faceted geometry, the next major constraint of developability was introduced. Developability can be ensured by the presence of uniform and zero Gaussian curvature throughout the mesh. A well-established discrete measure of Gaussian curvature is proportional to the sum of the angles subtended by the edges meeting at a vertex (Aleksandrov & Zalgaller, 1967). Thus a perturbation-based iterative solver was employed to 'relax' the input mesh towards developable or uniform Gaussain curvature solutions. The solver used a gradient descent method with mid-point integration to converge to a solution. We tested both an analytically supplied (Desburn et al., 2002) and a numerically computed gradient, with the analytical gradient predictably converging 2-3 times faster.

Beyond the refinement aspect of the solver, its convergent nature also presented an unexpected but welcome addition in the pipeline: the visual feedback of the iterative steps of the solver, its effects on the input geometry and its convergence being visualized on the mesh. This effectively allowed the designers to observe

the cumulative effects of the solver's logic on the global geometry. This proved invaluable to develop an intuition whilst iterating through the various steps of the pipeline to refine the design, in the face of changing design, and structural and manufacturing constraints.

Unfolding and boundary constraints

The surface mesh was required to be subdivided into panels (Figure 4) based on a 1.5m x 1.5m dimensional constraint, with each panel not containing more than two curved folds so they could be folded using three robotic arms. Each of these panels then needed to be unfolded into their respective flat configurations that could be used to physically re-fold each panel from flat sheet material to the correct 3D geometry.

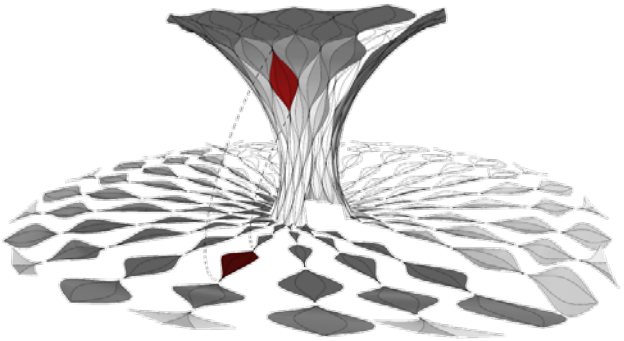

Figure 4: Subdivision of the surface mesh based on fabrication constraints

There is extensive literature, especially in the areas of computer graphics and cartography, related to this process of unfolding or computing a parametric mapping between a discrete mesh and its isomorphic and planar counterpart. We refer the reader to the paper parametrization of meshes (Desbrun et al, 2002) for various methods used to establish such a parametrization and their limitations. It is sufficient to state here that there are no perfect methods to compute a completely accurate mapping, and all current methods aim to minimize the deviations between the 3D mesh its planar counterpart. Some aim to minimize angular deviations (*conformal* mapping); others preserve areas (*authalic*). It can then be stated that we required our mapping to be *isometric*—i.e., both *conformal* and *authalic*. Another constraint was that we required the simultaneous unfolding of all ~500 panels in order to check that the adjacent boundaries coincided within tolerance (Figure 5). We chose to follow a spring-energy minimization route and a simplified particle-spring algorithm was employed to converge towards an unfolded solution edge set with minimal deviations in length from the original 3D states of each panel. Minimal angular deviations were ensured through the use of higher strength diagonal springs for each quad (Figure 6).

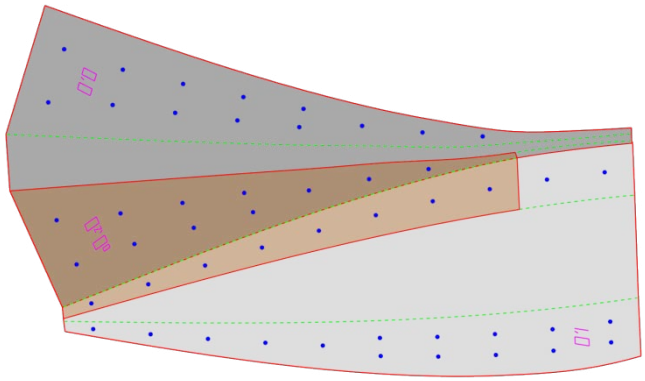

Figure 5: Simultaneous unfolding of all panels to check boundary correspondence between neighbouring panels

Learning from the previous stage, we also used built-in feedback to visualize the process of convergence. For more on parametrization with spring-like energy minimization, we refer the reader to (Zhong & Xu, 2006). It might be interesting to note that meshes from the previous step that were developable unfolded to greater accuracy than those that weren't.

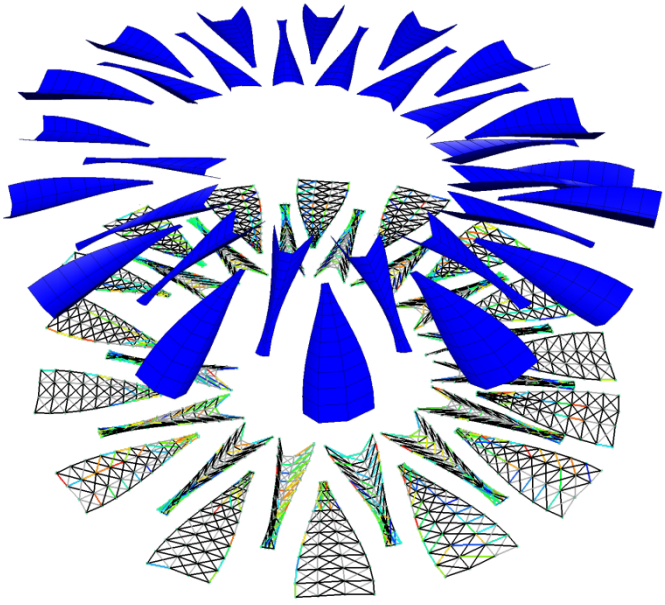

Figure 6: The spring layout of each panel in the particle-Spring based energy minimization method.

Refolding for robotic toolpaths

In order for the robots to be able to fold the sheet aluminium panels to the desired shape, we needed to generate an animation set of meshes for each panel that encoded a sequential transition from flat state to the 3D state, and an additional *over-bend* in order to accommodate for material spring-back (Figure 7). The robots held the metal sheets through suction grippers, which required the toolpaths to be generated from the face-centres of the mesh. Therefore, precision of fold angle had to be weighted higher than the precision in edge lengths and face area.

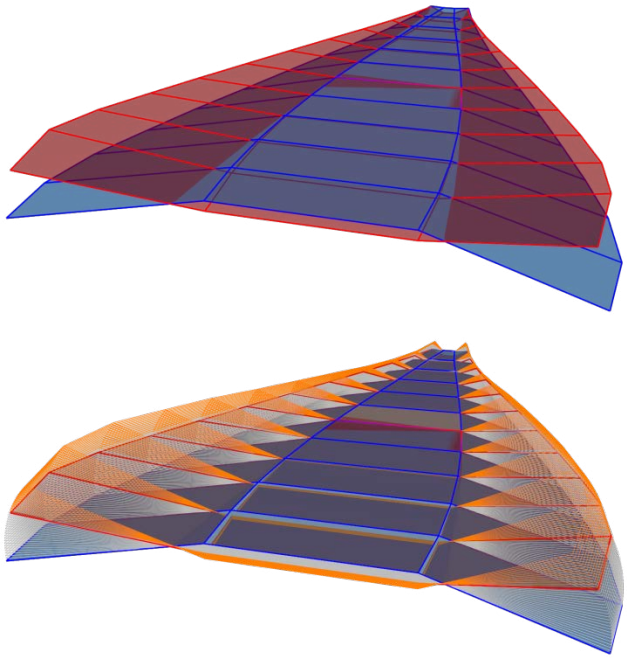

Figure 7: Above: Flat state in blue and the folded state in red. Below: Fold-state mesh sequence per panel. The orange lines indicate the overbend required to account for material springback

A set of 70 sequential mesh sets were required per panel, and considering there were ~500 panels resulting in a total of 35,000 meshes required, iterative methods such as a particle spring solver were quickly ruled out due to time constraints. Our approach to refolding differed from the unfolding for three primary reasons:

1) Each individual mesh was now only a panel whose fold sequence could be computed independent of the others, whereas the unfold had to be computed simultaneously for every panel in order to check for correspondence with neighbours.

2) The unfold process laid significant weightage to maintaining edge lengths and areas; these were less critical to the fold process.

3) The unfold process required output of only a single set of meshes per panel and all intermediate solver states were irrelevant; the fold process required a fixed number of highly accurate intermediate states for each panel.

We opted for a method that computed folds by applying rotations constrained along edges to the mesh vertices, similar to the one proposed by Tachi and used in his Rigid Origami Simulator (Tachi, T., 2009). The algorithm's non-iterative nature reduced solving time, and its weighting of fold-angle helped achieve an acceptable degree of precision. Our method differed from Tachi's in that it was set up to only require fold angles at the middle row of faces of the panel, computing the remaining vertices, edges and angles as a consequence of *actuating* the first set of folds. This ensured the highest angular accuracy at the middle row of faces that were to be used for generating the toolpaths (Figure 8). However, similar to Tachi's method, our method also required the triangulation of all quad faces as vertices with a valency of 4 did not offer enough degrees of freedom.

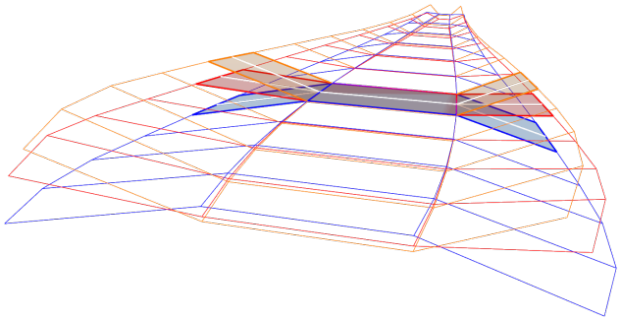

Figure 8: Fold Angles were only specified at the middle row of faces, as the toolpaths were generated from them.

3. CONCLUSION

The paper described a digital-design pipeline employed to design a self-supporting assembly of curve-crease folded panels. We described the benefits of a multi-stage process of error-distribution and reduction in an iterative and collaborative design process. We

speculate, on the basis of the case study, the following essential features for a general, physically-based form-finding method for curve-crease geometries that could negotiate the multiple objectives of tight time-scales of design projects, ease of use in exploratory design, and manufacturing constraints of their architectural-scale assemblies:

1) *Hierarchical description of geometry*: Architectural design usually involves multiple disciplines and widely disparate constraints—spatial, aesthetic, structural and manufacturing. Such constraints are difficult and/or unintuitive to include in a single-stage form-finding process. We presented the case for the benefits of Hierarchical description of geometry—*low-poly* to high-resolution subdivided meshes—in being able incorporate such constraints at different hierarchies. We believe a general form-finding method should include such affordances.

2) *Physical verification and establishment of tolerances*: Development of physically feasible geometries and establishment of the manufacturing tolerances at architectural scale is greatly aided by continuous production of paper models and mock-ups (Figures 9 and 10 – paper and aluminium mock-ups). Tolerances so established helped us fine tune our constraint solvers and also plan the strategic distribution of objectives. For instance, we were able to establish that the developability constraint, combined with accurate unfolding such that adjacent boundaries align, was more important than the absolute planarity of all faces of the mesh. We were also able to establish that the initial topological design intent set-out in the first, *low-poly* stage greatly impacted the rest of the downstream processes, especially the structural performance of the assembly. As such, we believe that a general method should afford the inclusion of key physical measurements / tolerances.

3) *Visual feedback for constraint solvers:* Visual observation of the process of convergence for the various solvers helped us understand the problematic areas of the mesh, and thus helped in directing our efforts towards fixing those areas.

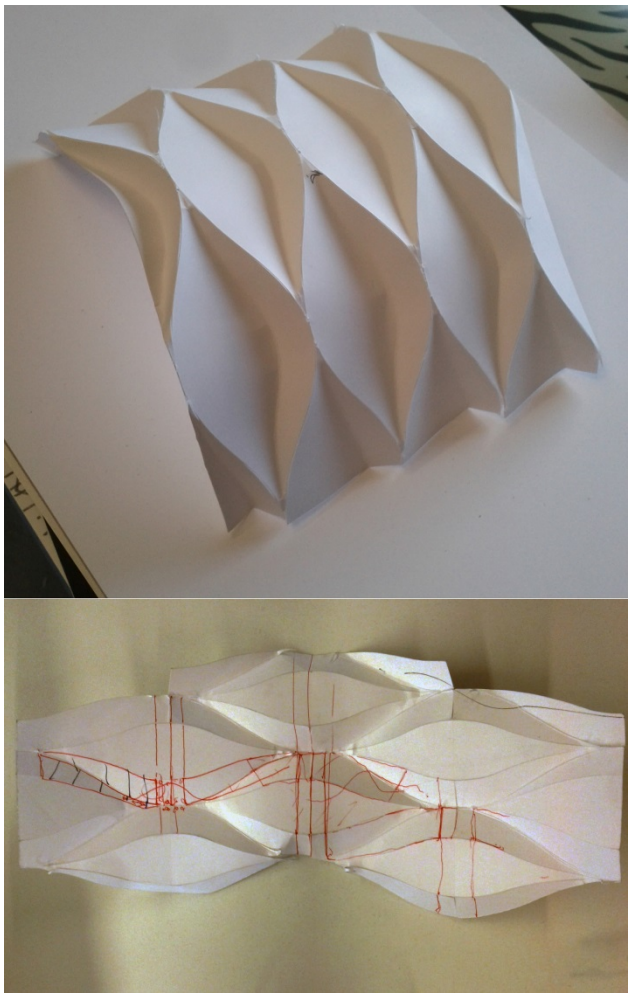

Figure 9: Paper mockups.

Further, such visual feedback from simple-yet-custom and real-time solvers helps in continuous iteration and design development, more than accurate, sophisticated black-box solutions.

We hope that the case study of a tight-timeline (3 months of design-to-completion), multi-disciplinary design effort will shed light on the opportunities, difficulties and requirements of a general method of physically-based, form-finding specifically catered to architectural design.

Figure 10: Aluminium Mockups

Acknowledgements

We would like to thank Patrik Schumacher, Zaha Hadid Architects for invaluable design guidance and Zaha Hadid Architects for sponsorship of the prototype. We would also like to thank Rasti Bartek, Buro Happold for structural engineering consultation and Gregory Epps for Robotic manufacture consultation and execution and also for sharing his paper-folding expertise.

References

HUI X , HONG, Q, 2002. A Physics-Based Framework for Subdivision Surface Design with Automatic Rules Control. Proceedings of the 10th Pacific Conference on Computer Graphics and Applications. p. 304.

KILIAN M., FLORY S., MITRA N. J., AND POTTMANN H. 2008. Curved folding, ACM Transactions on Graphics, Vol. 27, No. 3, pp. 1-9.

ALEKSANDROV, A.D., ZALGALLER, V.A. 1967. Intrinsic Geometry of Surfaces. American Mathematical Society, Providence, Rhode Island, 327 pages.

DEMAINE,E., DEMAINEM M., KOSCHITZ, D., AND TACHI, T. 2011. Curved Crease Folding: a Review on Art, Design and Mathematics, Proceedings of the IABSE-IASS Symposium: Taller, Longer, Lighter.

LÉVY. B, ETITJEAN. S, RAY, N, MAILLOT. 2002. ACM Transactions on Graphics Vol 21, N 3, pp. 362-371.

HUFFMAN, D. 1996. Geometric Paper Folding: Dr. David Huffman. http://www.graficaobscura.com/. Retrieved Nov 18, 2013, from http://www.graficaobscura.com/huffman/.

DEMAINE, E. 2010. Curved-Crease Sculpture. erikdemaine.com. Retrieved Nov 01, 2013, from http://erikdemaine.org/curved/.

SWEENY, R. Works. richardsweeney.com. Retrieved Nov 18, 2013, from http://www.richardsweeney.co.uk/menu.html.

SOLOMON, J., VOUGA, E., WARDETZKY, M., AND GRINSPUN, E. 2012. Flexible Developable Surfaces, Comp. Graph. Forum, Vol 31, N 5, pp. 1567-1576.

DESBRUN, M., MEYER, M., ALLIEZ, P. 2002. Intrinsic Parameterizations of Surface Meshes, Eurographics 2002 Conference Proceedings, Vol 21, N2.

ZHONG, Y., AND XU, B. 2006. A physically based method for triangulated surface flattening. Computer-Aided Design, Vol 38 N 10, pp. 1062-1073.

DESBRUN, M., MEYER, M., & ALLIEZ, P. 2002. Retrieved Nov 18, 2013, http://www.geometry.caltech.edu/pubs/DMA02.pdf

TACHI, T. 2009. Simulation of rigid origami, Proceedings of 4OSME: Origami 4, Massachusetts: A K Peters, Ltd., pp. 175-187.

STAM, J., (1998), Exact Evaluation of Catmull-Clark Subdivision Surfaces at Arbitrary Parameter Values, SIGGRAPH 1998 Conference Proceedings, pp. 395-404.

Session 7: Computational Fluid Dynamics **125**

Tensegrity Systems Acting as Windbreaks: Form Finding and Fast Fluid Dynamics Analysis to Address Wind Tunnel Effect 127
Panagiota Athanailidi, Ava Fatah gen Schieck, Vlad Tenu, Angelos Chronis
Bartlett School of Architecture, University College London.

Optimizing the Form of Tall Buildings to Achieve Minimum Structural Weight by Considering Along Wind Effect 135
Matin Alaghmandan, Mahjoub Elnimeiri, Andres Carlson, Robert Krawczyk
Illinois Institute of Technology; University of Southern California.

Approximating Urban Wind Interference 143
Samuel Wilkinson, Gwyneth Bradbury, Sean Hanna
University College London.

Tensegrity Systems Acting as Windbreaks:

Form Finding and Fast Fluid Dynamics Analysis to Address Wind Funnel Effect

Panagiota Athanailidi, Ava Fatah gen Schieck, Vlad Tenu, Angelos Chronis

University College London
Bartlett School of Architecture
100 Address Street West
p.athanailidi@gmail.com, ava.fatah@ucl.ac.uk, info@vladtenu.com, achronis@fosterandpartners.com

Keywords: Tensegrity Systems, Fast Fluid Dynamics (FFD), Form Finding, Wind Funnel Effect.

ABSTRACT

Wind speed in urban areas can create an unpleasant and dangerous environment, known as wind funnel effect, resulting in the non-use of urban spaces. This paper investigates a simulation-based method for designing tensegrity systems to mitigate the wind funnel effect in urban canyons, focusing on form finding of tensegrity systems. The following methodology was proposed: (1) modeling tensegrity structures accurately using Genetic Algorithms (GA) to find the most effective cubic units of struts and cables; (2) re-creating the wind funnel effect in a passage located between two parallel buildings; (3) finding the characteristics of the most porous windbreak structure that could effectively solve the funnel effect in the passage with the use of GA for optimization; (4) using tensegrity units acquired from step 1 to construct a windbreak with the characteristics found in step 3. All steps employed Fast Fluid Dynamic (FFD) simulations to test wind behavior in each environment. After this thorough investigation, the final results from the above steps showed that a proper combination of tensegrity units determined in step 1 is able to address the wind funnel effect effectively, creating a windbreak in a passage between parallel buildings.

1. INTRODUCTION

The majority of the world's population is concentrated in urban areas and it is expected that half of the earth's population already lives in urban settlements. Urbanization is changing city activities, causing serious problems in air quality and directly affecting the usability of urban spaces through issues such as the wind funnel effect.

Tensegrity systems, because of their geometrical and structural properties, may be a promising solution. Their dynamic loading assists with resisting wind and earthquakes, and they are able to exist as self-supporting structures.

This paper investigates the capabilities of tensegrity systems to act as windbreaks in a passage between parallel buildings, mitigating the wind tunnel effect. The aim of this study was twofold. The first part of the investigation was an attempt to simulate tensegrity systems using existing knowledge of particle spring systems in processing environments, and to implement Genetic Algorithms (GA) in unit scale using Fast Fluid Dynamic (FFD) simulation in the evaluation process in order to find the optimum tensegrity unit that can effectively front wind speed. The use of a particle-spring system as a tool in simulation gives the opportunity to include more parameters in the form-finding process, opening up new directions in computational design. GA was implemented with three different tensegrity units based on the number of struts, which is closely related to the porosity of each unit. The configuration of the fittest unit of each category was kept, in order to be used in later steps. The second part of the investigation relied on the exhibition of the wind funnel effect using FFD, and also on the use of GA to find the optimum combination of tensegrity units, identified above, to solve the problem. This bottom-up algorithmic strategy, using modular tensegrity components with different levels of porosity in order to create the final optimum configuration, offers a feasible approach to the design of windbreaks composed of tensegrity structures.

In the following sections we explain tensegrity systems and outline critical factors related to the wind funnel effect and windbreaks, highlighting related background research.

2. BACKGROUND

2.1. Tensegrity systems

The word tensgrity is a portmanteau of the words tensile and integrity. As its name suggests, a true tensegrity system is composed of two sets of components: integral compressive members (struts) that do not touch each other, and continuous tensile members (cables). Stability is provided by the self-stress state between these elements (Figure 1).

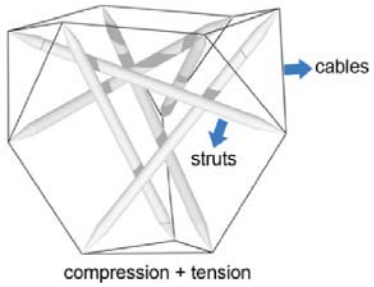

Figure 1. Tensegrity unit - explanation diagram.

The origins of tensegrity systems are linked to K. D. Snelson, R. Buckminster Fuller and D. G. Emmerich. Fuller and other scientists, through the deep exploration of these systems, started to conceive them as the basic principle of the Universe (Burrows, 1989) and the term tensegrity started to extend gradually to other fields like biology, robotics, and astronautics, as well as to other disciplines such as architecture, or civil and mechanical engineering. Researchers continue to explore properties of and applications for tensegrity. The significant advantages tensegrity systems can bring into play are their modularity, their ability to be easily folded and unfolded, and the fact that they are lightweight and cost-effective while at the same time giving a new aesthetic to their surrounding environment.

The geometrical complexity of tensegrity systems presuppose the existence of the appropriate tools that would ensure their constructability. As computation was gradually embedded into architectural and engineering design, designers were able to achieve complexity faster and bring automation into play. This advance is clearly expressed in the current discourse that two of the main research directions on tensegrity systems is form finding, and the attempt to model these systems using particle spring system simulation, which is the approach adopted by this paper.

In terms of form finding of tensegrity systems, there are quite a few methods that were implemented, such as dynamic relaxation. An interesting approach for form finding of irregular tensegrity systems using Dynamic Relaxation and Genetic Algorithms was applied by Chandana Paul et al (2005).

2.2. Wind funnel effect and air simulation

"Wind funnel effect, or double corner effect is where two adjacent surfaces squeeze the air between them, resulting in an increase in wind speed" (Reiter, 2010; Abohela, 2012). When wind is deflected from buildings because of the friction, turbulence increases causing changes in wind direction and speed, as well as a strong vortex at the pedestrian level. The average wind velocity is increased with building height, but on the contrary turbulence level and friction between the wind and earth are reduced with an increase in building height. The complex natural phenomenon of wind and all its effects can be simulated—and produce data like speed, direction and acceleration—through the use of wind funnel measurements, computational fluid dynamics (CFD) predictions or fast fluid dynamic simulation (FFD). FFD is the simulation method used in this paper to conduct experiments to assess the initial hypothesis. These experiments use software written by Chronis (2010) based on Stam (1999), and use the web-based programming language Processing.js. This paper focuses on assessing the wind funnel effect for a passage between two parallel buildings. This configuration is believed to be the more indicative situation, and can more accurately be brought into a simulation environment.

2.3. Windbreaks and porosity

Recent studies on the use of windbreaks are based on the assumption that the surrounding space is completely open, with no other obstacles. However, when referring to a built environment the presence of other buildings affects the effectiveness of a windbreak, and it is yet to be proven to what extent this is true. This paper tries to exploit work done on the basic characteristics of windbreaks and investigate how they fit into solving the phenomenon in question.

The most important factors that influence windbreak effectiveness during the design process are windbreak height, which determines the extent of the protected zone (Heisler and Dewalle, 1988; Forman, 1995) and the

aerodynamic porosity of the windbreak, which determines the ratio between airflow that passes through the barrier pores and airflow that diverges over the barrier (Vigiak et al. 2003). As is shown in the diagram below (Figure 2), the relationship between porosity and reduction of wind flow is directly correlated with the effectiveness of the windbreak, as follows: as porosity decreases, the air velocity decrease is more significant but yet does not exhibit exponential growth when moving away from the windbreak and out of the protection zone.

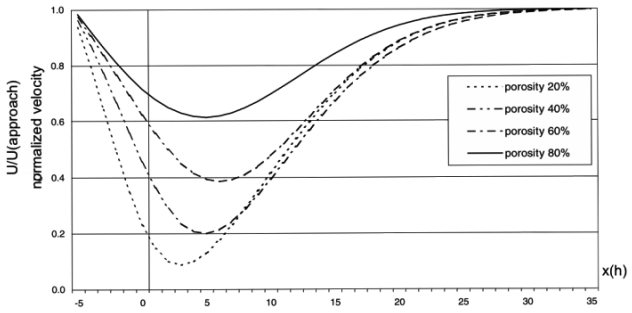

Figure 2. Normalized velocity, porosity, protection area (Vigiak et al. 2003).

Windbreaks can be categorized into three different clusters according to their porosity: porous, medium porous and non-porous (Abel, 1997). According to Forman (1995) the best solution that can mitigate wind is the use of medium porous windbreaks that show the same speed reduction properties as non-porous windbreaks but avoid the problems of turbulence and size distance protection that the latter creates. There is a constant tradeoff between porosity percentage and windbreak effectiveness and there is no optimal choice, but effectiveness is strongly correlated with the wind behavior in situ (Figure 3).

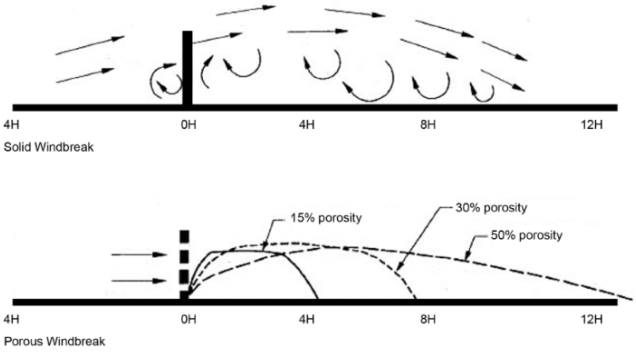

Figure 3. Porosity, windbreak, protection area.

2.4. Pedestrian wind comfort criteria

Wind is an environmental parameter of the microclimate that is directly connected with satisfaction in urban open spaces (Stathopoulos, 2006; Walton et al, 2007). There are many methods in literature to assess Pedestrian Level Wind: quantitative or qualitative, point or area methods, and mechanical, thermodynamic, optical or electric (Ghosh and Mittal, 2012). Lawson and Penwarden extended the "Land Beaufort Scale," presenting wind effects on pedestrians and giving useful wind speed thresholds that define the comfort criteria. (Lawson and Penwarden, 1975). This research adopts the extended Land Beaufort Scale method, both for tensegrity unit scale and macroscale in the process of wind evaluation, because it is directly correlated with the effect wind has on humans, hence closely related with the beneficial use of outdoor spaces.

To summarise, (i) the design of tensegrity systems in this paper is based on particle-spring system simulation, (ii) the final macroscale environment is a passage between parallel buildings, (iii) the threshold values for comfort criteria are based on extended Beaufort scale, and (iv) all the wind simulations were implemented with FFD.

In the following sections we outline the methodology followed and the results found. Section 3 highlights the experimental setup and outlines the findings.

3. METHODOLOGY

3.1. Step 1 - Tensegrity Unit Simulation

In order to be able to simulate the behavior of tensegrity structures in accordance with their physical environment, they were treated as particle-spring systems. The struts are defined as very strong springs and their rest length is defined to be equal to their physical length. The cables, on the other hand, are defined as weak springs with rest length equal to zero. The most significant properties that ensure the topological validity of the tensegrity unit are the number of

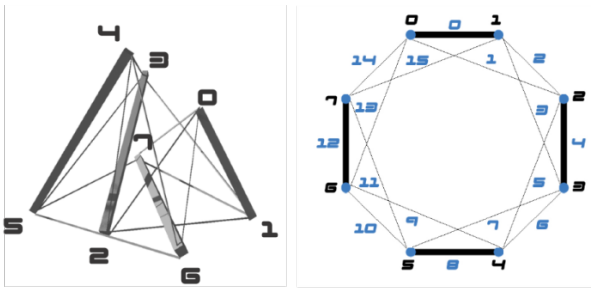

Figure 4. Initial connectivity pattern.

struts and the connectivity pattern that defines the connections between struts and cables. The connectivity pattern both forces the struts to have the same number of

connections with the cables, and also ensures that two struts cannot share a common joint (Chandana Paul et al., 2005). The initial connectivity pattern is presented in the diagram below (Figure 4).

Having understood the way the tensegrity structure is modeled in our simulation environment, the first choice we had to make was how to define the genes (in GA terms) our tensegrity would have. In our case we chose to describe a tensegrity unit with the following genes:

1) The length of struts,
2) The connectivity pattern,
3) The definition of type of connection (strut or cable).

These characteristics (*genotypes*) define a tensegrity structure as a whole, but its actual combination to create one entity is what we call a *phenotype* in GA terms. What is referred to as a population is a collection of individuals (25 in our case) that works as the initial seed of the process. A final important GA term that must not be overlooked is what we call *fitness*, which is closely related to the phenotype.

Our first step is to create an initial population of 25 individuals. A very important step, called the swap technique, takes place at this point and is explained in detail in the paper Evolutionary Form-Finding of Tensegrity Structures by Chandana Paul et al. (2005). The swapping technique is a clever way to create tensegrities with different connectivity patterns (hence different tensegrity units) but always ensuring that tensegrity properties are maintained. This technique randomly chooses two struts and swaps their places, honoring various constraints (Figure 5).

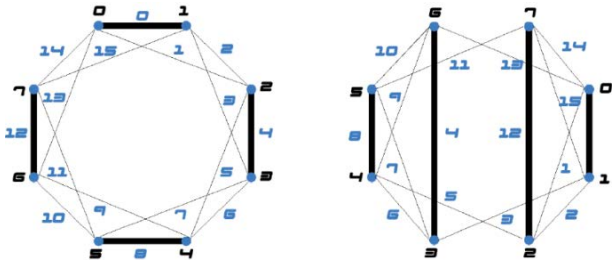

Figure 5. Swap technique.

The next step after careful population creation is to let the tensegrities form stable structures by performing particle-spring simulations until each system reaches equilibrium. This is generally referred to as a form-finding process in a tensegrity context. Once we ensure that all tensegrities have reached equilibrium, and are considered stable, our next step is to evaluate them. This is where fitness comes into play and in our case Fast Fluid Dynamic (FFD) simulation as well. FFD details will be explained in the following section, but this step can be described in general terms. Per individual, we create an FFD simulation environment and we simulate tensegrity behavior under it. The next figure (Figure 6) presents one individual during its evaluation process with its fitness calculation area (box behind tensegrity unit).

What is important at this stage beyond specific FFD information is defining what we consider to be fitness. We try to minimize the airflow that passes through our tensegrity unit, and hence we calculate the mean air velocity per area unit at a specific location "behind" the tensegrity and try to minimize it. All the values used are based on the extended Beaufort Scale and the wind speed at the starting point is number 4 on this scale.

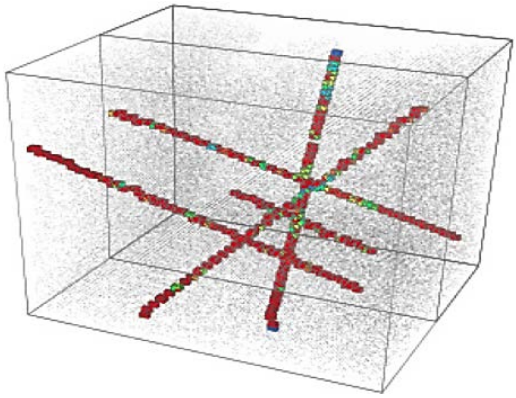

Figure 6. One individual in the evaluation process.

Once the whole population is evaluated it is then sorted based on individual fitness and we are ready to start what is called the evolution state. At this step we discard the 10 least fit individuals and create new ones (children) based mainly on the characteristics of the fittest ones. This is the part where the algorithm starts working toward finding the optimum solution. Four children are created with a single strut swap from the winner of the tournament selection process and six more are created with strut swaps for the rest of the individuals. When all children are created they are left to reach equilibrium state and then evaluated as explained above and we then move into the next-generation evolution.

This procedure is repeated for 20 generations and the fittest individual of all is the optimum result we were looking for. The whole GA procedure has been run for tensegrity units with different numbers of struts. The

optimal units with 5, 7, and 9 stucts are recorded later to be combined in various configurations during the final step of the proposed methodology (Figure 7).

Figure 7. Tensegrity unit winners (number of struts 5,7,9).

3.2. Step 2 - FFD | Wind funnel effect simulation

The target of this step is to try to mimic the wind funnel effect as accurately as possible using Fast Fluid Dynamics (FFD). A detailed explanation of the mathematics and algorithms behind the solver can be found in Chronis 2010. The parameters taken into account in the simulation process were:

1) Wind direction (parallel or perpendicular to passage),
2) Wind speed (3 different speeds from Beaufort Scale),
3) Building height (2 different types), and
4) Passage width (narrow or wide).

Based on the literature review and the experiments that took place, two buildings of equal height with a narrow passage between them and a wind direction perpendicular to this passage with speed 5 was chosen as the final simulation environment, as this configuration exhibited the phenomenon in the most accurate and consistent way.

A lattice of 60x100x40 voxels was created as the FFD simulation basis. To model the outdoor environment, two opposite vertical sides of the cube were not considered as external boundaries, with one chosen as the inflow side of the wind and the other acting as the outflow. The buildings were modeled as solid internal boundaries to be able to act as solid obstacles to wind flow (Figure 8).

3.3. Step 3 - Finding optimal tensegrity to address wind funnel effect

After completing the previous methodology, we turned to address the issue of the wind funnel effect. After careful consideration and deep study of windbreak literature, it was decided to follow a 2-step procedure. The initial step was to

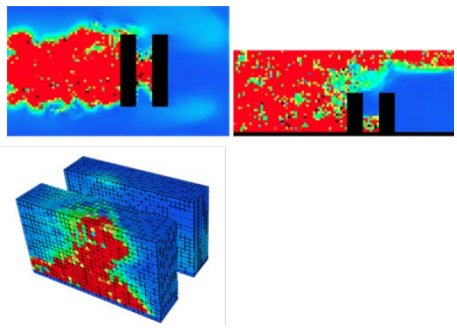

Figure 8. Wind funnel effect exhibition in a passage between parallel buildings.

gather data from the simulation environment and try to extract information on which exact areas were the most problematic with regard to allowing a large quantity of wind to enter the passage between the buildings.

The second step was to implement the GA in order to find the windbreak characteristics needed to resolve the issue. The GA was configured to try and find the optimal solution with regard to finding the most porous windbreak structure (as populated by the tensegrity units identified in step 1) to address the phenomenon. This optimization tactic was chosen as tensegrities are naturally porous structures and it could prove very hard or even impossible to use them to construct a windbreak with very low porosity. Another reason for choosing this optimization tactic is that porous structures would be very easy and cost effective to construct.

GAs were carefully designed to act as an optimization technique for this effort. The idea was to generate different configurations of blockages (solid single-voxel boundaries) to collectively act as windbreaks. In GA terms, a whole configuration is considered as an individual with genes consisting of the number of blockages and their locations. Extra care is needed here to always make sure that these blockages do not randomly appear but are always connected in a way that they define a structure that can be built. This was done by applying constraints and running extra checks during the gene generation to always make sure that every individual was using a valid configuration.

The evolution technique used in this implementation was to select the two individuals from the population with the highest chances of being amongst the fittest, and to breed them to create a child. In practical terms, this exercise created a child equally likely to adopt the blockages from

each parent (always taking extra care to make sure it will corresponded to a valid structure). Another point of interest in this step was balancing the need to minimize the number of blockages with the need to actually solve the issue.

When the evaluation was completed, the characteristics of the optimum configuration addressing the issue were stored. The final solution would act as a windbreak, so characteristics like porosity percentage, width and height were calculated for the final solution per section. Porosity was calculated by vertically intersecting the structure in the three facades and dividing the number of blockages over the whole surface.

The experiments that took place (Figures 9-10) show the ability of the algorithm to find the optimum solution that results in a reduction of the wind inside the passage with the least number of blockages used. The wind speed at the starting point is number 5 on the Beaufort scale (colored red), while the final speed inside the passage (colored blue) corresponds to number 1-2 (light air-light breeze) on the same scale. Figure 9 shows the worst case (maximum number of blockages) and Figure 10 shows the best case (minimum number of blockages).

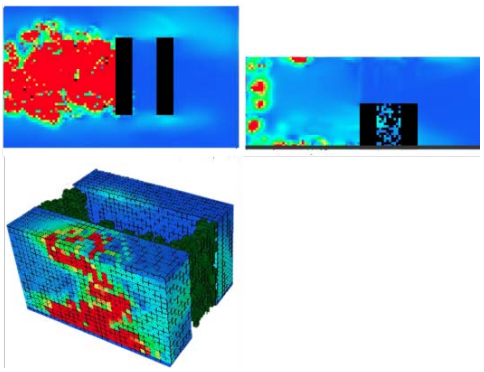

Figure 9. Worst case scenario. Maximum number of blockages (238).

3.4. Step 4 - Constructing tensegrity structure

The final step was to populate the configuration defined in the previous step, honoring the properties calculated. This step is the one responsible for actually implementing the tensegrity solution. The procedure is simple, as the previous steps have given us all the required tools to easily implement any solution. First, the structure is created using tensegrity units from step 1 and honoring at least the minimum percentage of porosity found on any section of the configuration. For example, if we assume that optimal configuration has a maximum porosity percentage of 50% at any given section (the structure is divided into tiles) and the tensegrity unit with three struts has 70% porosity, then it would not be chosen to populate the structure.

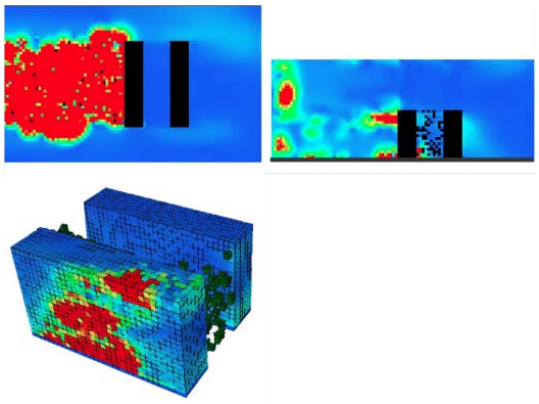

Figure 10. Best case scenario. Minimum number of blockages (126.)

The next step was to revisit tiles that needed less porosity than the maximum and add tensegrity units to create them, making use of the configuration depth properties. The task here is to try out solutions using tensegrity units with the minimum possible number of struts in order to find a valid implementation. The ability to use

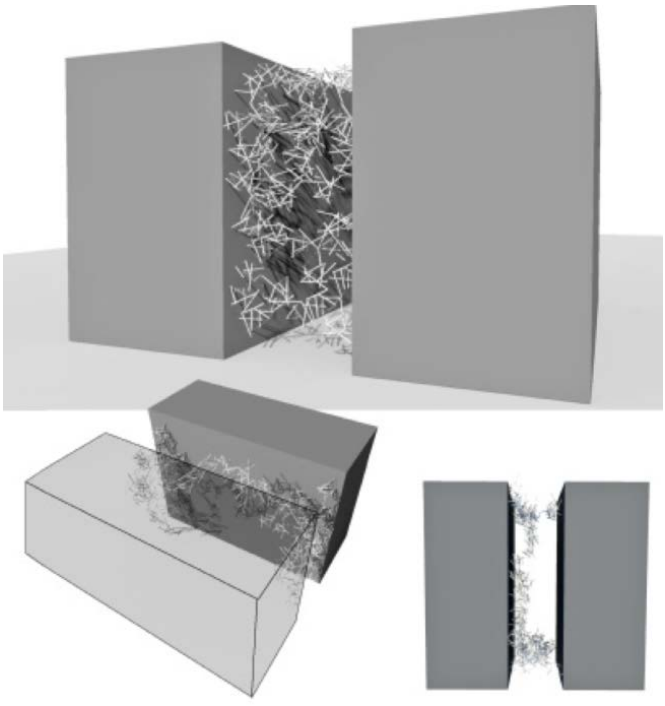

Figure 11. Final implementation.

different tensegrity units at this step provided great freedom both to implement visually interesting structures while honoring the configuration properties. So, it was the careful planning of the overall approach and previous methodology steps which enabled the use of tensegrities to address such a complicated phenomenon. In this final step it would have been computationally intractable to use FFD simulations due to the complexity of the geometry.

Some results visualizing final tensegrity windbreak implementation from various perspectives are presented in Figure 11.

4. DISCUSSION

Upon completion of the series of experiments explained above and analysis of results obtained, we are now in a position to safely judge and review the outcome of this effort. It has been shown that following the approach described in our methodology, tensegrities are able to act as windbreaks to address the wind funnel effect and improve pedestrian comfort levels. Being able to simulate and model the geometrically complex tensegrity structure by using particle-spring systems was one of the most significant reasons we had the ability to use tensegrities as components in the design process. Designers have long wanted to be in a position to investigate complex structures, but until computation lined up with architecture, this desire could only be described as a distant dream. This research, which combines accurate structural models of tensegrity systems with Fast Fluid Dynamic simulations, opens the door to ever more complex computational analysis. Designers now have a tool that offers them new paths to investigate and innovate on.

Furthermore, the initial hypothesis was proven through the final experiments in macroscale. By obtaining windbreak properties such as height, width and porosity (number of blockages) arising from GA optimizations and FFD simulations, we were able to construct a tensegrity windbreak against wind funnel effect by keeping the same characteristics. The results showed that wind speed, starting at 5 on the Beaufort Scale, was reduced to 2 or less inside the passage after the addition of the windbreak. At this reduced level, it is described as calm-light air.

At this point, it is beneficial to point out what exactly the assessment on whether tensegrity structures are eligible to act as windbreak in the environment consisted of. The tensegrity units acquired after the initial optimization had some very specific width, height, size and depth characteristics. The same holds for the windbreak structures found in methodology step 3. It was the ability to use tensegrity units as components to construct this structure that proved their eligibility to act as windbreaks and answered the research question. At this final assessment, tensegrities could have proven insufficient for this purpose if they were unable to create a structure with the desired characteristics.

4.1. Critical Review and Further Developments

This paper tried to suggest a new methodology for addressing a complex phenomenon. The approach followed needed to provide scope for designers to explore various possible solutions at the early design stage. With this scope in mind, it was important to keep things as computationally simple as possible, because increasing the time to obtain results in the early design stages is highly undesirable. This goal was achieved by using an FFD simulation environment, which has been proven to be reasonably accurate to use at the first stages of study. It has also affected other design decisions in accordance with the intention of the study.

The complexity of the work performed during this research allows for various points of further development to be suggested and implemented in the future, based on the required level of accuracy needed to be obtained from the analysis. Starting with the modeling of tensegrity systems, one suggestion is to improve the accuracy of the simulation. First, during the dynamic relaxation of the form-finding step, an extra kinematic relaxation approximation algorithm step can be applied to assist in finding the equilibrium point of the tensegrity. This extra step would reduce the time needed for the tensegrity to reach equilibrium, at the cost of some extra computations.

With regard to recreating the wind funnel effect, there is one factor that would certainly help make the simulation more accurate and closer to reality: by taking into account the roughness of buildings. Even if the first is relatively easy to model as an extra parameter affecting the wind speed during a collision with a solid boundary inside the simulation, it was not implemented under the scope of the current research, as it is believed it will not dramatically change the results obtained.

Both of these enhancements should be used in future applications where increased accuracy is desirable. For example, if this analysis is used to address wind funneling at a specific location.

Finally, in the last implementation step of the actual tensegrity structure, there are multiple fixes that could be implemented if the study is engineering-oriented and building stability is important. Obviously, accurate analysis on specific stability factors was out of the scope of the current research.

5. CONCLUSION

The use of tensegrity systems as a design-solution component for the wind funnel effect is innovative, and the number of projects that have dealt with this phenomenon is very limited. As a result, an extensive and combinatorial literature review was necessary. A thorough investigation in tensegrity systems and analysis of the different research directions offered a deep understanding of the capabilities these systems have and their potential uses. To address the general need to deal with environmental aspects of a city that might lead to non-use of outdoor urban spaces, we selected tensegrity systems as a design element that offers a unique solution to wind tunnel effect mitigation.

The particle-spring system approach and the implementation of GA with the modifications discussed were successfully integrated to tensegrity unit simulation. The evolutionary method (GA) used for form finding meets the requirements of the tensegrity simulation properties, and the use of FFD suits the needs in evaluation process. The experiments and results proved that the methodology that is followed could verify the initial hypothesis. It is evident that tensegrity systems can be used in outdoor spaces as windbreaks mitigating wind funnel effect. Despite the fact that FFD is used in early design stages that demand more time-efficiency rather than accuracy in results, it is clear that oenhancing the fluid solver used and implementing some other modifications discussed in the critical review could yield more accurate results for use in engineering projects.

Concluding, this paper proves the viability of the innovative approach of using tensegrity structures to address the specific environmental phenomenon. It also serves as the initial step for further research in the field. The whole applied methodology has been carefully selected for reuse in different urban design projects and investigations.

REFERENCES

ABEL, N. 1997. Design Principles for Farm Forestry. A Guide to assist farmers to decide where to place trees and farm plantations on farms. Canberra: Rural Industries Research and Development Corporation, p. 102.

BURROWS, J. 1989. Catalogue Introduction, Kenneth Snelson Exhibition: The Nature of Structure. New York: The New York Academy of Sciences.

CHRONIS, A. 2010. Integration of fast fluid dynamics and genetic algorithms for wind loading optimization of a free form surface. Thesis project on University College London (UCL).

CHANDANA, P. Lipson, H. & Valero-Cuevas, F. J., 2005. Evolutionary Form-Finding of Tensegrity Structures. Proceedings of the 2005 Genetic and Evolutionary Computation Conference, Washington D.C.: Cornell Creative Machines Lab, pp. 3-10.

FORMAN, R.T.T. 1995. Land Mosaics: The Ecology of Landscapes and Regions. Cambridge: Cambridge University Press, p. 632.

GHOSH, E., MITTAL, A.K. 2012. A review on pedestrian wind comfort around tall buildings. VI National Conference on Wind Engineering, pp.491-506.

HEISLER, G.M., DEWALLE, D.R. 1988. Effects of windbreak structure on wind flow. Agriculture Eco-systems Environment, (22) 23, pp. 41-69.

LAWSON, T.V., PENWARDEN, A.D. 1975. The effects of wind on people in the vicinity of buildings. Proceedings 4th International Conference on Wind Effects on Buildings and Structures. Heathrow: Cambridge University Press, pp. 605-622.

REITER, S. 2010. Assessing wind comfort in urban planning. Environment and Planning B: Planning and Design, 37(5), pp. 857 – 873.

STAM, J. 1999. Stable fluids. Proceedings of the 26th annual conference on Computer graphics and interactive techniques (SIGGRAPH '99). ACM Press/Addison-Wesley Publishing Co., pp. 121-128.

STATHOPOULOS, T. 2006. Pedestrian level winds and outdoor human comfort. Journal of Wind Engineering and Industrial Aerodynamics 94, pp. 769-780.

VIGIAKM O., STERK, G., WARREN, A., HAGEN, L.J. 2003. Spatial modeling of wind speed around windbreaks. CATENA, 52 (3-4), pp. 273-288.

WALTON, D., DRAVITZKI, V., DONN, M. 2007. The relative influence of wind, sunlight and temperature on user comfort in urban outdoor spaces. Building and Environment 42, pp. 3166-3177.

Optimizing the Form of Tall Buildings to Achieve Minimum Structural Weight by Considering Along Wind Effect

Matin Alaghmandan[1], Mahjoub Elnimeiri[1], Andres Carlson[2], and Robert Krawczyk[1]

[1]Illinois Institute of Technology
3410 S State St.,
Chicago, IL, USA, 60616
malaghma@iit.edu, elnimeiri@iit.edu, krawczyk@iit.edu

[2]University of Southern California
Watt Hall, Suite 204,
Los Angeles, Ca, USA, 90089
andersca@usc.edu

Keywords: Along Wind, Architectural Form, CFD Simulation, Design Method, GA Optimization, Parametric Design, Structural System, Tall Buildings.

Abstract

One of the most influential parameters in architectural and structural design of tall buildings, in addition to gravity loads, is the lateral load resulting from wind and earthquakes. Tall buildings have to be designed for a larger base shear resulting from wind forces rather than seismic forces; however, ductile detailing is required to account for seismic demands. The wind effect occurs primarily in two main modes of action: across wind and along wind. In this paper, a design method for tall buildings is presented that considers integrated architectural and structural strategies to reduce the along wind effect in an effort to achieve minimum weight for the structure. This method creates an innovative computational workbench to design efficient tall buildings in regard to the along wind effect. The workbench connects an architectural parametric design procedure by AutoLisp (AutoCAD), a Computational Fluid Dynamics program (ANSYS), a structural analysis program (ETABS), and a genetic algorithm-based optimization procedure of ParGen.

1. INTRODUCTION

There has been an increased growth rate in the number of tall buildings and also their average height over the past decade. This trend shows the importance of this type of building in future urbanism. Increased wind speeds and wind force through climate change will also impact the future of tall building design. Unprecedented heights and forces now require designers to consider architectural and structural factors that will improve the efficiency of the design process and of the building itself. Design time and building materials both carry substantial costs and an integrated approach such as the method described in this paper will reduce both. The maximum rentable floor area can be the major parameter of the architectural efficiency and the minimum weight of the structural elements can be the most important factor for the structural efficiency. Integrated design can also help to synthesize a more efficient design that the conventional design process is less likely to produce.

Wind produces three different types of effects on tall buildings: static, dynamic, and aerodynamic. These effects play an important role on the parameters of the architectural and structural efficiency of tall buildings, especially since the largest lateral forces on tall buildings are the result of wind. Thus, reducing the wind effects and also the dynamic response of tall buildings by architectural and structural concepts can positively influence the efficiency of these buildings.

In this paper, the traditional design method will be briefly illustrated. Then an innovative design method for tall buildings that considers efficient parameters will be introduced.

2. WIND CONSIDERATIONS

Wind is a phenomenon of great complexity because of many flow situations arising from the interaction of wind with structure, particularly with the structure of tall buildings (Taranath, 1998).

The wind effect occurs primarily in two main modes of action: across wind and along wind. A rectangular building with one face nearly perpendicular to the approaching wind will have two faces parallel to the mean flow; the far side is named the leeward side. The motion of wind measured

perpendicular to the mean flow is the *across wind direction* and the mean flow is in the *along wind direction*.

The across wind effect, which is not the object of this research, refers to the direction perpendicular to the mean wind direction, and primarily affects the two sides of the building parallel to the mean flow. In general, the across wind effect on a tall building is more complicated and more unexpected than the along wind effect. Across wind effects are typically modeled and predicted with wind tunnel tests because of the complexity of the behavior and the lack of reliability of measuring these dynamic effects using computer simulations. Hence, considering the across wind effect that causes vortex shedding and the dynamic response of tall buildings towards it will be included in future steps of this research.

The along wind effect, being in the direction of the mean wind flow, primarily results in pressure fluctuations on the building's frontal face hit by wind (windward) and the back face of the building (leeward) (Taranath, 1998). These effects are easier to simulate and results are more reliable than for across wind effects. In this paper, the along wind effect is considered as the only lateral load on tall buildings and the across wind effect is ignored.

To control the wind effect, both architectural and structural strategies have to be considered, preferably simultaneously. Designing aerodynamic forms and also modifying form and geometry, such as tapering and setback, are considered architectural concepts; whereas determining appropriate lateral-load based structural systems, such as a core-supported outrigger system or a diagrid system, are structural concepts. In this paper, the architectural and structural considerations to reduce wind effect and structural response are illustrated.

3. ARCHITECTURAL CONSIDERATIONS

The architectural strategies to reduce wind effect are basically divided into two main categories of micro and macro architectural concepts. Designing aerodynamic and tapering forms are the macro examples affecting the entire building geometry and rounded, cut and chamfered corners are the local or micro levels of architectural concepts that influence wind response. This definition is based on the quality of the effect of the modifications on the form and geometry of the buildings (Alaghmadnan & Elnimeiri, 2013).

Two important ideas have to be considered in the architectural concepts for mitigating wind effect. Firstly, the effect of wind on tall buildings can be reduced by deflecting or escaping from the wind. This means that the architectural strategies can reduce the effect of wind by providing a smooth flow behavior of wind around the building. Hence, in many of the most famous tall buildings, the aerodynamically favorable forms are currently preferred and their effectiveness is incredible. For instance, in Taipei 101 "corner modifications provide 25% reduction in the base moment when compared to the original square section" (Irwin, 2006).

Secondly, confusing (disrupting) the wind is a very effective solution to reduce the wind effect, particularly the dynamic effect of wind. The aerodynamic form of a building can act in an unexpected relationship with wind and in general can reduce the along wind response as well as the across wind effect by confusing the wind, particularly the across wind vortex-shedding effect (Irwin, 2009). It means that the aerodynamic form can disperse the wind and avoid gathering wind flow to have a huge integrated effect on the structure of tall buildings. Therefore, the cross-sectional form can be advantageous in reducing wind load effects and building responses.

However, recent studies such as (Sevalia, Desai, & Vasanwala, 2012) and (Kim & Kanda, 2010) have also shown that some architectural modifications are ineffective and even have adverse effects. Since there is no distinct consensus that the benefits of architectural concepts apply to the unique characteristics of all buildings, each individual building has to be tested with physical models in a wind tunnel to find out the effectiveness of the concepts, positive or negative (Alaghmadnan & Elnimeiri, 2013).

4. STRUCTURAL CONSIDERATIONS

There are two main structural concepts to reduce the response of tall buildings to wind: stiffening the structure of tall buildings and providing supplementary damping sources. Stiffening the structure of tall buildings can be efficient if accomplished by engaging and rearranging the structural systems, rather than just using more materials to provide more stiffness.

The structural systems of tall buildings are divided into two main categories of exterior and interior systems, depending on the location of the portion of the structural

system resisting the main lateral force. All types of tube systems, such as tube in tube or diagrid systems, are considered exterior. Core systems, such as braced or shear wall cores supporting outrigger systems, are the interior systems. Designing and choosing an efficient structural system for tall buildings not only is a critical and complex issue in itself, but also is dependent on the form and geometry of tall buildings. Therefore, the coordination between architectural and structural criteria to increase the efficiency of tall buildings is an important consideration in the design of this type of building.

The second main structural solution to reduce the response of tall buildings to wind is damping. Damping is the degree of energy dissipation that a structure can provide to reduce build-up of the resonant response. It comes from two main sources: intrinsic and supplementary. Intrinsic damping comes from within the structural material, such as steel, reinforced concrete, and soil. Unlike intrinsic damping, supplementary (or auxiliary) damping is primarily mechanical or heat releasing, and has to be added to slender tall buildings. If the geometry prevents the building from economically having enough stiffness to avoid dynamic resonance effects, supplementary damping can help to minimize building motion. This research is considering geometries that increase effeciencies, rather than requiring supplementary damping, so damping resources are not considered in this research.

5. DESIGN METHOD

The current design method of tall buildings needs to be reviewed, considering the aforementioned architectural and structural criteria, to find a better design method that improves architectural and structural efficiency.

The current design method for tall buildings is like that for most other architectural types of buildings, in that architects first design buildings schematically, and then transfer the main idea of the drawings to computing programs for implementing simulations. After architects finalize the main concepts of the design, structural and other related fields of engineering are added to the design team to design and analyze the structure and other components of the building, with minimal potential for building form changes either on the exterior or the interior. After the structural design has been developed sufficiently to identify dynamic properties of the building, a physical model is placed in a wind tunnel test to predict both static and dynamic forces and effects on the building. Thus, all the main design criteria and parameters are slowly developed and added throughout the design process, instead of being considered together from the first steps of design.

This model of sequential cooperation extends the design phase, while limiting the search for better solutions, and thus incurs extra costs for the construction of the building. Consequently, there is a gap in this kind of design process. Team collaboration and creative methods of design in the realm of tall buildings to cover these kinds of gaps are inevitable, and this research is providing one alternative.

For creating an innovative design method in the realm of tall buildings to achieve more efficient buildings, there needs to be a common workbench of architectural, structural and fluid dynamics computing programs to work together from the early steps of the design process. This method facilitates a comprehensive collaboration among architects, structural engineers and wind engineers in a non-linear back and forth process to gain the most efficient geometry and form with minimum wind impact and minimum structural weight, while still achieving the formal functional intents of the building.

5.1. The Main Design Steps

In the proposed design method, there are three main steps implemented on the basic workbench of ParaGen.

The first step is to design a model using an architectural parametric procedure. The 2D parametric model for a Computational Fluid Dynamics (CFD) simulation is implemented by DesignModeler, part of the ANSYS workbench. Another 3D parametric model is designed by AutoLisp in AutoCAD, and is used to set the parameters of the 3D model of the tall building for connecting to the ETABS program for the structural analysis and design process.

The second step is to simulate the CFD procedure, which is implemented by FLUENT of ANSYS. The model set on the DesignModeler is linked into the meshing module of ANSYS and then simulated in the CFD program (FLUENT) of ANSYS. Based on the CFD results, the lateral force of wind on the windward and leeward sides is obtained to use in the structural software simulation as the lateral wind load.

In the third step, every individual model subjected to CFD simulation is linked into the structural analysis program (ETABS) to be structurally analyzed and designed. The results of the ANSYS wind modelling are recalculated as the lateral load (wind) on the models in ETABS through a user-defined process to determine the corresponding wind load.

Between the CFD simulation and ETABS analysis and the design portions of the workbench, there is a script in MATLAB to get the results from FLUENT and create an Excel file of lateral forces as input to the ETABS model. All these steps and the computational workbench will be illustrated with more details in the following sections.

5.1.1. Architectural parametric design

In the parametric design method, the model is defined by parameters that modify shape and form. By assigning different values to the parameters and to the equations, different objects or configurations can be created through the generation process (Burry, 1999).

In the parametric design process of this research, the parameters of the models are set assuming equal gross area of the building for all the generations, with AutoCAD used for the structural modelling and DesignModeler used for CFD simulation. In order to provide a meaningful comparison of the solutions, it is necessary to base all models on the same architectural efficiency, which is dependent on the total gross area. Otherwise, the generations of models would not provide any meaningful comparison of solutions. In this process, designers can set the parameters of the building models based on the desired geometry and form, like aerodynamic form or setback, and then run the generations.

The basic model is a prismatic model with a 64 m by 64 m square plan and 360 m height. Tapering effects will be checked in this research, since the parameters of the models are set to achieve a generation of this type of architectural and form modification that is a macro architectural concept in only one direction (the reason will be explained in the next part). One of the important points of this part is to generate models with different tapering angles that keep the same total gross area and the same height (Figure 1), since the area of every floor can vary except for the 45th floor.

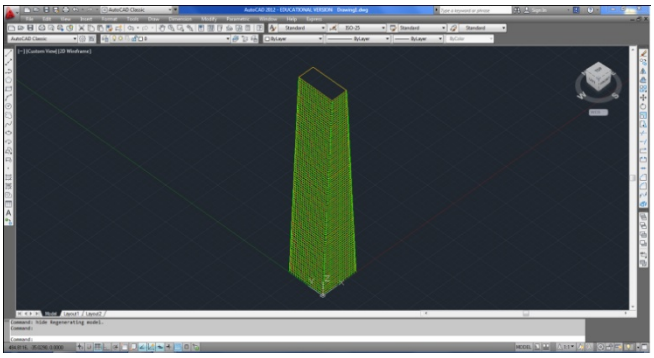

Figure 1: One generation of the parametric tapered models of tall buildings in AutoCAD.

In this step, it is necessary to mention that all the generations have to be evaluated and verified based on their function and acceptable architectural form; thus, every individual model of each generation has to be accepted by the design team before the model can go forward to the next steps. The parameters should be defined within acceptable boundaries to the design team up front so that the process can be streamlined to a solution space that is already acceptable.

5.1.2. CFD simulation (ANSYS)

All the generations of the models are linked in to the Meshing module (Figure 2) and then simulated with the FLUENT program of ANSYS. The parameter settings of the Meshing procedure and of FLUENT are very important to find enough accurate results, and are pre-required factors for using this program.

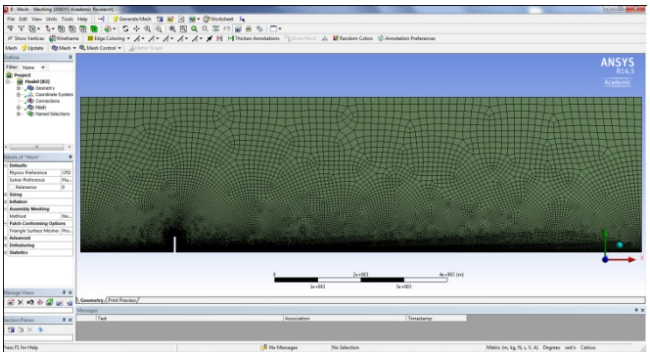

Figure 2: The gridding of the basic model in the Meshing module of ANSYS.

For this part, the AIJ (Architectural Institute of Japan) guideline and also COST (European cooperation in the field of Scientific and technical Research) are considered as the main guidelines for implementing the ANSYS program. The basic computational conditions—such as meshing

arrangements, boundary conditions and solution models —were specified by the guidelines. In this part, a couple of their major points are illustrated.

For the size of the computational domain, for a single tall building model, the lateral and the top boundary should be set at least 5H (where H=height of the tallest model) from the building, and the outflow boundary should be set at least 10H (based on AIJ) or 15H (based on COST) behind the building and the buildings included in the computational domain should not exceed the recommended blockage ratio (3%) (Tominagaa, et al., 2008; Franke, et al, 2007). However, in this research the top boundary is set to 9H and the upstream boundary size is set to 6H and the downstream boundary is 30H from the model, conservatively. In general, the outflow boundary needs to be far enough from the tall building for there to be negligible influence of the target building on the wind pattern.

The main points that should be confirmed in gridding or meshing is that the prediction result does not change significantly with different grid systems. In this case, the meshing is good enough to do the final CFD simulation (Figure 3). It is also necessary to ensure that the aspect ratio of the grid shapes does not become excessive on regions adjacent to coarse grids or near the surfaces of the obstacle. It is recommended to arrange the prismatic cells parallel to the walls or the ground surfaces for the unstructured grid system (Tominagaa, et al., 2008; Franke, et al, 2007).

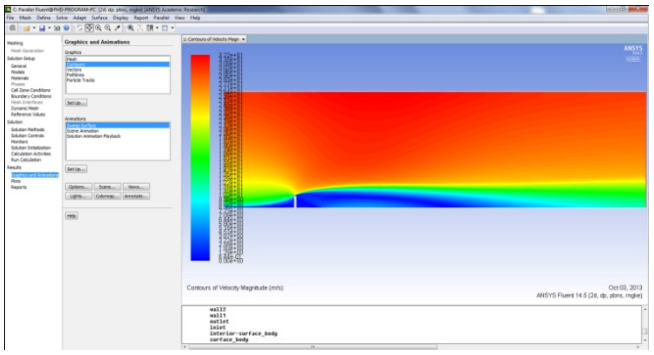

Figure 3: (Contour of Velocity) CFD simulation of the basic model in FLUENT of ANSYS.

Based on both these guidelines, the first-order upwind scheme is not appropriate for all transported quantities, since the spatial gradients of the quantities tend to become diffusive due to a large numerical viscosity; thus, the second order scheme is chosen for the simulations in this research.

The wind speed for the CFD simulation of this research is 7 meters/second or 25.2 km/h (around 15.6 mph). For comparison, the average annual wind speed in Chicago is 10.3 mph; Milton, 15.4 mph; Boston, 12.4 mph (20.0 km/h); New York City, Central Park, 9.3 mph (15.0 km/h); and Los Angeles, 7.5 mph (12.1 km/h) (http://en.wikipedia.org).

The final calculation also needs to include sufficient convergence of the solution. To avoid common problems, the aspect ratio and the stretching ratio of the gridding, the relaxation coefficient of the matrix and periodic fluctuations such as a vortex shedding must be carefully checked (Tominagaa, et al., 2008; Franke, et al, 2007). Figure 4 shows the static pressure diagram on the windward (white line) and on the leeward (red line) sides. These results by a MATLAB script can be placed into an Excel file as input to the ETABS program for structural analysis and design.

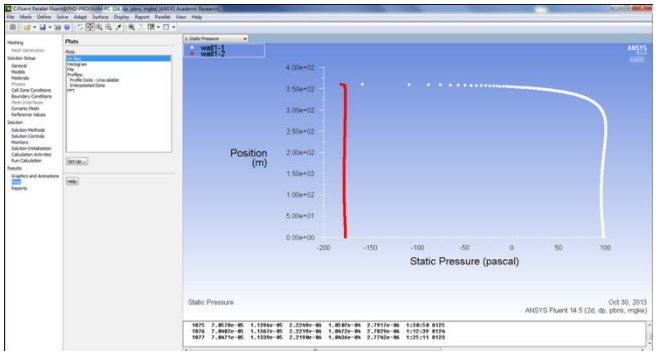

Figure 4: Static pressure plot of wind on the windward and the leeward sides of the basic model.

5.1.3. Structural analysis and design (ETABS)

After the CFD simulation, every individual model has to be transferred into the structural program (ETABS) to be structurally analyzed and designed against the lateral forces obtained from the ANSYS simulation.

In general, in design of tall buildings, structural designers “want to use the minimum material to resist a prescribed wind load without exceeding a deflection criterion such as tip deflection” (Baker, 1992). Hence, for designing an efficient structural system for a tall building with the least volume of material, it is useful to determine the deflection contribution of each member. This objective is essentially a virtual work or strain energy density that can be viewed as a measure of efficiency. In this case, all members of the structural system have to have equal energy densities to be of optimal efficiency (Baker, 1992). A desired roof displacement can be met through an

optimization process that reassigns groupings of members with different discrete shapes to try to make all groups of members in the structure have the same strain energy density or contribution to the displacement. As material is redistributed to this end, a lighter structure is achieved (Gilsanz & Carlson, 1991).

The models can be designed with a structural system based either on exterior lateral load or on interior load. In this part, designers can consider each structural system for all the generation models of buildings, and they can compare the weight of the structural elements of the models based on the different wind effects on the different tapering percentages. As mentioned before, the weight of the structure can be one of the most important factors for evaluating the structural efficiency.

In this research, the deflection limit is H/500 for the models. Therefore, because the basic model is 360 m tall, it can deflect 0.72 m horizontally from each side that is set in the ETABS displacement part. The analysis and design is based on AISC ASD steel code requirements (Figure 5). For this research, the steel framed tube system is chosen for the models, but clearly this does not mean it is the most efficient system for these models and height.

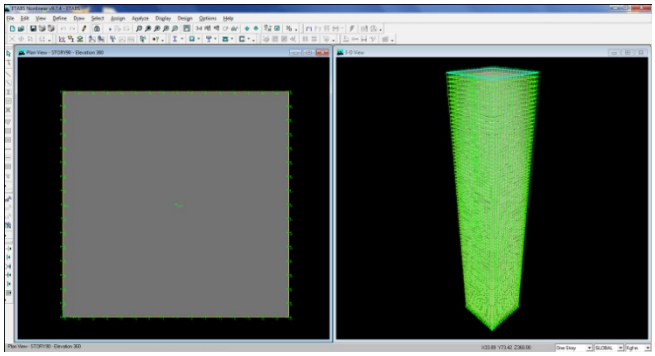

Figure 5: One of the examples of the structural analysis and design of the basic model in ETABS

The CFD results detailing the pressure on the windward and leeward sides of the models is exported into an Excel file. Then, the average pressure at every four meters (floor to floor height) is automatically calculated to consider lateral load on every floor system of the structural model.

6. PARAGEN

ParaGen is a parametric design tool using a Genetic Algorithm method of optimization for the exploration of form based on performance criteria. It is implemented/under development at the University of Michigan, Taubman College, where it has been used for structural form optimization; it is now being extended for interdisciplinary optimization (Von Buelow, 2012).

For this research, the performance and variable criteria were set up on the ParaGen web interface and the analysis and design part had to be implemented in parallel at Illinois Institute of Technology, School of Architecture. On the server side, both the original variable values along with the performance results are maintained in an SQL database, and linked to the data files. For the specific tapering example that is mentioned in this paper, the angle of tapering is the geometric variable of the models and the objective is to find the minimum weight of the structure in relation to the along wind effect. It is clear that this method can work for multi-objective optimization procedures as well.

Based on the capability of the ParaGen interface, the design team can view, compare and retrieve all the generations through the web interface. Another important point of the ParaGen is the ability to sort and filter the results in a variety of ways, such as the weight of the structure or any other defined parameter.

7. FUTURE STUDY

Nowadays, commercial tall buildings are getting taller, more slender, and with more complex architectural forms. For such buildings, the dynamic impact of wind loads is significant and has to be taken into serious consideration in both the architectural and structural design development stages.

The state of the art technique to evaluate the response of tall buildings to wind is through wind tunnel testing, with procedures that have been applied successfully through the years. However, such tests are expensive, time consuming, and for all practical purposes they are conducted at the final phases of the design.

Because of hardware limitations, our research has only considered the along wind effect. Future study can address the response of a slender tall building to cross wind and resultant vortex shedding. A process can be developed through which cross-wind accelerations and forces can easily be estimated during the early stages of the design. This will allow both the architect and the engineer to work together and interactively to produce an architectural shape

and a structural system that will respond well to such forces. The method is interactive, non-linear, and interfaces the 3D of the CFD modeling with computer/structural analysis programs such as Sap2000. The objective is not to seek an optimum solution, but to obtain an efficient structure which will work well within an accommodating architectural form. The method of approach is in no way an alternative to a wind tunnel test, but it is a valuable tool for establishing a good and sensible building.

8. CONCLUSION

The complexity of the form of tall buildings is going to increase because of the continued development of construction technologies, computational speed and progressive structural systems. However, the most important point that has to be considered by all design team members is architectural and structural efficiency. This research suggests a design method to model a comprehensive collaboration among the design team members towards designing efficient tall buildings. There are two specific findings of this study.

First, in the proposed method of design the following effects are known to reduce the overall weight of the structure, one of the main parameters of improved efficiency: (1) the effect of geometric modification on reducing wind effect and (2) the effect of determining and designing an appropriate lateral-load based structural system based on the geometry and form of the building.

Second, aerodynamic (geometric) modifications using architectural concepts and lateral-load based structural systems have to be considered and coordinated in the design of tall buildings from the early stages of design.

This method can take a generation of buildings based on the designers' criteria and parameters with equal total gross area to the basic model and sort the optimized solutions based on the least weight of the structure. Consequently, designers can achieve the desired geometry and form by considering the architectural and structural efficiency.

Acknowledgements

The authors would like to express their gratitude to Prof. J. Mohammadi, Prof. D. Sharpe and special thanks to Prf. R. J. Krawczyk for his contribution on the computing portion.

References

Alaghmandan, M., & Elnimeiri, M. (2013). Reducing impact of wind on tall buildings through design and aerodynamic modifications. AEI conference, Penn State university. College Station, Penn.

Baker, W. F. (1992). Energy-Based Design of Lateral Systems. Structural Engineering International , 99-102.

Burry, M. (1999). Paramorph. AD Profile 139: Hypersurface Architecture II. London: Academy edition.

Franke, J., Hellsten, A., & Schlunzen, H. a. (2010). The Best Practise Guideline for the CFD simulation of flows in the urban environment : an outcome of COST 732. The Fifth International Symposium on Computational Wind Engineering. Chapel Hill, North Carolina, USA.

Gilsanz, R., & Carlson, A. (1991). Optimization in Building Design. Boston, Massachusetts: International Conference on Computer Aided Optimum Design of Structures.

http://en.wikipedia.org/wiki/Origin_of_the_name_%22Windy_City%22#cite_note-ncdc-3. (n.d.). Retrieved 01 20, 2014.

Irwin, P. (2006). Developing Wind Engineering Techniques to Optimize Design and Reduce Risk. 7th UK Conference on Wind Engineering. Wind Engineering Society, ICE.

Irwin, P. (2009). Wind challenges of the new generation of super tall buildings. Journal of Wind Engineering and Industrial Aerodynamics , 328-334.

Kim, Y., & Kanda, J. (2010). Characteristic of aerodynamic forces and pressures on square plan buildings with height variations. Journal of Wind Engineering and Industrial Aerodynamics , 449-465.

Sevalia, J., Desai, A., & Vasanwala, S. (2012). Effect of geometric plan configuration of tall building on wind force coefficient using CFD. International journal of advanced engineering research and studies, 127-130.

Taranath, B. (1998). Steel, Concrete and Composite Design of Tall Buildings. NewYork: McGraw-Hill Book Company.

Tominagaa, Y., Mochidab, A., Yoshiec, R., Kataokad, H., Nozue, T., Yoshikawaf, M., et al. (2008). AIJ guidelines for practical applications of CFD to pedestrian wind environment around buildings. Journal of Wind Engineering and Industrial Aerodynamics , 1749–1761.

Von Buelow, P. (2012). paraGen: Parametric exploration of generative systems. Journal of the association for shell and spetial structures, 271-284.

Approximating Urban Wind Interference

Samuel Wilkinson, Gwyneth Bradbury, and Sean Hanna

University College London
14 Upper Woburn Place
London, WC1H 0NN
samuel.wilkinson.09@ucl.ac.uk
g.bradbury@cs.ucl.ac.uk

Keywords: Computational Fluid Dynamics (CFD), Generative Design, Machine Learning Approximation, Urban Wind Interference, Tall Buildings.

Abstract

A new approach is demonstrated to approximate computational fluid dynamics (CFD) in urban tall building design contexts with complex wind interference. This is achieved by training an artificial neural network (ANN) on local shape and fluid features to return surface pressure on test model meshes of complex forms. This is as opposed to the use of global model parameters and Interference Factors (IF) commonly found in previous work. The ANN is trained using shape and fluid features extracted from a set of evaluated principal (design) models (PMs). The regression function is then used to predict results based on shape features from the PM and fluid features from a one-off obstruction model (OM), context only, simulation. For the application of early-stage generative design, the errors (against CFD validation) are less than 10% centred standard deviation σ, whilst the front-end prediction times for the test cases are around 20*s* (up to 500 times faster than the CFD).

1. INTRODUCTION

CFD analysis in architectural design typically involves response times that are obstructive to the fast iterations of contemporary generative practice. In this parametric paradigm, architects can easily generate immense numbers of alternative scenarios but are then faced with the time-consuming task of evaluation and selection. One earlier solution focusses on early-stage design of tall buildings, using pre-computed procedural model sets, local morphological shape features, and machine learning via an artificial neural network (Wilkinson et al. 2013). It was shown that significantly faster prediction times can be achieved whilst minimising approximation errors to task-appropriate levels.

A limitation of this previous work, however, was the exclusion of surrounding context. That is, the approach treated the buildings in isolation, with unrealistically simplistic boundary conditions. In this work, the morphological features are extended with local fluid properties (upstream wind speed) to support complex urban scenarios. This is achieved by effectively superimposing an isolated building prediction of an infinitely variable generative model onto the surrounding conditions (a one-off, context-only simulation.

Many attempts have been made to approximate or generalise this kind of complex wind interference, i.e. the effect of multiple buildings in the domain (see Table 1). However, all have relied on a top-down problem definition in relating the position of identical surrounding building cuboids with a global Interference Factor (IF) for the design building. The new approach seeks to improve this significantly by: (1) allowing surrounding context of any degree of complexity; and (2) giving vertex-level resolution rather than global effect factors. A background review, general methodology, and experimental results for two test case complexities are presented in this paper, alongside a discussion on speed and accuracy.

2. LITERATURE REVIEW

The background review will explore the current state of performative generative design, various methods for approximative CFD, and the state of urban wind interference with machine learning. The intention is to highlight a gap in the research, specifically on approaches to CFD approximation and interference generalisation that do not rely on global parameters or over-simplification.

2.1. Performative Generative Design

In current generative design practice, enabled by the ubiquity of computation and advances in computer aided design, integrating performance behaviours into generative models has entered the foreground (Malkawi 2004). Examples can be seen in the use of structural, energy and thermal, materiality, fabrication, and air movement (either internally for comfort and indoor air quality; or externally for structural or façade aerodynamics, pedestrian comfort, or pollution dispersal).

Air movement, predicted through CFD, suffers the most from restrictive response times, predominantly because of the historical focus on accuracy rather than speed (due to low-tolerance high-risk scenarios in aircraft and spacecraft engineering). Arguably, the margins for acceptable error are more tolerant in building design, meaning that the simulation accuracy requirements can be relaxed or traded off for speed improvements (particularly at early design stages).

In these early stages of light-weight (fast and less-accurate) performance feedback, there can be more allowance for design exploration and optimisation. This is supported by the idea of speed-accuracy trade-offs (SATs, Chittka et al. 2009), which suggests that for low-risk problems it is often better to make faster, less accurate decisions. In other words, in the scope of the larger problem of building design, it is better to have a broader perspective on the performance variability rather than an extremely accurate but narrow perspective on fewer cases.

2.2. Approximating Computational Fluid Dynamics

CFD is one of the most intensive and time-consuming simulations in the performance assessment of tall building design. Specifically for wind analysis, it is of great importance for the safety, comfort, and efficiency of tall buildings and urban environments. Difficulty therefore typically arises in guiding massing and form decisions at early project stages due to the slow feedback from conventional CFD approaches, whilst this slow-and-accurate CFD simulation is better invested at later stages. It is therefore prudent to consider compromises in the speed-accuracy trade-off, sacrificing accuracy for speed, during these early stages so that many more design options can be explored. The need for application-specific simulation accuracy and speed that meets the demands of early design stages is proposed by Lu et al. (1991). They generate a range of reduced-order models of a combustion engine simulation, with varying accuracies and speed that can be used throughout the design process. The solution is posed as a Pareto front of non-dominated solutions, rather than a simpler trade-off curve based on biological decision making (Chittka et al., 2009).

Most approaches towards CFD approximation focus on simplification of the solver itself. For instance: simplified meshing routines; the use of lower-order discretisation; particle-based solvers; or the avoidance of turbulence models. These methods can be classed as type-one, *solver approximation*.

A typical example of this is the use of the 'Stable Fluids' fast fluid dynamics (FFD) solver developed by Stam (1999) for the computer graphics and games industry, which subsequently underwent some development for use in architectural practice (Chronis et al. 2011, 2012). Development and application for architectural design was motivated by three factors: a limited, low Reynolds number validation which suggested it as suitable for purposes beyond the scope of the validation (Zuo and Chen 2009, 2010); the qualitative appearance of accuracy for turbulent flows; and its remarkable speed. Zuo and Chen (2009) implemented the FFD with a zero-equation turbulence model but found that it performed worse since it was not designed or suited to the FFD approach. It should be noted, however, that with a lack of turbulence model, the solver relies on continuous interaction (such as game character movement) to compensate for numerical dissipation. The benefit is the availability of full fluid field data, although production of surface data is more difficult.

One other possible approach to this problem, type-two, is *solution approximation.* CFD originated in aeronautics and astronautics, as such there is a large quantity of work directed towards modelling and optimisation of airfoils, fuselages, and turbine blades. An optimisation routine will often generate large data sets of simulation data, from which knowledge of the problem can be extracted.

In one case, a large model set of turbine blades is used with a decision tree to analyse the relationship between point deformation of models and their change in surface pressure (Graening et al. 2008). Areas of high sensitivity can then be mapped onto a base geometry (pre-selected) and used to focus subsequent analysis. Ramanathan and

Graening (2009) extend this work further to incorporate an evolutionary optimisation process, so as to use the information extracted from previous cases to create non-random initial populations of solutions and to guide the evolution.

Another example of the solution approximation approach, this time applied to building design, is by Wilkinson et al. (2013). Predictions are made through training an ANN on shape features extracted from a set of evaluated procedural tall building models.

2.3. Interference

Interference refers to the increased or decreased effect that nearby buildings may have upon the wind behaviour of one another. Within an urban situation this is very common, and since the effects can be significant it is necessary to consider the context within the simulation. That is, independently designed buildings can not be treated in isolation. Along with the large research fields of bluff bodies and computational wind engineering, interference is also a significant area of study. Research on interference is especially concerned with creating generalised recommendations, a difficult issue due to the huge variation in potential scenarios.

A common misconception is that interference always reduces wind loads from the isolated case. Whilst this may be true for a uniformed array of similar buildings in close proximity, wind loads can be increased in the more complex, realistic case. The key factors in determining the effects of interference are the size, shape, and configuration of the buildings with respect to the direction of flow. The effects have been shown to be as great as up to 46% under-prediction and 525% over-prediction from regulatory loads on simple prismatic buildings (Stathopoulos 1984). An over-prediction of wind pressure is less dangerous than an under-prediction, since the latter may cause comfort or safety issues. Khanduri et al. (1998) present a thorough review of the full past and present state of interference. A summary of typical studies can be found in Table 1.

In all the cases shown in Table 1, simple cuboids were used with typical variables such as aspect ratio and position configuration. In other words, translating the objects over the two-dimensional horizontal plane. No studies have been performed which consider realistically complex shapes or contexts because the knowledge attained in evaluating them is typically esoteric and difficult to generalise.

A number of studies have, however, analysed the effects of a small number of adjacent structures, leading to the development of the *Interference Factor* (IF). This is a ratio between the wind loads with and without the interference from adjacent structures (see Table 1). In a few cases generalisation, or regression, has been attempted (the last three cases in Table 1) with the IF used as output response and basic scenario parameters as input features.

No.	Eval.	Variables	Source
2	WT	- Orientation - SD (x) - SD (y) - Aspect ratio	Agrawal et al. (2012)
2	WT + CFD	- Orientation	Zhang and Gu (2008)
2 & 3	WT	- Breadth ratio - Height ratio - Profile exponent - Configuration	Gu and Xie (2011), Xie and Gu (2004)
5	WT	- Orientation - Aspect ratio - Configuration	Jianguang (2008)
Multi.*	CFD	- Orientation - Configuration	Zhang et al. (2005)
No.	**Eval.**	**ANN Inputs**	**Source**
2	WT	- SD (x) - Profile exponent - Aspect ratio	English and Fricke (1999)
2	WT	- SD (x) - SD (y)	Khanduri et al. (1997)
2	WT	- Relative position - Profile exponent - Aspect ratio	Zhang and Zhang (2004)

Table 1: Summary of selected interference sensitivity studies (No. = Number of surrounding buildings in study, WT = Wind-Tunnel, SD = Separation Distance, x = along-wind, y = across-wind). * Multiple cuboids in a small number of configurations.

In these three cases, this method has been used along with a radial basis function (RBF) ANN. The IF was calculated from wind-tunnel data from new experiments or collected from existing literature. The limitations of this approach are the simplistic geometries (cuboids of a single height), basic configurations (typically two or three buildings), and lack of output data (only a single performance metric: the IF, rather than the varied surface pressure distribution). It should be noted that in nearly every case, the studies were constrained to a limited number of cuboids, a severe simplification in attempting to create generalised interference rules.

3. METHODOLOGY

The approach taken here is towards performance prediction of wind-induced surface pressure from shape analysis, developing previous work on morphological prediction (Wilkinson et al. 2013). It has previously been shown that it is possible, with a reasonable degree of accuracy and speed, to predict surface pressure for early-stage tall building design. The limitation of their work was that the models were treated in isolation without any urban context or interference: a simplification that is addressed in this section.

Considerable time and effort can be saved if it can be demonstrated that independent CFD simulations can be 'super-imposed' on one another with a reasonable accuracy. The end goal is to use a single, 'context-only' simulation, the *Obstruction Model* (*OM*), to make a limitless number of predictions for different designs, *Principal Models (PM*), using the fluid field data alone. The clear advantage of this is that the entire OM does not need to be re-run with every change of PM.

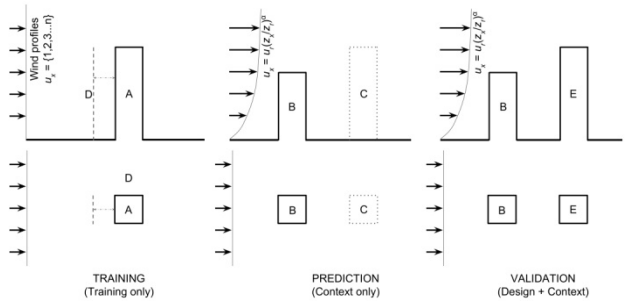

Figure 1: Local fluid features general method. (top) elevation view; (bottom) plan; (left) Training, A=Training model (in this case = PM), D=A projected upstream; (centre) Prediction, B=OM, C=Location of PM in field; (right) Validation, B=OM, E=PM.

The simulation of a complex urban wind environment without the PM is used as input feature for predictions on the PM in context. This is done by simulating the isolated PM under a variety of different wind speeds, and using the shape and fluid features to train an ANN and make predictions for the PM using the context-only model. The advantages of this method are in avoiding simulation of the full PM-in-context model and being able to use an existing context model to make predictions on a new PM. However, it is noted that in order to generalise this method to arbitrary PMs, a much greater training set would be required.

3.1. Simulation Methodology

The CFD solver used for the steady-state Reynolds-Averaged Navier-Stokes (RANS) simulations with a k-ε turbulence model is *ANSYS CFX 13.0*. Typically the models are meshed with roughly an equal number of cells (up to the maximum available computational resources), of around four million elements. The PM simulations, for the training set, therefore have a finer resolution than the OM used as the test case. The models themselves are created in GenerativeComponents (Bentley Systems).

The following simulation parameters were assigned: high-resolution advection and turbulence numerics; isothermal fluid at 25ºC; a scalable wall function; a convergence residual target of $1.0e^{-6}$ RMS; and a minimum mesh edge size of $0.3m$. With these parameters, the simulations take 30±10 minutes to converge to steady state. A transient large eddy simulation (LES) could alternatively be used instead of RANS to achieve more accurate and time-dependent surface pressures. However, due to time and resource limitations it was not possible to include a comparison in this study.

In both test cases, the wind speed is applied at an upstream inlet, with a reference speed (U_r) of $10ms^{-1}$ at a reference height (Z_r) of $10m$. The most commonly used distribution of mean wind speed with height is the 'power-law' expression:

$$U_x = U_r \, (Z_x / Z_r)^{\alpha}$$

The exponent α is an empirically derived coefficient that is dependent on the stability of the atmosphere. For neutral stability conditions it is approximately 0.143, and is appropriate for open surroundings, such as open water or landscapes (Hsu et al., 1994). In the training models a constant wind profile is used, albeit with varying speeds so as to generate a range of upstream wind speeds for every vertex.

3.2. Learning Methodology

In all cases, the learning process consists of a training set and a test set of features. For a training set, S^{Tr}, consisting of vertex feature vectors and simulated pressure extracted from the CFD, the ANN approximates the function $f^{ANN}: \boldsymbol{X} \rightarrow P$ where $\boldsymbol{X}$ is the vertex feature vector and P is the vertex pressure. $\boldsymbol{X}$ is defined as follows:

$$\boldsymbol{X} = [V_{upstream}, \boldsymbol{N}_{x,y,z}, \boldsymbol{N}\sigma^{1\text{-}5}_{x,y,z}, \boldsymbol{T}_{x,y,z}]$$

Where $V_{upstream}$ is the wind speed at the vertex's projected position upstream at a distance of $20m$ (approximately midway between PM and upstream OM), $N_{x,y,z}$ are the vertex normal components, $N\sigma^{1\text{-}5}_{x,y,z}$ are the vertex-ring (one through five) neighbourhood curvature (non-absolute) standard deviation components, and $T_{x,y,z}$ are the normalised vertex position within the model limits. For the test prediction, $V_{upstream}$ is replaced by V, the wind speed at the vertex's position on the PM but measured in the OM fluid field.

From the 15 training set models that have been evaluated with various wind speeds, a total of 210,000 vertex features are extracted (14,000 per model), from which 10,000 are randomly selected for training the model. This number is sufficient for convergence of the ANN. An ANN with a non-linear RBF activation function is used, with a network structure of 22:20:1, i.e. 22 inputs in the feature vector, X, 20 neurons in the hidden layer, and one output response, Y. The error is calculated as:

$$\%\ Diff. = (P_{prediction} - P_{simulation}) / (P_{simulation\ range}) * 100$$

The errors, or difference between the predicted and simulated model pressures, are reported as: the range's minimum and maximum; the mean of the absolute errors; and the standard deviation of the absolute errors (see Table 2). For both cases, a kernel density estimation is given which gives a continuous error density estimation. The smoothing kernels use a normal distribution and width of 0.1%.

4. RESULTS

There are two experimental cases: the first of simple geometric complexity, perhaps at the level of what may be found in the literature; and the second, of a real context and design case as might be found in practice.

4.1. Multiple Cuboid Context and Design

In the first case, five surrounding cubic buildings constitute the OM, with the PM at the centre. As training data, the PM is run independently with different wind speeds (1, 2, …, $15ms^{-1}$) without any wind profile. The shape and fluid features are extracted from each of these models and used in the training set. The OM is also run, and the fluid features extracted from the appropriate positions to use as test features. Finally, the surface pressures on the PM are extracted from the full model for validation. The geometric setup of the full design and context (validation) model is shown in Figure 2. Context buildings, OM, are labelled as A and design building, PM, as B.

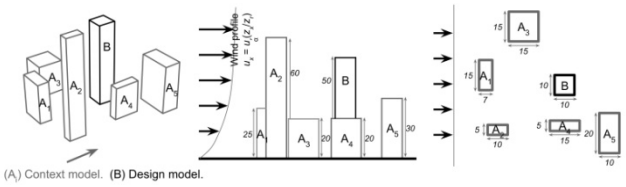

Figure 2: Case 1 – validation model setup: (left) perspective; (centre) elevation; and (right) plan views with respective wind profiles.

For each feature, or vertex, in the PM test case, the difference in pressure between the prediction and simulation is calculated. It is seen to converge with a mean absolute error of 6.73%, a standard deviation absolute of 4.02%, a maximum error of 33.76%, and a minimum of -26.37%. The distribution of prediction errors is shown by the kernel density estimation in Figure 3, giving a continuous error probability estimation (see Table 2 for percentiles).

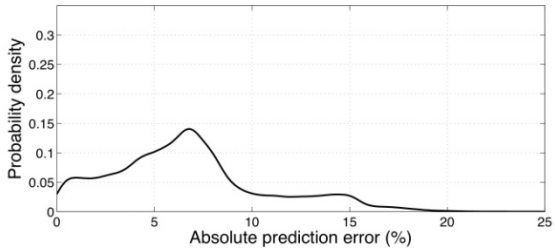

Figure 3: Case 1 – kernel density estimation of errors.

The difference between prediction and simulation is visualised in Figure 4: on the left is the surface pressure on the design model in the full context validation simulation; the centre is the predicted surface pressure; and on the right is the vertices' % pressure difference between the two.

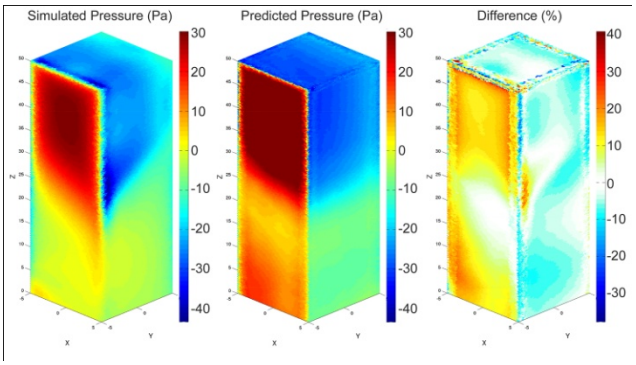

Figure 4: Case 1 – (left) simulation; (centre) prediction; (right) error.

Considering the complexity of the problem, this is a solid first step towards interference approximation in tall building design. The majority of the errors are less than 10 to 15% and the general pressure distribution is qualitatively correct, suggesting that the method has application in situations where accuracy can be compromised in order to facilitate rapid feedback.

4.2. Realistic Context and Design

In the second case, a realistic context model, the OM, of the dense City district in London, is used (Figure 5), along with a realistic design model, the PM (Figure 6). Both are put together for the validation model (Figure 7). The PM is relatively arbitrary, but is based on prior models generated at competition, massing, or form-finding project stages. The design model is 310m tall, as compared to the upstream Swiss Re (180m) and downstream Tower 42 (183m). The wind direction is shown in Figure 8.

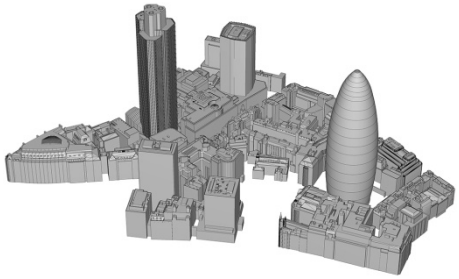

Figure 5: Case 2 – Context only model, OM, of the City, London. Raw geometry before simplification for meshing.

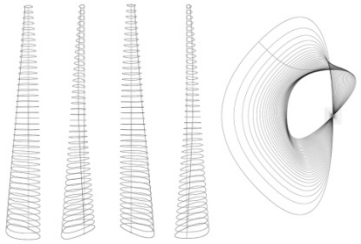

Figure 6: Case 2 – Design model, PM - wire-frame elevations and plan. Created in *GenerativeComponents*.

Figure 8 shows the test and validation CFD simulation results. Note that the lower image has the design model and the change in flow streamlines is visualised. It is also interesting to note that the addition of the new design model has effects on the entire flow field, upstream and downstream. It is evident that the use of a simple, global interference factor cannot do justice to the change in wind environment brought on by a new tall building.

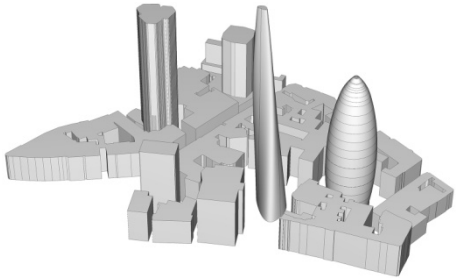

Figure 7: Case 2 – validation model setup. After simplification for meshing. Detail resolution greater than 1m.

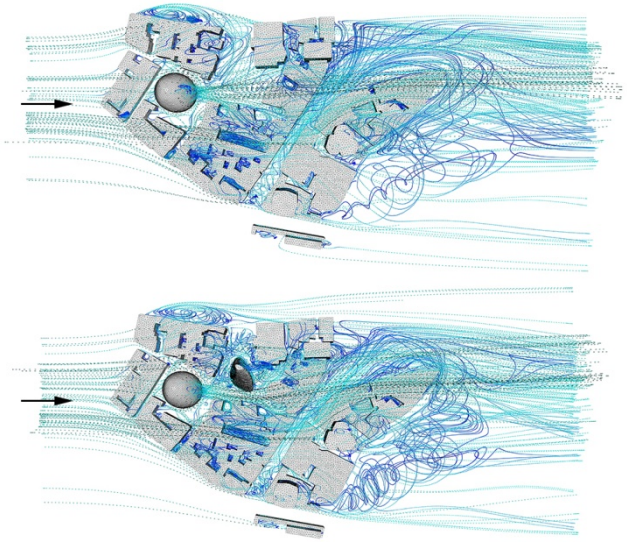

Figure 8: Case 2 – CFD simulation, streamline visualisation: (upper) context only for test data; (lower) context and design for validation.

The errors converge to a mean absolute of 5.80%, with a standard deviation of 9.01%, a maximum error of 11.99%, and a minimum of -55.71%. The distribution of prediction errors is shown by the kernel density estimation in Figure 9, giving a continuous distribution.

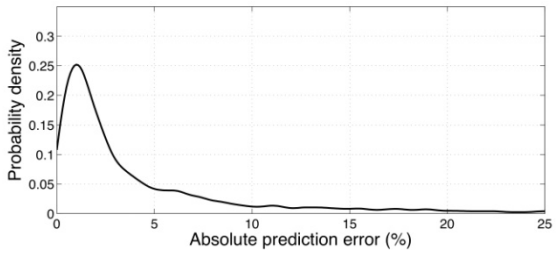

Figure 9: Case 2 – kernel density estimation of errors.

Figures 10 and 11 visualise the predicted surface pressures on the design model within the full context. The top image is the CFD simulation, the centre the ANN

prediction, and the lower the % difference between the simulated and predicted pressures.

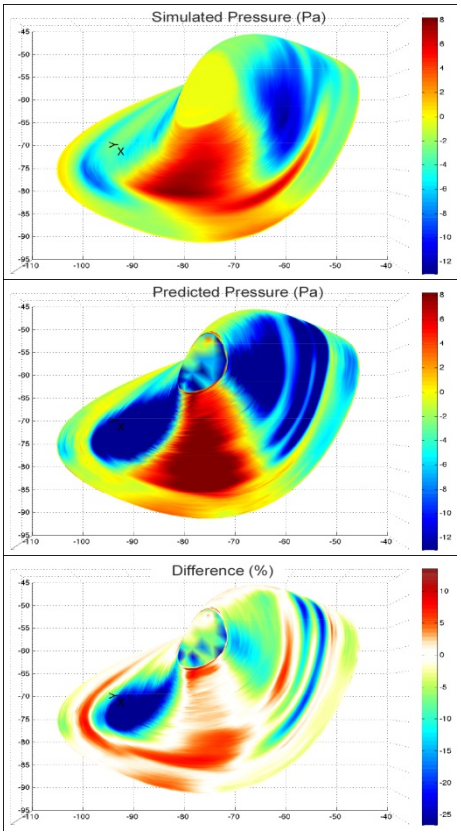

Figure 10: Case 2 – Design model in full context, plan view. (upper) simulation; (centre) prediction; (lower) error.

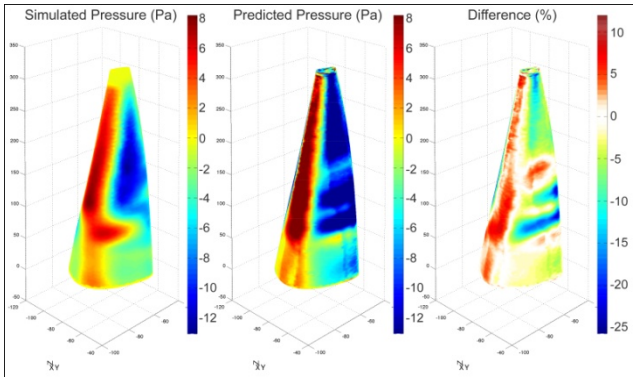

Figure 11: Case 2 – Design model in full context. (left) simulation; (centre) prediction; (right) error.

5. DISCUSSION

Compared to solver approximation techniques, such as the FFD solver and other low accuracy simulations, this solution approximation has the benefit of being based on a widely-used, validated CFD solver. In fact, it may be feasible to use a solver of any accuracy (such as LES or DNS, where the time improvements will be even greater). The comparative disadvantage is that the FFD can produce field rather than surface data, which is useful for identifying flow patterns, assessing pedestrian comfort, and gauging the secondary downstream effects that a new building will have on others.

These developments represent an alternative approach that is fundamentally different to previous attempts at interference generalisation found in the literature. The use of local features rather than global parameters allows for arbitrary complexity in the obstruction model and for vertex surface pressure visualisation rather than the global interference factor.

5.1. Response Times versus Accuracy

The errors are summarised in Table 2, and the process times for both cases and for the conventional and new approaches are given in Tables 3 and 4 respectively. Whilst the response times for the new method are approximately seven (case 1) and three (case 2) times greater than the conventional method, the true benefits are with repeatability. Therefore, in separating out the processes into front-end and back-end, the new method becomes 215 (case 1) and 510 (case 2) times faster.

6. CONCLUSION

The methodology and results presented here demonstrate an alternative approach to urban wind interference approximation for tall building design. Through the two cases it is demonstrated that significant improvements in response time (215 and 510 times faster when comparing front-end prediction times with conventional CFD) can be made with a reasonable trade-off in accuracy (mean absolute errors of 5.8 to 6.7%). Further improvements and generalisation can be made through the use of a procedural model to generate the training shape features, as well as through further testing on alternative models and optimisation of the training and test features.

	Case 1	Case 2
Min. / Max. range (%) *	-26.37 / 33.76	-55.71 / 11.99
Mean absolute (%)	6.73	5.80
Standard deviation absolute (%)	4.02	9.01

Table 2: Error summary. (* worst case vertex prediction)

	Time (s)	
Process	**Case 1**	**Case 2**
PM + OM simulation	4523	10709
Total	*4523*	*10709*

Table 3: Conventional CFD response times.

	Time (s)	
Back-end Processes (One-off)	**Case 1**	**Case 2**
PM simulations (15no.)	28535	22755
OM simulation	3793	10080
Feature extraction	300	300
ANN training	180	180
Total	*32808*	*33315*
Front-end Processes (Repeatable)	**Case 1**	**Case 2**
PM feature extraction	20	20
PM prediction	1	1
Total	*21*	*21*

Table 4: Proposed methodology response times.

Acknowledgements

This work was sponsored by the Engineering and Physical Sciences Research Council (EPSRC), Bentley Systems Incorporated, and PLP Architecture.

References

AGRAWAL, N., MITTAL, A.K. AND GUPTA, V.K. 2012. Along-Wind Interference Effects on Tall Buildings. In National Conference on Wind Engineering, India. pp. 193–204.

CHITTKA, L., SKORUPSKO, P. AND RAINE, N.E. 2009. Speed-Accuracy Tradeoffs in Animal Decision Making. *Trends in Ecology and Evolution*, 24(7), pp.400–7.

CHRONIS, A., TURNER, A. AND TSIGKARI, M. 2011. Generative Fluid Dynamics: Integration of Fast Fluid Dynamics and Genetic Algorithms for wind loading optimization of a free form surface. In SimAud 2011. pp. 79–86.

CHRONIS, A., TSIGKARI, M., DAVID, A. AND AISH, F. 2012. Design Systems, Ecology and Time. In ACADIA conference proceedings.

ENGLISH, E.C. AND FRICKE, F.R. 1999. The Interference Index and its Prediction using a Neural Network Analysis of Wind-Tunnel Data. JWEIA, 83, pp.567–575.

GRAENING, L., MENZEL, S., HASENJAGER, M., BIHRER, T., OLHOFER, M. AND SENDHOFF, B. 2008. Knowledge Extraction from Aerodynamic Design Data and its Application to 3D Turbine Blade Geometries. Journal of Mathematical Modelling and Algorithms, 7(4), pp.329–350.

GU, M. AND XIE, Z.-N. 2011. Interference Effects of Two and Three Super-Tall Buildings Under Wind Action. Acta Mechanica Sinica, 27(5), pp.687–696.

HSU, S.A., MEINDL, E.A. AND GILHOUSEN, D.B. 1994. Determining the Power-Law Wind-Profile Exponent under Near-Neutral Stability Conditions at Sea. *Journal of Applied Meteorology*, 33(6), pp.757-772.

JIANGUANG, Z. 2008. Interference Effects on Wind Loading of a Group of Tall Buildings in Close Proximity. The University of Hong Kong.

KHANDURI, A.C., BEDARD, C. AND STATHOPOULOS, T. 1997. Modelling Wind-Induced Interference Effects using Back-Propagation Neural Networks. JWEIA, 72, pp.71–79.

KHANDURI, A.C., STATHOPOULOS, T. AND BEDARD, C. 1998. Wind-Induced Interference Effects on Buildings - A Review of the State-of-the-Art. Engineering Structures, 20(7), pp.617–630.

LU, S.C.-Y., TCHENG, D.K. AND YERRAMAREDDY, S. 1991. Integration of Simulation, Learning and Optimization to Support Engineering Design. *Annals of the CIRP,* 40(1), pp.143–146.

MALKAWI, A.M. 2004. Developments in Environmental Performance Simulation. *Automation in Construction*, 13(4), pp.437–445.

RAMANATHAN, S. AND GRAENING, L. 2009. Knowledge Incorporation into Evolutionary Algorithms to Speed up Aerodynamic Design Optimizations. Universitat Stuttgart.

STAM, J. 1999. Stable Fluids. Proceedings of the 26th annual conference on Computer graphics and interactive techniques.

STATHOPOULOS, T. 1984. Adverse Wind Loads on Low Buildings Due to Buffeting. Journal of Structural Engineering, 110(10), 2374–2392.

WILKINSON, S., HANNA, S., HESSELGREN, L. AND MUELLER, V. 2013. Inductive Aerodynamics. In: STOUFFS, R. and SARIYILDIZ, S., (eds.) Proceedings of eCAADe 2013: Computation and Performance.

XIE, Z.-N. AND GU, M. 2004. Mean Interference Effects among Tall Buildings. Engineering Structures, 26(9), pp.1173–1183.

ZHANG, A., GAO, C. AND ZHANG, L. 2005. Numerical Simulation of the Wind Field around Different Building Arrangements. JWEIA, 93(12), pp.891–904.

ZHANG, A. AND GU, M. 2008. Wind Tunnel Tests and Numerical Simulations of Wind Pressures on Buildings in Staggered Arrangement. JWEIA, 96(10-11), pp.2067–2079.

ZHANG, A. AND ZHANG, L. 2004. RBF Neural Networks for the Prediction of Building Interference Effects. Computers & Structures, 82(27), pp.2333–2339.

ZUO, W. AND CHEN, Q. 2009. Real-Time or Faster-than-Real-Time Simulation of Airflow in Buildings. Indoor Air, 19(1), pp.33–44.

ZUO, W. AND CHEN, Q. 2010. Fast and Informative Flow Simulations in a Building by using Fast Fluid Dynamics Model on Graphics Processing Unit. Building and Environment, 45(3), pp.747–757.

Session 8: Learning from Buildings **151**

Comparison of Control Strategies for Energy Efficient Building HVAC Systems 153
Mehdi Maasoumy, Alberto Sangiovanni Vincentelli
Dept. of Mechanical Engineering, University of California, Berkeley; Department of Electrical Engineering and Computer Science, University of California, Berkeley.

Causality in Hospital Simulation Based on Utilization Chains 161
Gabriel Wurzer, Wolfgang E. Lorenz
Vienna University of Technology.

Full-Automated Acquisition System for Occupancy and Energy Measurement Data Extraction 165
Dimosthenis Ioannidis, Stelios Krinidis, Georgios Stavropoulos, Dimmitrios Tzovaras, Spiridon Likothanassis
Information Technologies Institute, Centre for Research & Technology Hellas; Pattern Recognition Laboratory, Computer Engineering and Informatics,, University of Patras.

Comparison of Control Strategies for Energy Efficient Building HVAC Systems

Mehdi Maasoumy
Department of Mechanical Engineering
University of California
Berkeley CA, 94720, USA
mehdi@me.berkeley.edu

Alberto Sangiovanni Vincentelli
Department of Electrical Engineering and Computer Science
University of California
Berkeley CA, 94720, USA
alberto@eecs.berkeley.edu

Keywords: Model predictive control, energy-efficient buildings, embedded platform.

Abstract

A framework for the design and simulation of a building envelope and an HVAC system is used to compare advanced control algorithms in terms of energy efficiency, thermal comfort, and computational complexity. Building models are first captured in Modelica [1] to leverage Modelica's rich building component library and then imported into Simulink [15] to exploit Simulink's strong control design environment. Four controllers with different computational complexity are considered and compared: a proportional (P) controller with time varying temperature bounds, a tracking linear quadratic regulator (LQR) controller with time varying tuning parameters, a tracking disturbance-aware linear quadratic regulator (d-LQR) controller with time varying tuning parameters which incorporates predictive disturbance information and a model predictive controller (MPC). We assess the performance of these controllers using two defined criteria, i.e. *energy* and *discomfort* measured with appropriate metrics. We show that the d-LQR and MPC, when compared to the P controller, manage to reduce energy by 41.2% and 46% respectively, and discomfort from 3.8 to 0. While d-LQR and MPC have similar performance with respect to energy and discomfort, simulation time in the case of d-LQR is significantly less than the one of MPC.

1. INTRODUCTION

We present an approach to optimize the energy efficiency of HVAC systems by designing smart controllers with full integration of several factors such as system dynamics, weather predictions, and occupancy schedules, with attention paid to the needed computational power of the embedded platform.

We leverage a number of previous results: A physics-based building model is proposed in [7, 9–12, 16]. A hierarchical control architecture is utilized and simulation results are compared with the ones obtained with a flat architecture. [18] lays out a simple model predictive control (MPC) formulation for building temperature control and presents the advantages and disadvantages of model predictive control when applied to building air temperature regulation. [3] uses a reduced-order model of the airflow in buildings and derive an optimal control law in closed form for rejecting a known disturbance while minimizing a quadratic cost.

In this paper, we build upon [13, 19], where we presented a building automation and control system, and the co-design of control algorithm and embedded platform with focus on sensing system accuracy. In this paper, we extend the co-design framework to include computational complexity of the control algorithm. Hence, we analyze the computational complexity of four control algorithms along with their performance in terms of energy and comfort metrics. We compare the performance of the following controllers: a proportional controller, a linear quadratic regulator (LQR), a disturbance-aware linear quadratic regulator (d-LQR), all suitable for platforms with limited computational power, and MPC, a computationally demanding control algorithm, which requires online computation of control policy through solving optimization problems [11, 12].

Our flow is as follows:

1) Modeling: We first model the building HVAC system and envelope in Modelica [1][1]. Building models are usually highly nonlinear. To automatically derive the mathematical model of the building for control purposes, we use Modelica's features to obtain the linearized systems about the operating point of the system. This model is then imported into Simulink that is particularly suited for simulation and control design.

2) Control Design: We design the control strategy using MATLAB and implement it using MATLAB/Simulink. The plant model (originally in Modelica) and the control algorithm (in MATLAB) are co-simulated using the MATLAB (Simulink) simulation environment. We adapted four controllers to the HVAC problem: a simple P controller, an LQR, a modified d-LQR, and an MPC. In particular, we modified the tracking LQR presented in [10] by using time-varying tuning parameters (matrices) reflecting different temperature bounds at

[1]The building library developed by LBNL [17] can also be used in our framework for a more detailed modeling of the system.

different times of the day. We also modified the LQR controller, called d-LQR, by using the a-priori knowledge of the disturbance data. The performance of the four controllers is compared and contrasted.

The paper is organized as follows. Section 2. introduces a mathematical model for building. Section 3. describes the four different control algorithms that have been used. It presents the derivation of the closed-form solution to the tracking LQR and d-LQR problems and lays out the formulation for MPC. Finally, Section 4. shows results obtained from simulations and discusses the performance and computational characteristics of the four controllers. Conclusions are drawn in Section 5..

2. MATHEMATICAL MODELING

In this paper, we use the model that was proposed in [10, 14] in which the building is considered as a network. There are two types of nodes in the network: walls and rooms. There are in total n nodes, m of which represent rooms and the remaining $n-m$ nodes represent walls. Temperature dynamics of the i-th wall is governed by the following equation:

$$C_{w_i}\frac{dT_{w_i}}{dt} = \sum_{j\in\mathcal{N}_{w_i}} \frac{T_j - T_{w_i}}{R'_{ij}} + r_i\alpha_i A_i q''_{rad_i} \qquad (1)$$

Where T_{w_i}, C_{w_i}, α_i and A_i are the temperature, heat capacity, absorption coefficient and area of wall i, respectively. R'_{ij} is the total resistance between wall i and node j. q''_{rad_i} is the radiative heat flux density on wall i. $\mathcal{N}_{w_i}$ is the set of all of neighboring nodes to node w_i and, r_i is equal to 0 for internal walls, and to 1 for peripheral walls.

The temperature of the i-th room is governed by the following equation:

$$C_{r_i}\frac{dT_{r_i}}{dt} = \sum_{j\in\mathcal{N}_{r_i}} \frac{T_j - T_{r_i}}{R'_{ij}} + \dot{m}_{r_i}c_p(T_{s_i} - T_{r_i}) + w_i\tau_{w_i}A_{w_i}q''_{rad_i} + \dot{q}_{int} \qquad (2)$$

Where T_{r_i}, C_{r_i} and $\dot{m}_{r_i}$ are the temperature, heat capacity and air mass flow into room i, respectively. c_a is the specific heat capacity of air, A_{w_i} is the total area of window on walls surrounding room i, τ_{w_i} is the transmissivity of glass of window i, q''_{rad_i} is the radiative heat flux density radiated to node i and $\dot{q}_{int_1}$ is the internal heat generation in thermal zone i. $\mathcal{N}_{r_i}$ is the set of all of the neighboring nodes to room i and, w_i is equal to 0 if none of the walls surrounding room i has window, and is equal to 1 if at least one of them has.

A detailed model of building envelope and HVAC system is captured in Modelica with the air mass flow into each thermal zone as inputs, and the temperature of each thermal zone and temperature of walls as outputs. This plant is imported into Simulink using the Dymola[2]-Simulink interface.

[2]Dymola is a commercial simulation environment for Modelica

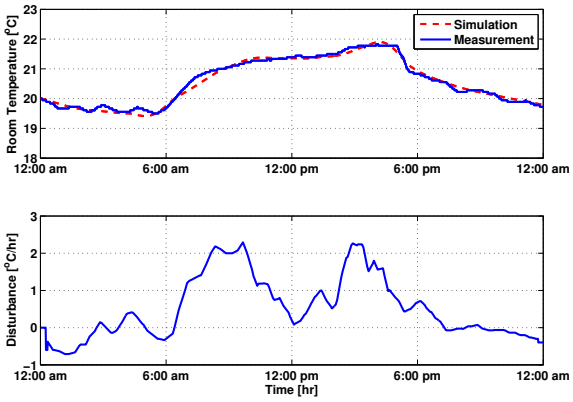

Figure 1. Validation of the proposed model against historical data. We concurrently estimate the model parameters and the unmodeled dynamics using parameterization of the unmodeled dynamics based on the measured data. Details can be found in [12].

The entire plant is imported into Simulink by using first the C-generation capability of Dymola and then encapsulating the code so generated into a DymolaBlock. The DymolaBlock is a wrapper around an S-function MEX block.

We capture the model obtained from (1), and (2) for a three-room model in Modelica. The model has been validated against historical data. The validation result is shown in Fig. 1.

3. CONTROLLER DESIGN

We implemented *a P controller, a tracking LQR, a tracking LQR with disturbance knowledge (d-LQR), and a model predictive controller (MPC).*

In general, a *P* controller is the least computationally complex, as the control input in this case is proportional to a temperature offset. LQR is more computationally complex than *P*, as it involves matrix multiplication and inversion. However, a closed form solution can be derived for the optimal control policy. *P* easily handles a large number of states. LQR with disturbance knowledge (d-LQR) makes use of the available predictive knowledge to enhance the control input to reject disturbances in a smarter fashion than LQR. The computational complexity of this controller is similar to that of LQR. MPC is the most computationally complex algorithm but it yields a solution that always meets the state and input constraints optimally as defined by the cost function.

We use system dynamics that is linearized about the equilibrium point of the system. Note that since the range of thermal zone temperature is small (usually 20 - 22 ° C). The four controllers adapted for the building problem are described as follows:

3.1. P Control

The proportional controller used in this paper is given by the following equations:

$$u_k = \begin{cases} K_p[\overline{T}_k - T(k)] & \text{if } T(k) > \overline{T}_k \\ 0 & \text{if } \underline{T}_k < T(K) < \overline{T}_k \\ K_p[\underline{T}_k - T(k)] & \text{if } T(k) < \underline{T}_k \end{cases} \quad (3)$$

Where K_p is the proportional gain of the controller which should be chosen for best performance. Note that we only consider this controller as a basis against which to compare the performance of other controllers.

3.2. Tracking LQR

We implemented a tracking LQR controller with time-varying tuning matrices on the plant model. Consider the plant model given by

$$x_{k+1} = Ax_k + Bu_k \quad (4)$$
$$y_k = Cx_k \quad (5)$$

Where the state vector $x_k \in \mathbb{R}^n$ at time $t = k$ contains the temperatures of all the nodes in the thermal network of the building: $x_k = [T_{w_1}(k) \ \cdots \ T_{w_p}(k) \ T_{r_1}(k) \ \cdots \ T_{r_m}(k)]$. Where p is the number of walls, m is the number of rooms, and $p+m=n$. The vector $u_k \in \mathbb{R}^m$ is the input at time k, $u_k = [\dot{m}_1(k) \quad \cdots \quad \dot{m}_m(k)]$. Vector y_k^d is the desired output trajectory (i.e. desired temperature for each room), specified for all $k = 1, 2, \cdots, N$ and $U_k := [u_k \quad u_{k+1} \quad \cdots \quad u_{N-1}]$. The LQR tracking problem is formulated as follows:

$$\min_{U_0} \frac{1}{2}(y_N^d - y_N)^T \mathbf{Q_N}(y_N^d - y_N) + \frac{1}{2}\sum_{k=0}^{N-1}\left((y_k^d - y_k)^T \mathbf{Q_k}(y_k^d - y_k) + u_k^T \mathbf{R_k} u_k\right) \quad (6)$$

The solution to the LQR problem is the optimal control input of a linear system according to a quadratic cost function of the states and the inputs, hence the name LQR. The offset from the desired trajectory and the inputs are penalized with weight matrices called $\mathbf{Q_k}$ and $\mathbf{R_k}$ at each time k, respectively.

$$\mathbf{Q_k} = \mathbf{diag}\ [q_k^1,\ q_k^2,\ ...,\ q_k^m] \quad (7)$$
$$\mathbf{R_k} = \mathbf{diag}\ [r_k^1,\ r_k^2,\ ...,\ r_k^m] \quad (8)$$

Where the superscript i refers to the room i in the building and the subscripts k implies the k^{th} time step.

Assumption 1: We assume that the matrices $\mathbf{Q_k}$ are positive semidefinite and symmetric and the matrices $\mathbf{R_k}$ are positive definite and symmetric. This translates to $q_j^i \geq 0 \ \ \forall i, j$ and $r_j^i > 0 \ \ \forall i, j$. Note that the symmetry assumption is fulfilled by the diagonal structure of these matrices.

The controller can be tuned by varying the weight matrices according to the occupancy schedules. Using *Bellman's principle of optimality*, a recursive relation can be obtained. The resulting optimization problem can be solved by *dynamic programming* backwards in time to determine the optimal control law. In [14] the optimal control law was shown to be as follows:

$$u_k^o = F_k - K_k x_k \quad (9)$$
$$K_k = [\mathbf{R_k} + B^T P_{k+1} B]^{-1} B^T P_{k+1} A \quad (10)$$
$$F_k = -[\mathbf{R_k} + B^T P_{k+1} B]^{-1} B^T b_{k+1} \quad (11)$$

Where P_k and b_k can be calculated backwards in time using

$$P_{k-1} = A^T P_k A - A^T P_k B[\mathbf{R_{k-1}} + B^T P_k B]^{-1} B^T P_k A + C^T \mathbf{Q_{k-1}} C \quad (12)$$
$$b_{k-1} = -A^T P_k B[\mathbf{R_{k-1}} + B^T P_k B]^{-1} B^T b_k - C^T \mathbf{Q_{k-1}} y_{k-1}^d + A^T b_k \quad (13)$$

with the terminal conditions being $P_N = C^T \mathbf{Q_N} C$ and $b_N = -C^T \mathbf{Q_N} y_N^d$. Note that K_k can be regarded as the feedback gain and F_k as the feed-forward gain [4].

3.3. Tracking d-LQR

The difference of LQR and d-LQR is that d-LQR integrates the predictive disturbance knowledge to enhance the performance of the LQR. The classic LQR problem solution can be found in the literature [5]. The solution to the non-homogeneous discrete time d-LQR was developed recently [3] using Lagrange multipliers for the state dynamics as constraints and then solving the problem using the Karush-Kuhn-Tucker (KKT) optimality conditions. Here we derive the same solution using a different method, namely *dynamic programming*. Assume the plant model given by (14) where d_k is the disturbance to the system at time $t = k$.

$$x_{k+1} = Ax_k + Bu_k + E\mathbf{d_k}$$
$$y_k = Cx_k \quad (14)$$

We consider the same cost function (6). We use dynamic programming to solve for the solution of this problem. The optimal control is given by

$$u_k^o = F_k - K_k x_k \quad (15)$$
$$K_k = [\mathbf{R_k} + B^T P_{k+1} B]^{-1} B^T P_{k+1} A \quad (16)$$
$$F_k = -[\mathbf{R_k} + B^T P_{k+1} B]^{-1} B^T (b_{k+1} + P_{k+1} E\mathbf{d_k}) \quad (17)$$

Where P_k and b_k can be calculated backwards in time using

$$P_{k-1} = A^T P_k A - A^T P_k B[\mathbf{R_{k-1}} + B^T P_k B]^{-1} B^T P_k A + C^T \mathbf{Q_{k-1}} C \quad (18)$$
$$b_{k-1} = -A^T P_k B[\mathbf{R_{k-1}} + B^T P_k B]^{-1} B^T (b_k + P_k E\mathbf{d_{k-1}}) - C^T \mathbf{Q_{k-1}} y_{k-1}^d + A^T (b_k + P_k E\mathbf{d_{k-1}}) \quad (19)$$

with the terminal conditions being $P_N = C^T \mathbf{Q_N} C$ and $b_N = -C^T \mathbf{Q_N} y_N^d$. Note the appearance of disturbances in the update

equation for b_{k-1}. The solution to the problem developed here agrees with the solution developed by [3] using a different method.

Note that the boundedness of the Riccati equation solution of the homogeneous LQR problem, and the asymptotic stability of the resulting closed-loop system is guaranteed [6].

3.4. Model Predictive Control

A model predictive control problem is formulated with the objective of minimizing a cost function which is a linear combination of the total cooling and heating power consumption and the peak of air flow and temperature-bound violation at each time subject to system dynamics and constraints. The predictive controller solves at each time step t the following problem

MPC Algorithm:

$$\min_{U_t,\bar{\varepsilon},\underline{\varepsilon}} \quad \{||\mathbf{U_t}||_1 + c_1||\mathbf{U_t}||_\infty + c_2(||\bar{\varepsilon}_\mathbf{t}||_1 + ||\underline{\varepsilon}_\mathbf{t}||_1)\}$$

subject to:

$$x_{t+k+1|t} = Ax_{t+k|t} + Bu_{t+k|t} + Ed_{t+k|t} \quad (20a)$$

$$y_{t+k|t} = Cx_{t+k|t} \quad (20b)$$

$$\underline{T}_{t+k|t} - \underline{\varepsilon}_{t+k|t} \leq y_{t+k|t} \leq \overline{T}_{t+k|t} + \bar{\varepsilon}_{t+k|t} \quad (20c)$$

$$u_{t+k|t} \leq \overline{u} \quad (20d)$$

$$\underline{\varepsilon}_{t+k|t},\ \bar{\varepsilon}_{t+k|t} \geq 0 \quad (20e)$$

where $\mathbf{U_t} = [u_{t|t}, u_{t+1|t}, \cdots, u_{t+N-1|t}]$ is the vector of control inputs, $\underline{\varepsilon}_\mathbf{t} = [\underline{\varepsilon}_{t+1|t}, \cdots, \underline{\varepsilon}_{t+N|t}]$ is the temperature violations from the lower bound, $\bar{\varepsilon}_\mathbf{t}$ the temperature violation from the upper bound, $y_{t+k|t}$ is the thermal zone temperatures, $d_{t+k|t}$ is the load prediction, and $\underline{T}_{.|t}$ and $\overline{T}_{.|t}$ are the lower and upper bounds on the zone temperature, respectively. $\overline{u}$ is the upper bound on the input air flow. c_2 is the penalty on the comfort constraint violations, and c_1 is the penalty on peak power consumption. Note that constraints (20a), and (20d) should hold for $k = 0, 1, ..., N-1$ and constraints (20b), (20c), and (20e) should hold for $k = 1, 2, ..., N$.

At each time step only the first entry of $\mathbf{U_t}$ is implemented on the plant. At the next time step the prediction horizon N is shifted leading to a new optimization problem. This process is repeated over and over until the total time span of interest is covered. The prediction horizon is $N = 24$. We used YALMIP [8] to formulate the MPC problem in MATLAB, and used IBM CPLEX [2] to solve the resulting optimization problem.

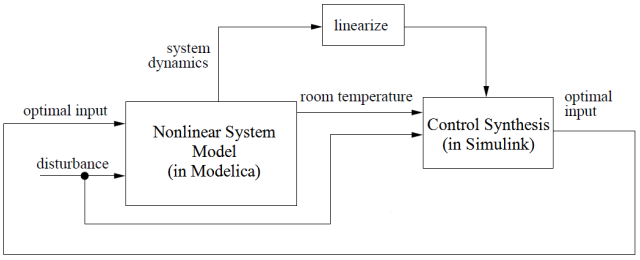

Figure 2. Schematic of the closed loop system including the nonlinear system model in *Modelica* and the control implementation in *Simulink*.

4. SIMULATION RESULTS

4.1. Simulating Heterogeneous Models

To verify the performance of the controllers, we simulated the combination of controller and plant (Fig. 2). We argued that modeling the plant in Modelica has several advantages while the design and implementation of the controller is best done in Simulink. There are two strategies to simulate the composed system:

- *Hosted Simulation* where either the Modelica model is imported into the Simulink input language and simulation occurs in Simulink or the Modelica model is imported into the Simulink environment and simulation occurs in Modelica.
- *Co-simulation.* where the two components are evaluated during simulation each in its own simulation environment (for Modelica, the simulation environment we chose is Dymola). In this case, a "master" is needed that orchestrates the actions of the two simulators while simulation progresses. Commercial co-simulation platforms have been developed to act as the "master", for example, EXITE, Silver and TISC [1]. EXITE, for instance, provides interfaces to Dymola, Simulink, ASCET, Rhapsody, ARTISAN Studio and C/C++. During co-simulation all models stay in their simulation environment and EXITE implements the communication among them via dedicated communication blocks.

Simulink has a feature (the S-Function C-Mex mechanism) that can be used to deal with models described in Dymola if the models are expressed in terms of input and output signals (Modelica has also the capability of capturing models in equation form where inputs and outputs are not explicitly identified, a feature that is not available in Simulink). The models can be imported into Simulink as an S-Function C-Mex file.

There are two mechanisms that can be used to perform simulation in the Dymola environment:

- *In-line Integration*. The simulation engine is Simulink. In this option, the user has to select a particular integra-

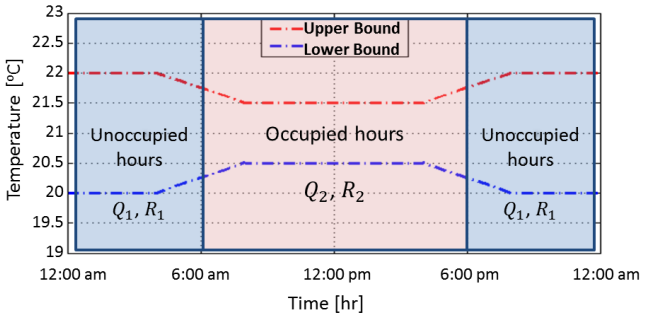

Figure 3. Temperature bounds for occupied and unoccupied hours.

tion method that is used by Dymola (e.g., *explicit/implicit Euler, trapezoidal method, explicit/implicit Runge Kutta*) to generate "C"-code that is then managed by the Simulink simulation engine.

- *In-line integration method not used*. The generated "C" code includes variable declarations and a call to the Dymola environment to evaluate the model. In this case, Simulink acts as the master.

For some integration methods such as *Explicit Euler*, the output diverges (this is to be expected because of the limited absolute stability region of this method), while no divergence is observed in the case of *No in-line integration* since the integration methods are dictated by the two tools that use robust numerical integration methods. Hence, we use "No in-line integration" for the simulations presented in this paper.

4.2. Comparing Controllers

We compare now the four different controllers described in Section (3.). The comfort zone is defined to be the space between the lower and upper temperature bounds as shown in Fig. (3).

For the disturbance model we assume that the disturbance load from the outside weather to the building is a sinusoidal load which is negative at night and positive during the day. We also assume an additive load due to a high density of occupants (e.g. a meeting) in the considered room from 11 am to 1 pm. The cumulative effect of both disturbances is shown in Fig. (4)

To be consistent and fair to all controllers we used a sampling time of one hour for all cases. In order to be fair for evaluation of the energy savings, we kept running simulations until we experienced a difference of less than 0.2 °C between the room temperature at the start time of one day (12am) and the end time of the same day (12am next day).

4.2.1. P Control

P control logic is given by (3).

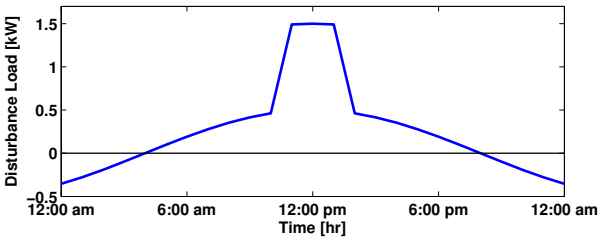

Figure 4. Aggregate effect of disturbance from outside weather and internal loads.

4.2.2. Tracking LQR

In this case we have considered the desired temperature, y_k^d to be a constant temperature of 21^oC. We consider time varying tuning parameters $\mathbf{Q_k}$ and $\mathbf{R_k}$ to reflect the occupancy schedule knowledge in the LQR control derivation.

We exploit the following strategy for tuning the weight matrices which reflects the temperature constraints at each time $t = k$:

$$\mathbf{Q_k} = \begin{cases} \mathbf{Q_1} & \text{if } 12am \le k \le 4am \\ \mathbf{Q_1} + \frac{(\mathbf{Q_2}-\mathbf{Q_1})*[k-4]}{4} & \text{if } 4am \le k \le 8am \\ \mathbf{Q_2} & \text{if } 8am \le k \le 4pm \\ \mathbf{Q_2} + \frac{(\mathbf{Q_1}-\mathbf{Q_2})*[k-4]}{4} & \text{if } 4pm \le k \le 8pm \\ \mathbf{Q_1} & \text{if } 8pm \le k \le 12am \end{cases} \quad (21)$$

Where $\mathbf{Q_1}$ and $\mathbf{Q_2}$ are the weight matrices corresponding to *unoccupied* and *occupied* hours, respectively, as shown in Fig. 3. The same strategy can be defined for $\mathbf{R_k}$ as well. In this case the disturbance knowledge is not used in the control derivation.

4.2.3. Tracking d-LQR

In this case we also assume a constant temperature of 21^oC as the desired temperature and pick the tuning parameters of $\mathbf{Q_k}$ and $\mathbf{R_k}$ based on the same strategy as (21). The difference of this case with case 1 is that the disturbance knowledge is used in the control derivation for a better tracking and disturbance rejection.

4.2.4. MPC

We have considered an MPC with soft constraints on the room temperature. However, to have a fair comparison among different controllers, we choose a large value for c_2 to force the temperature to stay within the upper and lower bounds (i.e comfort zone).

The results are shown in Fig. (5). A quantitative comparison of different controllers is depicted in Fig. (6). The controller parameters and the simulation time for each is provided in Table (1).

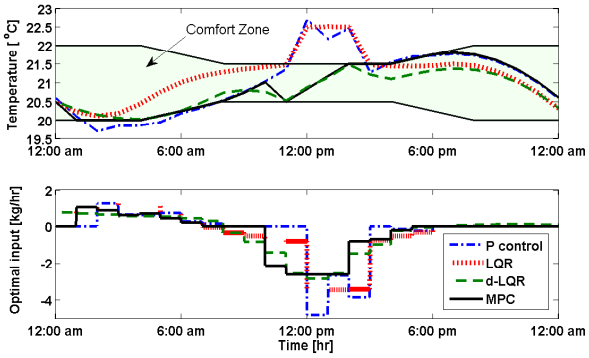

Figure 5. Temperature and optimal input for four different controllers.

4.3. Control Performance Comparison

To compare the overall performance of the proposed controllers we define two metrics to measure the energy consumption and comfort level provided by each controller. The energy metric is defined as:

$$I_e = \int_{t=0}^{24} [P_c(t) + P_h(t) + P_f(t)]\, dt \tag{22}$$

Where cooling power P_c, heating power P_h and fan power P_f are defined as

$$P_c(t) = \dot{m}_c(t) c_p [T_{out}(t) - T_c(t)] \tag{23}$$
$$P_h(t) = \dot{m}_h(t) c_p [T_h(t) - T_{out}(t)] \tag{24}$$
$$P_f(t) = \alpha \dot{m}^3(t) \tag{25}$$

The discomfort metric is defined as the sum of all the temperature violations during the course of a day.

$$I_d = \int_{t=0}^{24} \left[\min\left(|T(t) - \overline{T}(t)|, |T(t) - \underline{T}(t)| \right) . \mathbf{1}_{\mathcal{B}(t)^c}(T(t)) \right] dt$$

Where $\mathcal{B}(t) = [\underline{T}(t), \overline{T}(t)]$ is the allowable temperature boundary at time t and $\mathbf{1}$ is the indicator function.

Remark 1. As shown in the lower plot of Fig (5) the control input for the d-LQR is more similar to the MPC control input rather than to the LQR. On the other hand, the control input of the LQR is comparable to the one from P control.

Remark 2. The d-LQR and MPC use the disturbance knowledge to *pre-cool* the space several hours before the disturbance load hits as opposed to the LQR and P control which only react to the disturbance load instantaneously. The utilization of the disturbance knowledge results in a lower peak air flow demand and full satisfaction of temperature bounds for these two controllers versus the high peak air flow and constraint violation for the LQR and P controllers.

Remark 3. As shown in Table (1) the time required to simulate the MPC operations is three orders of magnitude higher than the one required for the simulation of LQR. This is because the LQR problems have closed-form solutions while the MPC solves optimization problems on the fly. The high computational effort and delay of MPC can be problematic as also indicated in [18], for implementing on embedded platforms with limited computational power. The *d-LQR* controller introduced in this paper can be regarded as a less computationally intensive alternative to MPC for large systems with a high number of states and inputs.

Table 1. Simulation time and Parameters for different controllers.

Controller:	P Ctrl	LQR	d-LQR	MPC
Simulation time $[s]$	1.31	0.13	0.11	115.1
Parameters	$K_p = 4$	$q_1 = 0.01$ $q_2 = 100$ $r_1 = 10$ $r_2 = 0.02$	$q_1 = 0.24$ $q_2 = 0.54$ $r_1 = 1$ $r_2 = 0.09$	$c_1 = 5$ $c_2 = 500$

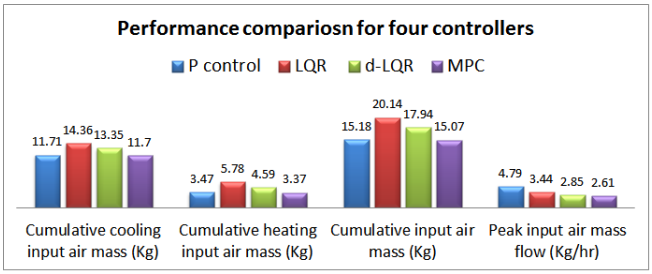

Figure 6. Quantitative comparison of different controllers.

The comparison result is shown in Fig. 7. From this comparison, we note that the LQR is not sensitive to parameter changes, the P controller is the worst controller among the proposed controllers and the performance of d-LQR and MPC are very close.

It was shown that the developed d-LQR controller acts more like an MPC rather than an LQR controller in terms of rejecting disturbances, and results in a smarter controller which uses disturbance knowledge to decrease both the total air mass and the peak air mass flow into the thermal zone.

5. CONCLUSION AND FUTURE WORK

We presented and compared four controllers for the control of an HVAC system in smart buildings. We presented and validated a heterogeneous model comprising a building envelope and an HVAC system model in DymolaBlock.It was shown that the d-LQR controller is able to reject the distur-

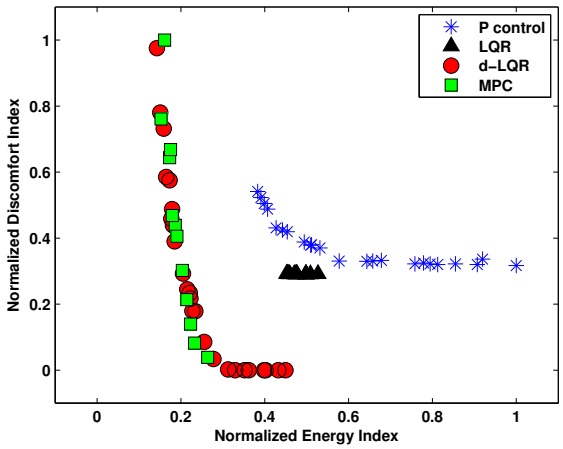

Figure 7. Normalized discomfort level versus normalized energy consumption for different controllers. It is shown that P control exhibits the worst performance; LQR, in the presence of disturbance is not so responsive to parameter changes; and d-LQR and MPC have similar performances. Normalized values along each axis are obtained by dividing the absolute values for each axis, by the maximum experienced value along that axis.

bance by using the knowledge of the disturbance and to keep the temperature within a set of given bounds at all times as opposed to the LQR derived with no a-priori knowledge of the disturbance characteristics. As a result the energy index of the d-LQR was reduced by 41.2% and the discomfort metrics from 3.8 to 0 when compared to the P control. A model predictive controller was also designed and implemented. This controller was shown to reduce the energy index by 46% and the discomfort index from 3.8 to 0 when compared to the P controller. d-LQR and MPC manage to keep the temperature within the temperature bounds at all times as opposed to P control and LQR which fail in doing so.

In future work, we will extend the co-design approach presented in [13] of control algorithm and embedded platform considering the computational complexity of the control algorithms and and the computational capabilities of the embedded platforms.

6. ACKNOWLEDGEMENT

Mehdi Maasoumy is funded by the Republic of Singapore's National Research Foundation through a grant to the Berkeley Education Alliance for Research in Singapore (BEARS) for the Singapore-Berkeley Building Efficiency and Sustainability in the Tropics (SinBerBEST) Program. BEARS has been established by the University of California, Berkeley as a center for intellectual excellence in research and education in Singapore. Alberto Sangiovanni Vincentelli is supported in part by the TerraSwarm Research Center,one of six centers administered by the STARnet phase of the Focus Center Research Program (FCRP), a Semiconductor Research Corporation program sponsored by MARCO and DARPA.

REFERENCES

[1] Modelica website: https://www.modelica.org, February 2012.

[2] IBM ILOG CPLEX Optimizer, September 2013.

[3] S. Ahuja, A. Surana, and E. Cliff. Reduced-order models for control of stratified flows in buildings. In *American Control Conference (ACC), 2011*, pages 2083–2088. IEEE, 2011.

[4] B.D.O. Anderson and J.B. Moore. *Linear optimal control*. Prentice-Hall Englewood Cliffs, NJ, 1971.

[5] D.P. Bertsekas. *Dynamic programming and optimal control*. Athena Scientific, 1996.

[6] D.P. Bertsekas. Dynamic programming and optimal control 3rd edition, volume i. 2011.

[7] D. Gyalistras and M. Gwerder. Use of Weather and Occupancy Forecasts for Optimal Building Climate Control (OptiControl): Two years progress report. *Terrestrial Systems Ecology ETH Zurich, Switzerland and Building Technologies Division, Siemens Switzerland Ltd., Zug, Switzerland*, 2010.

[8] J. Lofberg. Yalmip : A toolbox for modeling and optimization in MATLAB. In *Proceedings of the CACSD Conference*, Taipei, Taiwan, 2004.

[9] Y. Ma, F. Borrelli, B. Hencey, B. Coffey, S. Bengea, and P. Haves. Model predictive control for the operation of building cooling systems. In *American Control Conference (ACC), 2010*, pages 5106–5111. IEEE, 2010.

[10] M. Maasoumy, A. Pinto, and A. Sangiovanni-Vincenteli. Model-based hierarchical optimal control design for HVAC systems. In *Dynamic System Control Conference (DSCC), 2011*. ASME, 2011.

[11] M. Maasoumy and A. Sangiovanni-Vincentelli. Optimal control of HVAC systems in the presence of imperfect predictions. In *Dynamic System Control Conference (DSCC)*. ASME, 2012.

[12] M. Maasoumy and A. Sangiovanni-Vincentelli. Total and peak energy consumption minimization of hvac systems using model predictive control. *IEEE Design and Test of Computers*, Jul/Aug 2012.

[13] Mehdi Maasoumy, Qi Zhu, Cheng Li, Forrest Meggers, and Alberto Sangiovanni-Vincentelli. Co-design of control algorithm and embedded platform for HVAC systems. In *The 4th ACM/IEEE International Conference on Cyber-Physical Systems (ICCPS'13) (ICCPS 2013)*, Philadelphia, USA, April 2013.

[14] Mehdi Maasoumy Haghighi. Modeling and optimal control algorithm design for hvac systems in energy efficient buildings. Master's thesis, EECS Department, University of California, Berkeley, Feb 2011.

[15] N. Mendes, G.H.C. Oliveira, and H.X. de Araújo. Building thermal performance analysis by using matlab/simulink. In *Seventh International IBPSA Conference, Rio de Janeiro, Brazil*, 2001.

[16] F. Oldewurtel, A. Parisio, C.N. Jones, M. Morari, D. Gyalistras, M. Gwerder, V. Stauch, B. Lehmann, and K. Wirth. Energy Efficient Building Climate Control using Stochastic Model Predictive Control and Weather Predictions. In *American Control Conference (ACC)*, pages 5100–5105. IEEE, 2010.

[17] M. Wetter, W. Zuo, and T.S. Nouidui. Modeling of heat transfer in rooms in the modelica buildings library.

[18] A. Dally Y. Ma, A. Kelman and F. Borrelli. Model predictive control of thermal energy storage in building cooling systems. *IEEE Control System Magzine*, pages 1–65, 2011.

[19] Yang Yang, Qi Zhu, M. Maasoumy, and A. Sangiovanni-Vincentelli. Development of building automation and control systems. *Design Test of Computers, IEEE*, 29(4):45 –55, aug. 2012.

Causality in Hospital Simulation Based on Utilization Chains

Gabriel Wurzer and Wolfgang E. Lorenz

Vienna University of Technology
Treitlstrasse 3 (Architectural Sciences / 259.1)
Vienna, Austria, 1040
{firstname.lastname}@tuwien.ac.at

Keywords: Agent-Based Simulation, Analysis, Debugging.

Abstract

The operation of complex buildings (e.g., airports, hospitals, industrial facilities, penitentiaries) is commonly simulated forward in time: agents arrive and perform their prescribed tasks, utilizing resources and space as required. When trying to understand the model's state at a certain point in time, say, "why is this resource over-utilized?", one must either guess or run the simulation again to determine what the cause is. Our contribution lies in the introduction of causal chains into the workflow of an agent-based simulation, so that an end user (in our case, process planner and hospital architect) can get a further insight into the intermediate simulation result at a certain point in time, without having to re-run the simulation.

1. INTRODUCTION

In the past half year, we have been simulating a large central operations theater (eight operation rooms minimally, the total number dependent on simulation output). With this work, we regularly had to hunt down errors and inconsistencies. Even when having full access to the model's code (*white box approach*), this was already quite a challenge, as there are many causes for an observed behavior (activities of an agent, signals, queuing and prioritization, etc.). For someone without access to the code (i.e. *black-box approach*, typically end-users), finding the erroneous spot might be even more troublesome: one could either guess (basically using *trial and error*) or resort to more sophisticated protocol-based methods such as (Rogsch and Klingsch 2011). Clearly, it is hard to argue for the trustworthiness of a model under such circumstances. Our major goal is thus to give end-users a greater flexibility in exploring a model during its development phase.

2. END-USERS NEED MORE THAN RESULTS

Process planners and hospital architects (who are our end-users) are not confident in simulation results lest they can understand how they were computed. For example (see the left side of Figure 1), they will want to see not only a utilization graph but also *dependencies between different resources*. It is common to shift this responsibility to the visualization (see the right side of Figure 1), meaning that one has run a simulation multiple times in order to understand the relationships between the patients and resources fully.

Figure 1. No causality shown in utilization graphs (left) and simulation view (right).

What if we could instead *stop the model* at a certain point in time and find out the *chain of events* that led to the current state, without having to restart? This is the core idea and main contribution of our paper, which we detail under Section 4. Summarizing briefly, we might then ask—for a specific space under scrutiny—the following questions:

- *Why* are resources utilized (causal chains, Section 4.1)?
- *Who* is using certain resources (role-centric, Section 4.2)?
- *When* are resources utilized (time-centric, Section 4.3)?

It is our hope that, using such functionality, users will be less tempted to call for "realistic visualizations" for proving

the credibility of a simulation but can instead resort to proper argumentation.

3. BACKGROUND

3.1. Simulation Model

We use an agent-based model in which each agent follows a fixed sequence of functions to visit (that is, the *medical pathway*, which might consist of functions ARRIVAL > [HOLDING AREA] > PATIENT TRANSFER SYSTEM > OT > RECOVERY). This is similar to a schedule-calibrated occupant behavior simulation (Goldstein et al. 2010) or User Simulation of Space Utilisation (Tabak 2008). We use real (but anonymized) pathways exported by the Hospital Information System (see Wurzer et al. 2012; Glock et al. 2013 for details) or generate these by using "standard sequences" from which we eliminate steps based on probabilities, also determining step durations using min/max service times per function.

Functions form the dynamic aspect of our simulation: they are resources which can hold a finite number of agents at a time (*capacity*) and ultimately determine when an agent is able to proceed with its process. Thus, one might call our model a more discrete/client-server-based approach than agent-based approach, even though we also use agents for their ability to navigate in space (along the circulation, in the preliminary schema of the hospital, using a pedestrian movement model if required). Each function is situated in a space (e.g. OT1), which is the basic planning unit that our end users are after. There are two modes in which functions are acquired. First, an agent can utilize a function directly because it is in his process (*function as activity*). Second, a function is utilized *as queue* when another function is unavailable (e.g., preoperative holding area).

Histories are recorded for both agents and spaces: agents record at which time which function was sought or acquired, or a queue was entered, whereas spaces record which agents have visited or queued for a contained function. Using these basic recording mechanisms, we can later infer a causal chain.

3.2. Related Work

Techniques that can deliver the functionality we propose have already been available for some time in the context of debugging. An illustrative example of interrogative debugging techniques, (Ko and Myers 2004) have proposed a system that can interrogate a program over "why" or "why not" a certain program state was reached, by recording program states in between. In contrast to this approach, we need not "infer" causality (cf. Pearl 2009; Hluch 2014), as this is explicitly given in the medical pathway that each agent follows (see Section 3.1).

Visually, our approach uses Sankey diagrams (cf. Tufte 1983, p.176) to depict flow between spaces. A similar technique that depicts temporal events from medical records has been previously presented by Wongsuphasawat and Gotz (2012), albeit with no connection to the building layout on which our approach superimposes the visualization. Such an approach can be seen as Focus+Context technique (Card et al.1999) where a space under scrutiny is shown in full detail together with flows from other spaces leading there (giving context).

4. CONTRIBUTION

4.1. Why are Resources Utilized?

The answer to this question lies in all spaces that an agent has crossed before coming to a space under scrutiny. As we have recorded all utilizations for these spaces, we may thus speculate if these have led to a bottleneck (also refer to Figure 2). If agents are utilizing a space below its capacity, no queuing occurs (labeled green in the left part of Figure 2). If, on the other hand, agents queue for that space (labeled red, see again the left part of Figure 2), there is a potential for that space to have become a bottleneck.

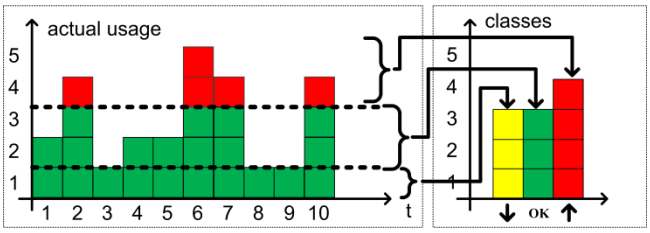

Figure 2. Utilization of a function. (left) Utilization with queuing depicted as red. (right) Classification into underutilized (yellow, <20% usage), well-utilized (20%-100%) and over-utilized (>100% =queuing).

The latter aspect deserves some attention, as there are two possible interpretations. Either we say that a space for which queuing occurs [even once!] can be the source of a bottleneck (*absolute utilization*). Or, we disregard minor queuing activities and focus on whether queueing occurs "most of the time" (*relative utilization*). In that context (refer to the right side of Figure 2), a space may be "under-utilized" (< 20% utilized), "well-utilized" (20-100%) or "over-utilized" (queueing occurs, thus >100%).

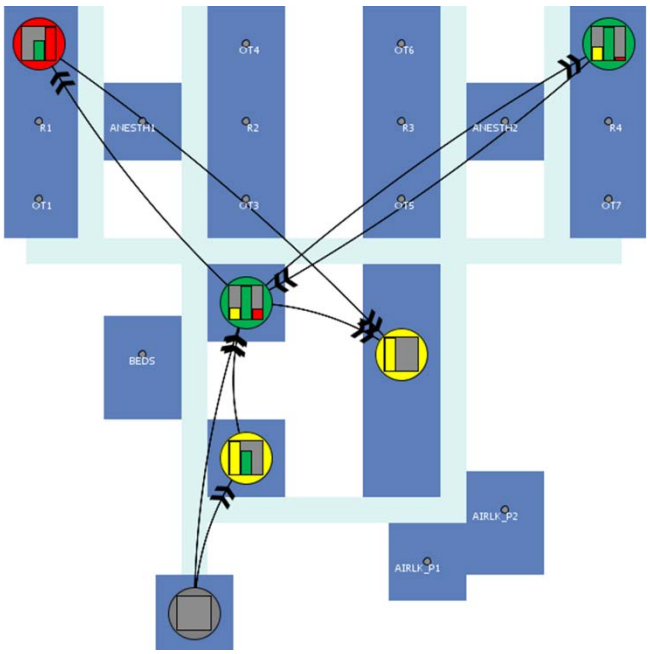

Figure 3. Causal chain depicting "why?" the space on the lower-right has been utilized (red = over-utilization, yellow = under-utilization, green = well-utilized). Actual screen shot from our simulation.

Figure 3 shows a utilization graph for the relative case. The overall utilization is shown by the color of each circle (yellow = under-utilized, green = well-utilized, red = over-utilized, inscribed into each space along the causal chain leading to the space under scrutiny). Under-, well- and over-utilizations are embedded into the same circle, allowing for an overview. Absolute utilization would be depicted in almost the same way, except that a space would turn red when a single over-utilization occurs (though this is only helpful in cases where resources are very scarce).

4.2. Who is Using Certain Resources?

To answer questions on utilization for a specific role (e.g. "are acute patients causing a bottleneck?"), a separation of causal chains *by role* is performed (refer to Figure 4). Colored edges now show patient type (red = acute, green = planned, red = day-clinic patients) and volume of patients crossing a space under scrutiny. As before, we show the relative utilization of the space as a circle (yellow = under-utilized, green = well-utilized, red = over-utilized), which we scale according to the patient volume. Large volumes of a specific patient type and visible utilization problems along the causal chain can help to pinpoint a bottleneck in the process for a certain group of building users.

4.3. When are Certain Resources Utilized?

This information is readily available in the utilization graphs (see the left of Figure 1); however, anchoring it to the chain of events may make patterns and dependencies in the temporal domain more obvious. We superimpose temporal utilizations over the causal chains (see Figure 5), by inscribing usage plots into circles showing relative utilization. A benefit of having such visualization is that planners can get a feeling for temporal dependencies without having to re-run the simulation.

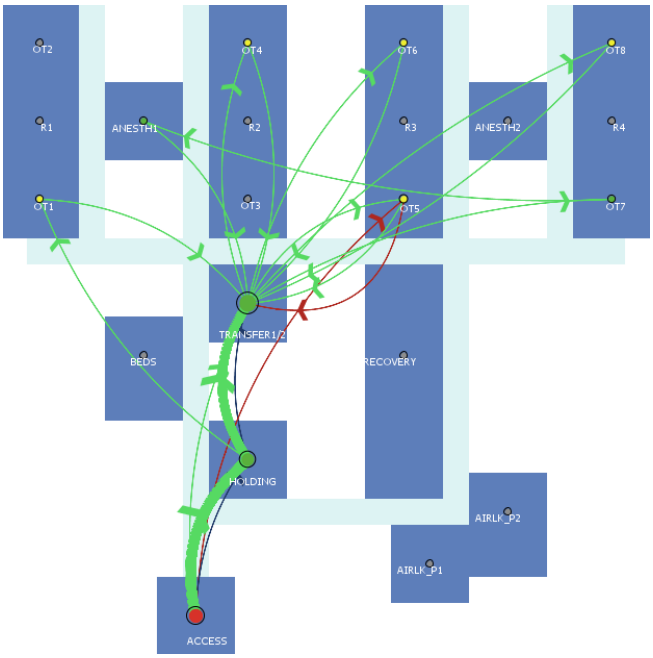

Figure 4. Utilization from a patient-centric perspective ("who?"). Patient flows depicted as colored edges (red = acute, green = planned, blue = day-clinic patients). Thickness of edges corresponds to patient volumes. Relative utilization of spaces shown as color-coded circles (red = over-utilization, yellow = under-utilization, green = well-utilized). Circle radius shows patient volume having crossed that space. Actual screen shot from our simulation.

5. DISCUSSION

Our approach is targeted at planners wishing to ask "why", "who" and "when" types of questions during the development of their model—either for analysis or for debugging purposes—leading to some confidence in the simulation results. The underlying model consists of agents visiting their respective medical pathways (or causal chains, as we would say). However, there is no need to have fixed sequences of visited functions as a basis for our approach -

it will just work fine with any other agent-based simulation for which agent histories and spatial utilization are recorded.

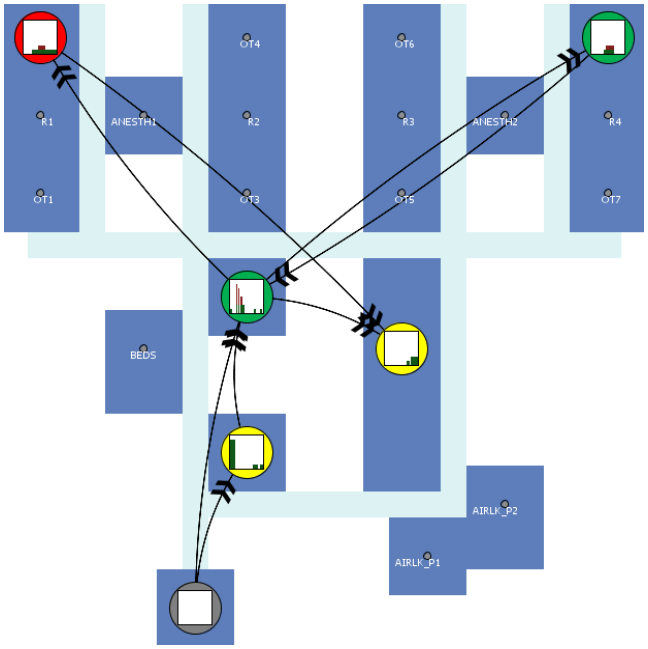

Figure 5. Superimposing utilization graphs over the utilization chain to show time-dependent causality. Actual screen shot of our simulation.

Another point worth discussing are the results of our underlying model (i.e., OT utilization, number of patients, room configuration and so on). We have intentionally left these out, since what we are interested in is *tool support* rather than a concrete case, even though our simulation was initially built with a 1100-bed clinic in Vienna in mind (but has since been extended so as to become more general-purpose OT planning software). Arguing further, we are only interested in preliminary phases of building design, where space programming takes place. In contrast, most papers in the same field target optimization of hospital units in the later phases of design, where concrete results can be given because the main decisions in space programming have already been made.

The chosen visualization types—"why", "who" and "when"—come from actually working with practitioners while developing our model. To be fair, we have yet no indication if our approach can be considered a "success" or "failure" in terms of aiding the design team for the general case. Proof or rejection of this statement would require us to test our model with one group using the visualization and one without—a task we have to leave for future work.

6. CONCLUSION

We have presented a visualization of utilization chains in agent-based models, which lets planners ask "why", "who" and "when" a certain space and its contained resources were utilized. Interrogating a model in this way can help users gain confidence and hunt down errors during the development of a simulation.

Acknowledgements

This work was sponsored in part by the ZIT MODYPLAN and the FFG STABLE HBO project. We wish to acknowledge fruitful discussions among the project members, especially with Anita Graser, Barbara Glock, Richard Wurglitsch, Niki Popper and Rudolf Linzatti.

References

CARD, S.K., MACKINLAY, J.D. AND SHNEIDERMAN, B. (Eds.) 1999. Readings in Information Visualization: Using Vision to Think. Morgan Kaufmann Publishers, San Francisco.

GLOCK, B., WURZER, G., BREITENECKER, F. AND POPPER, N. 2012. Reverse Engineering Hospital Processes Out of Visited Nodes. EUROSIM 2013, Cardiff. 312-317.

GOLDSTEIN, R., TESSIER, A. AND KHAN, A. 2010. Schedule-Calibrated Occupant Behavior Simulation. SimAUD 2010, Orlando. 79-86.

HLUCH, L. 2014. The Place of Causal Analysis in the Analysis of Simulation Data. Advances in Intelligent Systems and Computing. 245. 3.

KO, A.J. AND MYERS, B.A. 2004. Designing the Whyline: A Debugging Interface for Asking Questions about Program Failures. CHI 2004, Vienna. 6(1). 151-158.

PEARL, J. 2009. Causality: Models, Reasoning and Inference. Cambridge University Press, New York.

ROGSCH, C. AND KLINGSCH, W. 2011. To See Behind the Curtain - A Methodical Approach to Identify Calculation Methods of Closed-Source Evacuation Software Tools. PED 2010, Gaithersburg. 567-576.

TABAK, V. 2008. User Simulation of Space Utilisation. Ph.D. Thesis, Eindhoven University of Technology.

TUFTE, E.R. 1983. The Visual Display of Quantitative Information. Graphics Press, Cheshire.

WONGSUPHASAWAT, K. AND GOTZ, D. 2012. Exploring Flow, Factors, and Outcomes of Temporal Event Sequences with the Outflow Visualization. IEEE Transactions on Visualization and Computer Graphics. 18(12). 2659-2668.

WURZER, G., LORENZ, E.W. AND PFERZINGER, M. 2012. Pre-Tender Hospital Simulation using Naïve Diagrams as Models. I-WISH 2012, Vienna. 157-162.

Full-Automated Acquisition System for Occupancy and Energy Measurement Data Extraction

Dimosthenis Ioannidis[1,2], Stelios Krinidis[1], Georgios Stavropoulos[1], Dimitrios Tzovaras[1], and Spiridon Likothanassis[2]

[1]Information Technologies Institute
Centre for Research & Technology Hellas,
Thermi-Thessaloniki, 57001, Greece
{djoannid,krinidis,stavrop,Dimitrios.Tzovaras}@iti.gr

[2]Pattern Recognition Laboratory,
Computer Engineering and Informatics, University of Patras,
Rio, Patras, Greece
{djoannid,likothan}@ceid.upatras.gr

Keywords: Occupant-Aware Building Analysis, Human Presence and Movement Analysis, Building Energy Efficiency.

Abstract

There is ongoing research on reconciling the difference between predicted/simulated and actual energy consumption in buildings (either in the design or operational phases). In this paper a fully automated acquisition system for occupancy and energy measurement data is going to be presented. The proposed system comprises a depth camera cloud and RFID for occupancy extraction, a network of CO_2 and temperature sensors and separate energy meters for HVAC, lighting, wall sockets and equipment. The extracted occupancy and energy consumption measurements of the proposed system could be utilized in a variety of applications, such as real-time control strategies, performance simulation analysis, high semantic occupancy and energy consumption information extraction, and even business processes analysis and simulation. The proposed system has been evaluated in a large-scale experiment, and its accuracy and robustness will prove its significance to the occupancy simulation processes, as well as to any kind of application that exploits occupancy.

1. INTRODUCTION

Building occupancy and energy simulation is an essential task for building space refinement, new building design, etc. Building simulation can lead to designing buildings with higher energy efficiency, higher thermal comfort, etc. However, building simulation accuracy is highly related to accurate occupancy and energy information for buildings.

There is a variety of building simulation systems, which can be divided into three main categories. The first category includes building simulation systems where the occupancy and energy simulation are based on predefined functions without the use of any kind of measuring and training. These tools simulate the occupancy of a building based on stochastic models, such as Markov chain or probabilistic distribution (Gunathilak et al. 2013). The occupancy simulation in such a system is not accurate, since the exploited probabilistic models take into account only the geometrical information of the building. The second category includes systems that perform occupancy training and simulation processes based on information manually obtained from occupant responses to a questionnaire (Ioannidis et al., 2013; Liao and Barooah, 2011; Stevenson et al., 2010). However, one can question the accuracy of occupant responses and as a consequence the accuracy of the training and simulation results. Finally, the last building simulation systems category includes systems based on occupancy and energy consumption measurements. Most of them perform occupancy detection, utilizing passive infrared (PIR) motion detectors. These systems are simple, but have the drawback of failing to detect occupants who remain relatively still, as well as a distant passersby. Also, warm and cold airflows affect the efficiency of such systems. A variety of sensors, such as sonars, gas sensors, sound pressure level, illuminance, CO_2, temperature and humidity have been exploited in order to measure the occupancy of a building (Erickson and Cerpa, 2010; Hailemariam et al., 2011; Tarzia et al., 2009). Generally, there are very few systems in the literature that based their simulation results on occupancy and energy consumption measurements.

In the proposed system, a number of low-cost privacy preserving sensors of different types have been incorporated into the building of interest. The sensors used by the system could provide not only information about the exact building occupancy, but also the occupancy per space, occupancy per zone, as well as their corresponding energy consumption. All these sensors can measure several attributes of the building environment: global energy consumption, energy consumption per type (light, HVAC, etc.), energy consumption per space and/or zone, carbon dioxide (CO_2), temperature and, finally, occupancy per building, per space and per zone. All this data could lead to tackling the difference between predicted/simulated and actual energy consumption in buildings (either in the design or operational phases). The motivation for the presented framework is that there is lack of availability of a holistic framework providing detailed occupancy and energy consumption information correlating disjoined worlds, such as Building Information Model (BIM), Business Process Model (BPM) and occupant comfort aspects.

The rest of the paper is organized as follows. Section 2 covers the sensor and the data type that is collected by the proposed system. Sections 3 and 4 introduce the occupancy and energy consumption extraction subsystems, which represent the main scientific contribution of the paper. Experimental results are presented in Section 5, and conclusions are drawn in Section 7.

2. APPARATUS AND DATA COLLECTION

The system can be established in any existing building of interest using a variety of sensors to measure various building occupancy and energy consumption attributes. Specifically, some sensors measure directly the desired occupancy and energy consumption of the desired area, while other sensors measure environmental attributes directly correlated to occupancy and energy consumption. The selected sensors measure carbon dioxide (CO_2), temperature, electrical current (due to lighting, to HVAC, to wall sockets, or to equipment usage (such as photocopiers, monitors, PCs, etc.)), occupant presence, and occupant flows. Table 1 presents the measurement type, the period of data collection, and the quantity of each type of sensor utilized by the proposed system.

An example of the physical placement for each sensor in a department of a technology company is depicted in Figure 1. The test bed consists of three main areas with similar usage (offices). Cameras have been established, using the center area of the building as a characteristic one. The left space is 87.27 m^2, the center 71.34 m^2, and the right 162.29 m^2. In this setup, a number of types of sensors were established, as shown in Table 1.

Type	Measurement	Period	Qty
Depth cameras	Occupancy flows	20 fps	9
RFIDs	Occupancy presence	Event	1
CO_2	Carbon dioxide	15 mins	3
Temperature	Temperature	15 mins	4
HVAC	Energy consumption	15 mins	1
Lighting	Energy consumption	15 mins	1
Wall sockets	Energy consumption	15 mins	1
Equipment	Energy consumption	15 mins	5

Table 1: Sensors used in a department of a technology company (Figure 1).

The data acquired by the proposed system's sensors is of various types and provided at different time instances, depending on the sensor type (Table 1). The depth cameras monitor all the areas under interest—detecting, tracking and extracting occupancy details over the entire monitoring period. The specific cameras operate and extract real-time occupancy information at 20 frames per second (fps). The occupancy information extracted by the depth cameras carries not only the occupancy of the areas under interest, but also the occupancy trajectories.

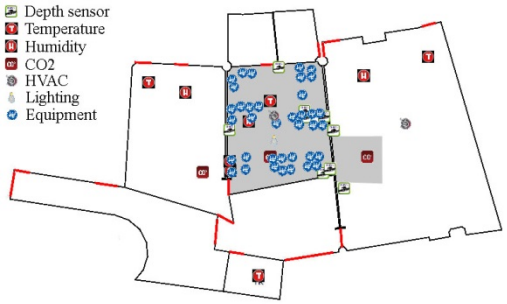

Figure 1. Physical configuration of sensors installed in a department of a technology company. The dark gray colored areas are the representative zones of the monitored area.

Depth cameras utilized by the proposed system exploit only the depth information (color information is discarded), so that the whole occupancy and energy consumption system takes into account all legal and ethical issues regarding individual privacy. Figure 2 illustrates such an example (second row), where individual cannot be discriminated from depth images. Furthermore, depth cameras exploiting by the proposed system are luminance and shadow invariance as shown in Figure 2. The first row of Figure 2 shows the color images of the same scene with

light illumination changes from one to another, whilst the second row depicts the corresponding depth images. (The color images are utilized here only for visualization purposes.)

Figure 2. Lighting invariance of the depth cameras utilized by the proposed system.

Another major issue that should be mentioned is time synchronization. The data aggregation module of the proposed system acquires data from a variety of sensors, which are plugged into different servers and workstations. It is of utmost importance that all this data is synchronized; data acquired by modules set up on unsynchronized systems could not be combined in the time sequence, and as a consequence would be useless. The synchronization of different workstations and servers is achieved by synchronizing each local computer's clock to the aggregator's clock every 100 milliseconds.

3. OCCUPANCY EXTRACTION

In this section, the methodology for the occupancy extraction subsystem utilized by the proposed system will be presented. The subsystem uses depth cameras and RFID sensors. RFID sensors are established in specific locations, where a semantic event occurs. These locations are the doors of the building, as well as the doors/entrances of all spaces and zones. In the proposed system, RFID sensors are installed at the doors of the spaces and zones of interest. Furthermore, RFID sensors play an assistant role to the depth camera output, verifying that an occupant has entered or left the areas of interest.

Depth cameras are utilized by the proposed system in order to extract occupancy information from the building. The proposed system exploits a depth camera cloud and as a consequence it inherits all the multi-camera system problems, such as camera calibration, overlapping views, camera error propagation, etc. One of the contributions of this paper is to tie camera calibration directly to the Building Information Model (BIM). Other algorithms performing calibration among cameras have a number of disadvantages, such as a need for overlapping areas, calibration error propagation, etc. The depth camera occupancy extraction subsystem is described in detail in the following subsections.

3.1. Multi-Camera Calibration Algorithm with the Building Information Model (BIM)

Calibration of the depth cameras utilized by the proposed system is of utmost importance, since it can transform the cameras' local coordinate system to a reference global one. One of the main concepts and innovations of the proposed calibration algorithm is that camera calibration is not achieved between the cameras, but each camera is directly calibrated to the BIM model. The global reference coordinate system that has been chosen in the proposed system is the coordinate system of the planar architectural map conveying the building of interest. The coordinates of this reference coordinate system (the building's planar architectural map) will be referred to as the real (reference) 3D coordinate system from now on. Camera calibration should be separately performed for each depth camera, and it is accomplished by exploiting a calibration pattern (e.g., with circles or squares). First of all, the real 3D coordinates of the pattern marks are calculated with a semi-automatic approach requiring the computation of only two points in the pattern. Knowing the coordinates of the two predefined pattern points, combined with knowing the pattern's plane on the same coordinate system, makes it possible to compute the real 3D coordinates for each pattern mark. The next step in the calibration process is the determination of the pattern marks' coordinates in the camera's coordinate system, which is accomplished by exploiting a pattern recognition technique based on Hough transformation.

Thus, the presented calibration algorithm is now able to compute the desired transformation matrices, rotation R and translation T, exploiting Singular Value Decomposition (SVD) methodology. The computed transformation matrices (R and T) can transform any 3D coordinate set from the camera's coordinate system to the real coordinate system. In

the same way, one can calibrate a large number of cameras. Each camera is completely independent, and it is not necessary to have overlapping areas for each camera view. Finally, any possible errors in the calibration or the detection procedure at later stages are not propagated and do not affect the rest of the cameras in the system.

3.2. Robust Human Presence and Movement Analysis in Indoor Environments

3.2.1. Human Presence Detection

Having correctly calibrated all the cameras adopted by the system, the occupancy detection algorithm is ready to start. Cameras extract the first available depth image (denoted here as img_c) and compare it with the adaptive background image img_b (see subsection 3.2.2). The comparison, $img_{c,b}$, of the current depth image with the background image img_b is exploited utilizing the L_1 norm on a local spatial neighbourhood $R_{i,j}$ around point $p_{i,j}$. The depth channel of the utilized cameras is a very noisy channel, causing a lot of problems to the detection procedure. In order to overcome this camera's hardware drawback, the algorithm applies a morphological filter eliminating all small parts (noisy parts) in the foreground of the image $img_f = \bigcap_{b \in B} img_{f-b}$. The final extracted foreground image img_f is fully free of any camera noise.

3.2.2. Adaptive Dual-Band Background Modelling

A very important issue in occupancy detection systems is the background depth image determination. Unfortunately, the background of the area under investigation does not remain the same (Barnich and Droogenbroeck, 2011). Thus, an adaptive dual-band depth background algorithm has been developed in order to overcome this restriction. It is based on the actual height h of the objects/pixels under investigation, where each pixel value is absorbed by the adaptive background model with a velocity depending on the band it belongs to. The band that a pixel belongs to, is determined by its height h. The absorption velocity is correlated with the number of processed frames. Thus, low-height staffs (chairs, tables, etc.) are quickly absorbed to the background (e.g., after 500 frames), whilst occupants are very slowly incorporated (e.g. after 35000 frames).

The adaptive dual-band background algorithm exploits two backgrounds, the current background img_b and the previous one, $img_{b_{prev}}$. The previous background image is used in order to capture the "empty" areas left by moving objects, which is achieved by using an intermediate image buffer img_{rest}, which, at each detection loop, stores the foreground data img_f that is detected on the current background img_b:

$$img_{rest} = H\left(img_{c,b} - thr_f\right)\left[1 - H\left(img_{c,b_{prev}} - thr_f\right)\right] \quad (1)$$

where thr_f is the predefined foreground threshold and $H(\cdot)$ the Heaviside function. This intermediate buffer img_{rest} stores all "foreground" data according to the current background and not according to the previous one. The current background image img_b is updated as follows:

$$img_b = H\left(img_f\right)\frac{img_b N_h + img_c}{N_h + 1} + H\left(1 - img_f\right)img_c \quad (2)$$

where img_c is the current camera's depth frame, img_f is the detected foreground image and N_h is a damping factor that controls how quickly a non-moving foreground object will be incorporated into the current background. The previous background image $img_{b_{prev}}$ is updated, exploiting the intermediate buffer img_{rest} in the same sense as in (2).

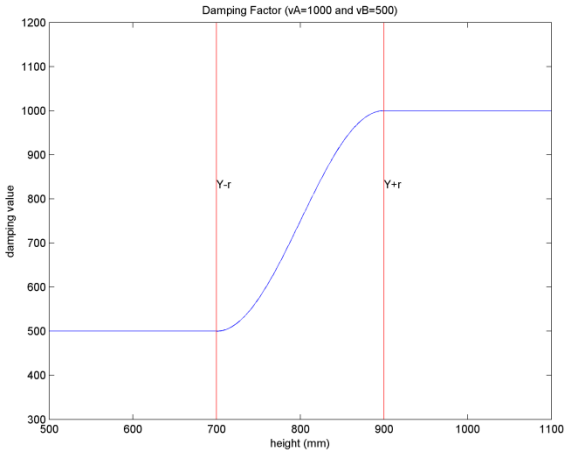

Figure 3. Example of the dual-band height function exploited by the adaptive background algorithm.

Furthermore, the damping factor N_h is dynamic and defined in a dual-band channel as follows:

$$N_h = \begin{cases} v_A, & h > Y + r \\ v_B, & h < Y - r \\ v_B + \frac{v_A - v_B}{2}\left(1 - sin\left(\pi\frac{h-Y}{2r} + \pi\right)\right), & \text{otherwise} \end{cases} \quad (3)$$

where v_A and v_B are two constants ($v_A \gg v_B$), h is the actual height of the pixel under investigation, Y is the height

that discriminates between the two background bands, and r is a height range among the two bands. Non-moving foreground objects with high height ($h > Y + r$) are enforced to be incorporated into the background very slowly (high v_A value), while the corresponding short objects ($h < Y + r$) are forced to be quickly incorporated (low v_B value). Objects of height belonging in the medium band ($Y - r \leq h \leq Y + r$) are incorporated into the background with a medium adaptive timing (3). Figure 3 illustrates an example of the dual-band adaptive function exploited for the non-moving objects' incorporation into the background by the described adaptive background algorithm.

The main achievement of the dual-band function incorporated into the adaptive background algorithm is that low-height objects are quickly absorbed into the background, whilst occupants are very slowly incorporated.

3.2.3. Virtual Camera Detection

The actual depth sensor could be placed anywhere in the monitoring area, but in order to enhance the occupancy system's robustness and reliability, a *virtual camera* is created by the system and is placed at the top of the camera's monitoring area. This virtual camera exploits orthogonal projection.

The transition from the normal view area to the virtual camera's view can be made by exploiting the transformation matrices (R and T) from the calibration process, which also provides the geometrical orientation of the camera according to the building. The main advantage of the utilization of the virtual camera is that it can efficiently handle occupants' partial occlusion.

3.2.4. Occupancy Tracking

Finally, the detected blobs are tracked exploiting the well-known Kalman filter. The combination of the Kalman filtering, the virtual camera utilization and the dual-band adaptive background have been proven efficient and robust.

Furthermore, occupancy tracking results are correlated with the results returned by the RFID sensors. When an RFID sensor detects an occupant, it sends an event to the tracking system, which looks for possible occupancy (extracted by the depth sensors) at the area nearby to the location of the RFID sensor. When the occupant is verified, then that specific occupant inherits all the information carried by the RFID sensor, such as role. In particular, the framework presented allows a correlation between occupancy trajectories and RFID information in the spatiotemporal domain. Moreover, by utilizing RFID-based information, occupant trajectories and equipment consumption enable inherently the association of equipment consumption to occupants in a space/zone.

3.3. Occupancy Information

The final occupancy results are sent to the aggregation module of the system. The occupancy information that is sent to the aggregation module is multi-fold, which means that a variety of information is stored. There are three types of information supported by the aggregation module: **(a)** S*pace occupancy*, the number of occupants per monitoring space. This type of message is sent periodically to the aggregation system, every 30 seconds. **(b)** *Occupant movemen*t, the movement of an occupant from one space or zone to another. This type of message is sent instantly when the event is occurring. **(c)** *Occupant trajectory*, the trajectory of each occupant. This information is sent periodically (e.g., every 30 seconds) to the aggregation module.

4. ENERGY CONSUMPTION AND ENVIRONMENTAL MEASUREMENT EXTRACTION

In this section, the methodology for energy consumption and environmental measurement extraction utilized by the proposed system is going to be presented. The environmental sensors measure carbon dioxide (CO_2), and the temperature of the area of interest. These sensors are locally measuring the environmental values of the spaces of interest. It is common knowledge that the environmental values have a low response time, so their measurements are sent aggregated to the aggregation module of the proposed system periodically (e.g., every 15 minutes).

The energy sensors measure the consumption by the equipment and the occupants in the area of interest. These measurements could be globally measuring the energy consumed in the whole area of interest. Furthermore, the energy consumption could be divided into categories (depending on the electrical board design) per device type, such as HVACs, lightings, wall sockets, etc. The energy consumption could be measured per equipment, which means that sensors attached to the equipment under interest return the energy consumed by them separately. Moreover, acquired data is sent periodically to the aggregation module (e.g., every 15 minutes). The sensors do not send the instant

energy consumption, but rather the energy consumed during the period between the transitions. Exploiting trial-and-error methodology (5, 10, 15, 20 minutes, and so on), it has been experimentally found that a good compromise between quality and quantity of data is a frequency of 15 minutes.

Sensors metering environmental values are common, while the energy consumption sensors exploited by the proposed system are attached on the switch board of the electricity control system of the building, as well as externally to wall sockets. These "smart" sensors measure the energy consumption of a device (light, monitor, PC, photocopier, etc.) by attaching to the cable of that device.

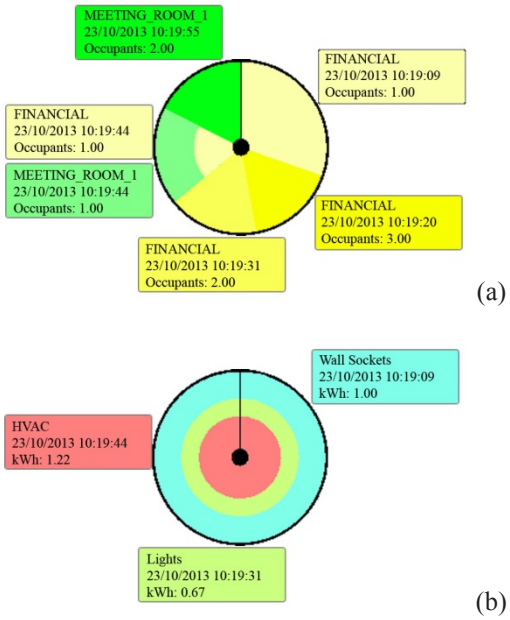

Figure 4. Clock charts of (a) occupancy per space and (b) energy consumption per category (HVAC, lighting, wall sockets) during a 1-minute period.

Finally, the aggregation module receives: (a) the environmental measurements per space and per zone of interest periodically, (b) the energy consumption per device type (HVAC, lighting, wall sockets, etc.) periodically, and (c) the energy consumption for the equipment under interest periodically.

5. EXPERIMENTAL RESULTS

In this section, a large-scale experiment conducted in a department of a technology company is going to be presented. A planar view of the area with all the sensors (depth cameras, environmental and energy consumption sensors) is shown in Figure 1. The type and the number of each sensor category installed at the experiment area are presented in Table 1. The area of interest covered by the proposed system includes the financial, the innovation, and the procurement departments of the company. The system ran for 46 consecutive days, covering a period from 11 October to 25 November.

The system is able to extract occupancy and energy statistics. Some examples are shown in Figure 4. Figure 4(a) illustrates the occupancy statistics of the monitoring area per space during a one-minute period in a clock-view diagram. Each slice of the clock-view diagram represents one second, while each slice is divided into parts depending on the space occupancy. Dark colors represent high occupancy values, while lighter colors represent low values. Figure 4(b) shows a similar clock-view diagram for the energy consumption per energy category for the same minute. Three kinds of energy devices are participating in the diagram: wall sockets, lights and HVACs. Tooltips nearby both diagrams depict the instant occupancy and energy consumption.

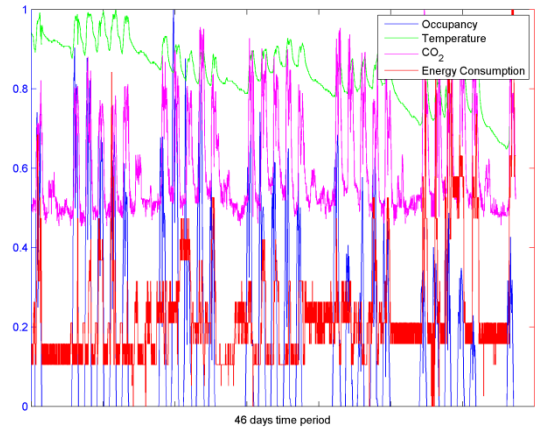

Figure 5. Energy consumption, temperature and CO_2 measurements versus occupancy over a 46-day period of time. All values are normalized.

Figure 5 illustrates the measurements (normalized values) of the experiment at the technology company after running 46 days. It illustrates occupancy versus energy consumption, temperature and CO_2 measurements. One can notice that the occupancy is directly related to the measurements. Furthermore, the specific measurements could be combined to provide real correlation with each other, rather than the probabilistic functions used in most other simulation programs in the literature.

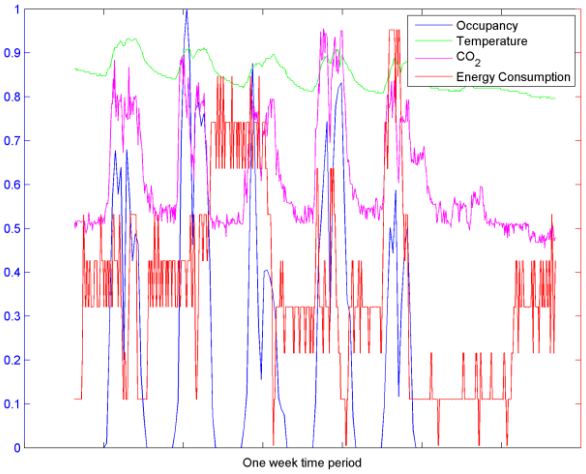

Figure 6. Energy consumption, temperature and CO_2 measurements versus occupancy over a randomly selected week. All values are normalized.

Figure 6 depicts the measurements (normalized values) of a randomly selected week, while Figure 7 shows the same plots for a randomly selected day (with normalized values). The relationships between the measurements is clearer in the latter figure due to its scaling. One can notice that when occupancy increases, energy consumption and environmental values follow with an increase; when occupancy falls, they follow with a decrease. The lunch time, when occupancy decreases and the other values fall also in Figure 7, verifies this statement.

True Positives	True Negatives	False Positives	False Negatives
38	0	0	2
Precision	**Recall**	**Accuracy**	**F_1-measure**
100.0%	95.0%	95.0%	97.4%

Table 2: Accuracy of the occupancy extraction system.

In order to evaluate the overall performance of the algorithm, a 37-minute video stream consisting of 1198800 frames was manually annotated. In addition, the selected minutes from the available dataset allowed us to perform extensive experimental evaluation of the proposed framework using several covariates that may affect performance (e.g., moving objects that affect background estimation, lighting and luminance differences, some human movements along different spaces, etc.). The annotation and measurement of this experiment has been performed based on the occupancy accuracy. Table 2 shows the accuracy metrics of the described occupancy extraction algorithm. The robustness of the proposed occupancy extraction system can be also visually verified by comparing the energy and environmental measurements with the occupancy in Figures 5 through 7.

6. DISCUSSION

Occupancy and energy consumption data extracted by the proposed system are useful in two ways. Firstly, they can be used for real-time control strategies. A decision support system can acquire the occupancy and energy consumption data extracted by the proposed system and make decisions about device and equipment use. It can make decisions such as when to switch on/off lights, HVACs, when to switch off specific equipment (photocopiers, printers, plotters, etc.) to power safe mode or to normal mode, and so on. The decision support system could be accompanied by an occupancy and energy consumption prediction system, which could predict in real-time—based on the current occupancy and energy consumption—the occupancy of the area under interest and as a consequence make further decisions about the usage of energy consumption devices and equipment.

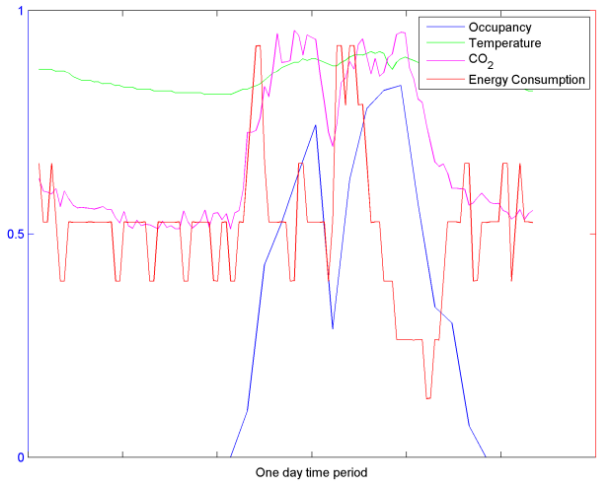

Figure 7. Energy consumption, temperature and CO_2 measurements versus occupancy for a randomly selected day. All values are normalized.

The occupancy and energy consumption data can be used to perform simulation analysis. It is common knowledge that occupancy and energy consumption are related, but their relationship differs from building to building depending on its geometry, its usage (company, hospital, etc.), its layout, and so on. Thus, the probabilistic model cannot accurately correlate occupancy with the energy consumption of a building (Hailemariam *et al.* 2011). On the other hand, the proposed system could

provide both the measured occupancy and energy consumption data for a long period of time, so as a performance simulation analysis it would be able to extract more realistic simulation results.

Furthermore, the proposed system could also extract the flows for each occupant and the energy consumed by specific devices. These two extra parts, which are not used in the above two cases, could be utilized for a Business Processes (BP) analysis tool. These flows provide the exact trajectories of each occupant, and can be correlated with the position and energy consumption of equipment to extract semantic information, such as what an occupant is doing at a specific time (e.g., photocopying, in a meeting, etc.). The spatiotemporal correlation of space utilization attributed to occupant roles, comfort, etc. would not be available directly using standalone sensing. Also, all this information combined could provide high-level semantic information about the BPs occurring in the area of interest, such as the day, the time, the location, the number of occupants, their roles, and the equipment used for a scheduled or even for a dynamic task. The BPs, and the tasks involved with them, could be detected and as a consequence they could be simulated, thus leading to more accurate energy performance simulation for a building, since BPs are the connecting link for different buildings that have similar usage. The raw data from the proposed framework can be utilized for facility management. The spatiotemporal correlation of raw data with the BPs occurring in the same monitored spaces could lead to better management of human resources, equipment, spaces (position and size), and so on.

Finally, setup difficulties for the system are mainly attributed to depth sensors installation, data (time) synchronization, and the storing and handling of large amounts of data. One limitation that could characterize the proposed system is the consideration of small and medium scale building installation, whilst the evolution of sensor cost is anticipated to allow large scale installations.

7. CONCLUSION

In this paper, a real-time, fully automated occupancy and energy consumption extraction system has been presented. The system utilized a depth camera cloud and a cloud comprised of a variety of sensors in order to measure the occupancy and the energy consumption of a building, spaces, and zones of interest. The occupancy and the energy consumption information extracted by the proposed system could be exploited by a variety of applications: (1) real-time control strategies, (2) performance simulation analysis, (3) high semantic occupancy and energy information extraction, and (4) business process analysis and simulation. In all cases, the energy consumption of the area of interest is available; thus, one can simulate its occupancy and energy consumption by exploiting real data and not probabilistic models. Finally, the accuracy and the efficiency of the results should be enhanced, using the data acquired by the proposed system.

Acknowledgements

This work was supported by the EU funded Adapt4EE ICT STREP (FP7-288150) and EU funded INERTIA ICT STREP (FP7-318216).

References

BARNICH, O. AND DROOGENBROECK, M., 2011. ViBe: A universal background subtraction algorithm for video sequences. IEEE trans. On Image Processing, vol. 20, no. 6, pp. 1709–1724.

ERICKSON, V. AND CERPA, A., 2010. Occupancy based demand response HVAC control strategy. Proceedings of the 2nd ACM Workshop on Embedded Sensing Systems for Energy-Efficiency in Building (BuildSys'10), pages 7–12, ACM, New York, USA.

GUNATHILAK, G., PRASANNAKUMAR, A., NAZARIAN N. AND NAEIMI, H., 2013. A Generalized Event Driven Framework for Building Occupancy. Proceedings of the Symposium on Simulation for Architecture and Urban Design (simAUD'13), pp. 227-230.

HAILEMARIAM, E., GOLDSTEIN, R., ATTAR, R., AND KHAN, A., 2011. Real-Time Occupancy Detection using Decision Trees with Multiple Sensor Types. Proceedings of the Symposium on Simulation for Architecture and Urban Design (simAUD'11), pp. 23-30.

IOANNIDIS, D., TZOVARAS, D. AND MALAVAZOS, C., 2012. Occupancy and Business Modeling. Proceedings of the 9th European Conference on Product and Process Modeling (ECPPM 2012), 3rd Workshop on eeBDM, eeBIM, Reykjavik, Iceland.

LIAO, C. AND BAROOAH, P., 2011. A Novel Stochastic Agent-Based Model of Building Occupancy. Proceeding of the American Control Conference, pp. 2095-2100, San Francisco.

STEVENSON, F. AND LEANMAN, A., 2010. Evaluating Housing Performance in Relation to Human Behavior: New Challenges, Building Research and Information, vol. 38, no. 5, pp. 437-441.

TARZIA, S., DICK R., DINDA, P. AND MEMIK, G., 2009. Sonar-based measurement of user presence and attention, Proceedings of the 11th international conference on Ubiquitous computing, pp. 89-92, ACM.

Session 9: Green Buildings and Cities **173**

Experimental Design of Energy Performance Simulation for Building Envelopes Integrated with Vegetation 175
Xiao Sunny Li, Ultan Byrne, Ted Kesik
John H. Daniels Faculty at the University of Toronto.

Transit-Oriented Development (TOD): Analyzing Urban Development and Transformation in Stockholm 179
Todor Stojanovski, Tesad Alam, Marcus Janson
KTH Royal Institute of Technology.

Scenario Modeling for Agonistic Urban Design 187
Trevor Patt, Jeffrey Huang
Ecole Polytechnique Federale de Lausanne.

Experimental Design of Energy Performance Simulation for Building Envelopes Integrated with Vegetation

Xiao Sunny Li, Ultan Byrne, and Ted Kesik

John H. Daniels Faculty at the Univeristy of Toronto
230 College Street,
Toronto, Ontario, Canada, M5T 1R2
sunnyxiao.li@mail.utoronto.ca, ultan.byrne@utoronto.ca, ted.kesik@daniels.utoronto.ca

Keywords: DIVA-for-Rhino®, Green Façades, Grasshopper™, Vegetated Cover.

Abstract

Green façades have many benefits, yet few software tools or methods have been developed for architects to assess the quantitative energy performance of green façades. This work-in-progress paper explores the methodologies of modeling and simulating the effects of green façades on wall surface temperatures. It proposes a partially parameterized workflow to compute the thermal performance of green façades within a platform based on Rhinoceros® (Robert McNeel & Associates, Seattle, WA) and its plug-ins. By calibrating the computed results with field measurements, the paper identifies the need for accurate information about vegetated covers and growth rates in modeling a green façade's performance. Also, the paper identifies evaporative cooling from the vegetation's transpiration as a key component contributing to cooling.

1. INTRODUCTION

Green façades, systems in which climbing plants are used to cover building walls, are known for their benefits in saving energy and moderating temperature in dense urban enviornments (Köhler 2008; Hunter 2014). Several studies have been conducted to quantify the thermoregulatory benefits of green façades (Alexandri and Jones 2008; Wong et al. 2010). However, these methods and software are not tailored to architects. In response, this paper explores a new methodology for using Rhinoceros along with its energy performance simulation plug-in, DIVA-for-Rhino (Solemma, LLC, Cambridge, MA, U.S.A.), to model the cooling effects of vegetation on wall surface temperature.

DIVA-for-Rhino is built on RADIANCE, a backward ray-tracer extensively studied since the late 1990s (Ibarra and Reinhart 2009), and EnergyPlus, developed by the U.S. Department of Energy to perform energy simulation for residential and commercial buildings. DIVA-for-Rhino can be used with Grasshopper™ to allow a fully parameterized simulation workflow. At this stage of the project, however, DIVA-for-Rhino's plug-in is used with Rhinoceros to take advantage of simulation metrics such as point-in-time illuminance. This particular metric allows the level of light to be measured at a specific date and time (Lagios 2014). The computed results from this metric can be compared with onsite measurements, allowing more precise calculations of shading effects in energy modeling. Furthermore, vegetated cover is said to be the key trait of the climbing plant in providing cooling effects (Koyama et al 2013). Visualizing the physical geometry of the leaf coverage would not only better assist designers in perceiving the formal quality of the green façade, but would also allow further simulation studies to be quickly done using architect-friendly simulation software.

2. METHODOLOGIES

2.1. Empirical data source and constraints.

The green façades investigated in this study are established by the Green Roof Innovation Testing (GRIT) Lab, which is located on the roof of the five-storey John H. Daniels Faculty of Architecture, Landscape and Design building at the University of Toronto St. George Campus in Toronto, Ontario. Six south-facing 3D greenscreen® façades are built against a building wall containing heated office and storage space. The trellises are 2.15m in height and set away from the exterior wall (MacIvor et al. 2013). The green façades contain Virginia creeper (Parthenocissus quinquefolia) and are set up along with two other green façades of the same modular width (1219mm), covered in River Bank Grape and Nugget Hops respectively. Each

green façade has a corresponding control wall, which also has the same width but is free of vegetation on the trellis. This project uses the green façades covered by Virginia creeper, which has been studied across the globe for its cooling effects on building surfaces (Ip, Lam, and Miller 2010).

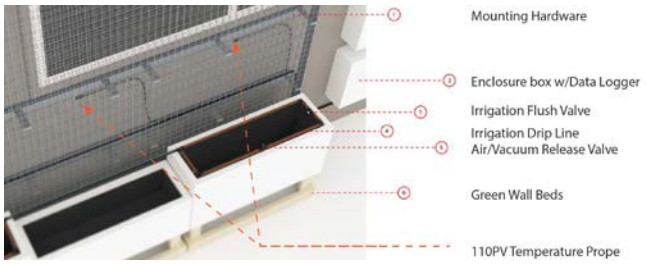

Figure 1. The thermal sensors, irrigation flush valves and green façade beds, and data logger for the green façade (Courtasy of GRITLAB 2013).

A single temperature probe (110 PV Surface Mount Thermistor, Campbell Scientific) was attached to the surface of the exterior wall, centered on both the control and vegetated façades. It measures the wall surface temperature, which is considered the sol-air temperature (Figure 1). In addition to the wall's surface temperature, the GRITLAB records weather data every five minutes. Although the output from all electronic probes is ample, this study is constrained by the frequency of field observations, which include photographic documentation of the vegetated cover and thermograph documentation of the wall surface temperature. So far, there are ten sets of data gathered between the end of May to the end of July. Each set of data consists of the following: the shaded and controlled wall surface temperature (a.k.a. sol-air temperature) recorded by the 110PV Temperature Probes; the shaded wall's surface temperature recorded from the FLIR thermographs taken of a 1x1 m section of the green façade surface at 1 p.m. every five to seven days; and a photograph of the 1x1 m section taken every five to seven days. These ten sets of data form the calibration data set for the following simulation results.

The simulation procedure starts with extracting pixel points from the field observation photographs to construct a series of simplified 3D models of the shading geometry in Rhinoceros. We first use Grasshopper to prepare an algorithmic definition to form points on a 1x1 m plane in Rhinoceros. These points correspond to the position of the pixels that share a given range of the RGB values of the documentation photographs. Then, we use the Eyedropper Tool in Adobe Photoshop (Adobe System Inc., San Jose, CA, U.S.A.) to survey the desired RGB values of the leaves on the documentation photographs. We take these RGB values from Photoshop as the inputs for the "given range of RGB values" in the Grasshopper definition. The algorithmic definition identifies the positions of points, which are matched with the pixels that share the values within the range of RGB values mentioned above. Still in Grasshopper, we construct circular surfaces, which are centred to these points with a desired radius so that any neighbouring circles are approximately tangent to each other.

In order to proceed to daylight simulation analysis with DIVA-for-Rhino, these circular surfaces are "baked" into the shading geometry. Grasshopper's "bake" component transforms the parametric form into a NURBS geometry that is permanent. More importantly, after "baking", the NURBS circular planes, an abstraction of the leaves on the green façade, can be assigned different RADIANCE material definitions to emulate the actual transparency of the leaf. However, at this stage in the investigation, we treated the leaf to be opaque to simplify the simulation procedure.

We first load the weather data, which is downloaded from the EnergyPlus Energy Simulation Software webpage (U.S. Department of Energy, 2013). The simulation metric is set to illuminance with the unit of Lux under Daylight Grid-Based analysis for Point-in-Time Illuminance. The date in the simulation setup will be set according to the date of the field observation photograph and thermograph recording. The time, in general, is set to 1 p.m., because eight of the ten thermographs were taken around 1 p.m. The amount of illuminance received by the wall behind the shading geometries is calculated by implementing these setup procedures for the ten distinct shading geometries, By considering the wall material with a relatively light colour (by choosing a value for α/h_o), a computed sol-air temperature value T_e, measuring the shaded wall surface temperature between the wall and the green medium is obtained by using the equation below.

$T_e = T_o + (\alpha/h_o) \times (I_t) - (\epsilon/h_o) \times (\Delta R)$

I_t = illuminance received the wall behind the green medium (lux) x (0.0079 W/m²/lux)*
* Approximation for conversion from the illuminance of sunlight to Solar Radiant flux or Solar Irradiance (Chua, 2013)

α = 0.75, h_o = 17 W/ (m² °C) (Hutcheon and Handegord, 1995)

2.2. Comparison and Calibration

The polynomial trendlines in Figure 2 illustrate that the computed T_e values are quite close to the T_e values

measured from the 110PV Temperature Probe for the 1x1 m shaded wall surface. However, it is noticeable that the computed T_e values are lower than the measured ones most of the time, especially for values before June 25th when the temperature is relatively cool. This shows that the reduction in wall surface temperature by shading is exaggerated. Koyama and his colleagues pointed out that the overall reduction in wall surface temperature by green façades is mainly contributed by two parts: the interception of solar radiation by the vegetation as well as the cooling effect by the evaporative cooling of the vegetation's transpiration (Koyama et al. 2013). The computed T_e values only account for the first component: the solar radiation interception. Therefore, the computed T_e values should be larger than the measured ones, at least for a significant portion of the observation period. The computed T_e values are directly proportional to the amount of illuminance that the wall received, and inversely proportional to the density of the shading geometry generated by the Grasshopper definition. It is clear that we need to calibrate the Grasshopper definition in processing the field observation photographs.

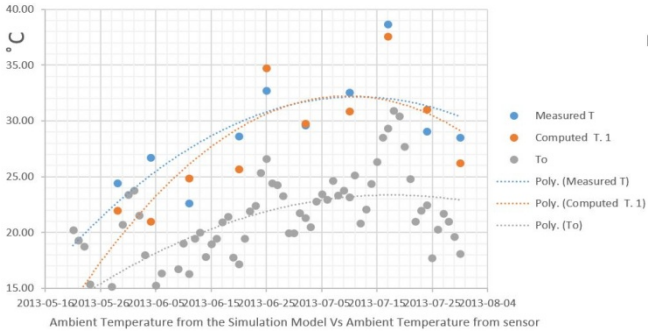

Figure 2. The computed Te vs. the measured Te vs. daily average T.

The Grasshopper definition is changed by replacing the intake field observation photograph with a binary image processed from the original photograph in Photoshop, and by narrowing the range of points accepted to generate the shading geometry. As illustrated in Figure 3, the slider component in the middle of the image is changed to 0.1, which limits most of the deviation from the black colour with RGB values of 0, 0, 0. This generates points with high fidelity to the selected black colour, avoiding over-estimation of the effect of interception of solar radiation by the vegetation. After adjusting the Grasshopper definition, the new set of circular surfaces—shading geometry—will be "baked" from Grasshopper for the second round of daylight simulation analysis with DIVA-for-Rhino as stated above.

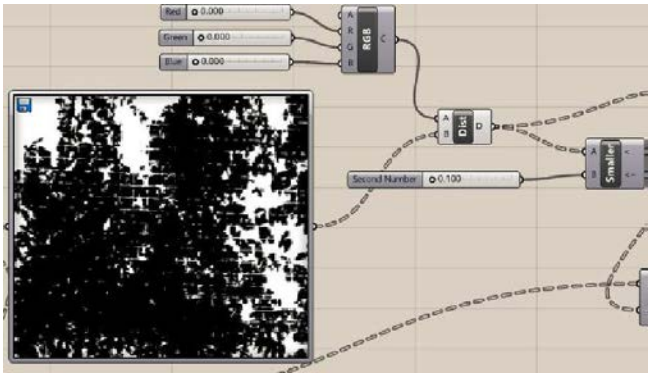

Figure 3. The binary image in Grasshopper to generate less dense shading geometry.

3. CONCLUSION

The calibrated illuminance values from the second-round DIVA point-in-time daylight simulation analysis generated higher T_e values, as shown in Figure 4. Compared to Figure 2, the newly computed T_e values show that the interception of solar radiation by the leafiness of vegetation will not be the only dominant factor in providing cooling to the wall surface, as the values on the computed T_e's trendline are higher than the ones on the measured T_e's trendline. As Price remarks, the percentage of cooling effect that could be maximally contributed by evapotranspiration is estimated to be 47%, which means 53% of the cooling effect is achieved by shading on a south-facing green façade in mid-Atlantic weather (Price, 2010). In these calibrated results, for instance, on June 25th, the ΔT between the control and computed wall surface temperatures is 2.68°C, which is 51.4% of the ΔT between the control and the measured wall surface temperatures—5.49%. In short, using DIVA-for-Rhino and the shading geometry generated from a given empirical field observation can produce a reasonably reliable estimation only of the effects that vegetation's shading has on the overall thermal performance of a green façade during hot summer days.

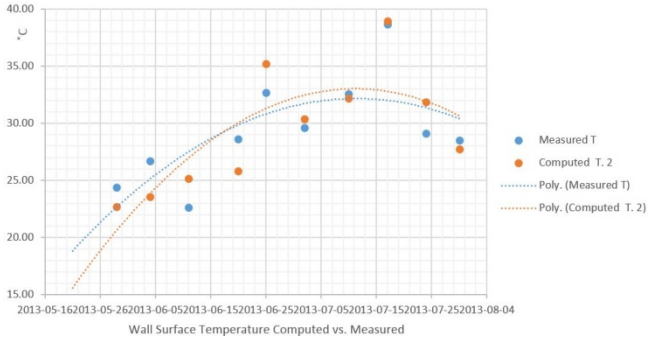

Figure 4. The computed Te vs. the measured Te.

In short, using DIVA-for-Rhino and the shading geometry generated from a given empirical field observation can produce a reasonably reliable estimation only of the effects that vegetation's shading has on the overall thermal performance of a green façade during hot summer days.

4. NEXT STEP

Although the calibration work has been performed and the shading geometry is more accurate, a large portion of the trendline of the computed shaded wall surface temperature during June and July is lower than the wall surface temperature measured on site. The downloaded weather file used in the simulations above was recorded at the airport, which is cooler than downtown Toronto due to the urban heat island effect noted by GRITLAB's weather records. This suggests that one should load a local weather file collected onsite to run the simulations in future studies. Also, the over-estimation of plant leaf size and its shading effect on the wall surface requires attention. It urges our future research to look into two areas: understanding the mathematical models of the growth rate of the plant, and finding an appropriate combination of RADIANCE material definitions to represent seasonal changes in the transparency of the vegetated cover. This could minimize human error and the constraints imposed by the observation frequency in the current empirical approach. For instance, the vegetated cover for vine plants is determined by the vine length (Koyama et al. 2013). If this relationship is modeled into a fully parameterized Rhinoceros-Grasshopper platform, the simulation can achieve higher accuracy in computing the plant's interception of solar radiation at any point in time. The modeling of evaporative cooling by plant transpiration is also crucial in order to achieve a complete simulation for the cooling effect of vegetation. Once these unknowns are resolved, one can apply the computed shaded wall surface temperature into DIVA-for-Rhino's Thermal Analysis, in which the indoor temperature of a structure with a vegetation-integrated envelope could be computed. Since most of the workflow stated above could be done in one single platform, Rhinoceros, this future works aligns with the objective of developing a reliable parameterized simulation workflow for computing the thermal performance of green façades.

Acknowledgements

All on-site measurments and photographs of the green façades, and the illustration in Figure 1, are provided by GRITLAB at the John H. Daniels Faculty of Architecture, Landscape and Design at the University of Toronto. We thank Liat Margolis, Liam O'Brien and Scott MacIvor for the experimental design. We also acknowledge Benjamin Matthews, Curtis Puncher, Catherine Yoon and Matthew Perotto for help installing the façades and planters and photo documentation, as well as Jennifer Drake and Gabrielle Gomes Calado for the thermal photography. We are also grateful to greenscreen® Bioroof, Tremco, IRC Building Science Group, Campbell Scientific, the University of Toronto Facilities & Services and the John H. Daniels Faculty of Architecture, Landscape, and Design, MITACS, RCI Foundation and the City of Toronto Environment Office for funding and/or materials and services.

References

ALEXANDRI, E. 2008. Temperature decreases in an urban canyon due to green walls and green roofs in diverse climates. Building and Environment. 43. 480-493.

CHUA, S. Light vs. Distance. UC Berkeley: Berkeley Center for Cosmological Physics. 12. (http://bccp.berkeley.edu/o/Academy/workshop_09/pdfs/InverseSquareLawPresentation.pdf).

HUNTER, A. et al. 2014. Quantifying the thermal performance of green façade: A critical review. Ecological Engineering. 63. 102-113.

HUTCHEON, N.B., AND HANDEGORD, G. O. P. 1995. Building Science for a Cold Climate. Institute for Research in Construction. 222-225.

IBARRA, D.I., AND REINHART, C. 2009. Daylight Factor Simulations —how close do simulation beginners 'really' get. Building Simulation 2009 Eleventh International IBPSA Conference. (http://web.mit.edu/tito_/www/Publications/BS09_DaylightingNovices.pdf).

IP, K., LAM, M., AND MILLER, A. 2010. Shading performance of a vertical deciduous climbing plant canopy. Building and Environment. 45. 81-88.

KÖHLER, M. 2008. Green façades—a view back and some visions. Urban Ecosyst. 11. 423-436.

KOYAMA, ET AL. 2013. Identification of key plant traits contributing to the cooling effects of green façades using freestanding walls. Building and Environment.66. 96-103.

LAGIO, K. 2014. Daylight factor and illuminance. DIVA for Rhion. (http://diva4rhino.com/user-guide/simulation-types/daylight-factor-illuminance).

PRICE, J. W. 2010. Green Façade Energetics. University of Maryland: Department of Envrionmental Science and Technology.

PUNCHER, C. 2012. Species fact sheet: Virginia creeper. GRITLAB. (http://grit.daniels.utoronto.ca/wp-content/uploads/2012/10/02.9_MATERIALS_ASSEMBLY_Green_Wall_SPECIES_FACT-SHEET_P_quinquefolia1.jpg).

U.S. DEPARTMENT OF ENERGY. 2013. EnergyPlus Energy Simulation Software. (http://apps1.eere.energy.gov/buildings/energyplus/cfm/weather_data3.cfm/region=4_north_and_central_america_wmo_region_4/country=3_canada/cname=CANADA).

WONG, ET AL 2010. Thermal evaluation of vertical greenery systems for building walls. Building and Environment. 45. 663-672.

Transit-Oriented Development (TOD): Analyzing Urban Development and Transformation in Stockholm

Todor Stojanovski, Tesad Alam, and Marcus Janson

KTH Royal Institute of Technology
100 44 Stockholm, Sweden
todor@kth.se, tesad@kth.se, marcusja@kth.se

Keywords: Transit-Oriented Development (TOD), Urban Morphology, Urban Analysis, Development Potential, Geographic Information Systems (GIS).

Abstract

Transit-oriented development (TOD) is a policy to design and develop dense, attractive and walkable urban environments that enhance the use of public transportation. In a broader perspective, TOD deals with synchronizing urban life—its growth and development, its everyday activities and mobility patterns—with public transportation systems.

Urban development is a product of negotiation, a political struggle between actors and stakeholders, their visions and interests, and their powers to induce urban change. In the background of urban politics, social and physical factors limit the potential to develop or transform. In this study, this potential for urban development and transformation is analyzed for three neighborhoods along the Tunnelbana, a subway line in Stockholm, with the help of geographic information systems (GIS) software. Two development scenarios are explored: one with TOD applied, the other with it dominating as a policy.

1. INTRODUCTION

Transit-oriented development (TOD) was introduced by Peter Calthorpe at the beginning of the 1990s as the design or development of moderate- or high-density mixed use urban environments at strategic points along a regional public transportation system (Calthorpe 1993). There are many definitions for TOD, depending on context, but TOD is almost always associated with high urban density, urban mixity and high-quality walking environments to enable access to public transportation (Cervero et al. 2004; Currie 2005). The argument of proponents for TOD and the compact city, its European parallel, is that urban density and diversity contribute to higher use of public transportation and more liveable cities (Pushkarev and Zupan 1977; EC 1990; Naess 2006; Susilo and Stead 2009; Ewing and Cervero 2010).

TOD is nothing new as a policy. Cities during industrialization grew near public transportation. Urban life pulsated in time to train schedules and thrived around train stations. Stockholm by example developed gradually along its public transportation systems for almost two centuries as a "transit metropolis" (Cervero 1996) and much effort in its planning and development, even today, is spent on improving public transportation access. It is a city that is growing quickly, with almost 30,000 new inhabitants per year, and there are ongoing discussions about extending the Tunnelbana, its subway network. A new subway line has been proposed to focus more urban growth around stations, improve regional connectivity and decongest the central station (Figure 1).

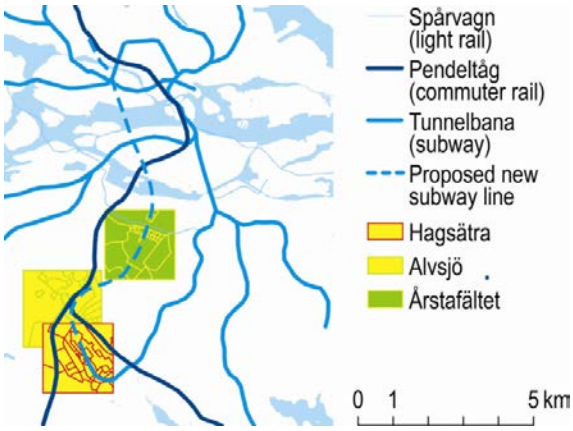

Figure 1: Transportation relationships and the potential for urban development and transformation in three Stockholm neighborhoods.

The newly proposed subway line links the Älvsjö, Hagsätra and Årstafältet neighborhoods (in the south of Stockholm), targeting them as three foci for new urban

growth and development. Hagsätra and Älvjsö are existing regional nodes of the Tunnelbana and the Pendeltåg (the commuter rail network in Stockholm). The Tunnelbana and Pendeltåg are primary radial lines in the regional public transport system. Årstafältet is tangentially traversed by a secondary orbital light rail system, the Tvärbana. The challenge is to transform and develop the three neighborhoods into walkable and lively urban environments where it is easy to take public transportation. What is the potential to develop these three neighborhoods? How rigid are the existing urban environments as social and physical systems to change and transformation? How have these neighborhoods developed in the last two decades?

2. METHODS

The city in urban morphology is a mosaic of urban areas or spaces. It is defined as a "complex individual" of different urban quarters (Reclus 1905:385) or "a mosaic of little worlds that touch, but do not interpenetrate" (Park 1925:40). This analysis focuses on neighborhoods as dynamic mosaics, where each piece of the mosaic has a distinctive meaning and status, recognized in society as unique or typical. We analyzed three neighborhoods, tessellated as mosaics, with the help of geographic information systems (GIS) software. ArcGIS and IDRISI are used for analysis and visualization. The data is from Lantmäteriet (National Land Survey of Sweden) and the basemap from Bing Maps.

The potential for urban development and transformation is analyzed and quantified, represented on a desirability map with a value from 0 to 100, where a higher value shows more potential for the place to develop or transform. The desirability map is a result of Multi-Criteria Evaluation (MCE), a powerful analysis tool in GIS when "multiple and conflicting criteria, interests and objectives are concerned" (Carver 1991). Analytic Hierarchy Process (AHP) is used to structure those factors that affect the potential for urban development and transformation, and to calculate the weights in between.

2.1. Conceptualizing potential

The potential for development and transformation is described by two factors: the attractiveness of the urban environment as a dynamic state, and the different drivers of urban change as processes. The potential for densification (*förtätningspotential*) is a measure described in the report "Denser Stockholm" ("Tätare Stockholm"). It includes need (*behov*) and pressure (*tryck*), available space (*utrymme*), and legislative freedom (*frihet*) for densification (SSL, 2009). These four factors are reduced to three to capture the interplay between attractiveness and development. 1. **Freedom** includes not only the maximum legislative freedom, but also the economic and technological capacity, to develop or transform. 2. **Pressure** is influenced by the political economy and physical state of the urban environment. Buildings have a life span and a life cycle; as a result, physical factors such as deterioration can increase the pressure. Other social and political factors, like status and popularity of neighborhoods, also affect the need to develop or redevelop. The economy continuously needs growth and more pressure to develop. 3. **Easiness** (to develop or transform) shows the political and physical possibilities to develop or transform the existing urban form: firstly by physical hindrance (newer and more complex urban environments are more difficult to develop) and secondly by opposition due to popularity and status of the existing built environment. The urban form is a major factor that links these factors and also defines attractiveness. Attractiveness also depends on proximity–-to urban cores and activity centers, to forests, parks and waterfronts, and to transportation, the TOD factor (Figure 2).

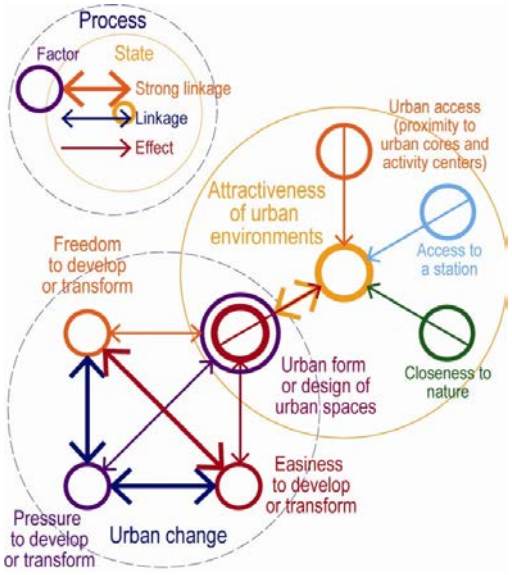

Figure 2: Relationships in the potential for urban development and transformation

2.2. Quantifying the potential

Swedish urbanization is characterized by a growth of distinctive neighborhoods, recognizable cityscapes that are described as urban characteristics (*stadskaraktärer*) or

Urban characteristic or type	Planning measures	Social perception and status	Development potential	Pressure	Easiness	Freedom
Äldre Förstad (older suburb centers)	Preserved and developed	High status	Very limited	10	50	100
Villastad (detached townhouses)	Infill development can occur when balance maintained	High status	Very limited	10	50	100
Smalhusområden (early modern blocks)	Preserved and developed	Neither low nor high	High potential	70	50	100
ABC radhusområde (modern row houses)	Preserved and developed by its origins	Neither low nor high	Limited potential	10	50	100
ABC centrum (modern suburb centers)	Preserved and developed by its origins	Low status	High potential	100	50	100
ABC lamellhus (modern apartment blocks)	Preserved and developed by its origins	Low status	High potential	100	50	100
ABC punkthus (modern apartment towers)	Preserved and developed by its origins	Low status	High potential	100	50	100
Miljonprogram (late modern apartment blocks and towers)	Developed with respect for the qualities in the original design	Low status	High potential	100	50	100
Institutionsområden (institutional areas)	Not specified	Low status	High potential	10	50	100
Verksamhetsområden (industrial areas)	Developed according to their different conditions	Depending on the type of industry	High potential	70	50	100
Småhusområden (detached houses)	Not specified	High status	Limited	10	50	100
Nyare stadsenklav (newer apartment blocks)	The areas' holistic view must be respected	High status. Newer areas.	Limited	10	10	100
Öppen mark (open space)	Develop or preserve depending on the area	Depends on the area	Either very high potential or assigned as preserve	100	100	100
Stations	Not specified	Not considered	Not considered	0	0	0

Table 1: Planning measures and development potential of the Swedish urban typology, with values for the urban development and transformation and urban attractiveness factors that derive from the social perception, popularity and status of typical neighborhoods. Derived from previous research on the attractiveness of typical urban environments.

types. Much research has been done on categorizing architecture and urban environments, in regard to architectural styles (Björk et al. 1983), social and economic epochs (Engström et al. 1988), planning paradigms (Rådberg 1988; Rådberg and Friberg 1996), or historical urbanization; for example of Stockholm (Forshed 1997; SSK 1997; 2000). The type is the underlining concept in this morphological tradition. The society creates types of buildings and neighborhoods, and architectural styles in order to simplify communication and promote values (Franck 1994:345). The typo-morphological research on Swedish cities is a background to quantify the strength of the urban form and the drivers of urban change factors. The values in Table 1 are defined by research on urban quality in Swedish urban typologies (Rådberg and Johansson 1997; Rådberg 2000), their social structure and status and possibilities to develop (Engström et al. 1988), and the urban legislation (SSK 1997; 2000). The urban politics, physical characteristics and the social perception (especially if a neighborhood is regarded as attractive or prestigious) influence the potential.

The proximity factors are defined by accessibility as Euclidean distance (Figure 3). Rings of buffers starting from the edges of the attractiveness cores are used in the maps. The values are stipulated to be different for the three factors. They drop more steeply for distance from natural frontages. The assumption is that prospects on a park, water body or forest are more attractive. On the other hand, urban attractiveness is assumed to fade away more slowly.

The buffers for access to a station, the TOD factor, show a different trend. The attractiveness value is very low in areas in direct proximity to a station, which is not a very attractive place. The most attractive ring has station accessibility, but not direct proximity: between 50 and 150 meters, or 1 to 2 minutes walk from the station. After 150 meters, the attractiveness value falls gradually as the distance increases.

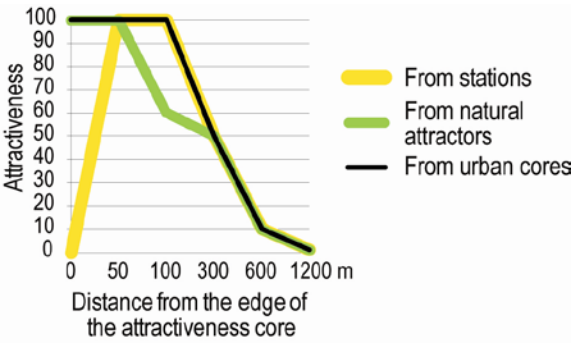

Figure 3: Relationships in the potential for urban development and transformation.

2.3. Description of scenarios

There are three scenarios to be applied: the baseline, the hypothetical TOD, and the Max development TOD, where TOD dominates as a policy and the development . The difference is seen in a change in the strength for the TOD factor and the freedom factor. The strengths and interrelationships between the various factors form the background for Analytic Hierarchy Process (AHP) and the factors range from extremely less important to extremely important for urban development (Figure 4).

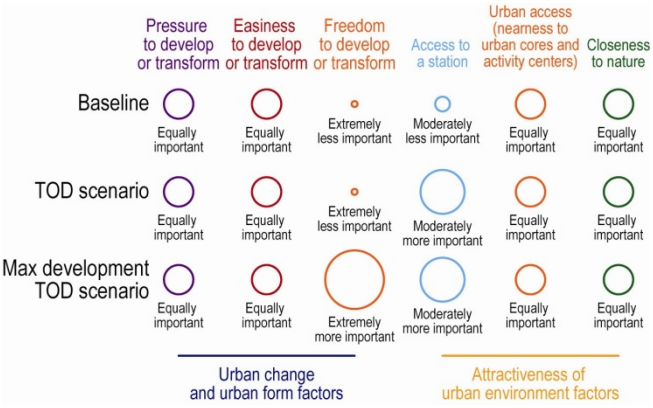

Figure 4: Strength of the factors in the different scenarios.

The pressure, easiness, urban attractiveness and access to nature are equally important factors in the baseline, while the freedom factor is extremely less important. The Swedish municipalities have a planning monopoly and the urban development is controlled by urban legislation. Thus the freedom factor is extremely less important than the pressure and easiness factors that are defined by the characteristics of urban form and social perception and status. The urban typology in Stockholm gives specific recommendations for development and transformation for the different urban characters (SSK 1997; 2000).

The TOD factor, indicating proximity to stations, is assumed in the AHP as moderately less important for the baseline. There is empirical evidence for this claim. The research in Sweden shows that the type of neighborhood and quality of the urban environment is a determinant for urban attractiveness, while proximity to a station is considered only half as important (Rådberg 2000). Similar results were replicated in TOD surveys of neighborhoods in Los Angeles, San Francisco and San Diego. More than half to two thirds of respondents listed type and quality of neighborhood as the reason why they moved to an area; only between a fifth and a quarter of the respondents listed proximity to a train station. San Francisco is an exception, where the proportion of respondents citing proximity to transportation was almost half, only slightly lower than those citing neighborhood quality (Lund 2006).

In the TOD scenario, the strength of the TOD factor and the other factors are reversed. The TOD factor is believed to be moderately more important than type of neighborhood and quality of the urban environment. This scenario assumes a dramatic change in the perception of public transportation and high demand for living in developments built close to stations.

In the last scenario, Max development TOD, the station proximity factor is the same as in the TOD scenario, but there is complete freedom for development (and corresponding lack of urban legislation). The freedom factor has a maximum value of 100 and is extremely more prominent than the other factors: pressure, easiness, urban attractiveness and access to nature. This scenario assumes extreme inclination towards TOD and the freedom to achieve this goal. Development targets not only the existing neighborhoods around the stations, but everywhere else. The TOD factor is highest in the hierarchy, but the other factors are also important.

Factors	Baseline	TOD scenario	Max development TOD
Pressure	0.2211	0.188	0.1075
Freedom	0.0212	0.0209	0.4026
Easiness	0.2211	0.188	0.1075
Urban access	0.2211	0.157	0.085
Access to a station	0.0944	0.2892	0.2124
Closeness to nature	0.2211	0.157	0.085

Table 2: Relative weights for the factors in the different scenarios.

The weights of the factors in the different scenarios are calculated with the AHP tool in IDRISI (Table 2). The consistency ratios between factors are acceptable (0.02 for the baseline, 0.03 for the TOD scenario and 0.05 for the Max development TOD).

2.4. Analyzing the neighborhoods

The morphological analysis of distinctive characteristics or urban types in the three neighborhoods, together with the mapping of the urban and natural attractiveness cores, are represented on Figure 5. The classification is done by mixing the official typology of urban characteristics of the city of Stockholm (SSK 1997; 2000) with Rådberg and Friberg's (1996) book "Swedish urban types" ("Svenska stadstyper"). Each urban characteristic or type has a specific value for pressure, easiness and freedom factors (Table 1). These values are input in the MCE and executed in IDRISI with the relative weights for the six factors from Table 2.

2.4.1. Älvsjö

Älvsjö is an industrial suburb ("äldre förstad" in the typology) in the southern part of the municipality of Stockholm. The Älvsjö railway station opened in 1879 and an urban village (*villastad*) developed around the station in the early 20th century. An expansion with infill of modern apartment blocks began during the 1940s and Stockholm International Fairs and Congress Centre (Stockholmsmässan) was established in the 1970s. Urban development continued during the 1980s with postmodern apartment buildings built north of the station.

Älvsjö is a major transportation hub and transfer point where the orbital trunk bus lines cross with the commuter rail line, Pendeltåg. Älvsjö is today seen as one of the most important urban development areas in Stockholm. The municipality considers the area to have great potential for housing and offices due to its central location and closeness to public transportation. Development is ongoing and the newer developments display a mix of residential units, workplaces and services, with a distinctively late postmodernist style.

2.4.2. Hagsätra

Hagsätra is a modern suburb (*ABC stad*) in the southern part of the municipality of Stockholm. Hagsätra includes the terminal station of one of the branches of the Green line and represents a rather typical Tunnelbana suburb in a Swedish context. The suburb was a consequence of modernist large-scale planning during the 1950-1960s, when the vision was to create neighborhoods around subway stations with proximity to workplaces, shops and services. The entire neighborhood developed simultaneously with the inauguration of the subway station and the community center (Hagsätra centrum) beside the station. The neighborhood is a mix of apartment blocks arranged freely in the landscape (ABC lamellhus), and towers (ABC punkthus) that surround the community center (ABC centrum) where shops, institutions and services are located. During the 1990s the area was complemented with new postmodern apartment buildings with partially enclosed blocks (*nyare stadsenklav*) in continuation from Hagsätra Centrum.

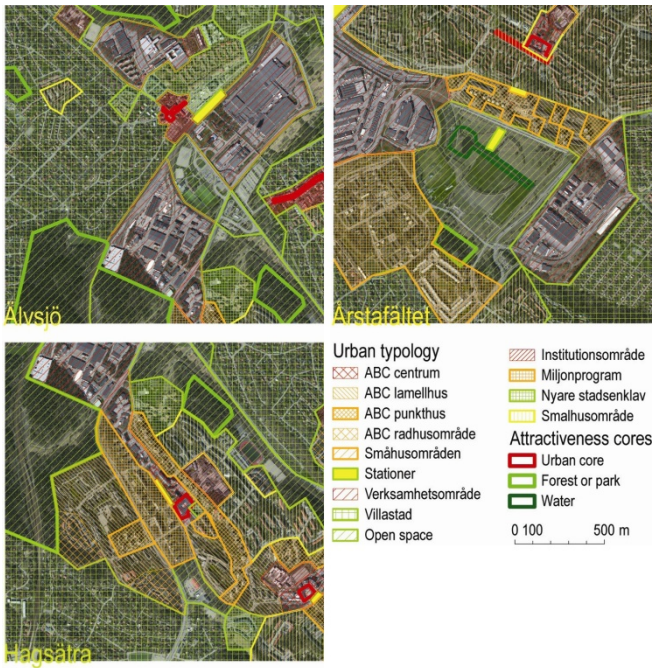

Figure 5: A typo-morphological study of the neighborhoods, with attractiveness edges. These maps are background for the desirability maps in the MCE. The values for the different factors for each urban characteristic or type are shown in Table 1. The attractiveness from urban and natural edges is shown in Figure 3. The desirability maps were created in IDRISI with the buffer tool.

2.4.3. Årstafältet

Årstafältet lies to the south of Årsta, one of the earliest modern suburbs of Stockholm, just adjacent to the urban core. Årsta developed in the 1940s primarily with apartment buildings (*smalhus*) characteristic for Sweden at that time, with 2-3 stories and small apartments with three orientations. The southern edge of Årsta, which is located in the northern part of Årstafältet, developed in the 1950s and 1960s as a mix of smaller apartment blocks (ABC lamellhus) and towers (ABC punkthus). New industrial

buildings and warehouses also developed in the 1980s. In the 2000s the Tvärbana, a new orbital light rail line, was built between Årstafältet and Årsta, introducing two new public transportation nodes: the Pendeltåg and light rail station, Årstaberg, opened in the northwest, and, the new light rail station Valla Torg between Årstafältet and Årsta. At the same time, the area around the light rail station Valla Torg was filled in with new buildings that were designed to fit in with the character of surrounding apartment blocks and towers from the 1950s and 1960s. The municipality of Stockholm has assigned Årstafältet as a new development zone. The new district will be characterized by apartment buildings in enclosed urban blocks (*nyare stadsenklav*), with mixed functions, where services along with housing are to be developed (SSK, 2010).

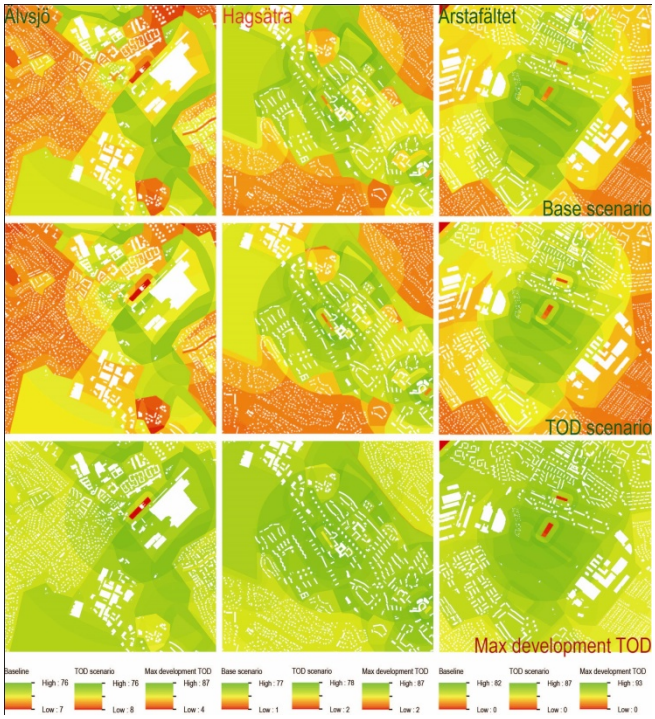

Figure 6: Map comparing the development potential of the different scenarios. Result of MCE of the values for the factors (Table 1 and Figure 3) with the AHP weights (Figure 4) in IDRISI.

3. RESULTS

Figure 6 illustrates the potential for development and transformation of the three areas. The greener the area on the map, the more desirable it would be for development; the least desirable areas are red. The analysis shows that there is space for urban development. There are contiguous areas with high development potential in Årstafältet and Älvsjö, whereas in Hagsätra the areas with higher potential are smaller and scattered. The TOD scenario puts an emphasis on the second ring around the station (areas within 5 minutes or between 100 and 300 meters from the station) as the zone with highest potential for TOD. The potential in the Max development TOD scenario does not consider the complexities behind friction or opposition to urban change, and thus shows a conical form. The potential is higher also in the open areas and areas in proximity to parks and urban forests.

4. DISCUSSION AND CONCLUSIONS

The potential for development and transformation is a concept that quantifies on a map the interplay between the attractiveness of urban environments and the processes of urban change and transformation. These factors are dynamic. The urban environments are continuously interpreted and revised in society. Namely, each stakeholder sees a different desirability map and it uses it as a stronger or weaker actor in the planning and development process. The political struggle between actors and stakeholders is not analyzed here, but it can be captured with an improved MCE method.

How does the potential compare to reality? The baseline conceived as a realistic or zero alternative is validated. The previously developed areas and ongoing projects are located in the areas for highest development potential. The newly proposed projects are also in zones with high development potential in the baseline and in the TOD scenarios (Figure 7). In a previous study evaluating the development potential along the new BRT line in Karlstad (Stojanovski 2011), the new zones assigned for growth and development by the new urban plan (Karlstads kommun 2012:71) had the highest potential.

How have these neighborhoods developed in the last two decades? Did historical development proceed according to the TOD principles? The accessibility to public transportation in Stockholm is considered as a 600 meter buffer (that is, roughly a 10 minute walk) from a Tunnelbana station. The results (Figure 7) show differences between neighborhoods, but in general the development followed a principle defined by a 600-meter distance to a station. The 600 meter buffer accessibility, however, does not reflect the real TOD attractiveness that is more a phenomenon of urban cores and attractive directions (Stojanovski 2013b). This is also a case for proximity to attractive urban and natural edges.

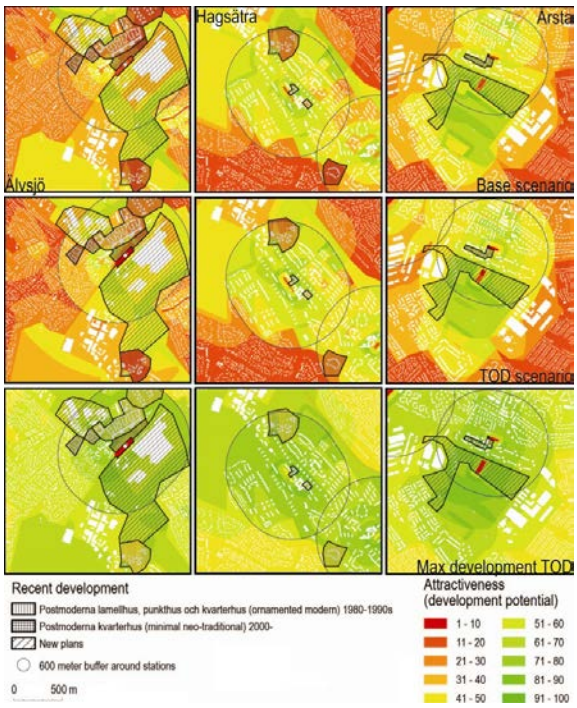

Figure 7: The different scenarios (normalized values) compared with the urban development and ongoing planning projects in reality. Result of MCE of the values for the factors (Table 1 and Figure 3) with the AHP weights (Figure 4) in IDRISI. The development areas were mapped in ArcGIS.

How does the potential for development and transformation relate to TOD? The guidelines for TOD describe a functional and architectural mix and density, regional connectivity, easy access to the station and high quality service with high frequency (Calthorpe 1993; Dittmar and Poticha 2004). The proximity to a station is the only TOD factor that is directly included in the analysis. The urban form aspects are indirectly considered through changes in the strength of factors in the scenarios. The transportation factors were excluded because the neighborhoods are located on the same branch of the line (similar regional connectivity and characteristics of public transportation service). GIS captures the attractiveness through checkboard cells or discrete objects and it is applicable for urban analysis around stations with no space-time convergence where the urban space is continuous. One urban region is more complex with its chorographic phenomenon of convergence of urban spaces and "death of distance". The method needs additional factors to better capture the mobilities between the pieces of the urban mosaic, as discrete objects (3D urban environments) that are in relation to other discrete objects, but represented on the 2D map (see Stojanovski, 2013a).

In GIS and urban modeling and simulation, the main focus is on cells, agents and automation (Batty, 2009). Urban morphology classifies physically and socially recognizable urban environments into objects with social meaning, states and potential for change. The cells and agents are merged into unique or stereotypical urban environments. In the context of Luhmann's social systems (1995) there are systems that continuously construct and revise the environments they are in. The urban typologies are constructs, and as pieces of the urban mosaic they are objects that also can be analyzed, modeled and simulated in a matrix. This is a compelling framework to analyze what will happen if a new policy, for example TOD, is applied in an existing urban environment with its social meaning.

Overall, the concept of development and transformation potential captures the friction and rigidity of urban environments and emphasizes zones with high potential that in reality are targeted by developers and planners in Sweden. It is very hard to predict precisely where within these zones a neighborhood will develop, or if it will develop at all, but the method shows all the choices.

For more detailed analysis, there is a need to classify the potential of individual buildings and plots. The analysis here is on the level of an urban block, because the differentiation of buildings requires more detailed data and building-by-building mapping. The attractiveness cores also need improved classification. There are differences between forests and parks, urban cores and centers, and differences in how attractiveness spreads from them. For example, in the urban cores the streets and squares are interconnected. Modern urban cores and centers have a frontage and a backside. The frontage is always attractive, whereas the backsides (of modern community centers, for example) are zones that are almost always unattractive and grey, asphalted open or enclosed spaces assigned for parking or logistics. The backside of a modern urban core is a detractor and spreads unattractiveness outward; while its core is very attractive. Another direction for future development is looking at the interplay between attractors and detractors. There are detractors in the urban environment too, such as rock outcrops or other terrain obstacles, unattractive urban environments (like the concrete cityscapes under or adjacent to transportation infrastructure), or deteriorated buildings or areas. The terrain in Hagsätra is much more difficult to develop than in Älvsjo and Årstafältet. The range from -100 to 100 for the development potential would be more appropriate.

Overall, the method is compelling and shows promise. It can deliver maps with a policy or actor perspective and bring them into the planning processes and negotiations. With the growing popularity of policies like TOD that prioritize redevelopment and growth within certain urban boundaries, urban transformation of existing neighborhoods will be stronger on the urban planning and design agenda.

References

BATTY, M. 2009. Urban modeling. International Encyclopedia of Human Geography. Oxford: Elsevier.

BJÖRK, C., REPPEN, L. AND KALLSTENIUS, P. 1983. Så byggdes husen 1880-1980: arkitektur, konstruktion och material i våra flerbostadshus under 100 år. Stockholm: Statens råd för byggnadsforskning.

CALTHORPE, P. 1993. The next American metropolis. Princeton Architectural Press: Princeton.

CALTHORPE ASSOCIATES. 1992. The TOD design guidelines. San Diego: City of San Diego.

CARVER, S. J. 1991. Integrating multi-criteria evaluation with geographical information systems. International Journal of Geographical Information Science, 5(3), 321-339.

CERVERO, R. 1998. The transit metropolis: a global inquiry. Island Press: Washington, DC.

CERVERO, R., ET AL. 2004. Transit-Oriented Development in the United States: Experiences, Challenges, and Prospects. TCRP Report 102. Washington, D.C.: Transportation Research Board.

CURRIE, G. 2005. Strengths and weakness of bus in relation to transit oriented development. Paper presented at the conference Transit Oriented Development–Making it Happen, Perth, Australia.

DITTMAR, H. AND POTICHA, S. 2004. "Defining transit-oriented development: the new regional building block", in Dittmar, H., and Ohland, G. (eds.). The new transit town: best practices in transit-oriented development. Washington D.C.: Island press.

EC (EUROPEAN COMMISSION). 1990. Green paper on the urban environment. EC.

ENGSTRÖM C.J, LINDQVIST A., LAGBO E. AND LANDAHL, G. 1988. Svensk tätort. Stockholm: Svenskakommunförbundet.

EWING, R. AND CERVERO, R. 2010. "Travel and the Built Environment". Journal of the American Planning Association, 76(3), 265-294.

FRANCK, K.A. 1994. "Types are us", in Franck, K.A. and Schneekloth, L.H. (eds.). Ordering space: types in architecture and design. New York: Van Nostrand Reinhold.

FORSHED K. 1997. "New Design Guidelines for Stockholm", in C.G. Guinchard (ed.), Swedish Planning Towards Sustainable Development. Gavle: Wesdund & Soner.

KARLSTADS KOMMUN. 2012. Översiktsplan för Karlstads kommun 2012: http://karlstad.se/filer/Bygga/Samhallsutveckling_planering/Oversiktsplan_2012_120916.pdf

LUHMANN, N. 1995. Social systems. Stanford: Stanford University Press.

LUND H. 2006. "Reasons for Living in a Transit-Oriented Development, and Associated Transit Use". Journal of the American Planning Association, 72(3), 357-366.

NAESS, P. 2006. Urban structure matters: residential location, car dependence and travel behaviour. London: Routledge.

PUSHKAREV, B. AND ZUPAN, J. 1977. Public transportation and land use policy. Indiana University Press: Bloomington.

PARK, R., BURGESS, E., AND MCKENZIE, R. 1925. The city. Chicago: University of Chicago Press.

RECLUS, E. 1905. L'homme et la terre, tome cinquième. Paris: Librarie universelle.

RÅDBERG, J. 1988. Doktrin och täthet i svenskt stadsbyggande 1875-1975. Stockholm: Statens råd för byggnadsforskning.

RÅDBERG, J. 2000. Attraktiva kvarterstyper: en undersökning av bebyggelse, befolkning och attraktivitet i Stockholm Söderort. Stockholm: Kungliga Tekniska högskolan.

RÅDBERG, J. AND FRIBERG, A. 1996. Svenska stadstyper: historik, exempel, klassificering. Stockholm: Kungliga Tekniska högskolan.

RÅDBERG, J. AND JOHANSSON, R. 1997. Stadstyp och kvalitet. Stockholm: Kungliga Tekniska högskolan.

SLL (STOCKHOLMS LÄNS LANDSTING). 2009. Tätare Stockholm - Analyser av förtätningspotentialen i den inre storstadsregionens kärnor och tyngdpunkter - Underlag till RUFS 2010 och Stockholms översiktsplan. Stockholm: SLL.

SSK (STOCKHOLMS STADSBYGGNADSKONTORET). 1997. Stockholms byggnadsordning. Stockholm: SSK.

SSK. 2000. Översiktsplan för Stockholm 1999. Stockholm: SSK.

SSK 2010. Översiktsplan för Stockholm. Stockholm: SSK. www.stockholm.se/PageFiles/267645/52638_Slutrapport_lowNY.pdf

STOJANOVSKI, T. 2011. The urban development along the newly proposed BRT line in Karlstad, manuscript published in Bus rapid transit (BRT) and transit-oriented development (TOD): How to transform and adjust the Swedish cities for attractive bus systems like BRT? What demands BRT? Stockholm: KTH Royal Institute of Technology, 239-258.

STOJANOVSKI, T. 2013A. City information modeling (CIM) and urbanism: blocks, connections, territories, people and situations. In Proceedings of the Symposium on Simulation for Architecture and Urban Design. Society for Computer Simulation International.

STOJANOVSKI T. 2013B. Public transportation systems for urban planners and designers: the urban morphology of public transportation systems. In Proceedings of the Third International Conference on Urban Public Transportation Systems. American Society of Civil Engineers.

SUSILO, Y. O., AND STEAD, D. 2009. "Individual carbon dioxide emissions and potential for reduction in the Netherlands and the United Kingdom", Transportation Research Record: Journal of the Transportation Research Board, 2139(1), 142-152.

Scenario Modeling for Agonistic Urban Design

Trevor Patt and Jeffrey Huang

École Polytechnique Fédérale de Lausanne
CH-1015 Lausanne, Switzerland
trevor.patt@epfl.ch, jeffrey.huang@epfl.ch

Keywords: Design Methods, Computational Urbanism, Urban Agriculture, Scenario Modeling.

Abstract

This paper describes a method for incorporating computational scenario modeling for integrated urban agricultural projections as an aid to the design process and the formulation of urban design guidelines. This method involves unique solutions for simplifying the input and management of large quantities of location-based data and hybridized processes for decision making among diverse and distributed behaviors. The project utilizes commonly available 3D modeling software (Rhinoceros with Grasshopper) to produce a responsively interactive simulation of urban potentials for given parameters as well as a contextualizing series of alternate scenarios using variable parameters.

1. INTRODUCTION

Despite a growing pressure on the cities of Switzerland to alleviate housing shortages there is a resistance to both vertical and horizontal expansion (Hayek et al. 2010). Vertical Density is seen as a threat to the visual culture of the cities and the urban landscape, while horizontal sprawl erases the connection of the city to the rural, agricultural patrimony of the country. (Diener et al. 2006).

The project described here works to negotiate the conflicting desires of urban densification and preservation of an agricultural landscape at the periphery of the city. Specifically, it develops a series of discrete 'best practice' recommendations for integrating urban agricultural development (Verzone and Dind, 2011) into a computational model for projecting different scenarios and hypotheses about potential urban futures. Though these recommendations seem straightforward and intuitive when conceived on their own, implementation on a real site leads to a complex interaction between competing interests, which is too complex to be sufficiently explored through a traditional design process without destructively reducing the problem. Furthermore, tracing these interactions is too time-consuming for a design team to produce more than a handful of possibilities. This project uses a computational model as a means for informing the design of complex urban situations, producing both potential massing volumes for direct testing of given parameters (Figure 1) and generates contextualizing data relating the given scenario to a broad range of other variation.

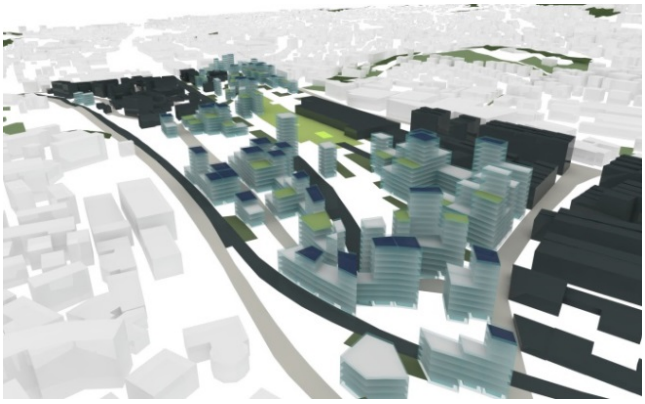

Figure 1. A rendering of one example of a generated urban scenario.

2. DESCRIPTION OF METHODS

The initial strategy for enacting the multiple interests and their interaction is to fragmentize the site into an urban grid, or meshwork, and to reinstantiate the diagram at each instance, effectively creating a set of immobile agents through which the diagram is routed as localized affinities or behaviors (Lehnerer 2009). This section will first detail the setup and interaction with the meshwork, then describe the decision making processes, and finally the output.

2.1. Data Structure and Management

A custom script reads the 'grid' and automatically formats it as a Half-Edge Mesh (de Berg et al. 2010), which is used as the standard reference for the entire model (Figure

2). The use of the Half-Edge Mesh (HEM) frees the base grid from reliance on geometrical properties for identification of face location or adjacency. The HEM has no restrictions on vertex valence and reconstructs topology on-the-fly for any edits. As implemented in this project, it is able to calculate 3-dimensional meshes, allowing the grid to follow the site topography. It has partial, but limited, ability to compute manifold meshes; however these are not a high priority in this kind of urban grid, which is assumed to be most often at ground level. The automation of this process gives the designer wide input as to the character of the grid and its parcels—their size, number, grain, direction—without requiring technical input or formatting beyond basic computer drafting skills.

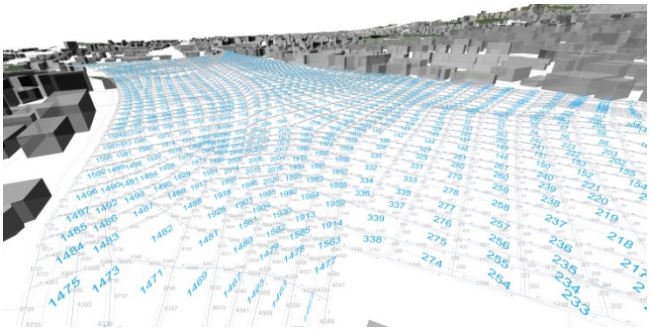

Figure 2. The final urban grid as a Half-Edge Mesh with face and half-edges labeled.

The mesh uses faces as the primary unit of identity, adding territory, shape, and orientation data to the system in addition to location. These additional qualities allow better approximation of and integration with the existing context as well as more meaningful location-specific data—whether calculated from the site model, like elevation change within a parcel, or user input, such as establishing a height zoning regulation. Each face is treated as though it were an immobile agent within a multi-agent system with the ability to communicate with neighbors, adjust internal values, and store associated state values as metadata.

However, the software used does not allow new class definitions, so all metadata was stored separately in a .csv file, which necessitates an element of centralized control to retrieve and overwrite face values. Because the face index is not determined by location in an intuitive way, data entry directly within this .csv file through a text editor, while possible, is not very practical. Datasets can be input or edited directly within the parametric modeling environment (Grasshopper) or by external members of the design team through an image map.

2.2. Behaviors

Because the agents in this system are immobile, their main action is the actualization of parcels as productive landscape or as built volumes through application of the original siting recommendations (Verzone and Dind, 2011).

The recommendations were abstracted from text-based rules to quantitative incentives or disincentives of various intensities for four possible outcomes: productive agriculture or garden usage, low-rise building (2-6 floors), mid-rise building (5-9 floors), or high-rise building (8-12 floors). These recommendations include passive reaction to the physical conditions, such as encouraging the use of flat ground for agricultural production, discouraging the replacement of existing buildings with volumes that would produce lower density, or ensuring a healthy amount of direct sunlight (Figure 3). These incentives are combined to produce a fitness value at each face for each type of usage (Figure 4).

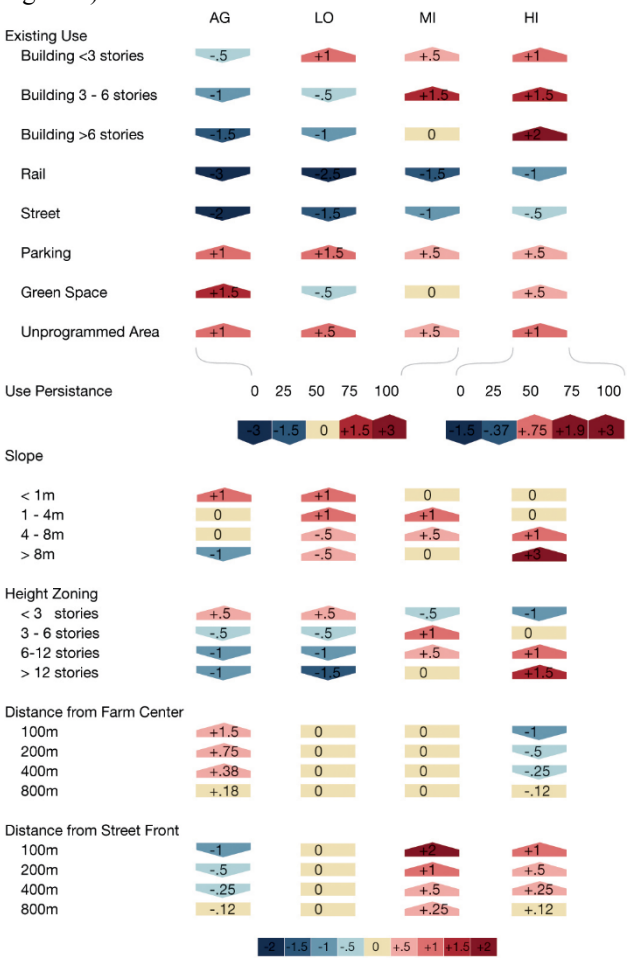

Figure 3. Diagram of site influences and their impact on use actualization.

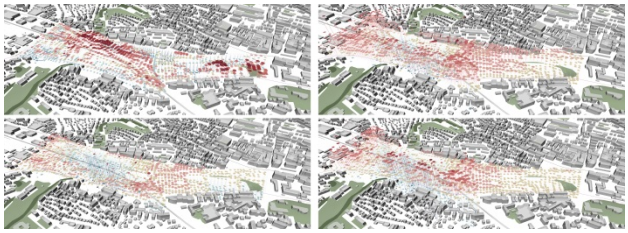

Figure 4. Datascapes of fitness value for each usage type: left column, agriculture and low-rise; right column, mid-rise and high-rise

The fitness values serve as a base for initiating actualization, but are not the sole input. During the actualization process, the computational model also computes more actively engaged responses (Figure 5). For example, building masses trigger adjustments to the adjacent faces, which are designed to encourage terracing and thus productive roof space as well as solar exposure. Similarly, agricultural use preserves its solar access by decreasing the fitness values for buildings (especially high-rise) where they might cast shadows over the crops.

In a more complex set of behaviors agricultural parcels are gathered together in an assemblage with more structured growth and location logic. The professional farm needs to be wholly continuous, whereas semi-professional plots are possible where faces connect to this area by only one edge (to increase the perimeter and the engagement with the urban public); finally, community gardens are sited completely separate from the farmland and in clusters of no more than three faces. This process of assemblage is used again on the building volumes to determine which areas might be suitable for roof gardens or photovoltaic arrays.

2.3. Output

The results of the locating process are visualized as three-dimensional surfaces and volumes within the site model (Figure 1). A variety of ancillary or derivative data useful to the designer for assessing the output can also be displayed, such as color coding the building volumes by height, plotting the height distribution on a bar graph, displaying the fitness values of actualized parcels compared to undeveloped parcels, projecting the FAR for different regions within the site, etc.

This data visualization was developed further by producing large sequences of scenarios (typically 750 solutions per sequence) with varying individual parameters (such as the target area for agricultural land or the desired m^2 of each scenario).

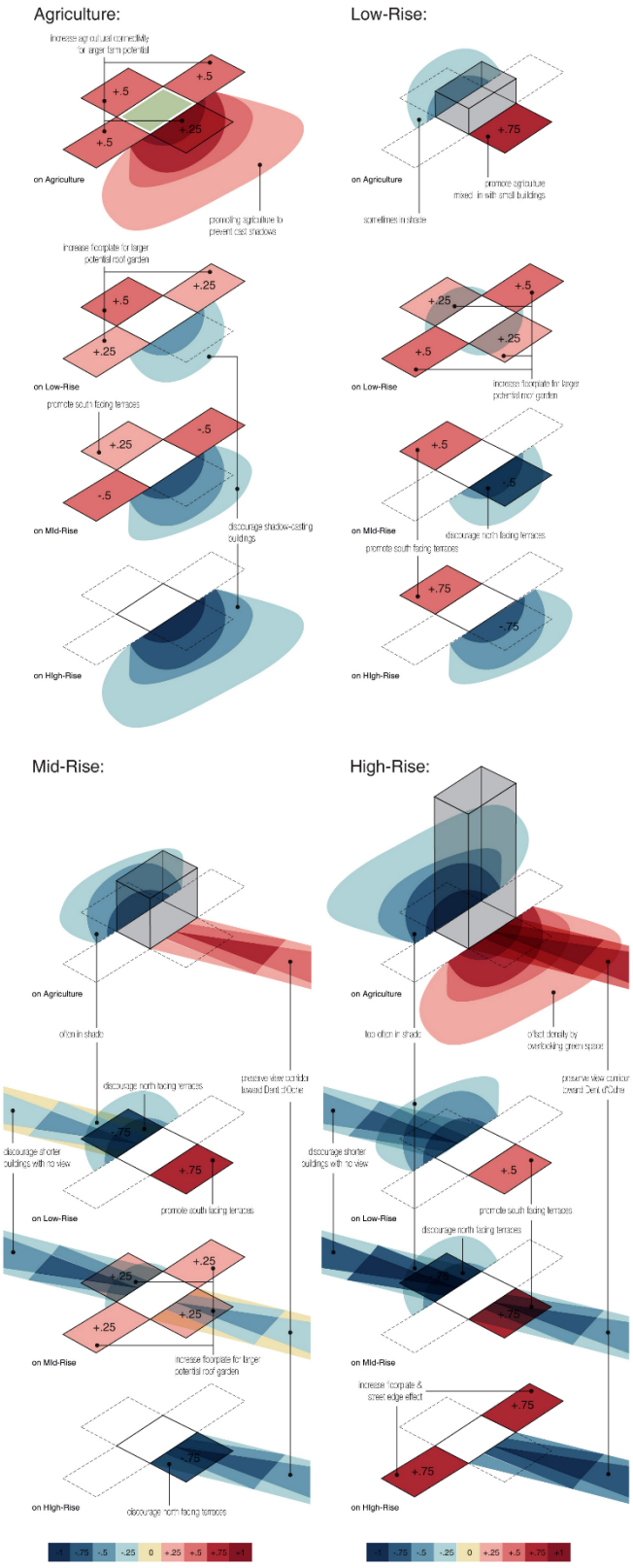

Figure 5. Diagram of adjustments to the fitness values (rows) of adjacent faces by different usage actualizations (columns).

These sequences could be viewed as an animation or charted as statistical plots to illustrate trends in how a set of behaviors manifest under different initial conditions. Individual scenarios can then also be identified within these plots and compared quickly and meaningfully to their alternatives (Figure 6).

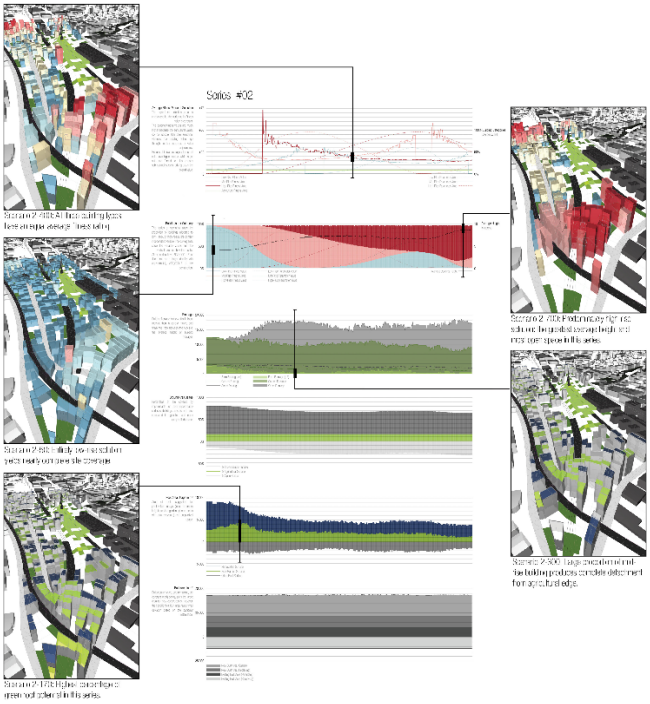

Figure 6. Five instances within a sequence of scenarios with a constant target of 625,000m^2 of new construction (bottom graph) and agricultural area of 1.75 hectares with a variation of the distribution of building heights (second graph: blue=low-rise, pink=mid-rise, red=high-rise). The remaining graphs show the fitness value of realized parcels (top); the total street, garden, and farm frontage (3rd); proportions of built, green, and open spaces (4th); the proportions of productive roof usage (5th).

3. CONCLUSION

This project developed a complex and robust parametric engine for the generation of computational urban scenarios, with a focus on flexibility and extensibility to other sites. The goal of these scenarios was to test the application of a diverse, and sometimes contradictory, set of siting recommendations for urban agriculture by simulating their interaction on an actual post-industrial site in Lausanne. The project succeeded in reproducing an environment of agonistic negotiation allowing the guidelines to respond sensitively to specific localized conditions without reducing the complexity inherent in the problematic or the site itself. Tools for visualization of the output were built into the computational model to aid the design process and convey differences in urban quality from one scenario to another.

4. FURTHER WORK

The robustness of the behavioral models (that is, the stability of relationships under diverse initial parameters) suggests that this method is less valuable as a way of producing 'blanket statement' guidelines for design (the role initially imagined by the research team) and more useful for testing the potential qualities of a set of behaviors across divergent conditions. This insight led to the production of the scenario sequences and the enhanced role of data visualization. This trajectory should be continued with more development of the statistical analysis and a method that makes adjustments to fitness values simpler to compare.

Acknowledging that many of the local behaviors that drive the actualization come from the architectural scale, it would be beneficial to incorporate more design parameters into the development process and not rely only on the abstract massings and usages. This should enable more complex interaction between the building volumes and the landscape and better link the local and global scales.

Acknowledgements

This project was carried out as part of the NRP 65 funded by the Swiss National Science Foundation.

The geographic data for Lausanne was provided by swisstopo through the GeoVITe portal: Reproduced with the authorization of swisstopo (JA100120), © 2013 swisstopo (JD100042).

References

DE BERG, M., CHEONG, O.,VAN KREVELD, M., OVERMARS, M. 2010. Computational Geometry: Algorithms and Applications. Springer, Berlin.

DIENER, R., HERZOG, J., MEILI, M., DE MEURON, P., AND SCHMID, C. 2006. Switzerland: An Urban Portrait. Birkhauser, Basel.

HAYEK, W., JAEGER, J.A.G., SCHWICK, C., JARNE, A., AND SCHULER, M. 2010. Measuring and assessing urban sprawl: What are the remaining options for future settlement development in Switzerland for 2030? Applied Spatial Analysis and Policy. Volume 4, Issue 4. Pages 249-279.

LEHNERER, A. 2009. The City of Kaisersrot: Not a Design, but the Result of a Mediated Process of Negotiation. Model Town: Using Urban Simulation in New Town Planning. INTI, Amsterdam. Pages 135-145.

VERZONE, C., AND DIND, J.P. 2011. De l'agriculture urbain au Food Urbanism: état des lieux et perspectives pour la Suisse. Urbia, Les Cahiers du développement urbain durable. Number 12. Pages 137-159.

Session 10: Smart and Sustainable Façades **191**

Acacia: A Simulation Platform for Highly Responsive Smart Facades 193
Daniel Cardoso Llach, Avni Argun, Dimitar Dimitrow, Qi Ai
Design Ecologies Laboratory, The Pennsylvania State University; Giner, Inc.

Sustainability Performance Evaluation of Passivhaus in Cold Climates 201
Kyoung-Hee Kim, Ph.D, Seung-Hoon Han, Ph.D
University of North Carolina at Charlotte and FrontInc.; Chonnam National University.

Acacia: A Simulation Platform for Highly Responsive Smart Facades

Daniel Cardoso Llach[1], Avni Argun[2], Dimitar Dimitrov[1], Qi Ai[1]

[1]Design Ecologies Lab
The Pennsylvania State University,
University Park, PA, USA, 16802
dzc10@psu.edu

[2]Giner, Inc
89 Rumford Ave,
Newton, MA, USA, 02466
aargun@ginerinc.com

Keywords: Responsive Architecture, Smart Windows, Simulation, Electrochromism.

Abstract

Recent advances in material science and high-precision digital manufacturing methods, as well as the increased availability of low-cost sensing technologies and processing power, are making programmable responsive surfaces viable alternatives to traditional building materials. These advances bring about opportunities to redefine building skins as interactive components with significant impact on the environmental and aesthetic dimensions of architecture. However, current modeling and analysis software systems largely consider building materials as static entities, making the design and assessment of programmable responsive surfaces (such as surfaces of variable optical transmittance) considerably difficult. Expanding on our previous innovative research on organic electrochromic smart windows as architectural components (Cardoso Llach et al. 2009), we report on a new simulation environment, Acacia, for the design and analysis of highly responsive building facades. Unique to Acacia is its capacity to enable the modeling and assessment of façade behaviors in response to both environmental and human inputs.

1. INTRODUCTION

The pre-alpha version of Acacia we introduce here is a Smart Façade simulator prototype demonstrating the relevance and feasibility of a user-friendly system to aid the design, analysis, and control of smart façades. The project's long term goals are to (1) allow users to easily model different smart façade scenarios involving both environmental and human input, testing their implications on a building's energy efficiency and comfort levels, and (2) facilitate a software/hardware interface with environmental and motion sensors to control a smart façade device in a real setting. Below we outline the environmental case for such a system, our prior work, Acacia's pre-alpha system contributions, limitations, and future steps.

Recent studies show that in developed countries the amount of energy spent on building operations ranges from 20% to 40% of total energy consumption (Pérez-Lombard et al 2008). In the U.S., a large portion of this energy (57%) goes into HVAC and interior temperature control (Ibid). Within this problematic context, building skins that change their transmittance level in response to the environment and occupancy may have great potential to reduce a building's cooling loads by responsively managing heat intake from solar radiation through transmittance change (Granqvist 2008; Granqvist et al 2003; James and Bahaj 2005). Transmittance is understood as the fraction of incident light passing through a window. Many researchers have shown that electric loads could be reduced significantly by implementing windows of variable transmittance (Carmody et al. 2004; Lampert 1998). Our own research confirms and further specifies these findings. Moreover, a building's capacity to adapt to its inhabitants' presence, gestures, and types of occupancy can greatly improve its comfort levels (James and Bahaj 2005)—opening up opportunities for innovative scenarios of interaction between human, environmental, and architectural actors (Cardoso Llach et al. 2009). Therefore, a smart façade element regulating the amount of sunlight entering a building in response to human and environmental inputs can significantly improve a building's energy efficiency

and comfort. Unfortunately, while current software systems such as Energy Plus, eQuest and IES provide tools for modeling basic switchable glazing behaviors, currently there are no user-friendly systems to holistically design, assess, and control smart façades. The challenge is to create a user-friendly simulation and control framework for meaningful and energy-efficient interactions between changing environmental conditions, human occupancy, and responsive buildings.

2. RELATED WORK

2.1. Electrochromic smart windows

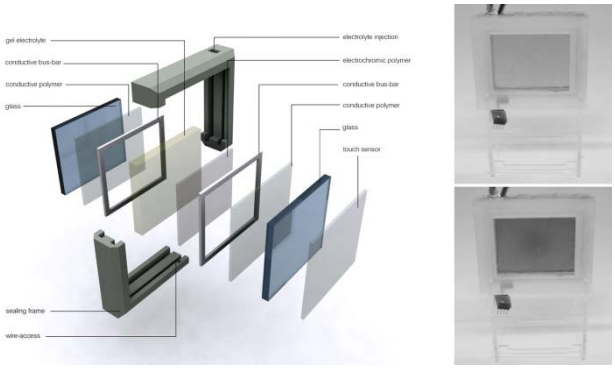

Figure 1. An example of an alternative "organic" smart window operation was demonstrated by the authors (Cardoso Llach et al 2009). A transparent pressure (tactile) sensor and a processor enabled an organic-polymer based touch-responsive tile. The transmittance change was clearly visible in this early prototype and the switching occurred in less than 5 seconds (substantially faster than any smart window based on inorganic metal oxides).

Current technologies for smart windows involve highly transparent conductive substrates coated with materials that have variable optical properties. These include liquid crystal displays (LCDs), suspended particle devices (SPD), and thermochromic, photochromic, and electrochromic systems derived from metal oxides, small organic molecules, and organic polymers (Baetens, et al 2010). Electrochromism, broadly defined as a reversible optical change in a material induced by an external voltage, can be obtained through reversible redox reactions of many inorganic and organic species to modulate light throughout the electromagnetic spectrum (Argun et al. 2004). For almost 40 years, technology has been developed for applications such as auto dimming mirrors, display devices, and smart windows for buildings. Despite the promise of energy efficiency from electrochromic windows, the commercialization of metal oxide-based (inorganic) windows like the systems mentioned above has been lagging due to a variety of factors. First, because of slow switching times and high initial material and processing costs—the increasing demand from display industries has driven the price of one required component, Indium tin oxide (ITO) to over $1,000/kg) (Chase 2011). . Our previous work on organic electrochromic windows addresses this point (Cardoso Llach et al. 2009) (See Figure 1).

The second reason for the lag, and crucial to Acacia, is the lack of an effective and user-friendly software platform for building designers and occupants to design, estimate, customize, and control smart facades. This lack severely limits the building industry's understanding of the potential environmental and social benefits of smart façade technologies, as well as the capacity of architects, engineers, and users to envision creative scenarios where smart facades interact with both the environment and human occupants for better energy efficiency and comfort. Providing this missing innovative software platform is the chief purpose of Acacia.

2.2. Context of Energy Simulation Software

There are hundreds of building simulation programs dealing with the multiple criteria involved in energy performance. However, the way each feature is interpreted and implemented varies considerably from system to system, to the point where there is not even a common language to describe the different tools and methods offered by building energy performance simulation programs (Crawley et al. 2008). While some programs consider basic switchable glazing behaviors (for instance IES, eQuest and EnergyPlus) by including elemental control parameters in relation to simple temperature thresholds and a few basic assumptions about occupancy, currently there are no systems to holistically design, assess, and control smart façades.

2.3. Assessing the potential energy savings of dynamic glazing

In order to better understand the potential energy savings of smart façades, we conducted a series of simulations to parametrically measure the effects of employing a switchable glazing system (such as electrochromic glazing). We analyzed three scenarios (switching, bleached, and tinted) and compared them on a baseline design. Based on the cost analysis, the switching case provides 20% annual savings over the bleached case,

and 6% annual savings over the tinted case. These results are comparable to results found in literature where savings of electrochromic glazing over double glazed units range between 28% and 40% in cooling dominated climates like Houston's, and ~7% in heating dominated climates like Pittsburgh's (Papaefthimiou et al 2006). Similar studies showed a 14% - 16% (Lee and Tavil 2007) and 13.5% (Roberts 2009) saving in peak energy demand was possible for both hot and cold climates in a spectrally selective low–e window baseline case. Our own simulations showed a 27% saving in peak energy demand over a fully bleached baseline case with a larger window size. A detailed discussion of our simulations and their implications will be published in a separate report. Key to our purpose here, however, is the simulation's result: an informed panorama confirming significant potential savings associated with dynamic glazing when implemented with a daylighting control scheme, in comparison with fully transparent (bleached) and fully tinted façade states.

3. ACACIA IMPLEMENTATION

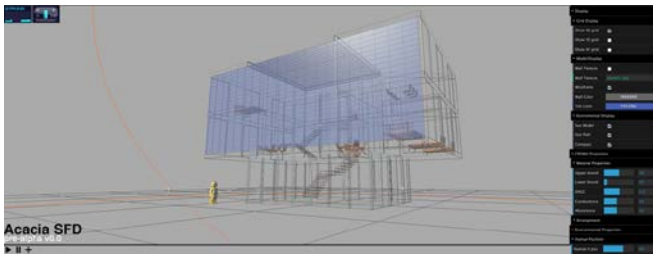

Figure 2. A screen shot from Acacia SFD pre-alpha version, under development at The Pennsylvania State University by the authors.

3.1. Overview

Acacia is a light, web-based prototype Smart Façade simulator developed to aid the design of highly responsive Smart Façades. Acacia features a user-friendly interface allowing users to interactively define and visualize in 3-D a façade's behavior in response to both environmental and human inputs. At its current state of development, a daylighting calculation module computes local variations in the façade's modules in response to basic environmental and human inputs in order to maintain adequate levels of light in the building's interior. Future steps include a robust connection with an energy model to assess performance savings, and a live link with a sensor-enabled smart façade system. The application is built from scratch on different web technologies. JavaScript libraries were used, such as: Three.js for building the 3D simulation; JQuery and Dojo for most of the client-side scripting and interaction functionality; dat.GUI for some menu components; Almene's Timeline.js for the timeline. HTML and CSS were used for the page layout and formatting. (See Figure 2). The pre-alpha version of Acacia can be freely accessed online (Cardoso Llach et al. 2013).

3.2. User Workflow

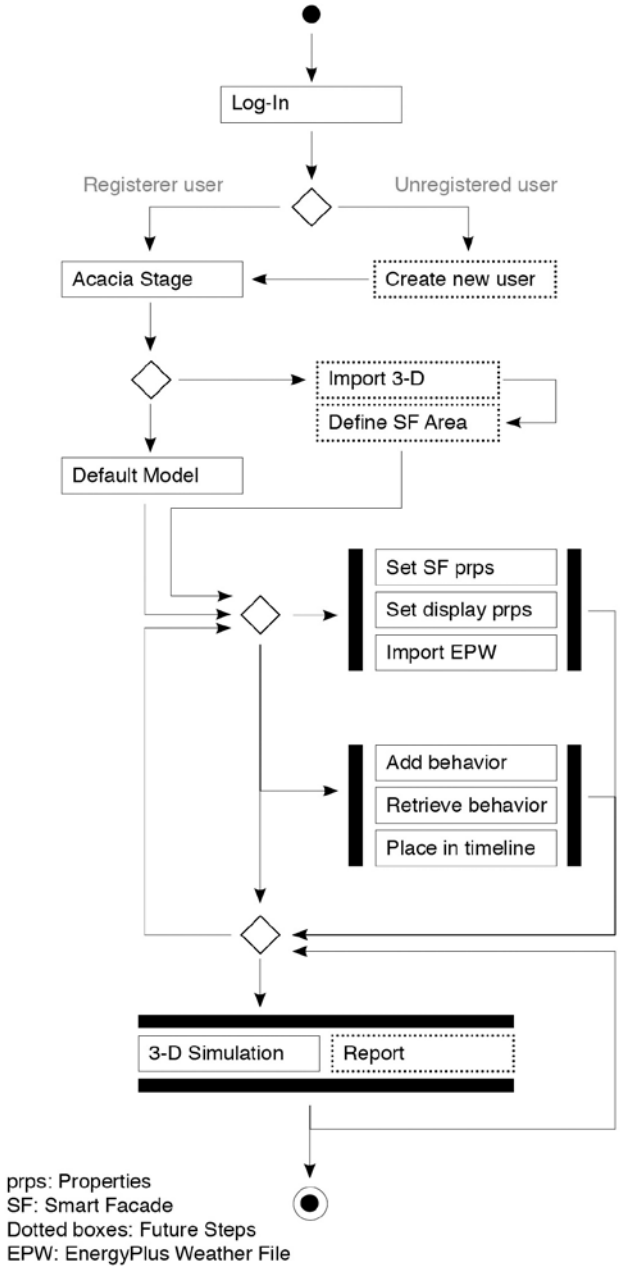

Figure 3. Activity diagram showing Acacia's typical use case scenario.

Acacia is designed to allow a user to import a geometric model of a building (.OBJ files) as well as weather data (.EPW files), define a smart façade's properties (transmittance variation range, conductance, absortence, among others), design façade behaviors responsive to environment and occupants, and visualize them in time in 3-D.

The user can model multiple façade behaviors taking into account both *environmental* and *occupant* data, and lay them out in time in a graphical timeline for simulation. At simulation runtime, Acacia calculates and displays the transmittance of each of the façade elements in response to (1) user-defined environmental parameters such as direct solar illuminance, solar path, and diffuse illuminance data, and (2) user-defined occupant parameters such as occupant proximity, motion, and decay, among others (See Figure 4). "Distance," for instance, determines the distance at which the presence of a human body will trigger the façade's responsive behavior. "Transmittance" determines the base transmittance of the area displaying responsive behavior (higher transmittance means higher transparency, and ranges vary according to the kind of electrochromic or responsive materials used). "Decay" determines the edge condition of the area displaying transmittance change. Lowest decay will yield a crisp edge. Highest decay will yield a blur. "Size" and "Shape" determine the aspect of the area displaying responsive behavior. "Persistence" determines the persistence of the behavior in relation to body movement (highest persistence means that the behavior remains in place indefinitely after the body has moved).

Once created, user-defined behaviors are automatically stored in a *library*. At any time, the user can select any behavior from the library and lay them out on a graphical *timeline*. On the timeline, the user can set a behavior's start and end time interactively to hour, day, and month precision. Using the timeline controls, a user can define the parameters of the simulation, start it, stop it, or ask for a report. The *library* and the *timeline* are the system's key features affording users the flexibility to easily configure and evaluate an infinite number of smart façade scenarios. Besides the *timeline* and *library*, a *viewport* and a *settings panel* are the other key components in the system's user-interface (See Figure 5). The *viewport* is a constantly updating in a 3-D window, allowing the user to visualize, select and manipulate the geometric model of the building, as well as other elements of the simulation such as the sunpath, people, and the smart façade elements themselves. The user can zoom in, orbit, pan, and navigate the 3-D space in order to examine different aspects of the model.

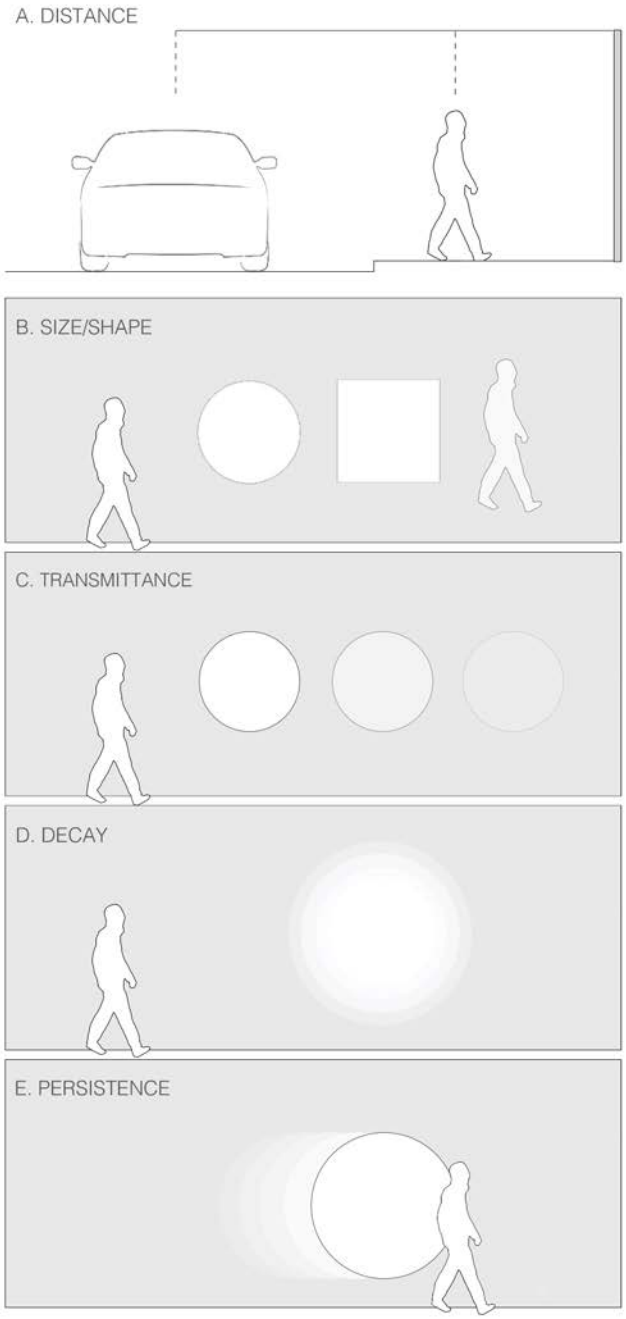

Figure 4. Users can define occupant-driven behaviors in Acacia easily by defining parameters such as distance, motion, and decay, among others.

The viewport shows the smart façade changes in real time (see Figures 2 and 6). The *settings panel* allows users to define the façade parameters and transformation ranges, including the transmittance variation range and base transmittance value of the façade components—as well as their distribution along the façade. It also enables users to choose from different visualization styles for the model, to toggle the sun path, as well as to select and import EnergyPlus weather data in .EPW format (See Figure 5).

Figure 5. A diagram of Acacia User Interface.

When the simulation runs, the software interactively computes the transmittance value of each of the smart-façade elements seeking to achieve comfortable levels of illuminance in the building's interior by balancing daylight requirements, user-defined behaviors, and solar gain reduction. Acacia can thus simulate a smart façade, maintaining adequate lighting comfort levels by iteratively adjusting the transmittance value of a matrix of smart façade elements in response to environmental and human conditions.

3.3. Daylight Calculations

Acacia calculates local levels of transmittance for the smart façade elements in order to preserve visual comfort during variable weather and occupancy conditions—by keeping a uniform illuminance gradient on the work plane. By importing data from any EnergyPlus (EPW) Weather File, Acacia extracts data for the site's geographical location, time of day, direct illuminance from solar, and diffuse illuminance from the sky, and uses a custom algorithm to calculate illuminance values on the work plane at different states of façade opacity. To develop the new algorithm, daylighting simulation software such as Radiance (Ward et al 1988) and Radiance-based Daysim (Reinhart and Herkel 2000) were studied for horizontal illuminance calculation. Radiance applies the daylight coefficients by extracting the field direct normal radiation and field diffuse radiation from the .EPW file (Walkenhorst et al. 2002; D Bourgeois 2008) and using the Perez sky model (Richard Perez et al. 1990; 1993) for illuminance calculation. While precise, this algorithmic approach is computationally expensive. In order for Acacia to be an effective real-time simulation tool, we developed a simpler method, which is relatively exact on the illuminance calculation, and can be almost independent of other daylight calculation software. The illuminance contributed by daylight at each of a set of critical calculation points in a given space constitutes the illuminance from the direct and diffuse sunlight. The horizontal illuminance can be calculated from the direct normal illuminance and diffuse horizontal illuminance from .EPW data (S. Wilcox 2008). When the façade transmittance is 1.00 (fully transparent), the horizontal illuminance on the work plane exposed to the direct sunlight is shown by the equation:

$$E_{hsun}=E_{sun}\cdot\sin\alpha_{alt}$$

Where E_{hsun} equals horizontal illuminance from the direct sunlight, E_{sun} equals field direct normal illuminance, and α_{alt} equals solar altitude angle (Dilaura et al. 2011). The solar angles (solar azimuth, solar altitude) can be achieved from the Duffie & Beckman algorithm (Duffie et al. 2013). The illuminance from diffuse sky light decreases as it goes deeper into the room at a rate that can be approximated from the calculation results from a test case in Daysim, compared to the diffuse illuminance from the EPW file. An important factor is the varying penetration depth of the sun at different times of the day. The penetration, hereby, is in terms of the distinct light spot on the floor produced by direct sunlight. The calculation of penetration depth is essential when investigating direct sunlight so as to apply the transmittance change for each tile. When the window faces south, the penetration depth is determined by the solar profile and the height of the space:

$$\alpha_p = \operatorname{atan}\left(\frac{\tan\alpha_{alt}}{\cos\alpha_z}\right)$$

$$L=H/\tan\alpha_p$$

Where α_p equals Solar Profile Angle, α_{alt} equals Solar Altitude Angle, α_z equals Solar Azimuth Angle, and H equals façade height (Dilaura et al. 2011). Besides direct sunlight, the illuminance in the "penetration area" is also created by the diffuse sky light. The illuminance outside the "penetration area" is due to the diffuse skylight, if we do not consider any other reflected light from the surroundings. In the calculation, the façade is modeled as a set of tiles stacked from bottom to top. Each tile is assigned to the "task" of illuminating its mapping calculation point. Based on the horizontal illuminance from daylight, a target illuminance can be set. Each of the tiles' transmittance values is adjusted at a ratio from bottom to top as the penetration goes from the window towards the inside of the room (See Figure 6 and Table 1).

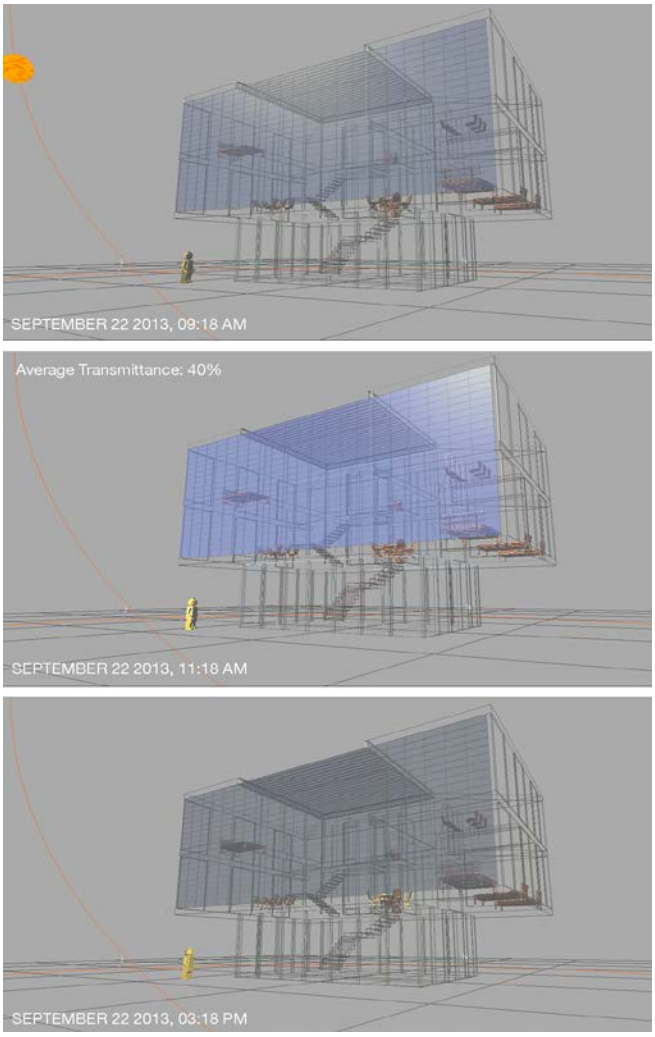

Figure 6. Images of an Acacia Smart Façade model responding to different weather conditions at different times of the day.

4. DISCUSSION

4.1. Applications

Current building simulation software does not provide tools for assessing visually and analytically the behavior of highly responsive smart façades. We have defined "highly responsive smart façades" as façades that are responsive to both direct environmental and human inputs. Because of the very unpredictable nature of environmental and human behaviors, these behaviors are hard to model and visualize. However, Acacia is a promising first step towards a system enabling different actors (smart window manufacturers, architects and engineers) to model and test new kinds of dynamic façade behaviors. As the system evolves, end users will be able to use it to customize their smart façades and easily establish different energy profiles for their buildings.

4.2. Contributions

Acacia's key contributions are (1) proving the relevance and feasibility of a new approach to smart façade modeling and analysis considering *both* occupancy and environmental data; (2) a first-of-its-kind user interface prototype for the design of occupant-responsive façade behaviors; (3) a fast daylight calculation algorithm allowing for the real-time visualization of a smart façade as it modifies its transmittance to maintain ideal interior lighting levels in response to *both* changing environmental conditions and user-defined behaviors.

Tile	Height (ft)	Depth from window (ft)	Total Illum.	Threshold	Transmittance
1	0.6	1	3348.864736	800	0.238886925
2	1.2	3	2215.531403	800	0.255391927
3	1.8	5	1837.753625	800	0.27189693
4	2.4	7	1648.864736	800	0.288401932
5	3	9	1535.531403	800	0.304906934
6	3.6	11	1459.975847	800	0.321411936
7	4.2	13	1406.007594	800	0.337916939
8	4.8	15	283.3333333		0.354421941
9	5.4	17	251.8518519		0.370926943
10	6	19	226.6666667		0.387431945
11	6.6	21	206.0606061		0.403936947
12	7.2	23	188.8888889		0.42044195
13	7.8	25	174.3589744		0.436946952
14	8.4	27	161.9047619		0.453451954
15	9	29	151.1111111		0.469956956
16	9.6	31	141.6666667		0.486461959
17	10.2	33	133.3333333		0.502966961
18	10.8	35	125.9259259		0.519471963
19	11.4	37	119.2982456		0.535976965
20	12	39	113.3333333		0.56898697

Table 1. Example of the transmittance response for one specific threshold value to the total illuminance

4.3. Limitations and Next Steps

Acacia's key limitations are (1) its dependency on backend datasets for daylight calculation (Daysim) and past weather data (EnergyPlus .EPW). To address this, we expect to implement a live "interoperability bridge" with EnergyPlus and test the system using sensor hardware in a real situation; (2) each tile's contribution to the overall room illuminance is not considered. The accuracy of the diffuse light calculation will be addressed through more research into the sky model; (3) energy and comfort analysis of occupant-driven behaviors are not implemented. We will further investigate connections between Acacia and a robust energy model, and on consolidating the system's quantitative reporting.

Acknowledgements

A Collaborative Design Research Grant, awarded by the Stuckeman School of Architecture and Landscape Architecture at Penn State, made this research possible. The team benefited greatly from the advice of Professor Richard Mistrick regarding Daysim, and our approach towards daylight calculation. Veronica R. Patrick assisted with illustrations.

References

ARGUN, AVNI A., PIERRE-HENRI AUBERT, BARRY C. THOMPSON, IRINA SCHWENDEMAN, CARLETON L. GAUPP, JUNGSEEK HWANG, NICHOLAS J. PINTO, DAVID B. TANNER, ALAN G. MACDIARMID, AND JOHN R. REYNOLDS. 2004. "Multicolored Electrochromism in Polymers: Structures and Devices." *Chemistry of Materials* 16 (23): 4401–12. doi:10.1021/cm049669l.

BAETENS, RUBEN, BJØRN PETTER JELLE, AND ARILD GUSTAVSEN. 2010. "Properties, Requirements and Possibilities of Smart Windows for Dynamic Daylight and Solar Energy Control in Buildings: A State-of-the-Art Review." *Solar Energy Materials and Solar Cells* 94 (2): 87–105. doi:10.1016/j.solmat.2009.08.021.

CARDOSO LLACH, DANIEL, AVNI ARGUN, DIMITAR DIMITROV, AND QI AI. 2013. "Acacia SFD (pre-Alpha v0.0 WIP)." *Designecologies*. November. http://designecologies.psu.edu/projects/croma/croma-dev/0.91/index_yellowBox.html.

CARDOSO LLACH, DANIEL, AVNI ARGUN, CARLOS A. ROCHA, AND JOSE GONZALEZ. 2009. "Drawing Transparencies: Responsible Responsiveness in Spaces Through Organic Electrochromism." In *Computation: The New Realm of Architectural Design*, 83–88. Istanbul (Turkey). http://cumincad.scix.net/cgi-bin/works/Show?ecaade2009_165.

CARDOSO LLACH, DANIEL, DENNIS MICHAUD, AND LAWRENCE SASS. 2007. "Soft Façade Steps into the Definition of a Responsive Facade for High-Rise Buildings." In *Predicting the Future*, 567–73. Frankfurt. http://www.docstoc.com/docs/52325870/Soft-Façade-Steps-into-the-Definition-of-a-Responsive.

CARMODY, JOHN, STEPHEN SELKOWITZ, ELEANOR S. LEE, AND DARIUSH ARASTEH. 2004. *Window Systems for High-Performance Buildings*. W. W. Norton & Company.

CHASE, J. 2011. "Next-Generation Smart Windows - Materials and Markets, Smart Window | NanoMarkets." *Nanomarkets.net*. March 28. http://nanomarkets.net/market_reports/report/next-generation_smart_windowsmaterials_and_markets_2011.

CRAWLEY, DRURY B., JON W. HAND, MICHAËL KUMMERT, AND BRENT T. GRIFFITH. 2008. "Contrasting the Capabilities of Building Energy Performance Simulation Programs." *Building and Environment* 43 (4): 661–73. doi:10.1016/j.buildenv.2006.10.027.

D BOURGEOIS, C. F. REINHART. 2008. "Standard Daylight Coefficient Model for Dynamic Daylighting Simulations." *Building Research and Information - BUILDING RES INFORM* 36 (1). doi:10.1080/09613210701446325.

DILAURA, DAVID L., KEVIN W. HOUSER, RICHARD G. MISTRICK, AND GARY R. STEFFY. 2011. *The Lighting Handbook: Reference and Application (Iesna Lighting Handbook)*. 10 edition. Illuminating Engineering.

DUFFIE, JOHN A., WILLIAM A. BECKMAN. 2013. *Solar Engineering of Thermal Processes*. 4 edition. Wiley.

GRANQVIST, C. G. 2008. "Electrochromics for Energy Efficiency and Indoor Comfort." *Pure and Applied Chemistry* 11 (80): 2489–98.

GRANQVIST, C.G., E. AVENDAÑO, AND A. AZENS. 2003. "Electrochromic Coatings and Devices: Survey of Some Recent Advances." *Thin Solid Films* 442 (1–2): 201–11. doi:10.1016/S0040-6090(03)00983-0.

JAMES, P.A.B., AND A.S. BAHAJ. 2005. "Smart Glazing Solutions to Glare and Solar Gain: A 'sick Building' Case Study." *Energy and Buildings* 37 (10): 1058–67. doi:10.1016/j.enbuild.2004.12.010.

LAMPERT, C. 1998. "Smart Switchable Glazing for Solar Energy and Daylight Control." *Solar Energy Materials and Solar Cells* 52 (3-4): 207–21. doi:10.1016/S0927-0248(97)00279-1.

LEE, E. S., AND A. TAVIL. 2007. "Energy and Visual Comfort Performance of Electrochromic Windows with Overhangs." *Building and Environment* 42 (6): 2439–49. doi:10.1016/j.buildenv.2006.04.016.

PAPAEFTHIMIOU, S., E. SYRRAKOU, AND P. YIANOULIS. 2006. "Energy Performance Assessment of an Electrochromic Window." *Thin Solid Films* 502 (1–2): 257–64. doi:10.1016/j.tsf.2005.07.294.

PEREZ, R., R. SEALS, AND J. MICHALSKY. 1993. "All-Weather Model for Sky Luminance distribution—Preliminary Configuration and Validation." *Solar Energy* 50 (3): 235–45. doi:10.1016/0038-092X(93)90017-I.

PEREZ, RICHARD, PIERRE INEICHEN, ROBERT SEALS, JOSEPH MICHALSKY, AND RONALD STEWART. 1990. "Modeling Daylight Availability and Irradiance Components from Direct and Global Irradiance." *Solar Energy* 44 (5): 271–89. doi:10.1016/0038-092X(90)90055-H.

PÉREZ-LOMBARD, LUIS, JOSÉ ORTIZ, AND CHRISTINE POUT. 2008. "A Review on Buildings Energy Consumption Information." *Energy and Buildings* 40 (3): 394–98. doi:10.1016/j.enbuild.2007.03.007.

REINHART, CHRISTOPH F., AND SEBASTIAN HERKEL. 2000. "The Simulation of Annual Daylight Illuminance Distributions — a State-of-the-Art Comparison of Six RADIANCE-Based Methods." *Energy and Buildings* 32 (2): 167–87. doi:10.1016/S0378-7788(00)00042-6.

S. WILCOX, W. MARION. 2008. "Users Manual for TMY3 Data Sets (Revised)." doi:10.2172/928611.

WALKENHORST, OLIVER, JOACHIM LUTHER, CHRISTOPH REINHART, AND JENS TIMMER. 2002. "Dynamic Annual Daylight Simulations Based on One-Hour and One-Minute Means of Irradiance Data." *Solar Energy* 72 (5): 385–95. doi:10.1016/S0038-092X(02)00019-1.

WARD, GREGORY J., FRANCIS M. RUBINSTEIN, AND ROBERT D. CLEAR. 1988. "A Ray Tracing Solution for Diffuse Interreflection." In *Proceedings of the 15th Annual Conference on Computer Graphics and Interactive Techniques*, 85–92. SIGGRAPH '88. New York, NY, USA: ACM. doi:10.1145/54852.378490. http://doi.acm.org/10.1145/54852.378490.

Sustainability Performance Evaluation of Passivhaus in Cold Climates

Kyoung-Hee Kim, Ph.D[1] and Seung-Hoon Han, Ph.D[2]

[1]University of North Carolina at Charlotte and FrontInc.
9201 University City Blvd
Charlotte, NC, USA, 28277
kkim33@uncc.edu

[2]Chonnam National University
300 Yongbong-dong, Buk-gu
Gwangju, Korea, 500-757
hshoon@jnu.ac.kr
(Corresponding Author)

Keywords: Energy Efficient Building, Passivhaus, Heat Transmission, Air Infiltration.

Abstract

Buildings are one of the major sectors that contribute to significant environmental impacts and energy consumption in the U.S.A. Building sustainability can be realized through enhancing energy efficiency and reducing energy demand. One sustainable strategy for meeting such goals is to adopt high performance building envelopes integrated with an energy-efficient HVAC system. Heat transmission (U-factor) and air infiltration of building envelopes are closely correlated to building energy conservation. The primary goal of this paper is to understand the energy implication of U-factor and air infiltration of building envelopes for energy conservation. The research is based on a case study project, a residential building in Calgary, Alberta, Canada designed based on Passivhaus (PH) criteria. In order to reduce the U-factor of the glazing façades of the case study building, a high performance glazing system is discussed and respective energy saving potentials are estimated using a building energy simulation tool. Air tightness of building envelopes is also discussed, as it plays a crucial role in the heating energy consumption of buildings in cold climates. The study confirms that both enhanced U-factor and airtightness reduce energy consumption by 30~40%. The proper choice of window technologies and field quality workmanship that enhance U-factor and air tightness becomes essential in building sustainability in severely cold climates.

1. INTRODUCTION

The energy efficiency of building environments significantly contributes to mitigating the challenges of climate change, resource depletion and wider environmental issues. Residential buildings in the U.S.A. account for 23% of the primary energy consumption (EIA, 2009) and residential buildings in Canada consume 20% of the primary energy consumption (NRC, 2006). The building sustainability can be achieved by two primary methods: maximizing energy efficiency and minimizing energy demand for a building. These methods are closely related to climate responsive design and sustainable technology integration. An example of sustainable technology integration includes high performance building envelopes coupled with passive space heating and cooling strategies. Among sustainable strategies for achieving high performance building envelopes, heat transmission (U-factor) and air tightness of building envelopes are known to be the most important parameters for building energy conservation, especially those located in cold climates. Their contribution to energy conservation becomes more apparent when a building has a relatively high window to wall ratio. This is due to the fact that a window wall offers relatively poor performance in U-factor and air tightness compared to an opaque wall. Despite poor energy performance of a window wall, it is often preferred over an opaque wall due to its positive psychological effect and energy saving from daylight. Currently, residential building energy codes in North America specify certain U-factors for different wall types. However, no building energy codes are available to regulate the air tightness of residential building envelopes. As a result, the air tightness is often underestimated and considered as a minor impact on building energy conservation.

The primary goal of this paper is therefore to investigate the effect of the U-factor and air infiltration rate on the annual energy consumption for a residential building using parametric building energy simulations. The paper also discusses state-of-the-art fenestration technologies and best practices that can improve U-factor and air infiltration. The study is based on a residential building designed by a

Seattle-based architectural firm, Olson Kundig Architects, that the researcher was involved in. It is a new residence with approximately 2300ft^2, 45 minutes west of Calgary, Alberta, Canada and designed based on Passivhaus (PH) criteria.

2. PASSIVHAUS STANDARDS AND RESIDENTIAL ENERGY SAVING

The *Passivhaus* (PH) standard is a voluntary program for residential buildings with ultra-low energy usage intensity (EUI). The standard requires buildings to meet specific EUI and airtightness. The target criteria include a total heating and cooling demand of < 15kWh/m2/yr (4.7 kBtu/ft2/yr) and total site energy use of <120kWh/m2/yr (11.5 kBtu/ft2/yr) with an airtightness 0.6 ACH@ 50 Pa (1.5psf) or less. The standard is recommended for buildings in cold climates such as zones 5~7 in accordance with ASHRAE 90.1 (American Society of Heating, Refrigeration, and Air Conditioning Engineers). Figure 1 illustrates the averaged EUI of a residential building in North America. A house with the PH criteria (37kWh/m2/yr (11.8kBtu/ft^2)) appears to consume approximately 13% of a typical Canadian residence (88kBtu/ft^2 (275kWh/m^2/yr)) and 33% of LEED homes (35.3Btu/ft^2 (111.3kWh/m^2/yr). The case study building targets for even lower EUI than a building with PH standard (Figure 1). This is realized through climate responsive passive design along with systems integration of high performance building envelopes and an energy-efficient HVAC system.

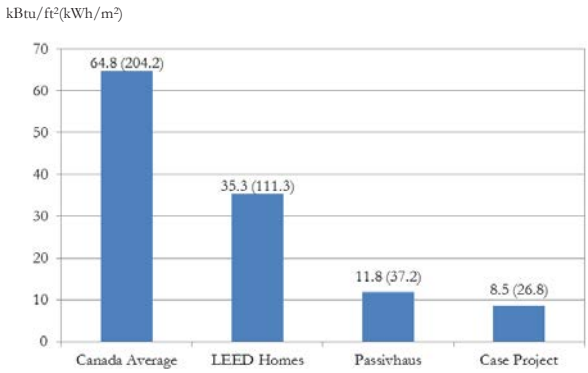

Figure 1. Averaged EUI of a residential sector in North America.

2.1. Glazing Thermal Performance

The energy attribute of a window system is defined by U-factor, solar heat gain coefficient (SHGC), and visible light transmittance (VLT). The U-factor is directly related to energy transfer through building envelopes, and therefore, a lower U-factor yields less heating and cooling energy consumption. VLT is related to daylighting transmission and higher VLT results in reducing artificial lighting loads, as well as cooling loads during summer. A higher SHGC is preferred during heating seasons but not cooling seasons. There are advanced window technologies available in the market that offer various energy attributes tailored to site location and building orientation. They include low-e coatings, gas type (e.g. argon, krypton) within an insulated glass unit (IGU), colored interlayer, and glass treatment (e.g. tinted glass, fritted glass).

Due to the harsh cold climate of the site location, the energy conservation of the case study project is focused almost exclusively on the reduction of space heating loads by maximizing winter heat gain and improving the U-factor and the air tightness of the building envelopes. The energy performance of a window is a balanced effect from solar heat gain and daylighting transmission year round. The summer cooling load is further minimized by using an external shading device and a high performance low-e coating that blocks excessive heat gain while maintaining an appropriate level of visible light transmittance. The summer insolation during early morning and late evening is blocked by an overhanging canopy on the east and west facades. Figure 2 shows energy efficient strategies provided by high performance building envelopes.

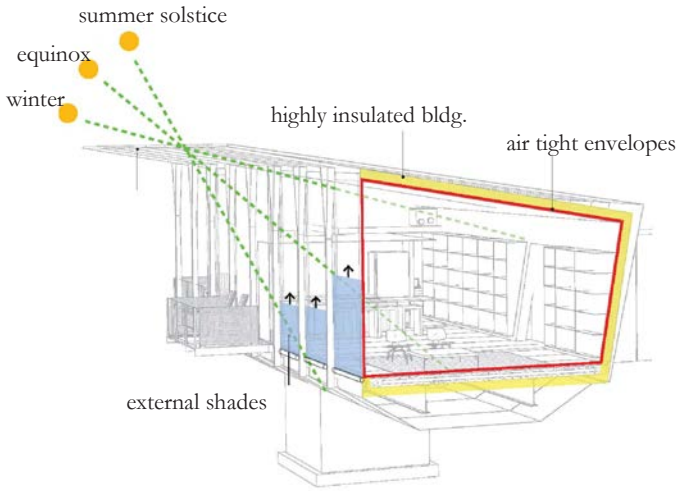

Figure 2. High performance building envelopes of the case study project.

3. ENERGY IMPACT FROM U-FACTOR AND AIR INFILTRATION

The design of the case study project uses significantly

more glass than is typically used in PH buildings. As a consequence, it demands specific U-factor and solar heat gain coefficient to regulate energy flow with passive heating in winter and without overheating in summer. Further, it is important to specify a best yet achievable level of airtightness for a window system.

3.1. Research Method

The goal of the study is to understand the implication of U-factor and airtightness in building heating and cooling loads. The study was carried out as a comparative analysis, simulating a single building model by changing a U-factor and infiltration rate, respectively. Whole building energy simulation is becoming more common with the increasing focus on energy efficient building design. The analysis model utilizes a Revit mass model built in Revit Massing platform (Figure 3). The Revit mass model of the case study building was exported as Green Building xml (gbxml) into DesignBuilder to run a whole building energy simulation. The gbxml contains information about building forms, glazing location, and envelope construction. DesignBuilder is a building thermal performance simulation program that analyzes hourly-recorded weather data and illumination data. It is a user-friendly visualization platform that utilizes EnergyPlus simulation engine. The simulation focuses specifically on calculating heating and cooling loads by changing the performance parameters of U-factor and air tightness.

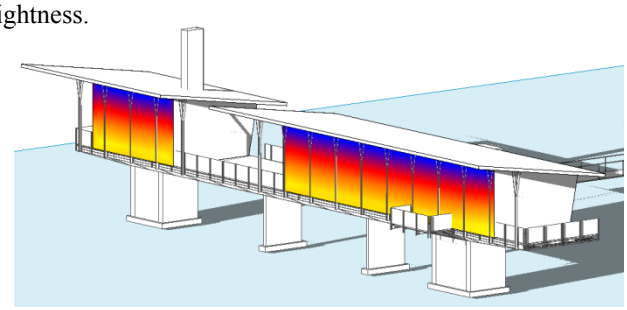

Figure 3. Gbxml model of the case study project in Revit.

Since the paper focuses on the impact of U-factor, the analysis in DesignBuilder keeps the same values for SHGC and VLT while changing the U-factor in accordance with Table 1. The air exchange rate per hour (ACH) of the building envelope was assumed to be 0.6 ACH as a baseline in accordance with the PH criteria. ACH was changed to 0.1ACH, 0.3ACH and 1ACH in order to understand its impact on energy consumption. The building operation schedule was a typical residential schedule set forth in DesignBuilder. The U-factor in Table 2 is dependent on a number of glass layers and low-e coatings as well as gas type. The lowest possible value of U-factor of a window would be in a range of U-0.065 (R-15) while being an economically and physically viable option. The desired U-factor and SHGC can be achieved by window technologies currently available in the market. The airtightness is determined by design, construction and its deterioration overtime (ASHRAE, 2009) and it can be best guaranteed by the installation quality workmanship of building envelopes in the construction field.

Window options	U-factor	SHGC	VLT
Triple IGU, two low-e's, argon gas (PH glazing, basis)	0.14	0.34	0.6
Triple IGU, three low-e's, Krypton gas	0.09	0.34	0.6
Quadruple IGU, three low-e's, Krypton gas	0.07	0.34	0.6

Table 1: Glass window energy attributes.

3.2. Analysis Results

The results show that improving the U-factor significantly reduces overall energy consumption by 15% compared to the case building enclosed with a baseline triple IGU (PH glazing). Specifically, enhanced U-factor reduces the both heating and cooling load by 20% and 15% respectively. The energy efficiency between a triple IGU and a quadruple IGU turned out to be marginal in this study. The air infiltration significantly affects energy consumption, especially heating load. As compared to a baseline of 0.6ACH (the PH criteria), the 0.1ACH yields a reduction of 80% in heating load and a 40% saving in space cooling, resulting in a 50% energy reduction in overall heating and cooling loads. Likewise, 0.3ACH yields a 40% reduction in the heating load and a 30% saving in the cooling load, resulting in approximately a 40% savings in heating and cooling energy consumption. On the other hand, 1ACH results in 10% increase in total energy consumption. Figure 4 shows annual EUI of the case study building with different U-factors and ACH. The case study project specified a Krypton gas infilled triple IGU with high performance low-e coatings. Due to the high performance window, coupled with the overhang roof and automatic external shading device, solar gain was maximized in winter and minimized in summer (Figure 4 (c)).

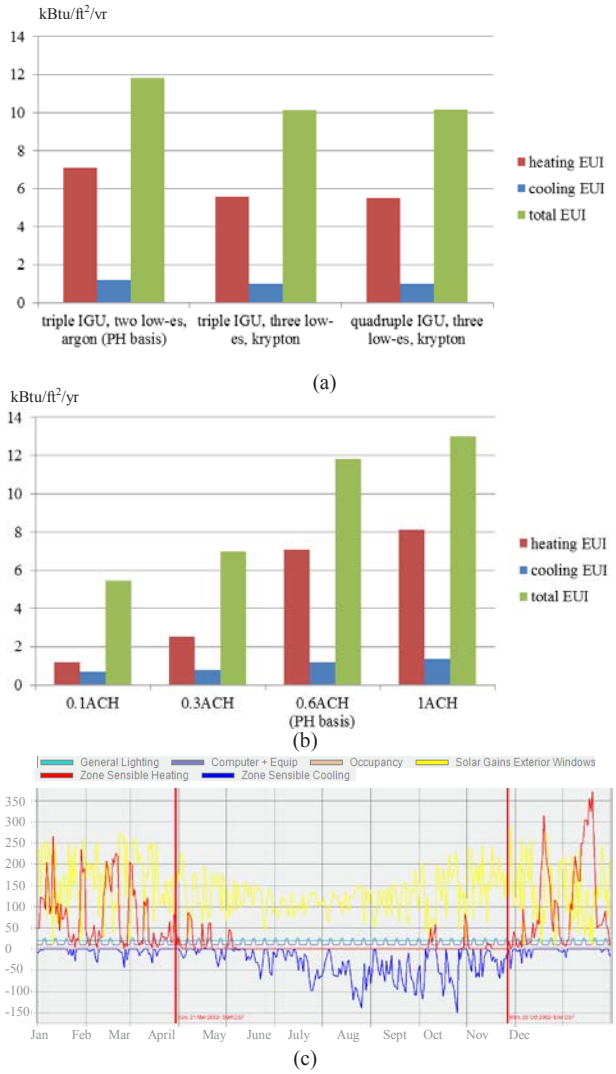

Figure 4. Annual EUI (kBtu/ft^2/yr) with different U-factors (a) and different ACH (b). Annual energy consumption of the case study project and solar gain (yellow line) through the high performance window (c).

4. CONCLUSION

The energy performance of a residential building in a cold climate was studied using DesignBuilder (EnergyPlus simulation engine). The performance parameters chosen in building the energy simulation were the U-factor of the glazing system and the air tightness of the overall building envelopes. This study confirms that both enhanced U-factor and airtightness reduce energy consumption by 30~40%. The proper choice of window technologies and field quality workmanship that enhance U-factor and air tightness becomes essential in severely cold climates. The case study project sets new levels of excellence in the use of high performance glass and façade design for Passivhaus criteria.

5. NEXT STEP

Future work includes the life cycle cost analysis of the case project and the in-depth study of the state-of-the-art fenestration technologies and best practices that can exceed Passivhaus standards. Further, the simulation data will be validated by carrying out field measurements after construction of the study project.

Acknowledgements

This research was supported by a grant (10High tech Urban B01) from the High Tech Urban Development Program funded by the Ministry of Land, Transport and Maritime Affairs of the Korean government.

References

ASHRAE. 2009. ASHRAE Handbook-Fundamentals. Atlanta: American Society of Heating Refrigerating and Air Conditioning Engineers, Inc.

AUTODESK. 2012. Autodesk Revit (Version 2012) [Computer software]. San Rafael: Autodesk.

CRAWLEY, D.B., HAND, J.W., KUMMERT, M., & Griffith, B.T. Contrasting the Capabilities of Building Energy Performance Simulation Programs. Building and Environment 2008; 43(4). pp. 661–73.

DBS. 2011. DesignBuilder (Version 2.3) [Computer software]. Gloucestershire: DBS.

EIA. 2009. Annual Energy Review. Washington: US Energy Information Administration.

EIA. 2009. Residential Energy Consumption Survey. Washington: US Energy Information Administration.

Energyplus Weather Data. Retrieved from http://apps1.eere.energy.gove.

LBNL. 2012. Window (Version 6.3) [Computer software]. Berkeley: LBNL.

LBNL. 2011. Therm (Version 6.3) [Computer software]. Berkeley: LBNL.

NFRC. 2004. NFRC 100-2004: Procedure for determining fenestration product U-factors. MD: National Fenestration Rating Council.

NFRC. 2004. NFRC 201-2004: Procedure for interim standard test method for measuring the solar heat gain coefficient of fenestration systems using calorimetry hot box methods. MD: National Fenestration Rating Council.

NR. 2006. Canada's Energy Outlook. Ottawa: Natural Resources Canada

STRAUBE, J. 2010. The Passive House (Passivhaus) Standard: A Comparison to Other Cold Climate Low-energy Houses. Sommerville: Building Science.

Presenting Author Biographies

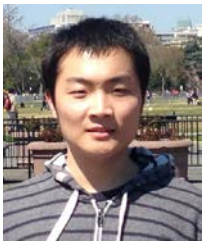

Qi Ai

Qi Ai is currently a graduate in the Architectural Engineering program at the Pennsylvania State University. Qi's research is related to daylighting simulation and photosensor control. He finished his undergraduate study in Fudan University, China in 2012. Qi joined the Design Ecologies Laboratory in September 2013, where he works on daylighting aspects of environmentally responsive smart facade systems.

Matin Alaghmandan

Matin Alaghmandan is a senior PhD candidate at Illinois Institute of Technology, School of Architecture. His research interest is the integration of architectural considerations with other related topics in building science and technology with computing tools. His current research focuses on the effect of the form and geometric modifications of tall buildings on the lateral loads-based structural systems regarding wind effect. Matin developed a design workbench including AutoCAD, SAP2000 and FLUENT (ANSYS) for his research.

Tesad Alam

Tesad Alam graduated from the Royal Institute of Technology, KTH with a M.Sc. in Sustainable Urban Planning and Design at the School of Architecture and the Built Environment in Stockholm, Sweden. Tesad began his studies in Stockholm University with a B.Sc. in Urban and Regional Planning. Tesad will during the SIMAUD conference present a part of his master's thesis together with Marcus Janson. The purpose was to contribute and examine the potential for future urban development along a new proposed subway line in Stockholm. Three areas along the new line were selected and thoroughly examined with the help of computer aided cartography software's such as Geographic Information Systems and IDRISI Selva. Tesad's professional interest is within geoinformatics as well as to understand the interaction between human activities and the physical environment.

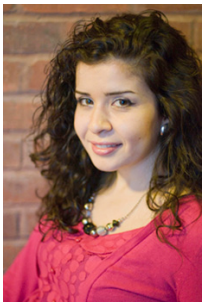

Alaa Alfakara

Alaa Alfakara is currently working on her Ph.D. at UCL Bartlett School of Graduate Studies where she is trying to use complex system simulations to obtain more accurate representations of dynamic occupant behavior in current buildings' energy performance simulation tools using agent-based modeling. After training as an architect at Al-Baath University in 2007, she developed a strong knowledge in sustainable building design, energy efficiency, and the application of technology into buildings while continuing her M.Sc. studies at the University of Reading. Her interest in sustainability led her to explore the sustainable features of vernacular building in the Mediterranean region. Then in 2009, Alaa joined the Bartlett School of Graduate Studies in Adaptive Architecture and Computation at UCL London, where she undertook a group project that investigated human interactions and behaviors in public spaces in the case of a digitally augmented environment, and, where the work was presented at MediaCity: Interaction of Architecture, Media and Social Phenomena conference in 2010. Throughout her graduate studies, Alaa developed a strong interest in the advances of simulation tools in building design and performance predictions. She investigated the application of multi-objective evolutionary algorithm into building design, which was applied to the case study of Niarchos Foundation Cultural Centre in Athens to optimize its solar canopy design.

Shajay Bhooshan

Shajay is a MPhil candidate at the University of Bath, UK and a Research Fellow at Institute of Technology in Architecture, ETH, Zurich where he is a research assistant in Block Research Group. He also heads the research activities of the Computation and Design (co|de) group at Zaha Hadid Architects, London and works as a studio master at the AA DRL Master's program. Previously he worked at Populous, London and completed his Master's Degree AA School of Architecture, London in 2006. His current interests & responsibilities include developing design research and maintaining computational platforms for the same at ZHA. He has taught and presented work at various events and institutions including SimAUD '14 ,Ingenio '13, Tensinet Istanbul '13, ICFF Bath '12 , Designers Gallery AU '11, Design Computation Symposium AU '10 , SimAUD '10 , SIGGRAPH '08, Yale University and University of Applied Arts, Vienna.

Erin Bradner

Erin is a Research Scientist with Autodesk Research. She holds a B.S. in Cognitive Science and a PhD in Information & Computer Science. Erin¹s dissertation research focused on the effects of communication technology on interpersonal behaviors such as persuasion, deception and trust. She has published in journals and proceedings in the field of Human-Computer Interaction and presented at conferences on the topics of distance collaboration and remote work. Erin has conducted numerous software ethnographies. She's observed Architects design skyscrapers from 3D virtual studios, observed children program gravity engines with the XBOX in their living rooms, and observed aeronautical engineers design emergency landings for the space shuttle. As an ethnographer, she uses inductive reasoning to extract patterns of interaction and to develop predictive models of behavior.

Johannes Braumann

Johannes Braumann is researching applications of industrial robots in architecture. He is a graduate of Master Building Science and Technology and fellow of the Austrian Academy of Sciences. Together with Sigrid Brell-Cokcan, he founded the Association for Robots in Architecture with the goal of making robotic arms accessible to the creative industry, organized Rob|Arch 2012, the first international conference on robotic fabrication in architecture, art, and design, and acted as co-editor of the Rob|Arch proceedings, published by Springer. He is the main developer of KUKA|prc (parametric robot control), a software tool for robotic fabrication and interaction which enables the accessible programming and simulation of robotic arms, directly within a CAD environment. His research on robotic fabrication has been presented at many international, peer-reviewed conferences, and published in research journals and books. In addition to teaching both technical classes and design studios at TU Vienna, Johannes Braumann has held robotic fabrication and Grasshopper workshops at international venues.

Daniel Cardoso Llach

Daniel Cardoso Llach is an architect, computational designer, and researcher. He is an Assistant Professor in Architecture at Penn State, where he directs the Design Ecologies Laboratory, a trans-disciplinary design research group investigating computation in design with a socio-technical lens. Daniel completed his PhD at MIT in 2012 with a dissertation investigating the ideas shaping Computer-Aided Design systems, with a focus on the 1960s MIT CAD Project, and its links to contemporary design. He has practiced with Gehry Technologies and KPF, and independently as a licensed architect in his native Colombia. Among his publications are: "The Poetics of Automation: Conceptions of human and non-human agency in design," 4S: Society for the Social Studies of Science (Tokyo: 4S, 2010); "Inertia of an Automated Utopia: Design Commodities and Authorial Agency 40 years after 'The Architecture Machine'," Thresholds 39 (2011); "Algorithmic Tectonics: how cold war era research shaped our imagination of design," AD (Architectural Design) (2012). His first book "Builders of the vision: software and the imagination of design" is now under contract with Routledge, and will be published in 2015.

Angelos Chronis

Angelos Chronis is a Design Systems Analyst in the Applied Research + Development group at Foster + Partners, and teaches at the Bartlett School of Graduate Studies of University College London. Angelos holds a diploma in Architecture from the University of Patras, Greece and an MSc in Adaptive Architecture & Computation from the Bartlett School of Graduate Studies, UCL, with distinction. He is a registered Architect in Greece. He has published papers in international conferences and journals, including the SimAUD symposium, at which he has received an "Outstanding Paper" award in 2011 and the eCAADe conference, at which his paper was selected for publication in the International Journal of Automation in Construction. Angelos's main research interest is the integration of simulation environments and performance optimization methods in the architectural process particularly in the field of computational fluid dynamics.

Mei Ling (Zan) Chu

Mei Ling (Zan) Chu is a Ph.D. candidate in the Civil and Environmental Engineering Department at Stanford University. She is also pursuing a Master's degree in Computer Science and Management Science and Engineering. Prior to her graduate study, she worked in Ove Arup (Hong Kong) as a structural engineer. At Stanford, she studies the effect of social behaviors on building egress by incorporating social science research into SAFEgress, the egress simulation framework built to model and predict crowd movement. Her research interests include studying user behaviors from real-life data and experiments, as well as incorporating behavioral factors in engineering designs.

Tim Frank

Tim Frank is an architect, designer, educator, and researcher. He currently occupies an Assistant Professorship within the College of Architecture Art + Design at Mississippi State and he maintains a nationally recognized interdisciplinary design studio based in Atlanta. Through a combination of research and practice, his work explores the role of design media technology in advancing the performance characteristics of architectural space. His studio has authored a number of award winning projects including first place in the 2012 AIA 10up competition and grand prize in the 2009 AIA 48 hours competition. His work has been exhibited in several museums and galleries including his 2010 solo exhibition of work entitled, “Sense & Sustain - ability” at the Museum of Design in Atlanta. His research has also been featured in many publications and venues around the world including his 2008 talk entitled, “Auditory Sketching” at the Palais des Congres in Paris, France.

David Jason Gerber

In 2009 Dr. Gerber was appointed Assistant Professor of Architecture at the University of Southern California. He has since been awarded a courtesy joint appointment at USC’s Viterbi School of Engineering. Upon joining the USC faculty he developed and taught primarily as a design studio and design technology professor in architecture for both undergraduate and graduate core and electives and curriculum in the Civil and Environmental Engineering Graduate sequence. Prior to joining the USC faculty Dr. Gerber was full time faculty at the Southern California Institute of Architecture from 2006-2009. Dr. Gerber has also taught at UCLA’s school of architecture and urban design, the AA’s DRL graduate program as a technical tutor, the Laboratory for Design Media at the EPFL in Lausanne Switzerland, Stanford University’s CEE department as a guest instructor, and the Tecnologico de Monterrey School of Architecture, Mexico. He is a frequent instructor at Tsinghua University in Beijing and lectures globally on architecture, digital practice, and design technology. Professionally, Dr. Gerber has worked in architectural practice in the United States, Europe, India and Asia including for Zaha Hadid Architects in London, England; for Gehry Technologies in Los Angeles; for Moshe Safdie Architects in Massachusetts, and The Steinberg Group Architects in California.

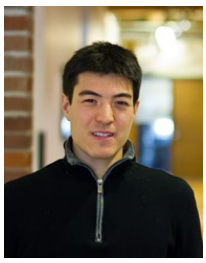

Rhys Goldstein

Rhys Goldstein is a Simulation Researcher at Autodesk Research in Toronto, Canada. His work combines building information modeling (BIM) with sensor data and simulation to help predict and ultimately reduce energy consumption in buildings. Rhys received the best paper award at the 2010 IBPSA-USA Conference for a new method to simulate the behavior of building occupants. He is currently investigating the use of open standards like the Industry Foundation Classes (IFC), as well as modeling conventions like the Discrete Event System Specification (DEVS), to help researchers collaborate in the development of simulation software.

Wassim Jabi

Wassim Jabi is Senior Lecturer at the Welsh School of Architecture, Cardiff University. He has a PhD in Architecture from the University of Michigan, Ann Arbor. Dr. Jabi is a past-president of the Association for Computer-Aided Design In Architecture (ACADIA) and a member of the Editorial Board of the International Journal of Architectural Computing (IJAC). He has published numerous papers in the area of computer-supported collaborative design, computer-aided visualization, parametric design and digital fabrication. He has recently published a book titled “Parametric Design for Architecture” (Laurence King, London, 2013). Dr. Jabi’s current research involves two areas of parametric design: the integration of building energy simulation in the early phases of design and the integration of robotic digital fabrication for architectural construction. Recently, he secured a $120,000 grant to purchase a large 6-axis high accuracy industrial robot to investigate innovative digital fabrication processes of architectural components and structures.

Marcus Janson

Marcus Janson graduated from KTH Royal Institute of Technology, School of Architecture and the built environment in Stockholm, Sweden. He has a bachelor degree within the built environment and a M.Sc. in Sustainable Urban Planning and Design. He will during the conference present a part of his master´s thesis together with Tesad Alam, where the purpose was to contribute and examine the potential for urban development in three selected areas along a new proposed subway line in Stockholm. Marcus professional interests include cities, urban morphology, geographic information systems and sustainability.

Kyoung-Hee Kim

Kyoung-Hee Kim is an assistant professor of the School of Architecture at UNC Charlotte. Kim holds a Ph.D and M.Arch from the University of Michigan and degrees of Bachelor of Engineering and Master of Engineering in Architecture from the Chonbuk National University, Chonju, Korea. Dr. Kim teaches core courses in Building Technology, Technology elective, and advanced topical studio incorporating performance-based design. Her scholarly research focuses on the development and implementation of building life cycle integrated design that identifies specific implications of sustainability during architectural design and execution. Her paper "A Feasibility Study of an Algae Façade System" in the 2013 International Sustainable Building conference was awarded as a best technical paper. In 2012, Dr. Kim co-chaired the Architectural Research Centre Consortium (ARCC) conference: the Visibility of Research at the University of North Carolina at Charlotte (UNCC). She was a PI for the P3 student competition in 2013 sponsored by the NSF-EPA, and has been served as a faculty advisor for the USGBC UNCC Student Chapter. Dr. Kim has been working as a building façade consultant in Front, New York since 2007, and involved with a wide range of buildings including Rutgers Business School (NJ, Completion 2013), World Trade Center Museum Pavilion (NYC, Completion 2012), High Line 23 (NYC, Completion 2011), Broad Art Museum (Lansing, MI, Completion 2012), Yas Island Marina Hotel (Abu Dhabi, Completion 2009), and King Abdullah University of Science and Technology (Saudi Arabia, Completion 2009). Current projects include the Amazon HQ's Biosphere Greenhouse in Seattle and a new conference center in Libreville, Gabon.

Stelios Krinidis

Dr. Stelios Krinidis is a postdoctoral research assistant in CERTH-ITI. He received the Diploma degree and the Ph.D. degree in Computer Science from the Computer Science Department of the Aristotle University of Thessaloniki (AUTH), Thessaloniki, Greece, in 1999 and 2004 respectively. He has also served as an adjunct lecturer at the Aristotle University of Thessaloniki, the Democritus University of Thace, and at the Technological Institute of Kavala during the period 2005-2012. His main research interests include computational intelligence, computer vision, pattern recognition, signal processing and analysis, 2D and 3D image processing and analysis, image modelling, fuzzy logic and visual analytics. He has authored twenty (20) papers in international scientific peer review journals and more than fifteen (15) papers in international and national conferences. He has also been involved in ten (10) research projects funded by the EC and the Greek secretariat of Research and Technology.

Xiao Sunny Li

Xiao Sunny Li is assistant researcher at the University of Toronto's Green Roof Innovation Testing Laboratory, His research focuses on digital simulation of the thermodynamic performance of green facades in relation to building envelopes. Li is an architect by training and has worked for a number of architecture and urban design firms in Canada, China and Germany. He holds a bachelor degree in physical geography and environmental science from the University of Toronto where he was involved in research at the Adaptation and Impact Research Sector of Environment Canada. Li received a Master in Architecture from the University of Toronto John H. Daniels Faculty of Architecture, Landscape, and Design. His thesis focused on the design of earthworks and topographical manipulations to better integrate architectural structures and ecological systems.

Mehdi Maasoumy

Mehdi Maasoumy is a PhD Candidate at the Mechanical Engineering Department of University of California at Berkeley. His research interests include modeling and model-based optimal control of linear, nonlinear and hybrid systems, with applications in energy efficient building control systems, smart grid and aircraft electric power distribution system. He has a B.Sc. degree in 2008 from Sharif University of Technology in Iran and a M.Sc. degree in 2010 from University of California at Berkeley both in Mechanical Engineering. He is a student member of IEEE and ASME. He is the recipient of the Best Student Paper Award at the ACM International Conference on Cyber-Physical Systems (ICCPS 2013), and Best Student Paper Award Finalist at the ASME Dynamic Systems and Control Conference (DSCC2013), and the IEEE American Control Conference (ACC2014).

Seoug Oh

Seoug Oh is an architect and a researcher currently completing his Masters at Penn State's Department of Architecture, where he is a member of the Design Ecologies Laboratory. Prior to Penn State, Seoug worked as an architect in Bangalore, Vienna and Beijing. He completed his bachelors of architecture at Seoul National University of Science and Technology, Korea. His current research interests include technology and science and their influence on architecture and society.

Veronica Patrick

Veronica Patrick is currently completing her final undergraduate semester in the Bachelor of Architecture and Dance minor programs at Pennsylvania State University. She is passionate for all realms and scales of design, with a focus on responsive architecture, movement, and interactive relationships between people, architecture and the environment. Passionate about collaboration, Veronica has participated in a number of interdisciplinary projects at Penn State, and has been a member of the Design Ecologies Laboratory since the Summer of 2013. Upon the completion of her undergraduate degree she plans to attend Columbia University's Graduate School of Architecture, Planning and Preservation.

Trevor Patt

Trevor Patt is a PhD candidate at the École polytechnique fédérale de Lausanne in Switzerland. Previously he received his M.Arch from the Harvard Graduate School of Design. His doctoral research is focused on thickening the interaction between architectural and urban design stages, encouraging bi-directional interaction and influence across scales and durations utilizing methods of computational urbanism and assemblage urbanism theories. He has lectured, published, and exhibited in Europe, Asia, and North America.

Alexander Robinson

Alexander Robinson is an assistant professor in the University of Southern California School of Architecture Landscape Architecture program, principal of the studio oOR Landscape + Urbanism and director of the Landscape Morphologies Lab. His research and practice explores the growing role of performance within landscape practice, both in terms of core landscape systems and landscape design within infrastructural territories. Robinson is the co-author of Living Systems: Innovative Materials and Technologies for Landscape Architecture (Birkhauser, 2007), a treatise on advanced material practices in landscape architecture. With his Landscape Morphologies Lab (lmlab.org) he continues this research into landscape infrastructures and other performance systems by developing innovative tools and methodologies to engage their design. Recent work includes a rapid landscape prototyping machine for the Owens Lake and augmented hydraulic modeling for the Los Angeles River. He has worked for Mia Lehrer & Associates, SWA Group and StoSS Landscape Urbanism on a range of projects, including the Los Angeles River Revitalization Master Plan. Robinson is a graduate of Swarthmore College and received a MLA from the Harvard Graduate School of Design.

Jenny Sabin

Jenny E. Sabin's work and research is at the forefront of a new direction for 21st-century architectural practice---one that investigates the intersections of architecture and science, and applies insights and theories from biology and mathematics to the design of material structures. Sabin is an Assistant Professor in the area of Design and Emerging Technologies in Architecture at Cornell University. She is Principal of Jenny Sabin Studio, an experimental architectural design studio based in Philadelphia USA and director of the Sabin Design Lab at Cornell AAP, a hybrid research and design unit with specialization in computational design, data visualization and digital fabrication. Jenny holds degrees in Ceramics and Interdisciplinary Visual Art from the University of Washington and a Master of Architecture from the University of Pennsylvania where she was awarded the AIA Henry Adams first prize medal and the Arthur Spayd Brooke gold medal for distinguished work in architectural design, 2005. Sabin was awarded a Pew Fellowship in the Arts 2010 and was recently named a USA Knight Fellow in Architecture, 1 of 50 artists and designers awarded nationally by US Artists. She has exhibited nationally and internationally most recently at Nike Stadium NYC, the American Philosophical Society Museum and at Ars Electronic, Linz, Austria. Her work is currently exhibited in the internationally acclaimed 9th ArchiLab titled Naturalizing Architecture at FRAC Centre, Orleans, France. Her work has been published extensively including in The Architectural Review, A+U, Mark Magazine, 306090, 10+1, ACM, American Journal of Pathology, Science, the New York Times, Wired Magazine and various exhibition catalogues and reviews. She co-authored Meander, Variegating Architecture with Ferda Kolatan.

Flora Salim

Dr. Flora Salim is a Lecturer at the School of Computer Science and Information Technology, RMIT University. She received her PhD in Computer Science from Monash University in 2009. Her research interests are context-aware, mobile, and pervasive computing and human computing interaction. She has been investigating sensor cloud infrastructure, real-time data analytics, and intelligent monitoring for industry-partnered projects in smart mobility, energy efficient and sustainable buildings, healthy ageing, lifestyle and wellness. She has published at least 50 international peer-reviewed articles in significant conferences, journals, and book chapters. She is a member of the team who secured an ARC Linkage grant on integrating real-time public transport data. She has secured other internal and external grants from the IBM Smarter Planet Industry Skills Innovation Award 2010, the RMIT Ian Permezel Memorial Award 2010, and RMIT and Siemens Greener Government Building Program funded by Victorian Government.

Andres Sevtsuk

Andres leads the City Form Lab at SUTD, which investigates the urban built environment and its influence on the social, economic and environmental performance of cities using state of the art computational and analysis tools. He joined SUTD in 2011 from MIT, where he spent the previous seven years, as a student and as a lecturer in Architecture and Urban Studies & Planning. Andres has worked as an architect, urban designer, consultant and researcher in Europe, United States and now in Singapore and developed ground-breaking methods for architectural and urban modeling, published and presented his work at various international events, including TEDx and the Venice Architecture Biennale.

Omid Oliyan Torghabehi

Omid Oliyan is currently a Ph.D. student at Taubman College of Architecture at University of Michigan. Having a background in structural engineering and some research experiences in Computational Mechanics and Artificial Intelligence, He is now pursuing his doctoral studies in architecture, focusing his research on exploring new performance based design strategies in architectural form finding and material systems.

Samuel Wilkinson

Samuel Wilkinson is currently a VEIV Eng.D research engineer in the Bartlett School of Graduate Studies' Complex Built Environment Systems group at University College London. Due to finish in 2014, the Eng.D is in partnership with Bentley Systems and PLP Architecture; the project is exploring a novel approach to wind analysis for generative design of tall buildings using machine learning to approximate CFD. Samuel holds a B.Arch + M.Eng in Architecture and Environmental Design from the University of Nottingham, and an M.Res in Adaptive Architecture and Computation from UCL.

Gabriel Wurzer

Gabriel Wurzer earned his Ph. D. degree in Process Visualization and Simulation for Hospital Planning from Vienna University of Technology in 2011. His research in architectural sciences focuses on tool support for early-stage planning of complex buildings, with regular contributions to both Pedestrian and Evacuation Dynamics conference (PED) and the Education and Research in Computer Aided Architectural Design in Europe conference (eCAADe), from which he was awarded the Ivan Petrovic Prize in 2009. He is also an active researcher in archaeological simulation, together with the Natural History Museum Vienna.

Conference Committees

Organizing Chair

David Jason Gerber, University of Southern California, Assistant Professor, School of Architecture and Viterbi School of Engineering

Organizing Co-Chair

Rhys Goldstein, Autodesk Research

International Program Committee

Ramtin Attar
Autodesk Research

Burcin Becerik-Gerber
University of Southern California

Martin Bechthold
Harvard University

David Benjamin
The Living

Shajay Bhooshan
Zaha Hadid Architects

Jordan Brandt
Autodesk

Sigrid Brell-Cokcan
Association for Robots in Architecture

Nathan Brown
Loisos + Ubbelohde

Jose Candanedo
Natural Resources Canada

Anders Carlson
University of Southern California

Joon Ho Choi
University of Southern California

Angelos Chronis
Foster & Partners

Jason Crow
McGill University

Daniel Davis
CASE

Xavier De Kestelier
Foster & Partners

Ipek Gursel Dino
Middle East Technical University

Stylianos Dritsas
Singapore University of Technology and Design

Forest Flager
Stanford University

Irene Gallou
Foster & Partners

Luisa Caldas
University of California, Berkeley

Tyler Garaas
Mitsubishi Electric Research Laboratories

David Gerber
University of Southern California

Rhys Goldstein
Autodesk Research

International Program Committee

Sponsors

Sponsored by

In co-operation with

Cover Image Credits

Simulating Human Behavior in Built Environments

Yehuda Kalay

Technion, Israel Institute of Technology

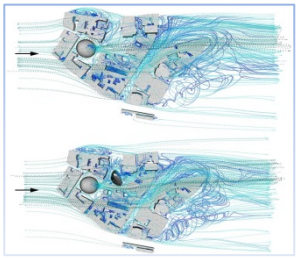

Approximating Urban Wind Interference

Samuel Wiklinson, Gwyneth Bradbury, and Sean Hanna

University College London

Design Agency: Prototyping Multi-Agent System Simulation for Design Search and Exploration

David J. Gerber, Rodrigo Shiordia, Sreerag Veetil, and Arun Mahesh

University of Southern California

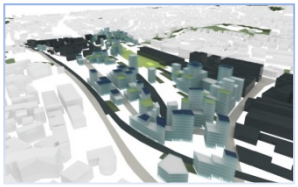

Scenario Modeling for Agnostic Urban Design

Trevor Patt, Jeffrey Huang

École Polytechnique Fédérale de Lausanne

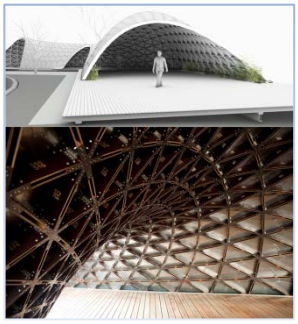

A Freeform Surface Fabrication Method with 2D Cutting

Andres Sevtsuk, Raul Kalvo

City Form Lab, Singapore University of Technology and Design

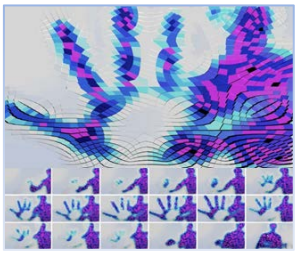

Prototyping Interactive Nonlinear Nano-to-Micro Scaled Material Properties and Effects at the Human Scale

Jenny E. Sabin, Andrew Lucia, Giffen Ott, and Simin Wang
College of Architecture, Art, and Planning, Cornell University
Sabin Design Lab
Jenny Sabin Studio

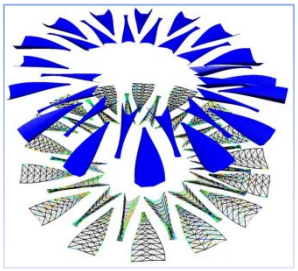

Design-Friendly Strategies for Computational Form-Finding of Curved-Folded Geometries: A Case Study

Shajay Bhooshan, Mustafa El-Sayed, and Suryansh Chandra
Zaha Hadid Architects

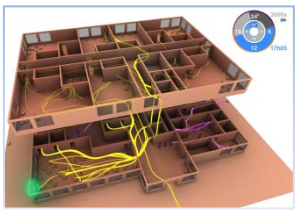

Towards Visualization of Simulated Occupants and their Interactions with Buildings at Multiple Time Scales

Simon Breslav, Rhys Goldstein, Alex Tessier and Azam Khan
Autodesk Research

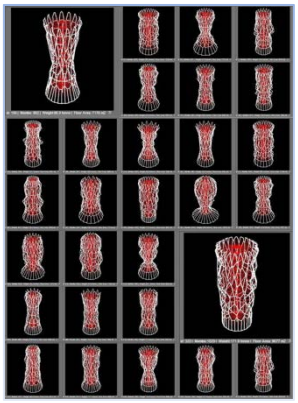

Genetic Based Form Exploration of Mid-Rise Structures Using Cell Morphologies

Omid Oliyan Torghabehi and Peter von Buelow
University of Michigan

Author Index

A
Ai, Qi 193
Alaghmandan, Matin 135
Alam, Tesad 179
Alfakara, Alaa 43
Argun, Avni 193
Athanailidi, Panagiota 127

B
Bhooshan, Shajay 117
Bradbury, Gwyneth 143
Bradner, Erin 77
Braumann, Johannes 101
Brell-Cokcan, Sigrid 101
Breslav, Simon 51
Byrne, Ultan 175

C
Carlson, Andres 135
Chandra, Suryansh 117
Chronis, Angelos 127
Chu, Mei Ling 35
Croxford, Ben 43

D
Davis, Mark 77
Dimitrow, Dimitar 193

E
El-Sayed, Mustafa 117
Elnimeiri, Mahjoub 135

F
Frank, Tim 25

G
gen Schieck, Ava Fatah 127
Gerber, David Jason 91
Goldstein, Rhys 51

H
Han, Seung-Hoon 201
Hanna, Sean 143
Huang, Jeffrey 187

I
Ioannidis, Dimosthenis 165
Iorio, Francesco 77

J
Jabi, Wassim 17
Janson, Marcus 179

K
Kalvo, Raul 109
Kesik, Ted 175
Khan, Azam 51
Kim, Kyoung-Hee 201
Krawczyk, Robert 135
Krinidis, Stelios 165

L
Latombe, Jean-Claude 35
Law, Kincho 35
Li, Xiao Sunny 175
Likothanassis, Spiridon 165
Llach, Daniel Cardoso 65, 193
Lorenz, Wolfgang E. 161
Lucia, Andrew 7

M
Maasoumy, Mehdi 153
Mahesh, Arjun 91

O
Oh, Seoug 65
Ott, Giffen 7

P
Parigi, Paolo 35
Patrick, Veronica 65
Patt, Trevor 187

R
Robinson, Alexander 73

S
Sabin, Jenny E. 7
Salim,Flora 61
Sevtsuk, Andres 109
Shiordia, Rodrigo 91
Stavropoulos, Georgios 165
Stojanovski, Todor 179

T
Tenu, Vlad 127
Tessier, Alex 51
Torghabehi, Ornid Oliyan 85
Tzovaras, Dimmitrios 165

V
Veetil, Sreerag 91
Vincentelli, Alberto Sangiovanni 153
von Buelow, Peter 85

W
Wang, Simin 7
Wilkinson, Samuel 143
Wurzer, Gabriel 161

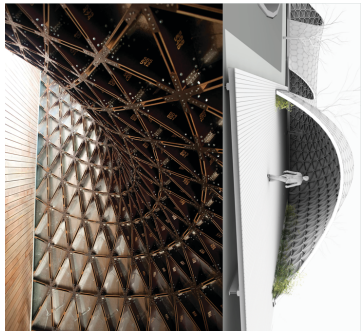
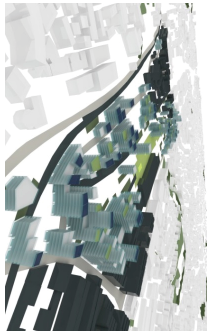

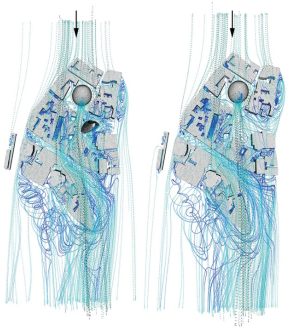


Symposium on Simulation for Architecture and Urban Design
2014